

REPORT NO. FRA-OR&D-79/19

TESTS OF THE AMTRAK SDP-40F TRAIN CONSIST
CONDUCTED ON CHESSIE SYSTEM TRACK

P. Tong
R. Brantman
R. Greif
J. Mirabella

U.S. Department of Transportation
Research and Special Programs Administration
Transportation Systems Center
Kendall Square
Cambridge MA 02142



MAY 1979

FINAL REPORT

DOCUMENT IS AVAILABLE TO THE PUBLIC
THROUGH THE NATIONAL TECHNICAL
INFORMATION SERVICE, SPRINGFIELD,
VIRGINIA 22161

Prepared for
U.S. DEPARTMENT OF TRANSPORTATION
FEDERAL RAILROAD ADMINISTRATION
Office of Research and Development
Washington DC 20590

REPRODUCED BY
**NATIONAL TECHNICAL
INFORMATION SERVICE**
U.S. DEPARTMENT OF COMMERCE
SPRINGFIELD, VA. 22161

NOTICE

This document is disseminated under the sponsorship of the Department of Transportation in the interest of information exchange. The United States Government assumes no liability for its contents or use thereof.

NOTICE

The United States Government does not endorse products or manufacturers. Trade or manufacturers' names appear herein solely because they are considered essential to the object of this report.

1. Report No. FRA-OR&D-79/19	2. Government Accession No.	3. Recipient's Catalog No. PB297711	
4. Title and Subtitle TESTS OF THE AMTRAK SDP-40F TRAIN CONSIST CONDUCTED ON CHESSIE SYSTEM TRACK		5. Report Date May 1979	
		6. Performing Organization Code DTS-74	
7. Author(s) P. Tong, R. Brantman, R. Greif, J. Mirabella*		8. Performing Organization Report No. DOT-TSC-FRA-79-14	
9. Performing Organization Name and Address U.S. Department of Transportation Research and Special Programs Administration Transportation Systems Center Cambridge MA 02142		10. Work Unit No. (TRAIS) RR919/R9357	
		11. Contract or Grant No.	
12. Sponsoring Agency Name and Address U.S. Department of Transportation Federal Railroad Administration Office of Research and Development Washington DC 20590		13. Type of Report and Period Covered Final Report June 1977 - August 1978	
		14. Sponsoring Agency Code	
15. Supplementary Notes *U.S. Department of Transportation Federal Railroad Administration Office of Rail Safety Research Washington DC 20590			
16. Abstract This report describes tests of an SDP-40F train consist conducted on Chessie System track during June, 1977. The tests consisted of the operation of two typical AMTRAK passenger consists, one powered by two SDP-40F's and the other by two E-8's, over a variety of track conditions. The objectives of the tests were to compare dynamic performance of the SDP-40F locomotive with the E-8, and to determine the sensitivity of the SDP-40F response to track geometry variations, operational parameters and truck configuration changes. Data was obtained on the lateral and vertical wheel/rail loads and carbody accelerations under a variety of speeds, track geometry and track surface conditions. Modifications of the SDP-40F trucks were also made and tested. Each locomotive was tested in a consist representative of passenger service over a variety of operational track conditions. In general, the SDP-40F lateral wheel/rail loads in selected curves showed a tendency to increase above curve balance speed at a faster rate than that of the E-8. A means was developed for accurately predicting lead axle lateral force levels in 2° curves as a function of speed and track geometry variations. A new strain gage configuration was developed which will greatly improve the accuracy of lateral rail loads measurements.			
17. Key Words Locomotive Tests Vehicle/Track Dynamics		18. Distribution Statement DOCUMENT IS AVAILABLE TO THE PUBLIC THROUGH THE NATIONAL TECHNICAL INFORMATION SERVICE, SPRINGFIELD, VIRGINIA 22161	
19. Security Classif. (of this report) Unclassified	20. Security Classif. (of this page) Unclassified	21. No. of Pages 251	22. Price A12-AC1

PREFACE

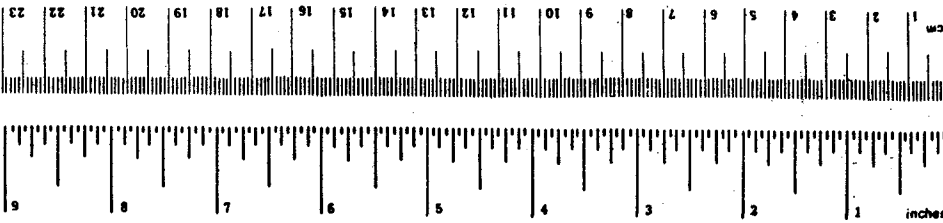
This report represents results of tests carried out and analyzed by a joint government/industry team. As in most tests, "insights" were gained beyond the pure factual information gathered. Although the prime emphasis of this report is on providing technical data on the relative performance of the SDP-40 consist under the specific conditions of tests made on trackage of the Chessie System, the format has been structured to convey the insights and the facts toward reaching the decision-makers involved in the "real world" problem of operating trains with this type of locomotive power.

Accordingly, the Executive Brief is aimed at railroad managers who can best assess and translate the importance of facts, trends, insights and judgments into meaningful actions. In addition, concise highlights are included at the beginning of each technical section.

METRIC CONVERSION FACTORS

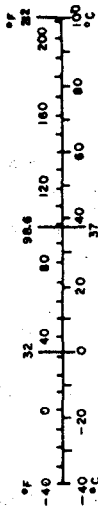
Approximate Conversions to Metric Measures

Symbol	When You Know	Multiply by	To Find	Symbol
LENGTH				
in	inches	2.5	centimeters	cm
ft	feet	30	centimeters	cm
yd	yards	0.9	meters	m
mi	miles	1.6	kilometers	km
AREA				
in ²	square inches	6.5	square centimeters	cm ²
ft ²	square feet	0.09	square meters	m ²
yd ²	square yards	0.8	square meters	m ²
mi ²	square miles	2.6	square kilometers	km ²
	acres	0.4	hectares	ha
MASS (weight)				
oz	ounces	28	grams	g
lb	pounds	0.45	kilograms	kg
	short tons (2000 lb)	0.9	tonnes	t
VOLUME				
teaspoon	teaspoons	5	milliliters	ml
Tablespoon	tablespoons	15	milliliters	ml
fl oz	fluid ounces	30	milliliters	ml
c	cups	0.24	liters	l
pt	pints	0.47	liters	l
qt	quarts	0.95	liters	l
gal	gallons	3.8	liters	l
ft ³	cubic feet	0.03	cubic meters	m ³
yd ³	cubic yards	0.76	cubic meters	m ³
TEMPERATURE (exact)				
°F	Fahrenheit temperature	5/9 (after subtracting 32)	Celsius temperature	°C



Approximate Conversions from Metric Measures

Symbol	When You Know	Multiply by	To Find	Symbol
LENGTH				
mm	millimeters	0.04	inches	in
cm	centimeters	0.4	inches	in
m	meters	3.3	feet	ft
m	meters	1.1	yards	yd
km	kilometers	0.6	miles	mi
AREA				
cm ²	square centimeters	0.16	square inches	in ²
m ²	square meters	1.2	square yards	yd ²
km ²	square kilometers	0.4	square miles	mi ²
ha	hectares (10,000 m ²)	2.5	acres	ac
MASS (weight)				
g	grams	0.035	ounces	oz
kg	kilograms	2.2	pounds	lb
t	tonnes (1000 kg)	1.1	short tons	ton
VOLUME				
ml	milliliters	0.03	fluid ounces	fl oz
l	liters	2.1	pints	pt
l	liters	1.06	quarts	qt
l	liters	0.26	gallons	gal
m ³	cubic meters	35	cubic feet	ft ³
m ³	cubic meters	1.3	cubic yards	yd ³
TEMPERATURE (exact)				
°C	Celsius temperature	9/5 (then add 32)	Fahrenheit temperature	°F



ACKNOWLEDGEMENTS

The work described in this report was conducted under the direction of the Office of Rail Safety Research of the Federal Railroad Administration (FRA). Guidance for the testing and analysis efforts was provided by a government-industry Review Group composed of representatives of the FRA Office of Safety, Association of American Railroads (AAR), National Railroad Passenger Corporation (AMTRAK), Electro-Motive Division of General Motors Corporation (EMD), and the Chessie System (Chessie). Analysis of past derailment histories was provided by J. H. Wiggins Co. and EMD.

During the tests, instrumentation and data collection support was provided by EMD and AAR for the SDP-40F locomotive, and by ENSCO, Inc. for the E-8 locomotive. Track geometry data were obtained by the FRA measurement cars T1 and T3, which were placed in the E-8 consist and operated by ENSCO. Wayside measurements of wheel/rail loads were performed by Battelle Columbus Laboratories (BCL). Initial data review was performed by Arthur D. Little, Inc. (ADL). Robert Vanstone assisted the Test Director in coordinating the testing.

Upon completion of the tests, analysis of the data was performed by the Transportation Systems Center (TSC) with support provided by ADL, BCL, and ENSCO. TSC would like to extend special recognition to these analysis support contractors for their exceptional performance.

A very special acknowledgement is due to the Review Group, whose active participation and comments proved invaluable in providing guidance during the conduct of the analysis and on the organization and interpretation of the final results. Finally, special thanks are due to AMTRAK for providing the equipment used in these tests, and to the Chessie System for permitting use of their track and for their active and complete cooperation during all phases of the test and analysis activity.

TABLE OF CONTENTS

<u>Section</u>	<u>Page</u>
1. EXECUTIVE BRIEF	1-1
1.1 Background	1-1
1.2 Chessie Tests Overview	1-1
1.3 Findings and Recommendations	1-3
1.3.1 Comparative Characterization of SDP-40F Consist Performance	1-4
1.3.2 Evaluation of the Contribution of Track and Operational Variations	1-9
1.3.3 Evaluation of the Contribution of Various Wear and Equipment Maintenance Conditions	1-11
1.3.4 Development of Guidelines for Evaluating and Ensuring the Safety of New Locomotive Designs Over Their Life-Cycles	1-14
1.3.5 Future Study/Needs Potentials	1-16
2. BACKGROUND OF TEST	2-1
2.1 The SPD-40F	2-1
2.2 Restrictions and Other Tests	2-4
2.3 The Chessie Test	2-5
2.4 Test Objectives	2-6
3. TEST DESCRIPTION	3-1
3.1 Test Consists and Vehicle Instrumentation	3-1
3.2 Site Selection	3-8
3.3 Track Instrumentation	3-14
3.4 Test Operations	3-17
4. DATA ANALYSIS PROCEDURES	4-1
4.1 Overall Approach	4-1
4.2 Track Geometry Descriptors	4-3
4.3 Vehicle Response Descriptors	4-3
4.4 Statistical Correlation Analysis	4-5
4.5 Important Vehicle Response Descriptors	4-6
4.6 Analysis of Repeat Runs	4-6
4.7 Data Analysis Task Force	4-7

TABLE OF CONTENTS (Cont'd)

<u>Section</u>	<u>Page</u>
5. TEST RESULTS	5-1
5.1 Dynamic Response of Baseline Locomotive Configurations	5-2
5.1.1 Effect of Speed	5-2
5.1.2 Effect of Track Geometry	5-31
5.1.3 Effect of Rail Surface Condition	5-49
5.1.4 Effect of Operating Modes	5-52
5.2 SDP-40F Configuration Changes	5-52
5.2.1 Vertical Primary Damping	5-54
5.2.2 Wheel Diameter Mismatch	5-66
5.2.3 Lateral Axle Clearance	5-68
5.3 Baggage Car/Locomotive Interaction	5-68
5.4 Future Implications	5-80
6. REVIEW GROUP COMMENTS, OPINIONS AND VIEWPOINTS	6-1
BIBLIOGRAPHY	7-1
APPENDICES	
A. Derailments of SDP-40F Consists	A-1
B. Track Geometry Data Analysis	B-1
C. Track Geometry Data in Test Zone	C-1
D. Use of L_{95} as a Vehicle Response Descriptor	D-1
E. Statistical Regression Analysis of Survey Run Data	E-1
F. HTC Truck Low Temperature Dynamic Response Characteristics	F-1
G. Correction of Lateral Force Data from Wayside Instrumentation	G-1
H. Simulation of Locomotive Vertical Response	H-1

ILLUSTRATIONS

<u>Figure</u>		<u>Page</u>
1-1	Comparison of Lateral Force Trends Versus Speed for Lead Axles	1-4
1-2	Comparison of Maximum Single-Axle Lateral Force for Middle Axles	1-5
1-3	Comparison of SDP-40F and E-8 Upper Bounds of Lateral Force on High Rail for Trailing Truck	1-6
1-4	Comparison of First and Middle Axle Lateral Forces	1-8
1-5	Upper Bound of Maximum Single-Axle Lateral Force on E-8 and SDP-40F Baggage Cars	1-9
1-6	Effects of Simulated Wheel Mismatch	1-12
1-7	Baggage Car Vertical Effects	1-14
3-1	SDP-40F Test Consist	3-3
3-2	E-8 Test Consist	3-4
3-3	SDP-40F and E-8 Test Consists	3-5
3-4	Interior View of EMD's ET-800 Car	3-9
3-5	SDP-40F Test Site on Chessie System	3-11
3-6	Partial View of Test Zone	3-12
3-7	Track Chart of 4-Mile Test Zone, Chessie System, Clifton Forge Division	3-13
3-8	Plan View of Instrumented Track Site, Milepost 257.6, Chessie System	3-15
3-9	Typical Wayside Gage Installation	3-16
4-1	Analysis Methodology	4-2

ILLUSTRATIONS (Cont'd)

<u>Figure</u>		<u>Page</u>
4-2	Organizational Flow For Data Reduction and Analysis of the SDP-40F and E-8 Locomotive Tests Conducted on Chessie System Track	4-8
4-3	FRA/TSC Data Reduction and Analysis Sequence for the SDP-40F and E-8 Locomotive Tests	4-9
5-1	Comparison of E-8 and SDP-40F Axle 10 Lateral Force Traces Under Power and Drift Near 60 MPH (Wayside Data)	5-4
5-2	Typical E-8 and SDP-40F Lateral Force and Gage Traces at 60 MPH	5-5
5-3	Maximum Single-Wheel Lateral Force and L/V Versus Speed for Lead Axle in Each Truck of the E-8 Consist (Baseline Runs, Wayside Data)	5-6
5-4	Maximum Single-Wheel Lateral Force and L/V Versus Speed for Lead Axle in Each Truck of the SDP-40F Consist (Baseline Runs, Wayside Data)	5-7
5-5	Comparison of E-8 and SDP-40F Lateral Force Envelopes for All Lead Axles Versus Speed (Baseline Runs, Wayside Data)	5-8
5-6	Comparison of E-8 and SDP-40F Maximum Single-Wheel Lateral Force Versus Speed for Each Lead Axle (Baseline Runs, Wayside Data)	5-9
5-7	Comparison of E-8 and SDP-40F Axle 11 Lateral Force Traces Under Power and Drift Near 60 MPH (Wayside Data)	5-11
5-8	Maximum Single-Wheel Lateral Force for Axles 10 and 11, E-8 and SDP-40F (Baseline Runs, Wayside Data)	5-12

ILLUSTRATIONS (Cont'd)

<u>Figure</u>		<u>Page</u>
5-9	Maximum Single-Wheel Lateral Force Versus Speed for Middle Axle in Each Truck of the E-8 and SDP-40F Consists (Baseline Runs, Wayside Data)	5-14
5-10	SDP-40F and E-8 Envelopes of Maximum Single-Wheel Lateral Force Versus Speed for all Middle Axles (Baseline Runs, Wayside Data)	5-15
5-11	Maximum Single-Wheel Lateral Force and L/V Versus Speed for Trailing Axle in Each Truck of the E-8 and SDP-40F Consists (Baseline Runs, Wayside Data)	5-16
5-12	E-8 Truck Lateral Forces on High Rail (Baseline Runs, Interpolated Wayside Data)	5-17
5-13	SDP-40F Truck Lateral Forces on High Rail (Baseline Runs, Interpolated Wayside Data)	5-18
5-14	Comparison of E-8 and SDP-40F Maximum Lateral Force on High Rail for Truck 3 (Baseline Runs, Interpolated Wayside Data)	5-20
5-15	Comparison of E-8 and SDP-40F Maximum Lateral Force on High Rail for Truck 4 (Baseline Runs, Interpolated Wayside Data)	5-21
5-16	Mean Exceedance Time Vs. L/V Ratio Threshold for Axle 10 in the Test Curve (Onboard Data, Nominal Configuration)	5-23
5-17	Mean Exceedance Time Vs. Lateral Force Threshold in the Test Curve (Onboard Data, Nominal Configuration)	5-24
5-18	Definition of Underbalance	5-26

ILLUSTRATIONS (Cont'd)

<u>Figure</u>		<u>Page</u>
5-19	Influence of Underbalance on the SDP-40F and E-8 L_{95} Forces for Axle 10 (Survey Run Data)	5-27
5-20	Comparison of Axle 10 L_{95} and $(L/V)_{95}$ For E-8 and SDP-40F Versus Speed in Test Curve (Baseline Runs, Onboard Data)	5-28
5-21	Comparison of Axle 10 L_{95} and $(L/V)_{95}$ for E-8 and SDP-40F Versus Speed in Curve at MP 257.2 (Baseline Runs, Onboard Data)	5-30
5-22	Influence of Various Track Descriptors in Equation for L_{95} on Axle 10 of SDP-40F and E-8 Based on Results of Regression Analysis	5-32
5-23	Comparison of Predicted SDP-40F Axle 10 Response from Regression Analysis with Baseline Run Data, in Test Curve, As a Function of Underbalance	5-35
5-24	Comparison of Predicted E-8 Axle 10 Response from Regression Analysis with Baseline Run Data, in Test Curve, As a Function of Underbalance	5-36
5-25	Comparison of Axle 10 Sensitivity Predictions for E-8 and SDP-40F from Statistical Regression Analysis	5-37
5-26	Regression Analysis Prediction for L_{95} of Axle 10 for E-8 and SDP-40F, As a Function of Underbalance, for Category A Track	5-38
5-27	Regression Analysis Prediction for L_{95} of Axle 10 for E-8 and SDP-40F, As a Function of Underbalance, for Category B Track	5-39
5-28	Regression Analysis Prediction for L_{95} of Axle 10 for E-8 and SDP-40F, As a Function of Underbalance, for Category C Track	5-40

ILLUSTRATIONS (Cont'd)

<u>Figure</u>		<u>Page</u>
5-29	Regression Analysis Prediction for L_{95} of Axle 10 for E-8 and SDP-40F, As a Function of Underbalance, for Category D Track	5-41
5-30	Influence of Various Track Descriptors in Equation for V_s on Axle 10 of SDP-40F and E-8 Based on Results of Regression Analysis	5-44
5-31	Influence of Various Track Descriptors in Equation for $(L/V)_{95}$ on Axle 10 of SDP-40F and E-8 Based on Results of Regression Analysis	5-45
5-32	Possible Mechanism Explaining Coincidence of Peak Lateral Loads and Peak Gage Variations Near High Rail Joints	5-46
5-33	Brush Chart Recording Showing Verification of Gage Variation with Respect to High Rail Joint Locations	5-47
5-34	Typical Axle 10 Lateral Force Traces at Test Site, E-8 and SDP-40F Near 60 MPH (Wayside Data)	5-48
5-35	Effect of Wet and Sanded Rail Surface Conditions on Performance of Axle 10 of SDP-40F in Test Curve (Power Mode, Onboard Data)	5-50
5-36	Effect of Wet and Sanded Rail Surface Conditions on Performance of Axle 10 of SDP-40F at Test Site (Wayside Data)	5-51
5-37	Effect of Operating Mode on Axle 10 Maximum Lateral Force for E-8 and SDP-40F at the Test Site (Baseline Runs, Onboard Data)	5-53
5-38	Effect of Variation in Vertical Primary Damping on RMS Primary Spring Deflection at High Wheel of SDP-40F Versus Speed in Test Curve	5-55

ILLUSTRATIONS (Cont'd)

<u>Figure</u>		<u>Page</u>
5-39	Effect of Variation in Vertical Primary Damping on SDP-40F Front Hood End Vertical Acceleration (All Runs for Trailing Locomotive at Road Crossing Near MP 257.5 in Power Mode)	5-56
5-40	Comparison of E-8 and SDP-40F Rear Cab End Vertical Accelerations	5-57
5-41	Effect of Secondary Spring Rate and Primary Damping on HTC Primary Suspension Performance (SP Test Results)	5-59
5-42	Analytical Simulation of Effect of Variation in the Vertical Primary Damping on SDP-40F Rear End Vertical Accelerations	5-60
5-43	Analytical Simulation of Effect of Variation in the Vertical Primary Damping on SDP-40F Maximum Wheel Unloading for Leading Wheelset of the Trailing Truck	5-63
5-44	Analytical Simulation Comparing the Maximum Wheel Unloading of the Leading and Trailing Wheelsets of the Trailing SDP-40F Truck	5-64
5-45	Analytical Simulation of Effect of Variation in the Vertical Primary Damping on the Vertical Wheel Force Trace of the Leading Wheelset of the Trailing SDP-40F Truck at the Bounce Resonance	5-65
5-46	Effect of Shimmed Axles 11 and 12 on V_s Response of Axle 10 of SDP-40F in Test Curve (Onboard Data)	5-67
5-47	Effect of Shimmed Axles 11 and 12 on $(L/V)_{95}$ Response of Axle 10 of SDP-40F in Test Curve (Onboard Data)	5-69
5-48	Effect of Axle 12 Wheel Diameter Mismatch on $(L/V)_{95}$ Response of Axle 10 SDP-40F in Test Curve (Onboard Data)	5-70

ILLUSTRATIONS (Cont'd)

<u>Figure</u>		<u>Page</u>
5-49	Effect of Wheel Diameter Mismatch on Minimum Single-Wheel Vertical Force for Axle 12 of SDP-40F (Wayside Data)	5-71
5-50	Effect of Increasing Lateral Axle Clearance of the Trailing Truck of Trailing Locomotive on L_{95} Response of Axle 10 of SDP-40F in Test Curve (Onboard Data)	5-72
5-51	Maximum Single-Wheel Lateral Force for Lead Axles of E-8 and SDP-40F Baggage Cars (Baseline Runs, Wayside Data)	5-73
5-52	Coupler Oscillation Between Trailing Locomotive and Baggage Car in the SDP-40F Consist	5-75
5-53	Trailing Locomotive/Baggage Car Lateral Acceleration Interaction for SDP-40F Consist Versus Speed (Baseline Runs, Onboard Data)	5-76
5-54	Vertical Carbody Accelerations of SDP-40F Locomotive and Baggage Car Over Adjacent Trucks at Road Crossing Near MP 257.5 (Power Mode)	5-77
5-55	Vertical Acceleration of SDP-40F Baggage Car Rear End at Road Crossing Near MP 257.5 (Power Mode)	5-78
5-56	Effect of Shimmed Axles 11 and 12 of SDP-40F on Front End Vertical Acceleration of the Baggage Car at Road Crossing Near MP 257.5	5-79
6-1	Comparison of Lead and Middle Axle Wheel Loads in Chessie & ICG Tests (Wayside Data from Baseline runs in Both Tests)	6-7
6-2	Comparison of Lead Axle Wheel Loads & L/V Ratios in Chessie Test	6-10

TABLES

<u>Table</u>		<u>Page</u>
1-1	SUMMARY OF DERAILMENTS AND TESTS CONDUCTED (1 of 2)	1-18
	SUMMARY OF DERAILMENTS AND TESTS CONDUCTED (2 of 2)	1-19
2-1	LOCOMOTIVE DATA	2-2
2-2	COMPARISON OF SDP-40F AND E-8 LOCOMOTIVE TRUCKS	2-3
3-1	TEST RUN LOG	3-19
5-1	SUMMARY OF TRACK GEOMETRY CHARACTERISTICS USED IN PREPARING FIGURES 5-25 THROUGH 5-29	5-42
5-2	RMS AMPLITUDES OF VERTICAL DISPLACEMENT AND ACCELERATION AT THE FRONT AND REAR TRUCK ATTACHMENT POINTS	5-61

1. EXECUTIVE BRIEF

1.1 BACKGROUND

The SDP-40F locomotive was introduced in Amtrak passenger service in June, 1973, and by August, 1974, a total of 150 SDP-40F locomotives were in service. This locomotive, a 3,000-hp, 6-axle, 6-motor unit like the SD40-2 locomotives which are widely used in freight service is equipped with HTC trucks. These passenger models have steam generators and water tanks and weigh nominally 396,000 lbs. with full supplies.

The SDP-40F locomotives generally replaced E-8 and E-9 locomotives originally delivered to the railroads between 1950 and 1962. These "E" type locomotives utilizing swing hanger type trucks were designed for passenger service and were 2250- to 2400-hp, 6-axle, 4-motor models weighing nominally 335,000 lbs. with full supplies. They were generally considered as dependable with no widely recognized safety problems.

By January, 1978, Amtrak passenger trains powered by SDP-40F locomotives had been involved in 21 derailments at speeds of 30 mph or greater. Concurrently, between 1974 and 1977, several special tests were conducted to factually determine the derailment tendencies of these consists as operated by Amtrak. Table 1-1 summarizes the essentials of prior derailments and the major test activities (page 1-18).

1.2 CHESSIE TESTS OVERVIEW

To provide data that would complement and extend the findings of the referenced tests, the FRA Office of Rail Safety Research, in cooperation with the AAR, Amtrak and EMD, conducted a series of controlled tests using typical Amtrak SDP-40F and E-8 locomotive consists over Chessie System track in June, 1977. The data analyses of these tests concentrated primarily on 2° to 3° curves on Class 3 jointed track with train speed ranging from 30 to 60 mph.

A comparative test procedure involving the predecessor E-8 power was dictated since absolute criteria for specific safe limits of wheel/rail force or force ratios were not available. The design of the test and the subsequent data analysis was established based on a recognition that SDP-40F derailments are rare events. While a given difference in wheel/rail force levels between the SDP-40F and baseline E-8

consists may not be significant in itself, the potential force levels reachable may be far above test results due to cumulative effects, i.e., additive increments in force due to the effects of sanding, maintenance states and operating practices. Thus, detection of marked differences in performance trends rather than absolute levels were considered especially important since unfavorable locomotive consist combination of conditions could conceivably occur in actual operations at the same time that "marginal" track conditions are encountered. Accordingly, the subsequent analysis was aimed at uncovering trends in those factors that could contribute to adverse performance even if a particular factor or level of force in itself may not justify attention as a sole cause of derailments. Since the focus of inquiry was on determining the mechanism for SDP-40F powered train derailments, concentration of efforts centered primarily on analysis of those portions of the test data where the performance of the SDP-40F consist exhibited unfavorable trends in comparison to the E-8 baseline case. (This is not meant to infer that the SDP-40F never compared favorably to the E-8 during the tests.) Also, a number of measurements were made in relationship to the SDP-40F consist which were not correspondingly done on the E-8.

The stated objectives of the tests and subsequent data analysis were:

1. Comparative characterization of SDP-40F consist performance,
2. Evaluation of the contribution of track and operational variations,
3. Evaluation of the contribution of various wear and equipment maintenance conditions, and
4. Development of guidelines for evaluating and ensuring the safety of new locomotive designs over their life-cycles.

Key elements in accomplishing these objectives were:

1. Continuous onboard wheel/rail force measurements on each of the two separate locomotive consists,
2. Selection of a specific test site based upon comparison of performance of the two locomotive consists operating over hundreds of miles of representative track,

3. Complementary wayside measurement of wheel/rail forces for each vehicle of entire consists at the selected test site,
4. Simultaneous measurement of track geometry for all trackage traversed by the consists, and
5. Application and validation of fresh analytical approaches toward establishment of trends.

1.3 FINDINGS AND RECOMMENDATIONS

At the risk of oversimplifying the results of a many faceted study, the findings and recommendations of this Executive Brief are intended to minimize the communication obstacles often posed by technical complexities. Since emphasis is on highlighting those comparative trends which best address the regime of actual SDP-40F consist derailment experience, the body of the report must be referred to for a more in-depth understanding as to performance differences over the broader spectrum. Obviously, incorporation of this approach:

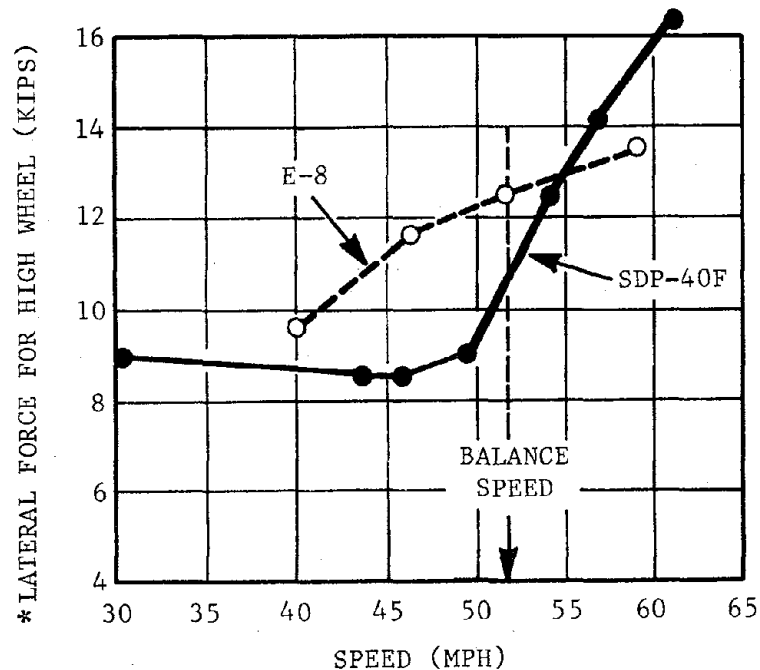
1. is aimed at reaching the largest possible audience with maximum clarity,
2. relies upon judicious selection of important factors,
3. assumes that extrapolation of comparative trends is justified,
4. supports individual conclusions with varying degrees of certainty, and
5. does not include all the details of caveats and/or qualifications which are contained in the body of the report.

This section presents the major results of the testing program. Findings are based on the test data and analysis which are provided in greater detail in the body of the report. The graphs included illustrate pertinent results but are not the sole basis for arriving at conclusions and/or recommendations.

1.3.1 Comparative Characterization of SDP-40F Consist Performance

Locomotive Single Axle Forces

1. The SDP-40F maximum single axle lateral load tended to exhibit greater increase in levels with increasing speed beginning near the "balance" speed. Figure 1-1 shows a severe case selected from actual data to illustrate this characteristic.



*95th Percentile - 5% of the time the forces exceeded this level.

Figure 1-1 Comparison of Lateral Force Trends Versus Speed for Lead Axles

2. A statistical regression analysis of 25 other curves supports an increasing force trend for the SDP-40F. At some point above the balance speed the SDP-40F lateral forces exceed those of the E-8 by increasing amounts.

Locomotive Middle Axle Forces

3. The middle axle lateral force tended to be higher for the SDP-40F than the E-8 virtually over the entire tested speed ranges; which contributed to higher lateral truck forces (Figure 1-2).

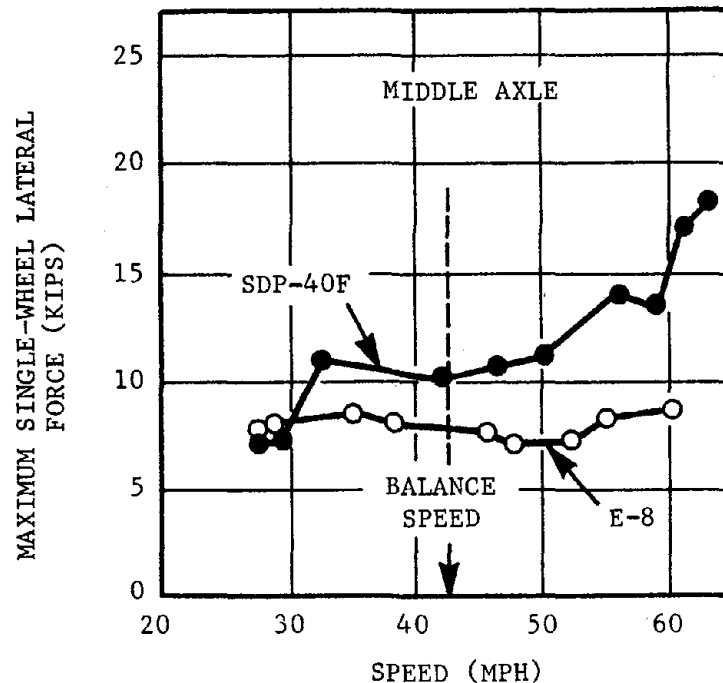


Figure 1-2 Comparison of Maximum Single-Axle Lateral Force for Middle Axles

Locomotive Third Axle Forces

4. The third or trailing axle lateral forces of the SDP-40F and E-8 were roughly comparable and at relatively lower levels.

Locomotive Truck Forces

5. Total truck lateral loads, which may be most significant for the reported causes of SDP-40F powered train derailments, were derived from measured axle data and tended to be higher on the SDP-40F than on the E-8 with the differences increasing with speed (Figure 1-3).

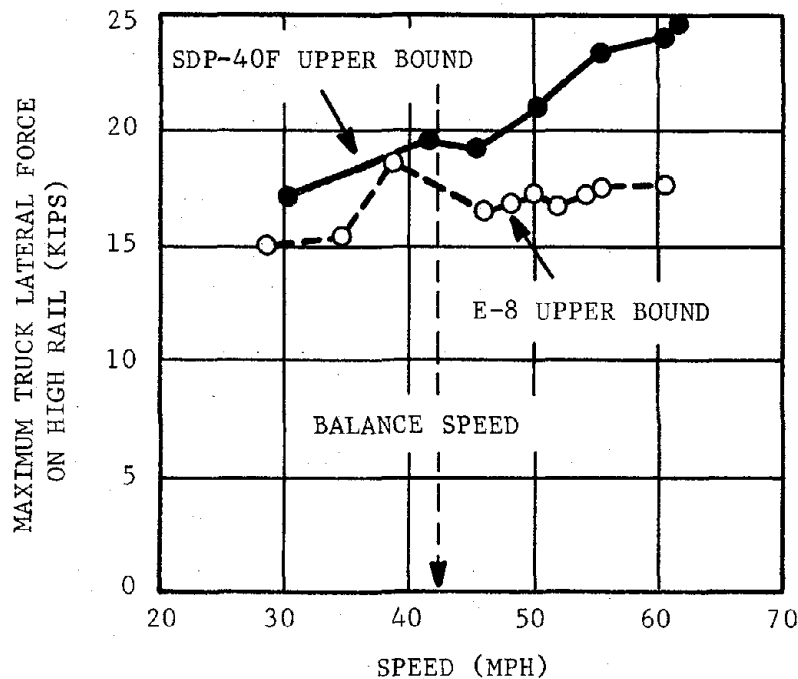


Figure 1-3 Comparison of SDP-40F and E-8 Upper Bounds of Lateral Force on High Rail for Trailing Truck

Locomotive L/V Ratios

6. The regression analysis of 25 curves indicated that the L/V ratios were higher on the E-8 than the SDP-40F. Specific individual runs showed that for the SDP-40F (consistent with lateral force findings), the L/V ratio had a definite trend towards higher rates of increase beyond the balance speed. The L/V ratios measured are below the derailment criteria commonly applied in the industry.

Locomotive Force Levels

7. Although the levels of forces measured for nominal consist configurations at the test site would not in themselves be considered excessive, the totality of results indicated that the important wheel/rail force trends uncovered can be augmented by other more unfavorable combinations of equipment configurations, maintenance/operations and track geometry conditions

(i.e., gage, cross level and alignment). These additives could produce more critical train derailment tendencies.

Locomotive Recommendations

- Based on the Chessie System Tests, and under the criterion of equivalence to E-8, SDP-40 powered trains can be operated to maximum speeds corresponding to about 1-1/2" unbalance on typical Class 3 track. With greater track strength and smaller rates of changes in track geometry deviations, consideration could be given to various degrees of relaxation of this limit.
- In view of the increase in lateral force with speed which the SDP-40F exhibits in operation above balance speed, precautions should be taken with SDP-40F locomotive consist operations to ensure that trains are not operated in excess of recommended speed limits (over speed).

Locomotive Vertical Dynamics

8. Application of vertical 1800/1800-lb. shock absorbers to the SDP-40F resulted in reductions in vertical carbody accelerations of up to 25% at the resonant conditions.

Locomotive Recommendations

- Apply vertical 1800/1800-lb. shock absorbers to the SDP-40F locomotives. This has the potential of lowering L/V ratios and improving the coupling interface dynamics with adjacent vehicles.

Locomotive Curving Characteristics

9. The tests indicate differences in curving characteristics of the SDP-40F and the E-8 locomotives. While the SDP-40F frequently produced second axle high-rail dynamic lateral force levels which approached or exceeded lead axle lateral forces, this was not the case for the E-8. On the E-8, the leading wheel on the high rail (commonly thought of as the "guiding" wheel in curve negotiations) consistently exhibited

wheel/rail lateral force levels greater than the wheels on the trailing axles (Figure 1-4).

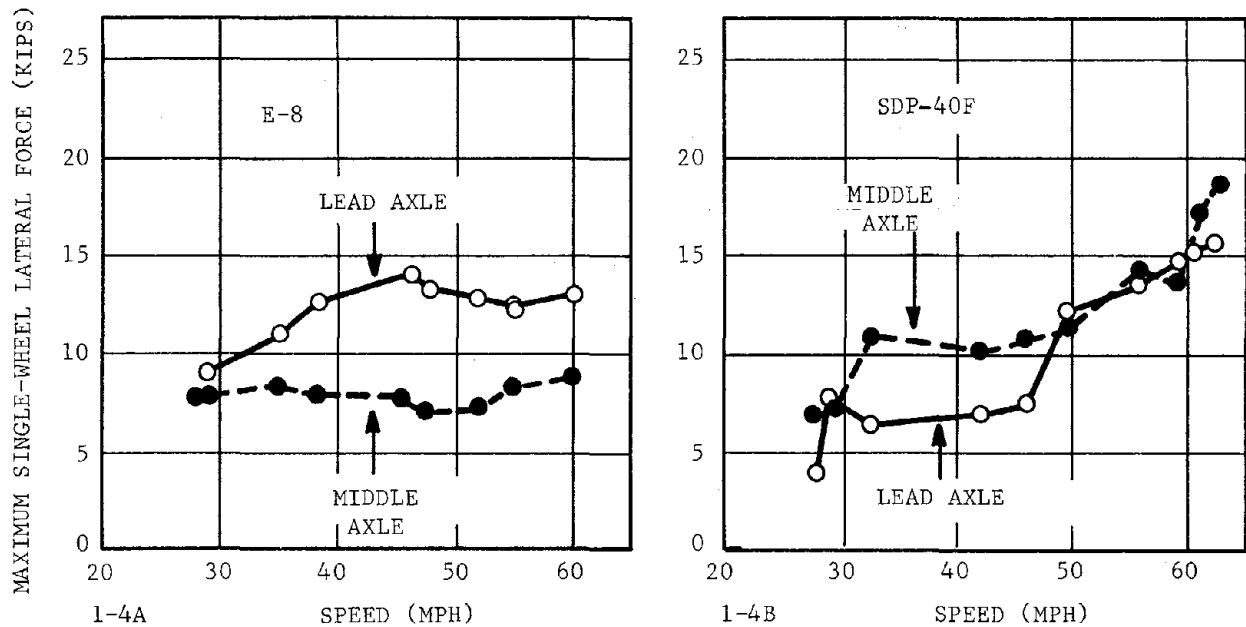


Figure 1-4 Comparison of First and Middle Axle Lateral Forces

Locomotive Baggage Car Coupling

10. The tests produced evidence of interactions between the locomotive and adjacent baggage car which will be referred to as coupling. Both vertical coupling and lateral coupling were observed. A strong indication of lateral coupling between the locomotive and baggage car was seen in the tests. The baggage car behind the SDP-40F (which has alignment control) generated maximum axle lateral loads twice as high as the baggage car behind the E-8 (which does not have alignment control) (Figure 1-5). Although there were some indications of alignment control involvement, it was not possible to accurately quantify the influence on performance.

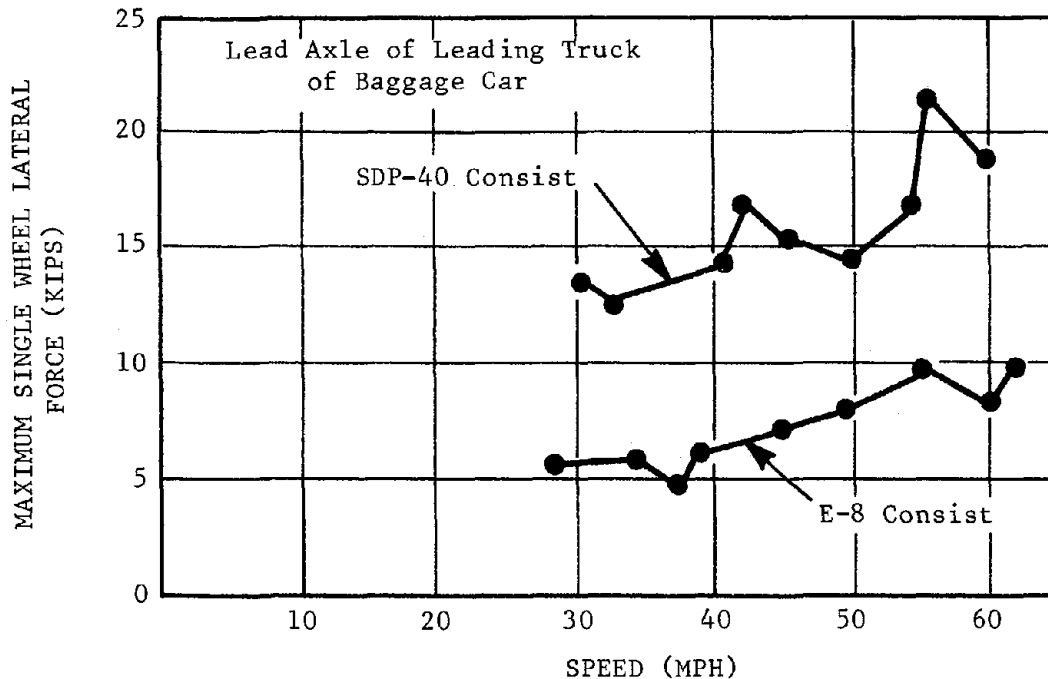


Figure 1-5 Upper Bound of Maximum Single-Axle Lateral Force on E-8 and SDP-40F Baggage Cars

Locomotive Recommendations

- Remove the alignment control from SDP-40F locomotives to eliminate any locomotive-baggage car lateral coupling which may result from its use (only if it can be verified that alignment control is not necessary for the relatively short passenger train consists used by Amtrak).

1.3.2 Evaluation of the Contribution of Track and Operational Variations

Track Influence

1. It was found that SDP-40F and E-8 lateral wheel-rail loads were generally higher in the vicinity of rail joints in the high rail than in other places on the track. These loads were associated with rapid changes of gage and/or alignment. The maximum dynamic lateral loads occurring in the immediate vicinity of joints

were commonly 2-4 times the steady state loads associated with curved track with minimal geometry deviations.

2. A technique was developed to assist in identifying, quantifying and determining the sensitivity of dynamic vehicle performance to specific variations in track geometry parameters. This tool was applied and is available for use in predicting force levels for given track geometry conditions.
3. The results indicate that for low curvatures (2°-3°), the SDP-40F lateral force is more sensitive than the E-8 to track lateral irregularities that periodically occur over distances of greater than or equal to 2 rail lengths (i.e., "curvature" as measured in these tests). On the other hand, the E-8 lateral force is more sensitive than the SDP-40F to periodic track lateral deviations occurring within about one rail length (i.e., "gage" as measured in these tests).

Track Recommendations

- *Priority maintenance should be directed at lateral track strengthening to provide greater rail fastening capacity in curves - including those of moderate degree of curvature which are sometimes considered almost "tangent" and do not always receive the speed reduction warranted. In jointed track, special attention should be given to tamping and improved fastening, e.g., additional spiking, in the immediate vicinity of joints.*
- *Railroads should give emphasis to maintaining track in curves to avoid large rates of change of track geometry and combinations of track geometry variations even though individual minimum standards allow such conditions.*
- *Railroads should give serious consideration to periodically utilizing an instrumented locomotive for the purpose of detecting those track locations which produce maximum dynamic responses. Critical track maintenance needs could thus be determined -- especially for routes where new passenger equipment which might have different degrees of sensitivity to track/operating variations will be used.*

Rail Surface Condition

4. In the tests at speeds up to 35 mph, sanding nearly doubled the maximum dynamic lateral wheel/rail force in curves. Conversely, the lateral loads were significantly reduced with rain on the rails.

Operating Recommendations

- *Both unnecessary manual and improperly triggered automatic use of sand in curves should be avoided. The benefits/problems associated with the use of onboard lubricator systems (similar to Swiss applications) which might reduce lateral forces in curves should be investigated and tested.*

Train Handling Practices

5. For the relatively short Amtrak passenger train consists, normal train handling practices involving changes in power or braking modes had little effect on lateral wheel-rail loads.

1.3.3 Evaluation of the Contribution of Various Wear and Equipment Maintenance Conditions

Locomotive Wheel Size Variations

1. The tests showed that increases in wheel L/V ratios of 40% can be produced with a simulated 1-1/4 inch radial wheel mismatch between axles (Figure 1-6).

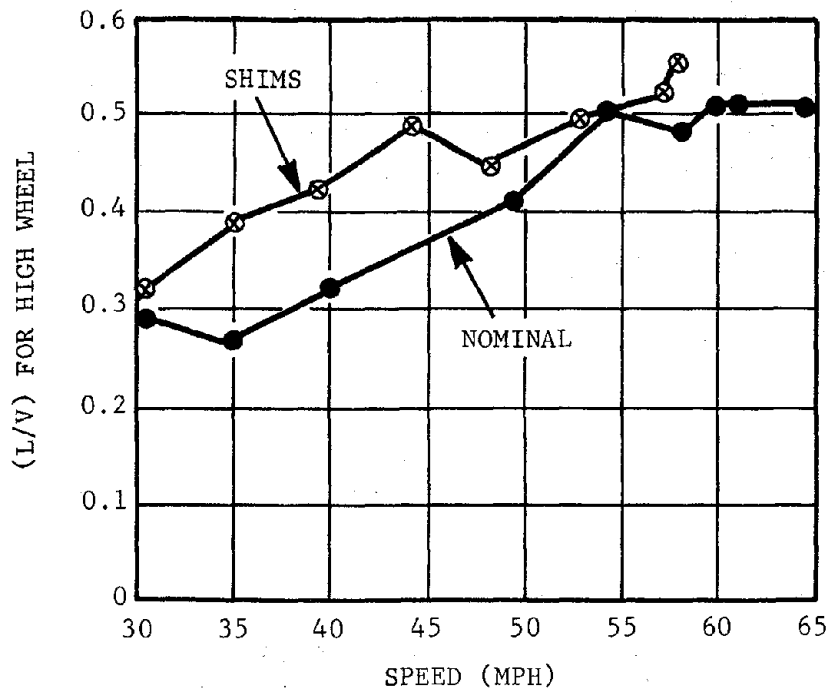


Figure 1-6 Effects of Simulated Wheel Mismatch

Locomotive Wear and Maintenance Recommendations

- EMD releases of June 1, 1971, and July 12, 1971, provide recommendations on wheel size variations and journal spring shimming. If wheel size mismatch within a 3-axle truck exceeds 1/4 inch on the radius (but less than the maximum allowable variation of 5/8 inch on the radius), shimming should be used to equalize vertical wheel loads. Excessive mismatch (even if properly shimmed) can induce false wheel slip indications and subsequent sanding. Maintenance procedures and practices should be aimed at ensuring that mismatches beyond limits specified do not occur.

Locomotive Lateral Axle Clearances

2. For the relatively short Amtrak passenger train consists, increasing lateral axle clearance on the SDP-40F had a negligible effect on lateral wheel-rail loads.

Control of Vertical Accelerations

3. The maximum vertical baggage car accelerations were about 45% higher than the maximum vertical accelerations of the SDP-40F locomotive with nominal vertical shock absorbers.
4. Resonant speeds for baggage car body bounce and pitch (48-58 mph in Chessie Tests) can overlap the resonant speeds for SDP-40F body bounce and pitch (40-50 mph range in Chessie Tests), depending on the baggage car load and the locomotive supplies. The overlap of resonant speeds can accentuate the vertical interaction between locomotive and baggage car if the couplers are vertically misaligned.

Baggage Car/Locomotive Vertical Coupler Alignment

5. Vertical coupling (forced interactions) between locomotive and baggage car increased when test variations in locomotive wheel diameters produced conditions wherein the couplers were misaligned vertically. Figure 1-7 indicates the extent of the resulting higher accelerations measured in the baggage car.

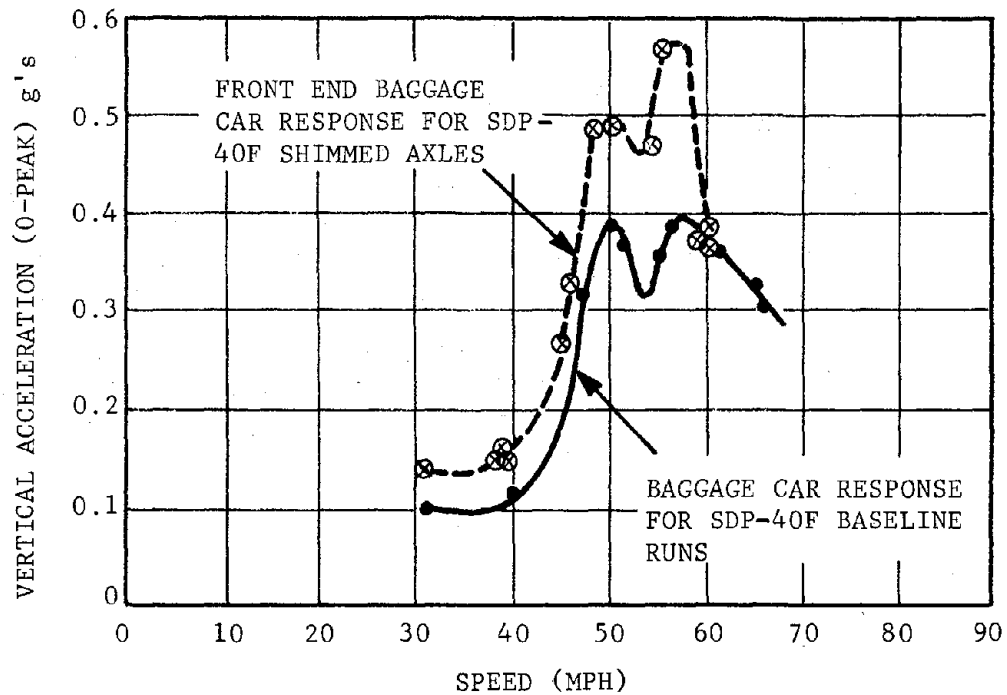


Figure 1-7 Baggage Car Vertical Effects

Baggage Car/Locomotive Wear and Maintenance Recommendations

- *Maintain proper coupler heights on locomotive and baggage cars. Allow for variations in locomotive/baggage car coupler heights as fuel, water supplies and baggage car lading changes.*
- *Maintain the spring-load coupler carrier on locomotives and baggage cars.*
- *Install and maintain vertical shock absorbers on all baggage cars.*

1.3.4 Development of Guidelines for Evaluating and Ensuring The Safety of New Locomotive Designs Over Their Life-Cycles

Facilitation of Future Testing

1. The Chessie Tests and the previous individual tests (referenced in the Background) incurred large

expenditures of manpower, equipment and other resources in reoccurring type tasks basically associated with setting up test procedures, instrumentation, establishment of logistics, means to support data collection, searching for a representative site, tear down, etc. In spite of prior intentions and careful planning, "field" tests inevitably cannot be "efficient" since the conduct of tests must fit in with critical railroad operations and time changing physical states. Additionally, such individual tests invariably take place under varying conditions which require extended time and effort to arrive at any meaningful comparison between different individual tests. More control, standardization and reduction in costs per test is needed.

Testing Guideline Recommendations

- *The feasibility of structuring a dedicated section of trackage which incorporates a known and representative range of track conditions and appropriate support facilities to minimize test costs and maximize the reliability of performance comparisons should be rigorously explored. Such a site could serve as the nucleus for arriving at more objective quantification of track/rolling stock/operations derailment criteria and results could be supplemented by limited field tests where warranted.*

Measurement and Analysis Tools

2. Tests predating the Chessie Tests did not clearly show the trends revealed in this report, apparently because instrumentation techniques and analytical tools that were especially developed for this series of tests were not practically employable. Without these aids, the statements contained in the report could not be made with reasonable confidence. Because of the potential importance to both the railroad and supply industries, definitive descriptions of improved instrumentation and analytical methods developed for/during this program are being included in this report. These advancements should prove valuable in future evaluation efforts.

1.3.5 Future Study Needs/Potentials

The findings of the tests on the Chessie System, together with the data provided in previous tests and from the derailment statistics, suggest several areas to be considered in future research.

Coupler Design

While proper coupler height on locomotive and baggage cars is important to minimize vertical coupling between the vehicles, consideration might also be given to using an "E" type coupler in place of the "F" type interlocking coupler on the locomotive to further minimize transmission of vertical loads through the couplers between locomotives or between a locomotive and a baggage car. Since it is desirable to keep the vehicles coupled together in the event of a passenger train derailment, an "E" type double shelf coupler might be a good candidate for evaluation.

Track Geometry

While initial steps have been taken to study the relationships between track geometry and vehicle response, additional work needs to be done to clarify these relationships and to make the information a useful input to track maintenance decisions. This includes development of guidelines on maximum rates of change of gage and alignment and the effects of combinations of cross level, gage and alignment deviations.

Seasonal Effect on Derailments

The higher incidence of Amtrak train derailments in the winter months indicates that vehicle and track characteristics and operating practices at low temperatures should be addressed. The FRA has sponsored laboratory testing of low temperature properties of the rubber bolster springs used on many locomotives including the SDP-40F. Additionally, available data for low temperature characteristics of track indicate that frozen roadbed can produce very large increases in track stiffness. Consideration should be given to investigating wheel-rail loads under the combination of frozen roadbed effects, low-temperature vehicle effects, and combinations of track geometry deviations. Truck lateral forces applied under rigid roadbed conditions might well roll over the rail in

cases which would have resulted in no damage with a less rigid roadbed.

Derailment Criteria

Although still somewhat controversial, derailment criteria for wheel climb associated with wheel L/V ratios over stipulated time durations have been proposed by several sources. However, there is definitely a lack of adequate grounds for derailment criteria for lateral wheel loads, lateral truck loads and truck L/V ratios. There is a need to develop and validate criteria which will directly address the reported predominant causes of SDP-40F consist derailments.

TABLE 1-1 SUMMARY OF DERAILMENTS AND TESTS CONDUCTED (1 of 2)

Derailments

- Twenty of the 21 derailments involved occurred at reported speeds of 40 to 70 mph with an overwhelming majority occurring in curves of less than approximately 30°.
- In 12 of the cases, locomotives derailed. In 11 of these 12 derailments, the car adjacent to the locomotive was a baggage car and was also derailed. In 10 of these 11 derailments, the derailed locomotive was the trailing unit of a multi-locomotive consist.
- In 10 of 14 cases where the mechanism of derailment was identified, the reported causes were excessive lateral force, rail spreading, wide gage, and rail rollover. Wheel climb was never designated as the mechanism of the derailment.
- In 9 cases, locomotives did not derail. In 4 of these, the first derailed car was a baggage car immediately following an SDP-40F locomotive.
- The derailment analysis indicated a seasonal trend, with the majority occurring in the winter months.
- Exposure and derailment rates (miles per derailment) varied widely from railroad to railroad.

Major Testing

- In 1974, EMD conducted tests of the SDP-40F locomotive up to 120 mph to study the influence of new and worn wheels and to investigate complaints that the locomotive exhibited an uncomfortable ride under some conditions. As a result of these tests, SDP-40F locomotives were equipped with wheels having a 1:40 taper profile and lateral shock absorbers.
- In 1975, EMD conducted a series of tests on similar freight locomotives to confirm and extend the work done with wheel profiles and lateral damping.
- In 1975, tests sponsored by the FRA were conducted on the Northeast Corridor to measure lateral loads of various vehicles, including the SDP-40F locomotive.

TABLE 1-1 SUMMARY OF DERAILMENTS AND TESTS CONDUCTED (2 of 2)

- In early 1976, Amtrak sponsored a test program on the ICG Railroad to compare the dynamic wheel-rail loads and ride performance of SDP-40F and E-8 locomotives. The FRA participated in the planning and observation of these tests. As a result of this work, EMD recommended in 1976 that the SDP-40F locomotives be retrofitted with softer rubber springs and increased lateral clearance in the secondary suspension.
- In the spring of 1977, Amtrak, EMD and the AAR began an SDP-40F baggage car test series on the Burlington Northern Railroad. The program included survey runs with an SDP-40F over several thousand miles of track and tests comparing SDP-40F and F40PH locomotives at selected sites. The analysis of this test data is currently being performed by the AAR.

2. BACKGROUND OF THE TEST

Highlights

- Six-axle SDP-40F for passenger trains evolved from prior "SD" equipment utilization in freight operations.
- Six-axle SDP-40F passenger use was preceded by previous 6-axle locomotive power such as the E-7, E-8, and E-9.
- The SDP-40F design employs traction motors on all three axles of each truck, whereas the E-8 middle axle is unpowered.
- Complaints of poor ride quality and a developing pattern of derailments caused concern for safe SDP-40F operation.
- Subsequent accident analysis, dynamic simulations and preliminary field tests established areas of concern.
- Based on existing data, operational restrictions were imposed on SDP-40F consists.
- Special field tests on the BN were commenced, and, with full participation by FRA, provision for an extension of the scope of these tests on the Chessie System was made.
- These tests were designed to provide comparative insights into the dynamic performance of the SDP-40F compared with previous AMTRAK locomotives.

2.1 THE SDP-40F

AMTRAK has owned and operated a fleet of 150 SDP-40F diesel-electric, passenger locomotives since mid-1973. A series of derailments and complaints of poor ride quality raised concerns about the safety of this locomotive. It was decided that a more complete testing program was needed for evaluating the dynamics of locomotives in order to assure high levels of safety. The Chessie Test was conducted towards this end.

The SDP-40F is one of the heaviest locomotives in use today, weighing approximately 395,000 pounds when fully loaded with fuel and water. Six-axle SDP-40F for passenger trains evolved from prior "SD" equipment utilization in freight

operations. Six-axle SDP-40F passenger use was preceded by previous 6-axle locomotive power such as the E-7, E-8, and E-9. Table 2-1 gives information on the SDP-40F and E-8 locomotives. The E-8 locomotive was compared with the SDP-40F during the Chessie Test series.

TABLE 2-1 LOCOMOTIVE DATA

<u>DESCRIPTION</u>	<u>SDP-40F</u>	<u>E-8</u>
Body Weight (lbs.)	295,700	239,400
Total Weight When Fully Loaded (lbs.)	395,000	345,000
Mass Moment of Inertia in		
(a) Yaw (in lb.-sec ²)	36 x 10 ⁶	17.3x10 ⁶
(b) Roll " " "	1.2 x 10 ⁶	1.94x10 ⁶
(c) Pitch " " "	36 x 10 ⁶	17.3x10 ⁶
C.G. Height Above Rails (in)	64	60.5
Truck Center Spacing (ft)	46	43
Length Over End Plates (ft)	68.17	68

The SDP-40F is equipped with two three-axle HTC trucks, each axle being powered by axle-mounted traction motors. The HTC trucks used in the SDP-40F are essentially the same as those used in the popular six-axle SD40-2 or SD45-2 freight locomotives. The main difference is that the SDP-40F is equipped with high-speed gearing for passenger service. For the E-8, only the lead axle and trailing axle of the truck are powered. The characteristics of the locomotive trucks are compared in greater detail in Table 2-2.

AMTRAK scheduled the SDP-40F locomotives into revenue service throughout the country when they were delivered during 1973 and 1974. During these initial years of service, several derailments occurred along with numerous complaints of poor ride quality. Between January 1974 and January 1976, the SDP-40F was involved in 14 derailments, each entailing injuries and property damages. The ride quality problem, coupled with safety considerations, led AMTRAK and General Motors - Electro-Motive Division (EMD) to conduct tests on the Illinois Central Gulf (ICG) Railroad. The FRA participated in the planning and observation of these tests.

TABLE 2-2 COMPARISON OF SDP-40F AND E-8 LOCOMOTIVE TRUCKS

	SDP-40 TRUCK (HT-C)	E-8 TRUCK
No. Wheels per Truck	6	6
Wheel Diameter	40"	36"
Truck Weight	54,600 lbs	52,500 (complete)
Axle Spacing	79-5/8" - 83-3/4"	Equal - 84-1/2"
Center Plate Location	Equidistant from ends; 1 1/4" outboard of truck center	Center of truck equi- distant from ends
Center Plate Diameter	28"	24" dia
Traction Motor/Gear Orientation	All gears on same side	gear on one side, 1 on other side
Adhesion Efficiency at 30% Adhesion	94.0%	
Brake	Truck Mounted	Truck Mounted
Frame Configuration	2 Inner Transoms, plus 1 End Transom forming U- shape frame; asymmetrical	2 Inner and End Tran- soms symmetrical closed frame
<u>Primary Suspension System:</u>		
No. and Type Springs over Each Journal Box	2 Double coil	Equalizer between mid- dle and end axles, 2 triple coils per equalizer (8 total)
Spring Rate/Box	6,846 lbs/in.	7,900 lb./in./coil
Spring Free Height	18-5/8"	12 7/8"
Vertical Snubbing	2 - 1200/400 lb/in. displacement hydraulic snubbers on center journal box only	None (some damping in secon- dary elliptical springs)
<u>Secondary Suspension System:</u>		
Bolster Support, Vertical	4 Elastomeric pads, 1 at each truck corner; compression rate 110,000 lbs./in. (Tested Configuration) 75,000 lbs./in. (Soft Configuration)	4 swing hangers, 4 elliptical leaf springs
Bolster Snubbers, Longitudinal	None	None
Total Axle Lateral Clearance in Journal Boxes	~3/8	3/8" - 9/16"
Longitudinal Clearance Between R.B. Driving Force Liners	~1/8"	~1/4"
Type of Pedestal Liner	Nylatron	?

2.2 RESTRICTIONS AND OTHER TESTS

The ICG tests were conducted in March and April 1976 on both tangent and curved track, with SDP-40F locomotives operated singly and in tandem.* Baseline runs were also made with an E-9 locomotive for comparison purposes. Lateral and vertical wheel loads, lateral/vertical load ratios, and carbody accelerations were measured. The test site tangent track was "marginal" class 5 jointed rail with unloaded alignment deviations of 3/4" and crosslevel deviations up to 1-1/8". The curved track test site track contained gage variations up to 7/8" and unloaded alignment deviations of 1-1/4".** These tests indicated that ride vibration for the SDP-40F at high speeds could be diminished by reducing secondary suspension stiffness. The tests did not detect any significant difference between SDP-40F wheel/rail forces and those of the E-8 locomotive. However, primarily as a result of the ICG test, AMTRAK and EMD proceeded with the modifications of secondary suspension on all 150 SDP-40F locomotives to improve ride quality.

During the winter of 1976-1977, three derailments of the SDP-40F powered trains occurred within a 1-1/2 month period. In one of the three derailments, the locomotive did not derail and in another the NTSB cited "weakened crosstie spikehole condition." In February 1977, the National Transportation Safety Board (NTSB) issued recommendations to the Administrator of the Federal Railroad Administration.*** The letter stated that at speeds above 48 mph on curves which exceeded 1-1/2 degrees of curvature, SDP-40F locomotives caused the outside rail to move laterally or to roll outward, thus widening the gage and allowing the locomotive (and following cars) to derail. The NTSB letter stated that the gage widens even though this particular six-axle locomotive did not appear to deviate from design

*ENSCO, Inc., Presentation of SDP-40F Test Results on June 3, 1976: AMTRAK, ENSCO, EMD, BATTELLE.

**W.R. Klinke and C.A. Swenson, "Tracking and Ride Performance of Electromotive 6-Axle Locomotives," in Railroad Engineering Conference, Pueblo, October 1976, Proceedings: "Railroading Challenges in America's 3rd Century, Improved Reliability and Safety," pp. 106-108, FRA/ORD-77/13.

***National Transportation Safety Board, Safety Recommendation R-77-1 and 2, Issued February 3, 1977; revised April 4, 1977.

standards and the track involved complied with Federal Track Safety Standards for the authorized speeds.

The NTSB recommendations to FRA were as follows:

Investigate immediately the interaction between SDP-40F--locomotives of passenger trains and train conditions to determine the causes for the widening of the track gage and act to correct the causes. (Class I, Urgent Follow-Up, R77-1)

Until such investigation and corrections are completed, restrict passenger trains with SDP-40F--locomotives to speeds that will permit safe operation around curves of one degree, 30 minutes or more on Class 4 or less track. The speeds should not exceed the equilibrium speed on such curves. (Class I, Urgent Follow-Up, R77-2)

Responding to NTSB's recommendations and to the FRA Office of Safety, AMTRAK issued orders to generally restrict the speed of the SDP-40F locomotives to 40 mph on curves of two degrees or more. While railroads meeting certain criteria are exempted from the restriction, some railroads have actually imposed even more stringent speed restrictions on the SDP-40F.

With these restrictions in effect, AAR, AMTRAK and EMD performed a series of tests on the Burlington Northern (BN) Railroad in March 1977. These tests were intended to pinpoint a "trigger" mechanism, or underlying cause of SDP-40F locomotive derailments, and to determine whether the "slow" order that BN had placed on this locomotive was justified. Two SDP-40F locomotives and a baggage car were instrumented. A variety of measurements was made on vehicle dynamics, wheel/rail force, and track geometry under simulated revenue service. Based on this data, specific sites were selected over which runs were made at various speeds. Limited baseline comparison runs were made using an F40-PH locomotive for both over-the-road and selected-site runs. The test data are now being reduced and analyzed by the AAR.

2.3 THE CHESSIE TEST

The Chessie Test described in this report was designed to provide a broader base of experimental information on the SDP-40F dynamic characteristics. The previous testing and operating experience with the SDP-40F indicated that

problems might exist in one or more of the five following areas:

1. locomotive/track interaction;
2. baggage car/track interaction;
3. locomotive/baggage car/track interaction;
4. low temperature characteristics of the locomotive and/or track; and
5. poor track conditions

The Chessie Test was designed to obtain greater insight into the first three of these areas. A team of participants was organized, with the FRA and the AAR jointly leading the planning and conducting of the test. AMTRAK and the Chessie System provided the railroad equipment and trackage, with EMD, AAR, ENSCO and Battelle providing the test instrumentation. Post-test data analysis was led by the Transportation Systems Center, with support from Arthur D. Little (ADL), ENSCO and Battelle.

Conducted from June 8 to June 25, 1977, the Chessie Test included an initial site-selection run of two instrumented consists over 600 miles of track between Huntington, W.VA, and Charlottesville, VA, and repeated runs of different speeds within a four-mile zone.

2.4 TEST OBJECTIVES

The overall goal of the Chessie Test program is to develop a technically sound basis for evaluating the dynamics of locomotives in order to assure that an appropriate level of safety is maintained. In support of this goal, the following four objectives were established for the test and the subsequent data analysis:

1. To compare the dynamic performance (safety-related effects--wheel/rail forces, carbody accelerations, etc.) of the SDP-40F locomotive with the E-8, a baseline six-axle locomotive which has a general history of safe operation, in order to determine the range of operating conditions under which dynamic responses of the two locomotives differ significantly.
2. To identify key track-geometry and operational parameters of these locomotives and determine empirical relationships between these parameters and locomotive dynamic performance. This information will be used to establish track maintenance and vehicle operating

requirements for improving locomotive dynamic responses.

3. To determine the sensitivity of the dynamic performance of the SDP-40F to variations in selected truck configurational parameters, simulating the effects of component wear and varied maintenance practices. Such information would establish a basis for vehicle maintenance and inspection requirements and for improvements of those equipment components that appear to be significant factors in derailment.
4. To generate substantive data and findings which will help both government and industry to develop guidelines for acceptable levels of safety in new locomotive designs. Such guidelines would accommodate the full range of operational situations which would be encountered during the life of the locomotive.

3. TEST DESCRIPTION

Highlights

- Separate but similar SDP-40F and E-8 consists were tested on the Chessie System under a variety of identical conditions typical of AMTRAK operations - in order to identify significant differences in dynamic responses.
- Dynamic response measurements over several hundred miles of track were made on each consist over a wide range of track conditions which were quantified by the DOT track-geometry measurement cars.
- In addition to the onboard measurements, concurrent wayside force data was collected at a carefully selected location where the range of the many variables in speed and operating modes was covered for both consists.
- Several maintenance states were simulated and tested for the SDP-40F.
- The onboard wheel/rail force measurements were made on the leading wheels of the trailing truck of the last locomotive of both consists.
- Additional measurements included vertical and lateral accelerations, braking status, coupler orientations and loads, and exact track locations.
- Ride quality measurements were also made on the SDP-40F baggage car.
- All pertinent locomotive and consist conditions were assessed and recorded prior to the test runs.
- Most data were recorded and are preserved on magnetic tape as part of a data bank which is available for future analyses.

3.1 TEST CONSISTS AND VEHICLE INSTRUMENTATION

Two test consists which were intended to be as identical as possible were used during the Chessie Test, one powered by two SDP-40F locomotives and the other by two E-8

locomotives. The SDP-40F consist is shown in Figure 3-1, and the E-8 consist is shown in Figure 3-2.

SDP-40F Test Consist

An SDP-40F test consist was assembled and tested on the BN during April and May of 1977. After the BN test was completed, the SDP-40F consist moved to the Chesapeake and Ohio at Huntington, W.VA, where it was reassembled in the same configuration as that used in the BN test. The consist make-up is shown in Figure 3-3. The SDP-40F's used in the tests were obtained from operational service. They had not yet been retrofitted with the softer rubber bolster springs and stiffer vertical shock absorbers which were being installed on later versions of this locomotive.

Locomotive instrumentation was installed in the trailing unit. A strain-gaged wheelset was placed on the leading axle of the trailing truck of the trailing locomotive, axle No. 10. Only a single wheelset was instrumented due to limitations of time and funds. The choice of the axle to be instrumented was based on two considerations:

1. The trailing truck of the trailing locomotive was the truck most often involved in the SDP-40F derailments (see Appendix A for further details).
2. The lead axle of a truck usually experienced the highest lateral loads.

The following data was collected:

- Vertical and lateral wheel forces on both wheels of axle No. 10.
- Vertical and lateral carbody accelerations at both ends of the locomotive and baggage car.
- Truck-to-bolster lateral displacement of both trucks of the locomotive and baggage car.
- Truck-to-carbody yaw angle of locomotive trailing truck and baggage car leading truck.
- Baggage car suspension.
- Locomotive axle-to-truck frame vertical motion (at middle axle of each truck on each side)
- Coupler load (longitudinal, vertical and lateral)



FIGURE 3-1 SDP-40F TEST CONSIST

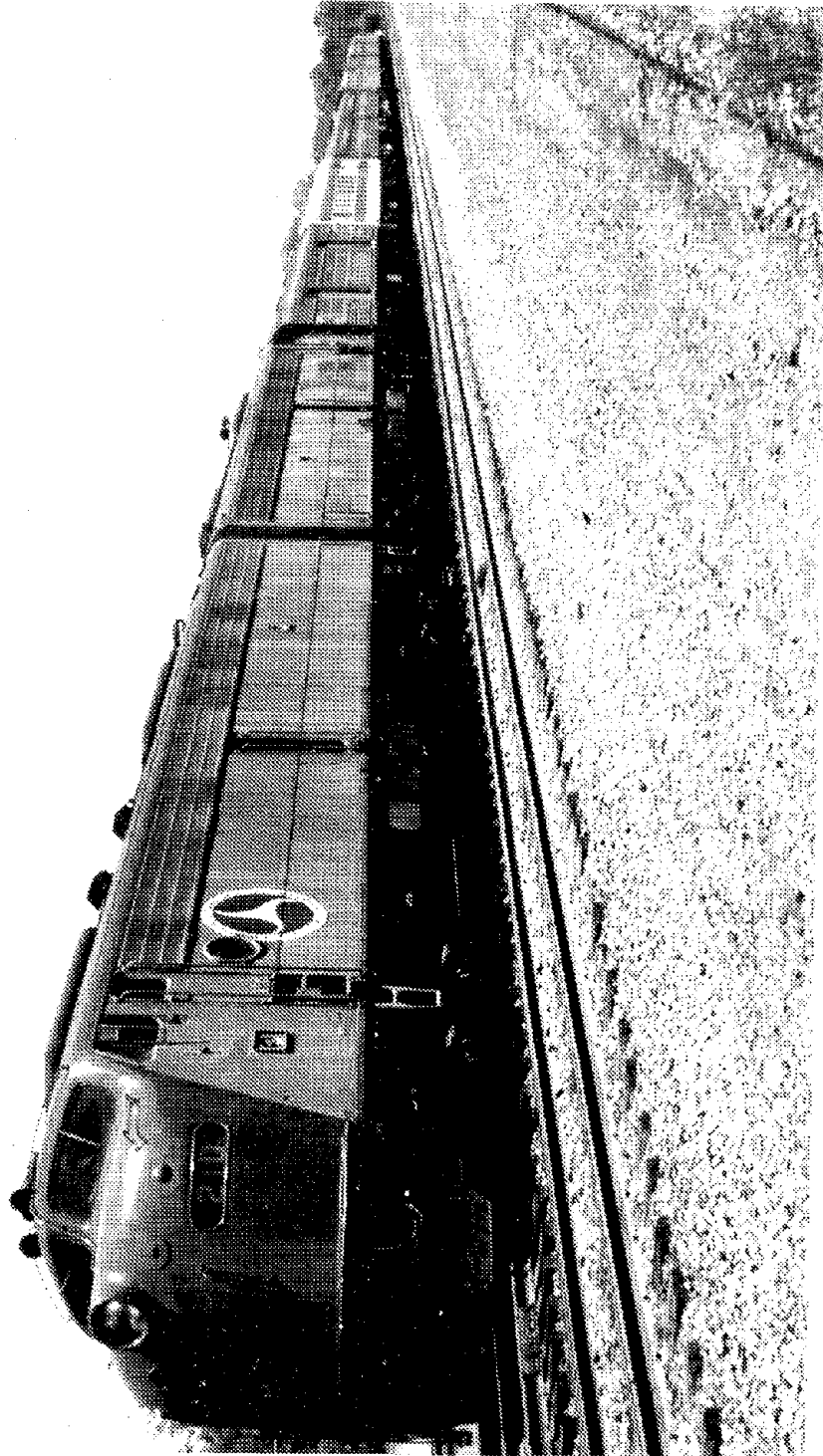
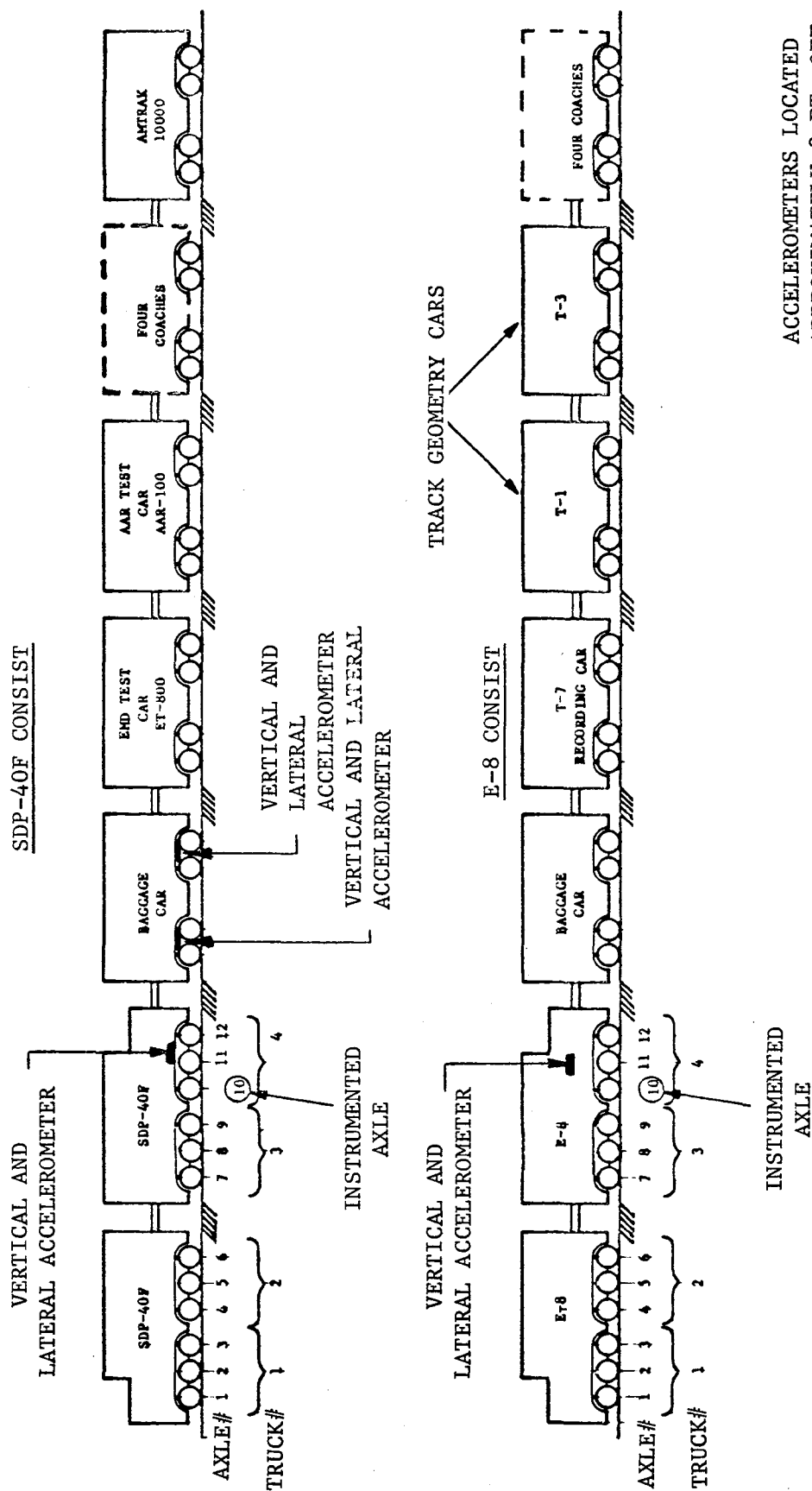


FIGURE 3-2 E-8 TEST CONSIST

TEST DIRECTION (WEST)



ACCELEROMETERS LOCATED
APPROXIMATELY 2 FT. OFF
THE LONGITUDINAL CENTERLINE
OF CARS.

FIGURE 3-3 SDP-40F AND E-8 TEST CONSISTS

- Coupler angle (horizontal)
- Throttle position
- Braking status (independent brake pipe, automatic brake pipe and locomotive brake cylinder)
- Dynamic gage (installed next to the instrumented wheelset)

The instrumented wheelset used a wheel surface gage pattern for lateral load sensing and a gage pattern in four holes drilled into the wheel plate for vertical force sensing. The SDP-40F instrumented wheelset had been trued prior to the BN test and had accumulated approximately 7,000 miles before the Chessie Test began. The signal processing for vertical forces used peak detection and a sample-and-hold procedure at each 1/4 revolution of the wheel. The strain gages were arranged to provide an approximately continuous modulated sine and cosine signal for lateral forces. A continuous lateral force signal is approximated by taking the square root of the sum of the squares of the two signals. The vertical and lateral force information from wheelset #10 is obtained from the rotating system through sliprings and was recorded in real time on strip charts and magnetic tape.

The baggage car in the SDP-40F consist was instrumented to measure and record lateral and vertical carbody accelerations. The baggage car was loaded with 21,000 pounds of bagged sand in equal piles over the two trucks to simulate a typical load.

The EMD test car, ET-800, was equipped with two six-channel Brush recorders and two 16-channel Honeywell visi-corders for displaying data on strip charts. No permanent magnetic tape recording was done on the ET-800.

The AAR test car, AAR-100, was equipped with two Brush strip chart recorders for real-time data display. Information on data channels cabled from the ET-800 was recorded on magnetic tape by an onboard computer (Eclipse S-200). Digital sampling was at 250 samples per second. Prior to sampling, the data was filtered at 100 Hz.

E-8 Test Consist

The E-8 consist and its instrumentation was modeled after the SDP-40F test consist. Due to the tight schedule, the

instrumentation installed on the E-8 locomotive measured only wheel/rail forces and carbody accelerations. The design of the wheelset instrumentation for the E-8 was similar to that of the SDP-40F in order to facilitate comparisons. The E-8 test consist is shown in Figure 3-3.

The lead E-8 locomotive unit was provided by the Transportation Safety Institute of the Department of Transportation. Locomotive instrumentation was installed in the trailing locomotive provided by AMTRAK. The instrumented wheelset was placed in axle position No. 10 of the consist, as it had been in the SDP-40F test consist. Locomotive instrumentation was installed in the trailing unit. Measurements were made of:

- Lateral and vertical wheel forces on both wheels of axle No. 10, and
- Carbody acceleration (vertical, lateral and longitudinal at both ends of the locomotive).

The instrumented wheelset employed the same strain gage pattern design as the EMD wheelset used in the SDP-40F. This wheelset was a new wheelset at the beginning of the Chessie Test. Raw strain gage bridge signals were recorded to preserve the direction of the lateral force through all later data processing.

The baggage car was of the same type as the one used in the SDP-40F consist. Snubbers on the baggage car were not used in either E-8 or SDP-40F consists. Sandbags were used in the baggage car for load simulation as they had been in the baggage car of the SDP-40F consist. Because of time limitations, no instrumentation was installed on the baggage car in the E-8 consist. Periodic visual observations of baggage car motion were made.

FRA Test Car T-7 was equipped with electronic equipment to condition signals coming from the locomotive and from the track geometry car T-3. A wheel-signal processor was installed to convert strain gage outputs to wheel forces and lateral/vertical force ratios. A Hewlett-Packard HP-2100 minicomputer installed in the T-7 was used in the recording of data on digital magnetic tape. A sampling rate of 250 Hz was used, which was consistent with the rate used by the AAR. Filtering was provided on all channels by filters having a corner frequency of 100 Hz. Carbody acceleration channels were filtered at 10 Hz. Three six-channel Brush recorders were used in the T-7 to display the vehicle

dynamic and the track geometry data. These charts were used for site selection and in preliminary post-test analysis. An interior view of the ET-800 car is shown in Figure 3-4.

Track geometry car T-3 was operated in its standard track inspection configuration. One eight-channel and two six-channel Brush recorders were used to display distance-based charts: one for the FRA file, one for the FRA Office of Safety and one for the C&O engineers. An onboard, Raytheon 704 minicomputer was used to process the test geometry sensor signals and to record the data on digital magnetic tape. The track-geometry parameters measured by the T-3 include:

- Rail profile of left and right rails (measured by a 62-foot midchord offset)
- Gage (measured by a servo magnetic system with a capacitive system as back-up)
- Crosslevel, i.e., superelevation (measured by a compensated accelerometer system)
- Track curvature (measured by an inertially-based curvature system in degrees per hundred feet)
- Track location and location targets (measured by a capacitive automatic location detector)
- Speed

The geometry measurements obtained included whatever rail deflections occurred under T-3 dynamic loadings. The size of these deflections is unknown.

3.2 SITE SELECTION

The initial test plan included a survey run by both consists over representative operational track. Track geometry data collected from earlier surveys on the Chessie System were used as the basis for choosing the route of these survey runs. The criteria for selecting the route of the survey runs were:

1. Substantial stretches of Class 3 track to ensure adequate excitation of locomotive dynamic response; and

Reproduced from
best available copy.

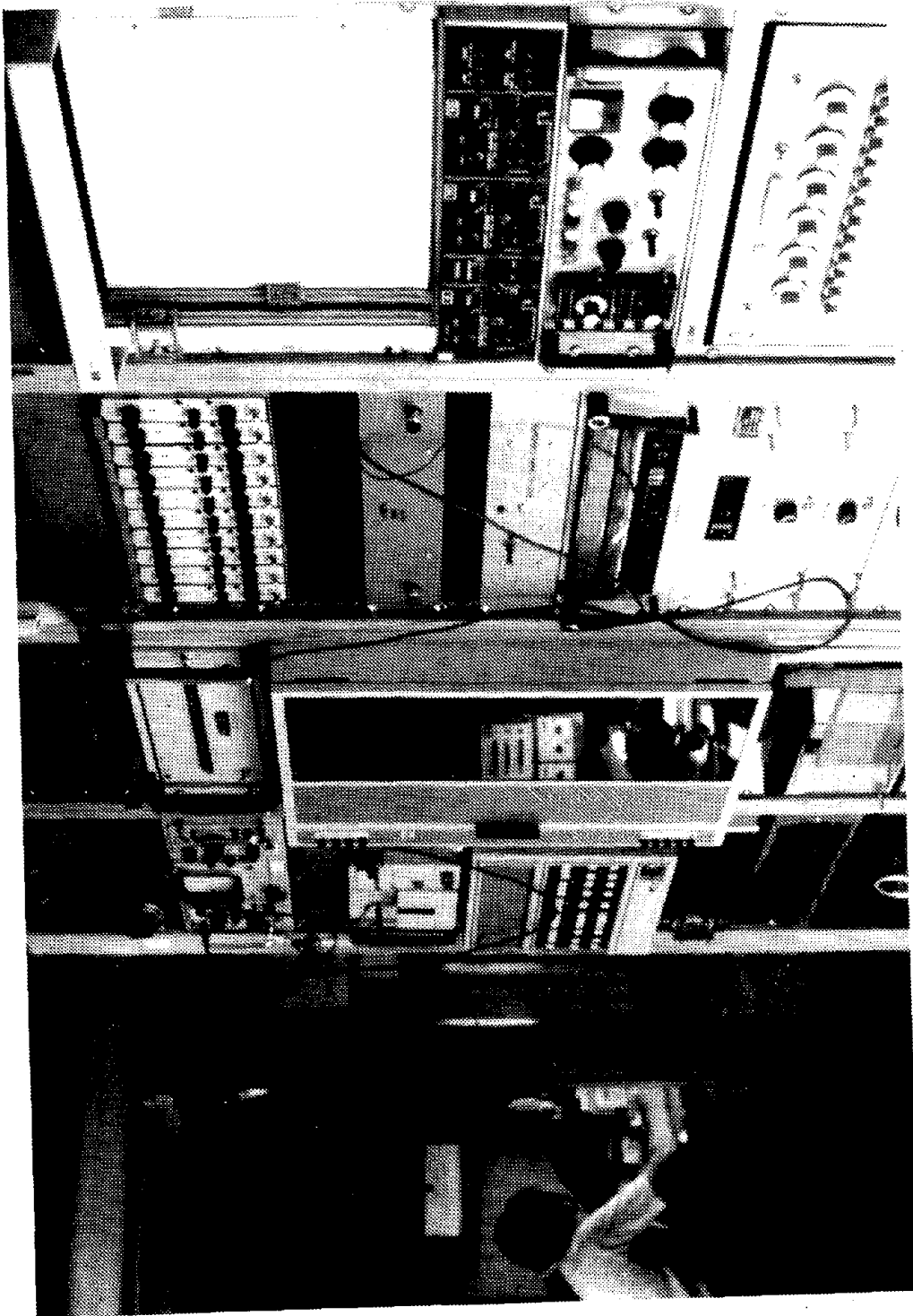


FIGURE 3-4 INTERIOR VIEW OF EMD'S ET-800 CAR

2. Frequent track curvature in the range of 2° to 3° , representative of conditions existing at several SDP-40F derailment sites (see Appendix A).

The route of the survey run is shown in Figure 3-5.

The test plan also called for repeated test runs over a more restricted test zone which was to include an instrumented track site. The data obtained on the survey runs were used to select the test zone. The selection criteria for the test zone were:

1. Track curvature of 2° to 3° , representative of conditions existing at several SDP-40F derailment sites;
2. Evidence of substantial locomotive dynamic response during survey runs; and
3. Acceptable track grades.

The test zone selected is illustrated in Figure 3-6. Figure 3-7 gives a track chart of the test zone. The rails in the test zone are jointed and staggered at approximately a half rail length. This four-mile section, according to measured data, satisfies at least FRA Class 3 track standards. Class 3 permits a maximum speed of 60 mph for passenger trains and 40 mph for freight trains. Going westbound, the ascending grade starts from MP 253 and attains a maximum grade of 1.51% at MP 255, gradually leveling out at MP 257. There are two curves in the one-mile segment between MP 257 and 258. The first is a right-hand curve (westbound) starting at MP 257.2. A tie marker indicates the curve as being $2^{\circ}38'$ with $4\frac{1}{2}"$ superelevation. This curve is followed by a short tangent segment and then a left-hand curve at about MP 257.5. This curve is marked as being $2^{\circ}06'$ with a $2\frac{1}{2}"$ superelevation.

Analysis of the site selection data led to the identification of 31 potential sites. This list was reduced by eliminating sites based on the criteria listed below:

Poor accessibility

Curvature too great or too small

No E-8 data

Low lateral forces

5. TEST RESULTS

Highlights

- Differences in dynamic response exist between the SDP-40F and previously operated E-8 consists under identical operating and track conditions.
- The maximum measured SDP-40F lateral loads are not due to a discrete single cause but rather are the result of a probabilistic event in which combinations of factors occur on top of basic lateral force characteristics which at times are higher than those of the E-8 consist.
- A predictive capability was developed which was used to quantify the degree of sensitivity of the SDP-40F and E-8 dynamic behavior in curves to track variations and speed.
- Operating factors such as sanding can significantly increase axle lateral forces, while rail lubrication appears to substantially reduce these forces.
- Operation above balance speed can produce significant lateral track forces for the SDP-40F.
- Variations in wheel diameter, axle shimming, and coupler vertical alignment can significantly influence the dynamic performance of the typical AMTRAK SDP-40F train consists.
- Configuration changes can improve the dynamic performance of the SDP-40F as demonstrated by the heavy shock tests.
- Track irregularities which were found to have the greatest influence on lateral loads were deviations in curvature, and rapid variations in gage due to local alignment deviations at high rail joints.
- There are good grounds for establishing guidelines for equipment dynamic performance testing and evaluations (under known and standard conditions) prior to routine use in passenger service.
- It is feasible to design and construct a calibrated test track for the a priori determination of vehicle performance.

The test results presented in this section contain only a portion of the total data collected. The analysis of test results concentrated on the data that was thought to be most applicable to the understanding of the SDP-40F dynamic characteristics in curves of 2° to 3°, and in particular, the dynamic behavior of the trailing truck of the trailing locomotive. This priority of analyses of the test results was based on the analyses of the SDP-40F derailments outlined in Appendix A.

The test results are presented in three categories:

1. Dynamic Response of Baseline Locomotive Configurations,
2. Effects of SDP-40F Configuration Changes, and
3. Baggage Car/Locomotive Interaction.

5.1 DYNAMIC RESPONSE OF BASELINE LOCOMOTIVE CONFIGURATIONS

The results of tests for which the locomotives and consists were in their nominal, or "baseline", configuration will be presented first. The primary variables during these tests were:

1. Speed,
2. Track geometry,
3. Rail surface condition, and
4. Locomotive operating mode.

5.1.1 Effect of Speed

In order to better understand the influence of speed on the dynamic response of the two locomotives, a series of runs was made at various speeds through the test zone under fixed locomotive operating modes. The influence of speed on the lateral loads occurring on individual wheels at the instrumented test site will be described first, followed by the findings on total truck lateral loads. A discussion of the analysis results of the survey run data and repeat run data for the instrumented axle (axle 10) completes this section.

Wheel Loads (Instrumented Site)

Since it is very difficult to compare lateral loads of the various wheels using the data in the form of continuous time histories, some more compact means had to be found. One approach which proved to be effective was to compare the maximum lateral loads measured at the test site using the wayside instrumentation. Appendix G describes how this data was corrected for instrumentation "cross talk" and how the resulting wayside loads measurement compared with the onboard data. At the instrumented site, at the higher speeds the maximum single-wheel lateral forces usually occurred at the first gage location past the joint, as shown for axle #10 in Figure 5-1. At lower speeds, these maximums occurred farther down the rail from the joint. However, in all cases, the maximum axle forces occurred within 1/4 rail length after the joint. This is not a unique property of the test site, as can be seen from Figure 5-2, in which there is a clear relationship between the peak loads and the maximum gage variations which occur at each joint.

The maximum values of lateral wheel loads occurring at the instrumented site have been summarized in the next three figures for all axles. For the E-8, the lead axle of the trailing truck of the trailing locomotive (axle 10) typically develops the highest maximum value of lateral force for all the lead axles at all speeds except 60 mph, as shown in Figure 5-3. For the SDP-40F, axle 10 is the lowest responding lead axle over much of the speed range, as shown in Figure 5-4. The maximum lateral load for the SDP-40F was usually produced by axle 7, the lead axle of the leading truck of the trailing locomotive. This difference in the relative severity of axle 10 forces is important to note since, other than at the test site, all comparisons between the axle forces of the E-8 and SDP-40F must be based on axle 10, the instrumented axle. It may also be seen from the figures that the curves for $(L/V)_{\max}$ and L_{\max} tend to have the same characteristic shape as a function of speed. This trend occurred on all axles. In Figure 5-5, a comparison of the range of lateral loads of all lead axles is presented. The highest lateral load for the E-8 lead axles (typically axle #10) and the highest lateral load for the SDP-40F leading axles (typically axle #7) generally have comparable force levels below about 45 mph. Above this speed, the E-8 maximum lead axle lateral loads tend to level off, while the SDP-40F loads continue to increase, becoming 33% greater than the E-8 loads at 60 mph.

Figures 5-6A through 5-6D compare the corresponding axle loads of the E-8 and SDP-40F for each lead axle in each

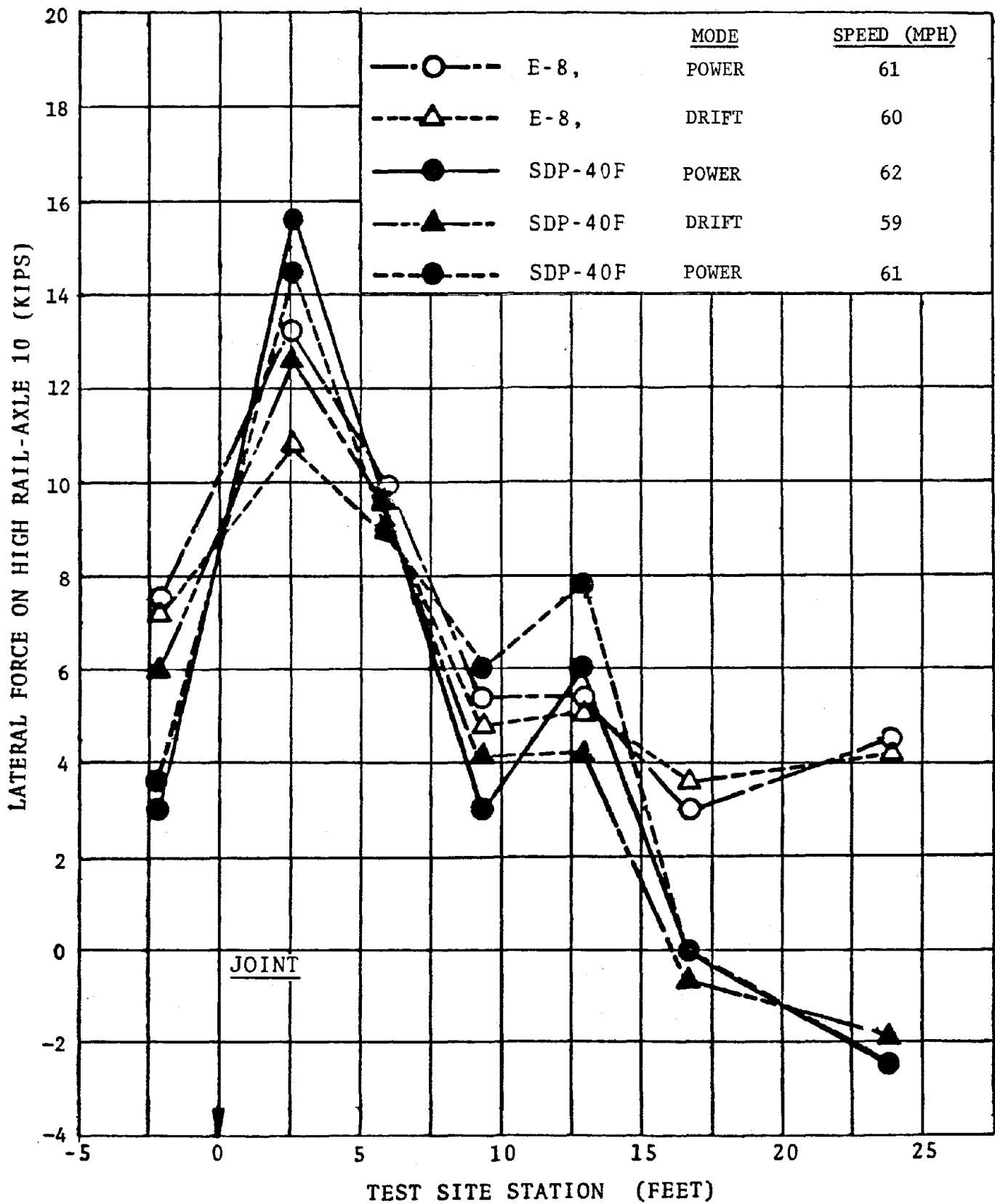
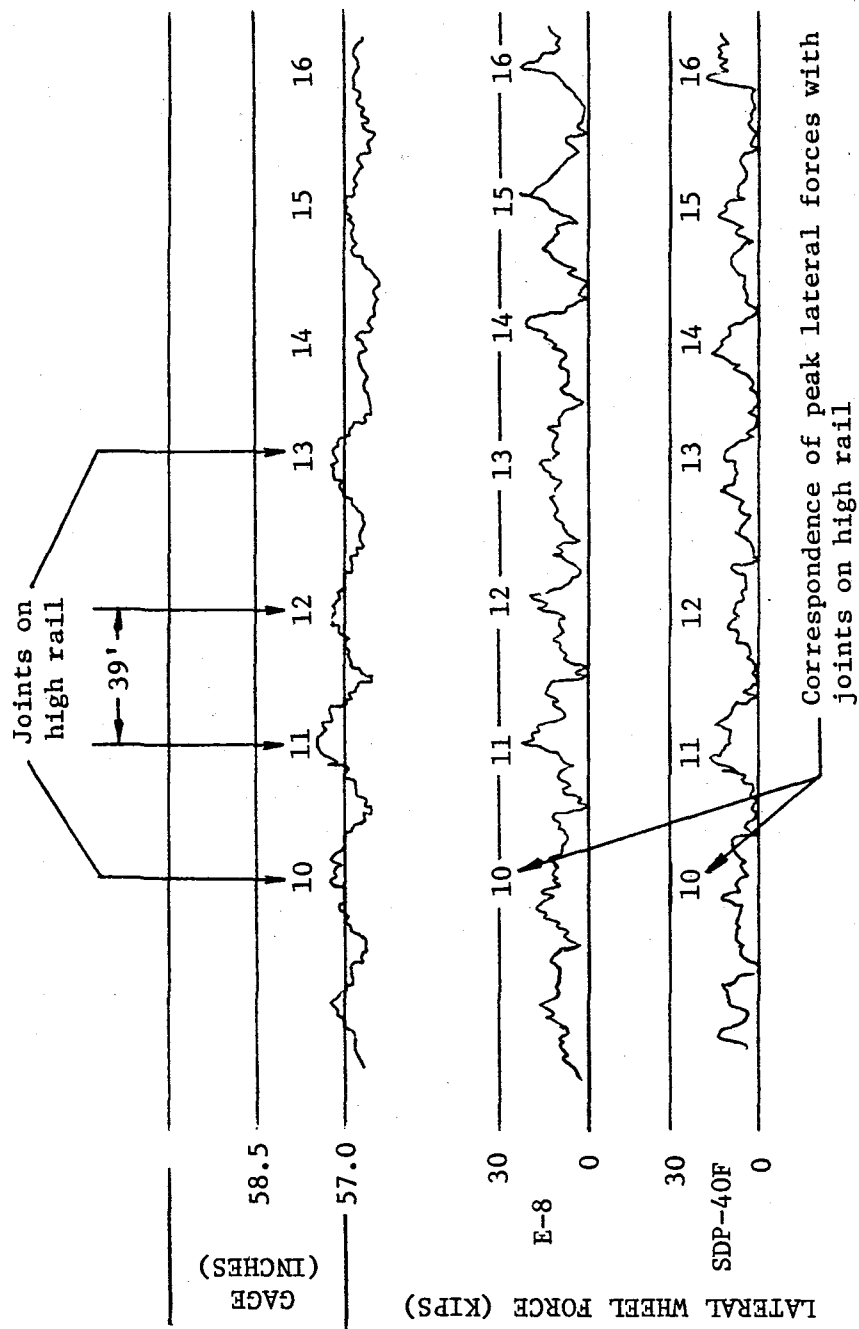


FIGURE 5-1 COMPARISON OF E-8 AND SDP-40F AXLE 10 LATERAL FORCE TRACES UNDER POWER AND DRIFT NEAR 60 MPH (WAYSIDE DATA)



Note: Numbered points correspond to joint locations.

FIGURE 5-2 TYPICAL E-8 AND SDP-40F LATERAL FORCE AND GAGE TRACES AT 60 MPH

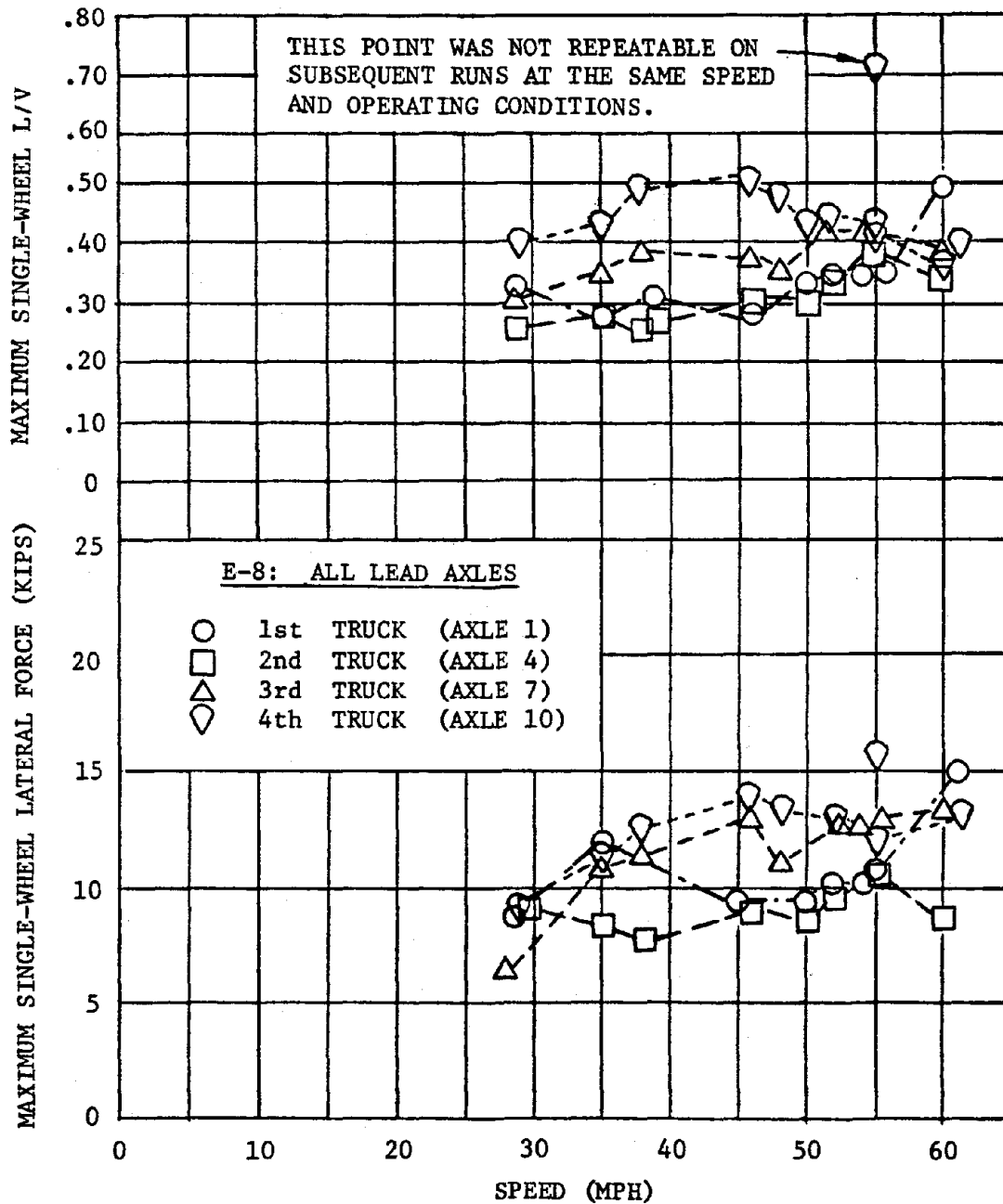


FIGURE 5-3 MAXIMUM SINGLE-WHEEL LATERAL FORCE
AND L/V VERSUS SPEED FOR LEAD AXLE IN EACH TRUCK
OF THE E-8 CONSIST (BASELINE RUNS, WAYSIDE DATA)

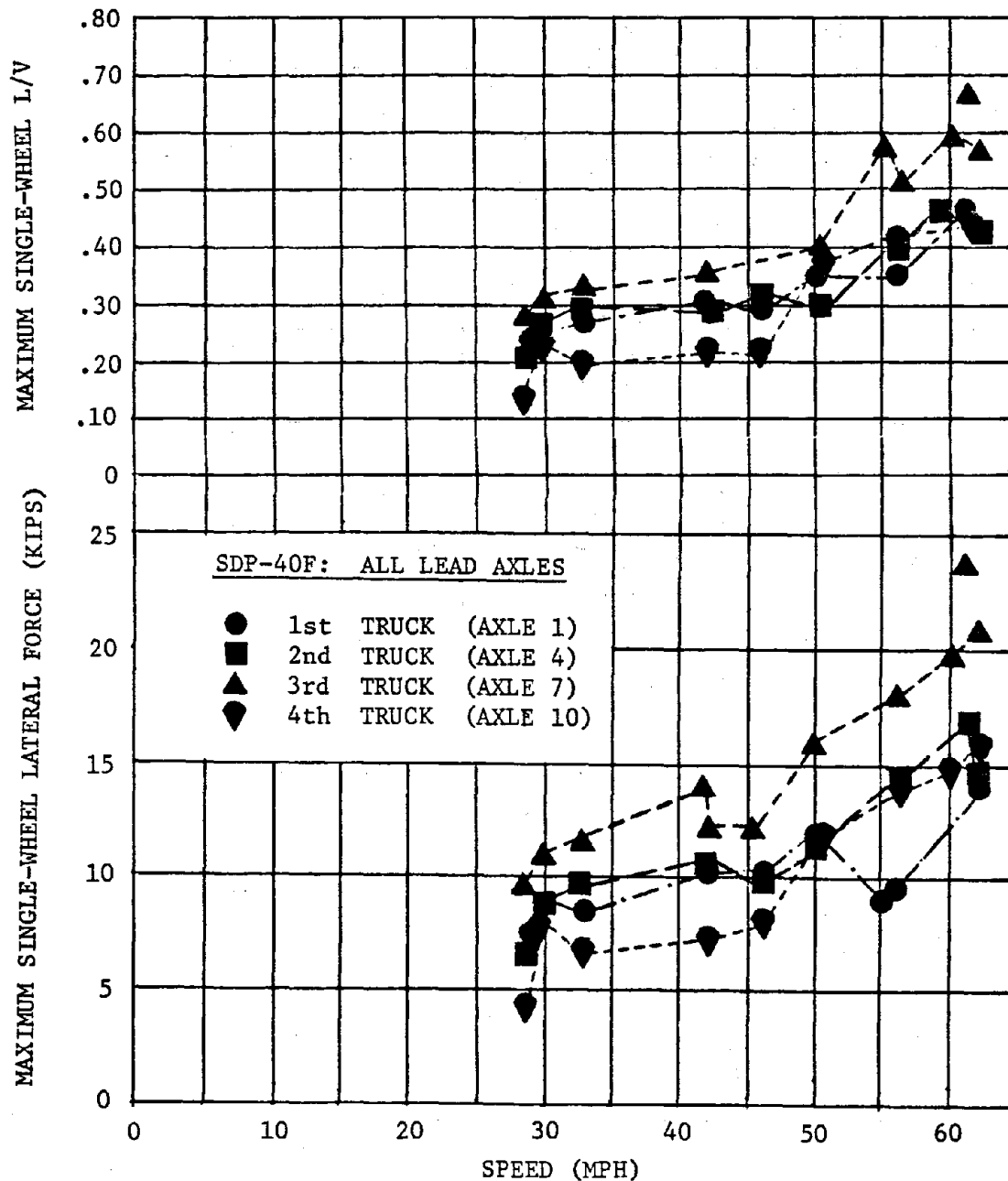


FIGURE 5-4 MAXIMUM SINGLE-WHEEL LATERAL FORCE AND L/V VERSUS SPEED FOR LEAD AXLE IN EACH TRUCK OF THE SDP-40F CONSIST (BASELINE RUNS, WAYSIDE DATA)

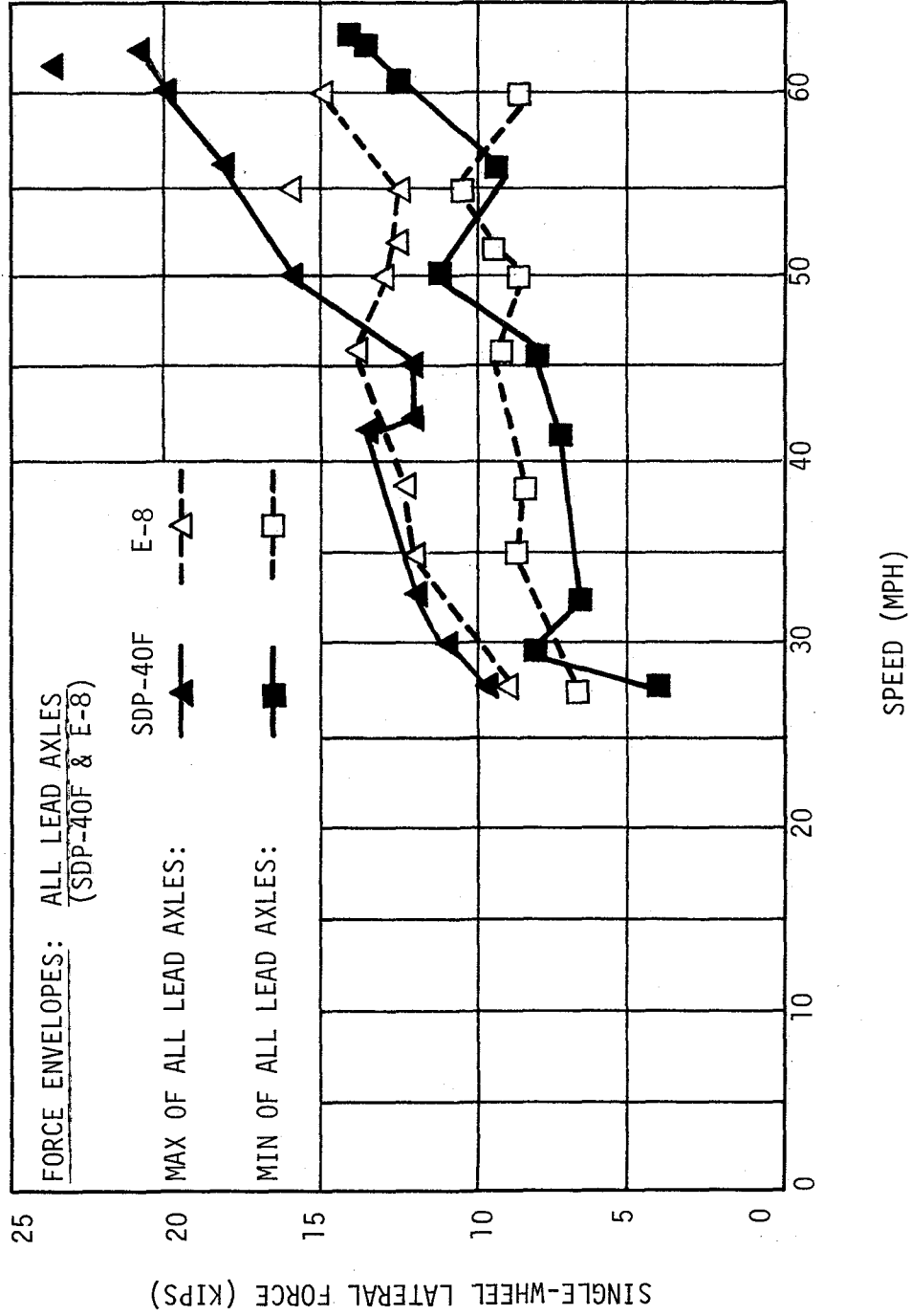


FIGURE 5-5 COMPARISON OF E-8 AND SDP-40F LATERAL FORCE ENVELOPES FOR ALL LEAD AXLES VERSUS SPEED (BASELINE RUNS, WAYSIDE DATA)

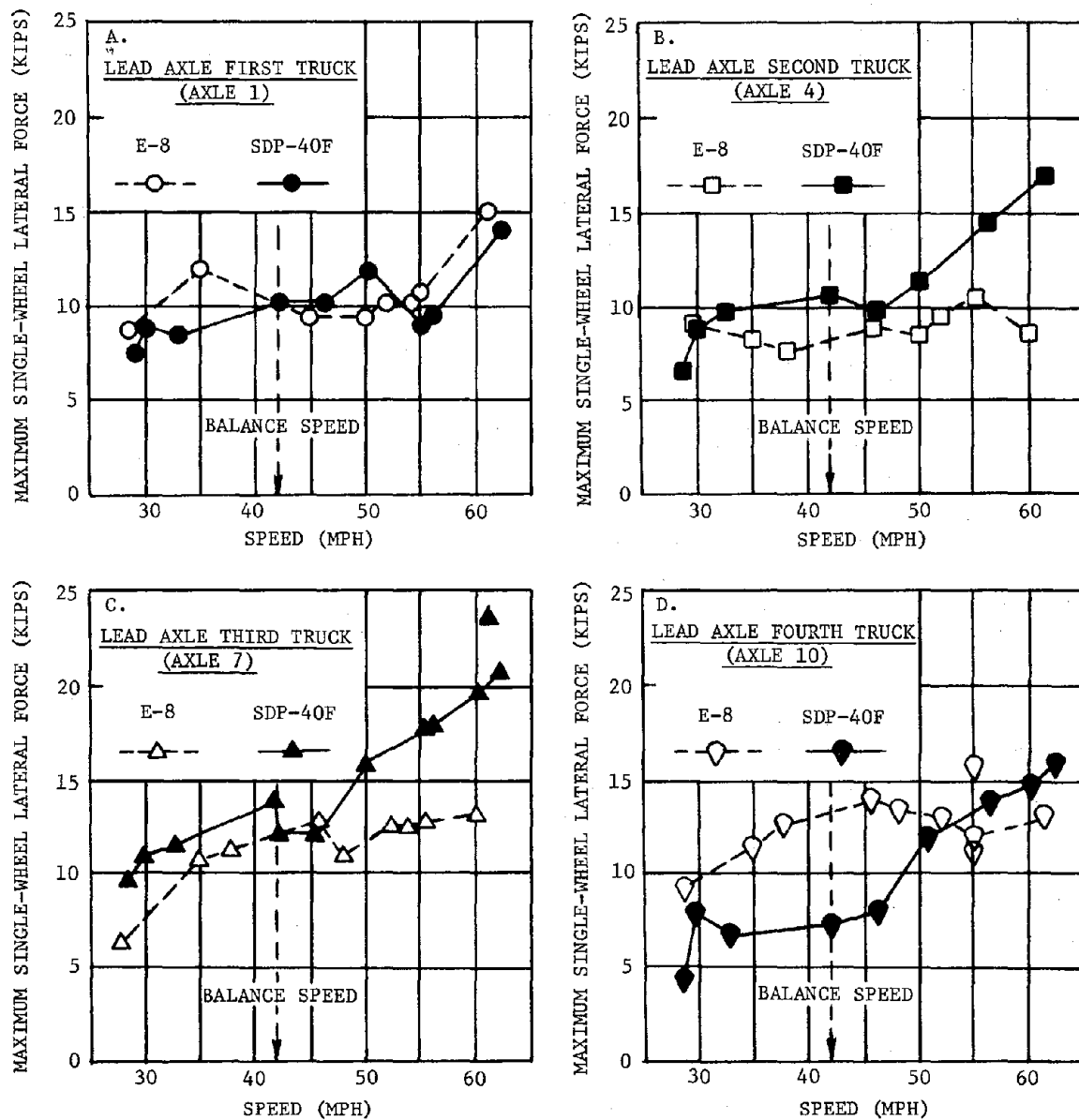


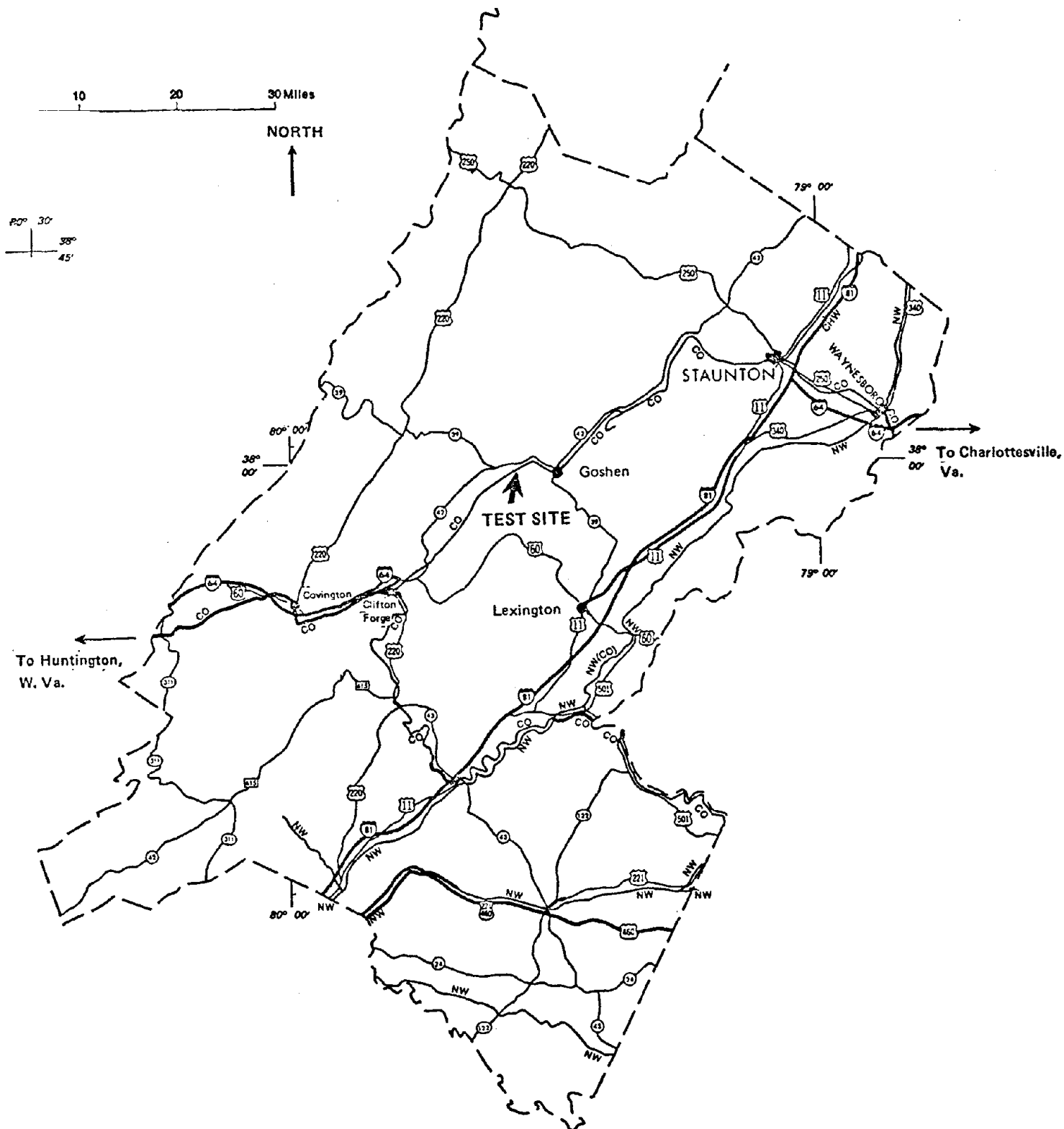
FIGURE 5-6 COMPARISON OF E-8 AND SDP-40F MAXIMUM SINGLE-WHEEL LATERAL FORCE VERSUS SPEED FOR EACH LEAD AXLE (BASELINE RUNS, WAYSIDE DATA)

truck at the instrumented test site. These figures indicate what appears to be a major difference in the lateral force versus speed characteristics of the E-8 and SDP-40F lead axle responses. Except for axle 1 (which behaves almost identically for the two locomotives), each of the remaining lead axles of the E-8 and SDP-40F consists appears to exhibit the following characteristic difference in response between the two locomotives:

1. Below balance speed, the SDP-40F lead axle lateral forces tend to remain relatively flat, and are either comparable to or less than those of the E-8.
2. Above balance speed, the E-8 lead axle lateral forces tend to level off while those of the SDP-40F start to increase rapidly, resulting in significantly higher forces for the SDP-40F somewhere above balance speed.

That this characteristic difference is in fact related to balance speed rather than absolute speed will be demonstrated later on in this section using the data from the instrumented axle. One additional point to note from Figures 5-5 and 5-6 is that, while the SDP-40F axle 10 lateral forces are much lower than those of the E-8 below balance speed, and are only marginally higher at 60 mph, this is not the case when the maximum SDP-40F lead axle loads are compared with those of the E-8. As was shown in Figure 5-5, these SDP-40F loads are almost identical with the E-8 maximum loads below balance speed, and begin to grow considerably greater than the E-8 loads once above this speed. This point should be kept in mind when later comparisons are made between the E-8 and SDP-40F based upon the onboard data from axle 10.

The spatial distribution of lateral force at the instrumented test site for axle 11, the middle axle of the trailing truck is shown in Figure 5-7. The E-8 lateral loads tend to have a relatively flat spatial response, while the SDP-40F response is similar to its axle 10 response, i.e., high force just past the joint and gradual moderation with distance from the joint. A comparison of the axle 11 response versus speed in Figure 5-8 shows that the maximum lateral force on axle 11 for the SDP-40F is greater than the corresponding E-8 maximum lateral force throughout the entire speed range. There is a significant difference in the relative behavior of the axle 10 and axle 11 loads as speed increases. The maximum axle 11 lateral force for the E-8 has a flat distribution. The lateral loads on axle 11



Source: United States Transportation Zone Maps, Office of Policy and Program Development, FRA; Zone 190, Staunton, Va.

FIGURE 3-5 SDP-40F TEST SITE ON CHESSIE SYSTEM



FIGURE 3-6 PARTIAL VIEW OF TEST ZONE

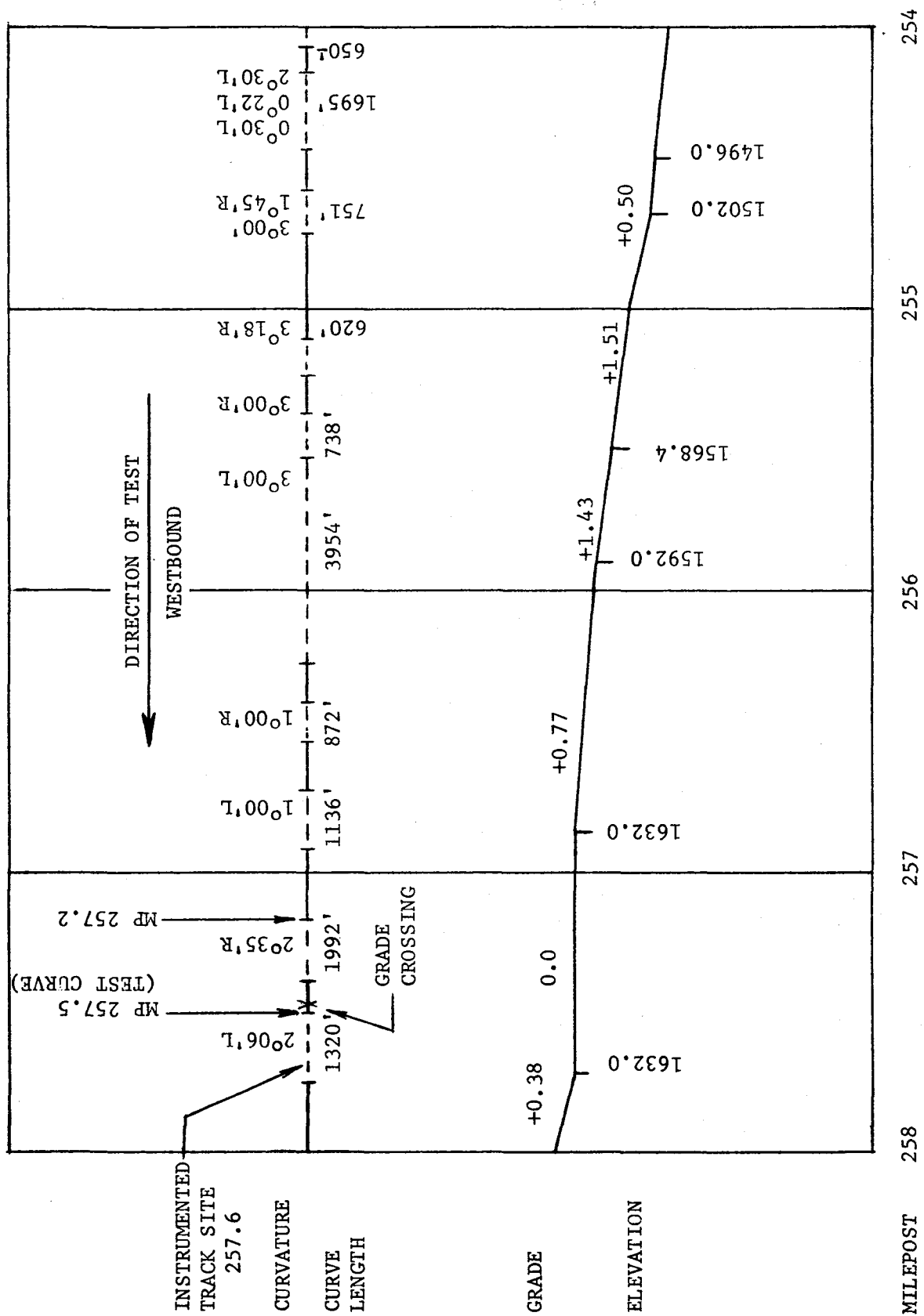


FIGURE 3-7 TRACK CHART OF 4 - MILE TEST ZONE
CHESSIE SYSTEM
CLIFTON FORGE DIVISION

Little difference in force

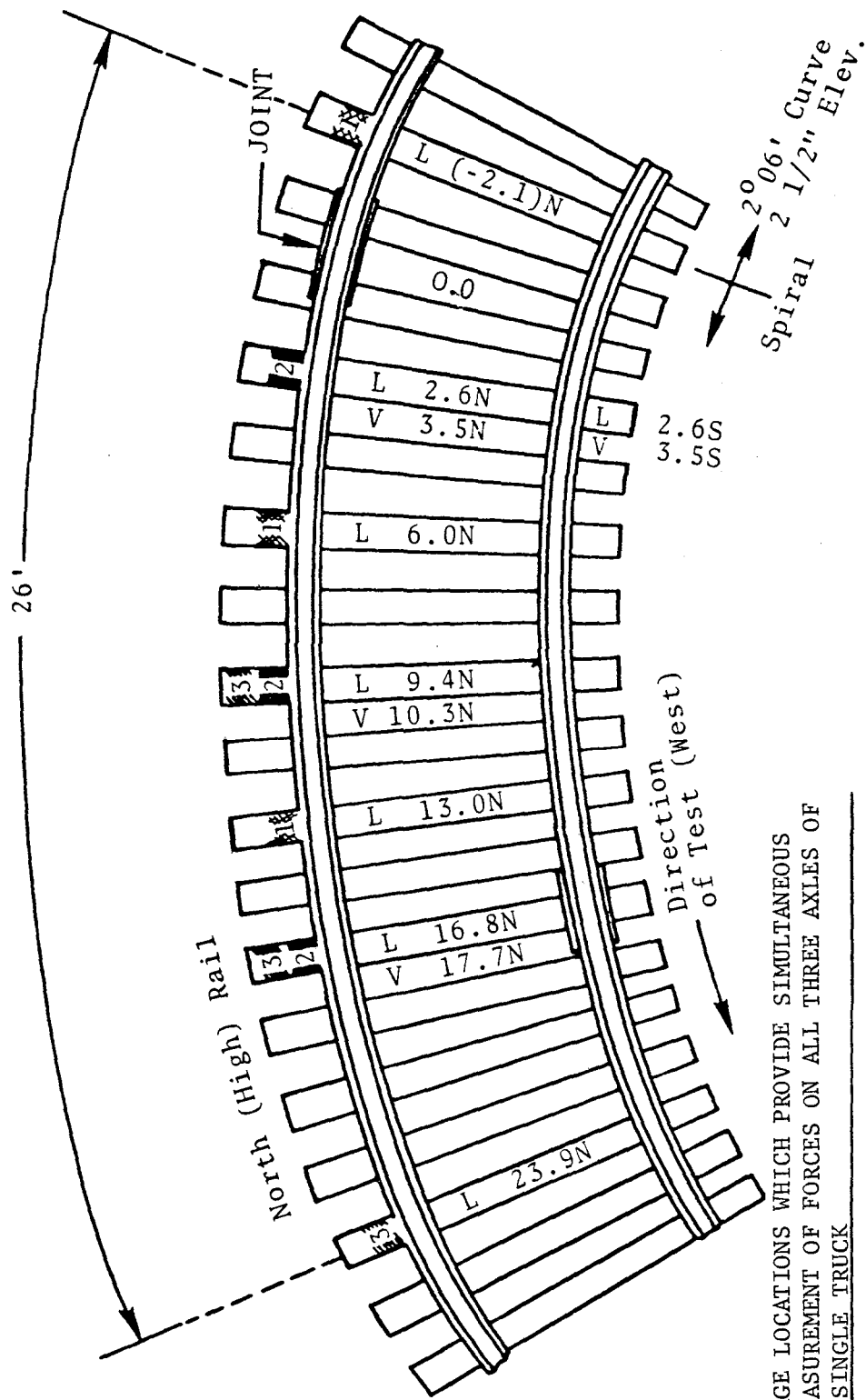
High speeds not attainable due to maintenance

The process of elimination thus left the 2°06' curve at Milepost 257.5.

The track at the selected test site was laid in 1945 with 131 lb. rail, 8" x 13" tie plates, 2 rail holding spikes/plate, 22 ties/panel and 36" joint bars. Most of the rail anchors were not directly against the ties and the rail showed signs of running 1" or more. The tie condition was fair and there was good shoulder ballast on the low rail side; however, the shoulder on the high rail side was marginal at best. The rail showed some minor signs of curve wear, rolling out and tie plate movement of up to 1/8". In addition, many of the joint bars had loose bolts. Gage ranged from in-gage to 1" wide, and, at one point, had changed by 1" in 10 feet. Almost every rail length had at least a 1/2" gage change associated with it. The surface characteristics of this curve were very poor, with 1" profiles (midchord offset of 62') in evidence. Pumped ties were found at many of the joints in the first half of the curve, and free clearance of up to 1/2" was seen between the bottom of the rail and top of the tie plate.

3.3 TRACK INSTRUMENTATION

The track site chosen for instrumentation ran about 26 feet, starting at the westbound exit spiral of the 2°06' left-hand curve at approximately MP 257.6. A plan view of the instrumented track site is given in Figure 3-8. Seven lateral force measuring strain gage patterns were applied to the high rail, along with three vertical force measuring patterns. A typical wayside gage pattern is shown in Figure 3-9. Based on the gage spacing, an approximate value of a truck's total lateral force could be measured at three instants, as shown in Figure 3-8. A lateral and vertical load gage pattern was also placed at a single point on the low rail. At each location, these trackside strain gage patterns provided a spatial sample of passing wheel loads. Gage position in Figure 3-8 is designated by the distance in feet from a joint on the high rail, designated as location 0.0. All 12 channels of wheel load data were recorded on the light beam oscillograph at a frequency bandwidth of 300 Hz.



GAGE LOCATIONS WHICH PROVIDE SIMULTANEOUS MEASUREMENT OF FORCES ON ALL THREE AXLES OF A SINGLE TRUCK

SITE 1:

SITE 2:

SITE 3:

L: Lateral
V: Vertical
N: North (High) Rail
S: South (Low) Rail
(7L & 3V locations)
(1L & 1V locations)

FIGURE 3-8 PLAN VIEW OF INSTRUMENTED TRACK SITE, MILEPOST 257.6, CHESSIE SYSTEM

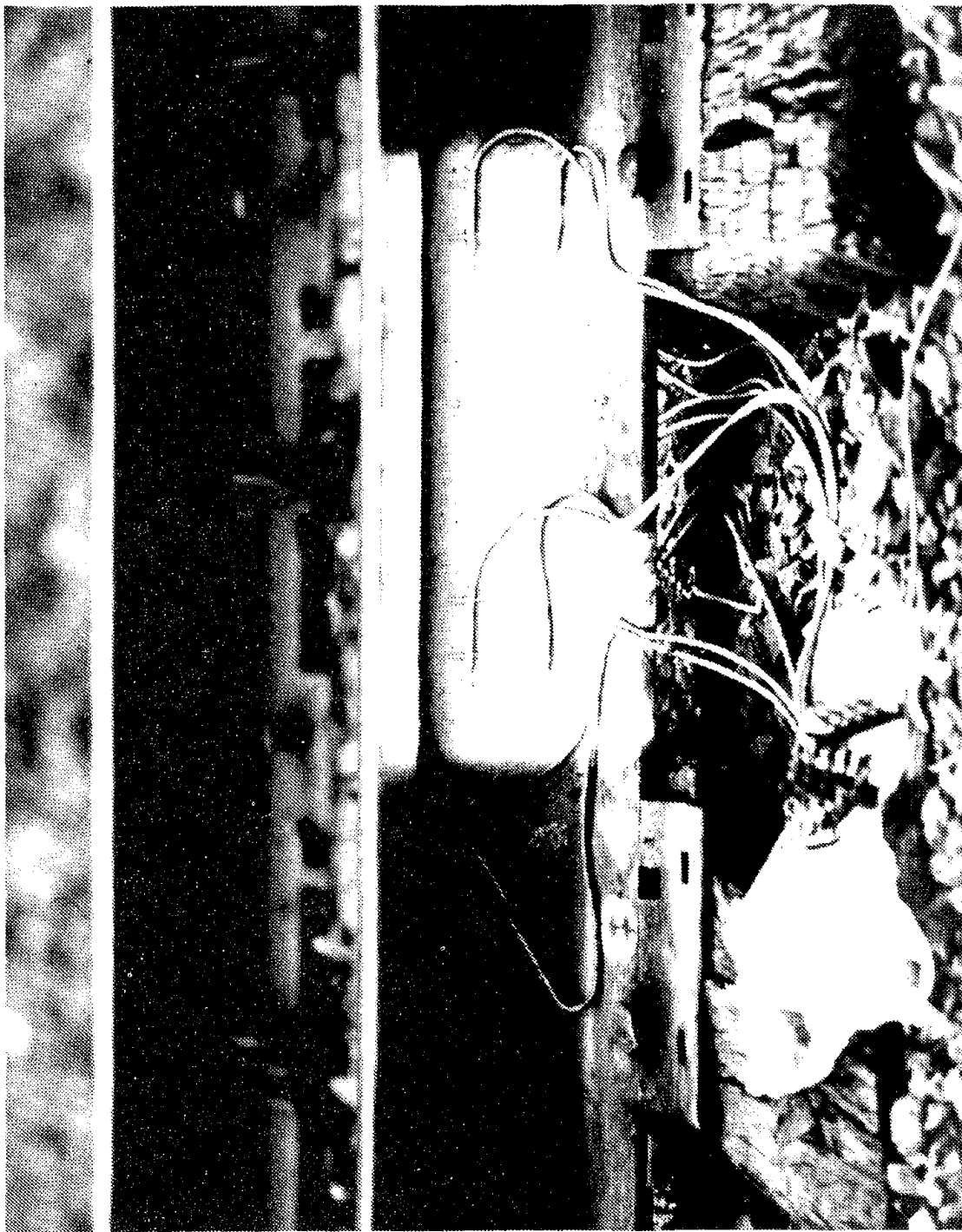


FIGURE 3-9 TYPICAL WAYSIDE GAGE INSTALLATION

The spacing of the gage stations was arranged to measure forces on all three axles of a truck simultaneously. Since the lateral force circuit must be installed over a tie, the gage station spacing cannot be matched exactly with the axle spacing of the truck.

3.4 TEST OPERATIONS

The initial survey runs were conducted between June 8 and June 10, 1977, over 600 miles of Chessie track between Huntington, West Virginia, and Charlottesville, Virginia. During the site selection runs, both consists followed the posted track speed and all speed restrictions imposed on standard passenger trains. Speed restrictions were waived with the exception of four locations where SDP-40F speeds were limited to less than normal speeds. The two consists always operated along the site selection route within a few hours of each other. This was to insure that track and weather conditions were similar when each consist passed a given point.

Test runs of the E-8 consist at the instrumented site were made on June 16, 17 and 18. All tests were made westbound between MP 254 and MP 258, over a speed range of 28 mph to 61 mph. Modes of operation included power mode, drift mode and power braking mode. All E-8 runs were made in a nominal locomotive configuration. No changes to the trucks were introduced. The locomotive dynamic data and the track geometry data were recorded on magnetic tape in the computer onboard test car T-7. The wayside data on wheel forces were recorded on analog magnetic tape.

The SDP-40F tests at the instrumented site were conducted starting June 19 and running through June 25. All tests were run westbound, between MP 254 and MP 258, over a speed range of 27 mph to 64 mph. Modes of operation included power mode, drift mode, dynamic braking mode and power braking mode.

Test runs of the SDP-40F consist included baseline tests of a nominal locomotive configuration and tests of modified locomotive configurations. The modified configuration included changes in lateral axle clearance, primary vertical damping, and wheelset diameter mismatch. The configuration changes were made only to the SDP-40F trailing locomotive to assess its sensitivity to truck component wear and design modifications. Tests were made with a single configuration change at a time.

Modifications to the primary vertical hydraulic snubbers involved changing the shocks between the center axle and the truck frame for both trucks of the trailing SDP-40F locomotive. Configuration variations included the standard shocks (1200/400), heavy-duty shocks (1800/1800), representing a design change, and no shocks, representing failed shocks.

To study the effect of wheel diameter mismatch, runs were made for a mismatched wheelset on axle No. 12, with each wheel of axle No. 12 having a 3" smaller diameter than nominal to represent the effect of worn wheels. It was also desired to test smaller diameter wheels on the leading axle; however, this would have required removing the instrumented wheelset. This condition was approximated by shimming the middle and trailing axles. Shimmed axle tests involved placing of additional metal spacers (shims), 1-1/4" thick, between the journal box and the primary (coil) springs of axles 11 and 12 of the trailing truck of the trailing locomotive.

Change of lateral axle clearance was accomplished by placing metal shims between the journal and its cover on each wheel of the trailing locomotive. In this way, the lateral clearance was increased by 1/4" per side.

During the course of the repeated site runs, there were several instances where rail surfaces were not dry and smooth. Specifically, test runs were made during rain, leading to damp rail surfaces. Three runs were made with the locomotive sanding dry rail, and one run was made with the locomotive sanding damp rail.

The E-8 consist was disassembled during the SDP-40F tests. The track geometry cars T-1 and T-3 were incorporated in the SDP-40F consist on the last test day to determine if changes in track geometry occurred during the locomotive tests. Table 3-1 provides a list of all runs conducted at the test site.

TABLE 3-1 TEST RUN LOG

<u>LOCOMOTIVE</u>	<u>RUN NO.</u>	<u>SPEED</u>	<u>POWER MODE</u>	<u>CONFIG. CHANGE</u>
E-8 #417	17-1 thru 18-6	28-61	Power, Power Brake	None
SDP-40F #620	19-1 thru 20-9	32-64	Power, Dynamic Brake, Drift, Power Brake	None
	20-10 thru 22-10	31-62	Power, Drift, Power Brake	Lateral Axle Free Clearance Increased from 3/8" to 7/8"
	22-11 thru 22-12	27-33	Power	No Vertical Shocks
	23-1 thru 23-10	31-48	Power, Drift	No Vertical Shocks
	23-11 thru 23-15	42-56	Power	1800/1800 lb. Shocks
	24-1 thru 24-12	31-59	Power, Power Brake, Drift	#11 & 12 Axles Shimmed by 1-1/4"
	25-1 thru 25-10	30-60	Power, Power Brake, Drift	37" Diameter Wheels on Axle 12

4. DATA ANALYSIS PROCEDURES

Highlights

- As a result of overall reviews of the characteristics and quality of data collected covering all measurements, a detailed analysis methodology was derived and applied.
- The analysis concentrated primarily on the output from extensive runs made on the single section of instrumented track, a road crossing, and from survey runs on 2° to 3° curves.
- Special analysis methods were developed and validated to ensure that the results from the instrumented test site could be extended to other such trackage.
- Special efforts were made to correlate onboard and trackside measurements so that the trackside data could be utilized with confidence to supply information not collected onboard the consists, i.e., wheel/rail forces on all the axles of the consist.
- The analysis efforts developed and used the 95th percentile wheel loads as a response descriptor, providing a more reliable means for comparing dynamic responses than peak loads often used in previous tests.
- Mean curvature and standard deviations of curvature, gage and crosslevel were used as track geometry descriptors for relating to locomotive performance.
- Descriptions of the track inputs and consist responses in terms of standard deviations and rates of change as well as absolute values were essential elements of the analysis.
- A high degree of cooperation, coordination and interaction between involved safety interests greatly aided the planning and implementation of the tests and analysis.

4.1 OVERALL APPROACH

The major features of the data analysis process are illustrated in the flow diagram in Figure 4-1. Each of the five main steps in the methodology will be outlined briefly

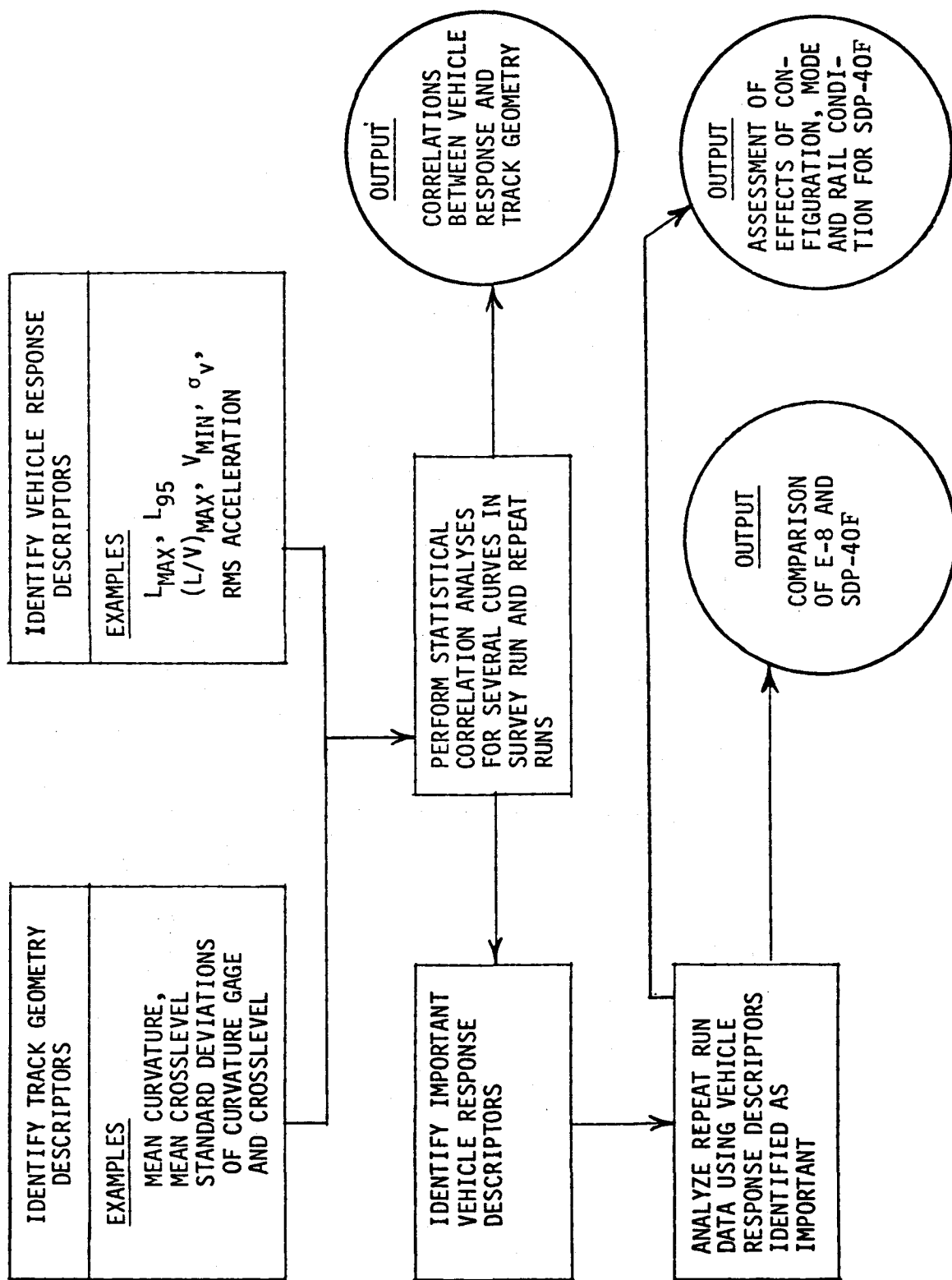


FIGURE 4-1 ANALYSIS METHODOLOGY

followed by a presentation of the test results of the analysis.

4.2 TRACK GEOMETRY DESCRIPTORS

Based upon a comparison of repeated runs at various speeds from 20 to 60 mph, the track geometry car appears to provide a consistent, speed-independent measurement of track geometry. Comparison of track geometry (gage, crosslevel, and surface) before the repeated site tests, after the E-8 tests and also after the SDP-40F tests, indicated that, within measurement accuracy, neither locomotive caused any permanent changes in track geometry within the 4-mile test zone. The accuracy of the track geometry measurements is approximately ± 0.2 inches.

The analysis of the track geometry data is outlined in detail in Appendices B and C. The particular descriptors selected for analyzing this data were, in general, dictated by what the geometry car measures:

- Gage - distance between the inside faces of each railhead measured across the track at points $5/8$ of an inch below the top of the railhead. (inches) (Figure C-1)
- Crosslevel - the elevation of the left rail surface minus the elevation of the right rail surface. (inches) (Figure C-2)
- Profile - (right and left) the vertical 62-foot mid-chord offset (MCO) of the rail surface. (Figure C-3)
- Curvature - track curvature in degrees subtended by 100 feet of track. Calculated from the measured path of the trucks through a given curve. (Figure C-4)

Root mean square values of the variation of these values about its steady state value were also computed and made available for later correlation analyses.

4.3 VEHICLE RESPONSE DESCRIPTORS

Selection of the appropriate vehicle response descriptors was guided primarily by the accident reports. The NTSB

assessment of SDP-40F accident causes and the analysis contained in Appendix A indicate a high frequency of rail lateral displacement as part of the derailment mechanism. This in turn suggests the existence of excessive lateral loads or high ratios of lateral to vertical wheel forces, (L/V), or both. Therefore, the maximum values of lateral force and L/V and the minimum values of vertical force are obvious response descriptors. Acceleration levels at various locations also provide valuable insights to vehicle characteristics and are particularly useful in validation of analytical models. The principle response descriptors used in the data analysis are summarized below:

- L_{\max} = the maximum value of lateral force on the high rail measured by the wayside instrumentation during a single consist passage.
- L_{TRK} = the sum of the instantaneous lateral forces on the three high rail wheels of the same locomotive truck.
- L_{95} = the value of lateral force on the high rail wheel of the leading (instrumented) axle of the trailing locomotive truck which is exceeded only 5% of the time during a single passage through a curve.
- V_5 = the value of vertical force on the high rail wheel of the leading (instrumented) axle of the trailing locomotive truck which is exceeded 95% of the time during a single passage through a curve.
- $(L/V)_{\max}$ = the maximum value of the instantaneous ratio of lateral to vertical high rail force measured by the wayside instrumentation during a single consist passage.
- $(L/V)_{95}$ = the value of the instantaneous lateral to vertical load ratio on the high rail wheel of the leading (instrumented) axle of the trailing locomotive truck which is exceeded only 5% of the time during a single passage through a curve.

locomotive = the maximum vertical and lateral
carbody accelerations at the front and rear of the
accelerations trailing locomotive during transit of a
 specific track perturbation (grade
 crossing).

baggage car = the maximum vertical and lateral
accelerations accelerations at the front and rear of the
 baggage car during transit of a specific
 track perturbation (grade crossing).

From the analysis of the onboard data over many miles of track, including the survey runs, it became apparent that definitions of maximum or minimum force levels were difficult to use because of the large random component associated with the true maximum or minimum. In addition, for examining force levels over many miles of track, isolated maximum or minimum values taken from a measurement are of some interest but are not the best variables for characterizing the behavior of the vehicle. The solution to this difficulty involved the use of the 95th and 5th percentile loads as indicators of the characteristic force differences among different test conditions. More information on the benefits of using other-than-maximum values is outlined in Appendix D. The analysis of the wayside data involves data taken at several fixed locations over 26' of instrumented track. Following a single axle through the instrumented site only yields seven data points for lateral force. This does not produce a large enough data base to permit a meaningful statistical analysis of the wayside data using typical descriptors such as L_{95} . Therefore, L_{max} has been chosen as the vehicle response descriptor associated with the wayside data. It should be noted that L_{max} from the wayside data may not include the maximum lateral wheel/rail force produced in the immediate vicinity of the test site since the wayside measurements produce only a sampling of the lateral force time history. For this reason, L_{max} of the wayside data and the maximum value of lateral load from the onboard data are not directly comparable. However, the wayside sampling procedure provides one advantage in that it acts to filter out forces of inconsequential time duration.

4.4 STATISTICAL CORRELATION ANALYSIS

Regression analysis techniques were employed to try to separate the individual effects of speed, gage, curvature, profile and alignment. The manner in which this was ultimately accomplished is outlined in Appendix E. This

methodology was able to relate the test results at the test site with those from the survey runs by means of an estimating equation for lateral wheel loads and L/V.

4.5 IMPORTANT VEHICLE RESPONSE DESCRIPTORS

Analysis of the test results to this point in the methodology provided the basis for judging which parameters had significant effects on wheel/rail loads and which were secondary. One technique developed to supplement the locomotive vertical response data was the use of a ten degree of freedom simulation model. The analysis done with this model provided important insight into the effects of some of the locomotive configuration changes. A description of the model and its calibration is provided in Appendix F.

4.6 ANALYSIS OF REPEAT RUNS

Within the four-mile test zone, performance descriptors for the instrumented test site and two curves, having curvatures of approximately 2°, but with balance speeds ten miles per hour apart, have been analyzed for the effects of a broad spectrum of varied test control parameters. The control parameters include:

Locomotive Type: E-8 or SDP-40F

Vehicle Speed: 30 to 60 mph

Track Balance Speed: 42 and 52 mph

Mode of Operation: power, drift, dynamic brake, power brake

SDP-40F Truck Configurational Changes: vertical primary damping, lateral clearance, mismatched wheels, shimmed axles

Rail Surface Condition: wet, dry, sanded

The vehicle dynamic data include displacement and acceleration measurements in the E-8 and SDP-40F test locomotives and in the baggage car in the SDP-40F consist. Continuous wheel force data was collected on axle 10, the lead axle of the trailing truck of the trailing locomotive, in both consists. Wayside wheel forces were obtained for each axle of the locomotives and baggage car as they passed through the 26' test site.

It was found necessary to correct the wheel/rail loads data derived from the instrumented rail at the test site. Wayside lateral loads did not agree with the lateral loads measured with the instrumented wheelset. The cause of this discrepancy was found to be excessive "cross talk" between vertical and lateral loads because of the locations and arrangement of the strain gages on the rail web. Laboratory tests and analytical procedures provided a correction factor for the lateral loads which brought this data into agreement with the onboard data sufficient for use in comparative analysis. The details of the correction procedure are provided in Appendix G.

4.7 DATA ANALYSIS TASK FORCE

A data analysis task force was assembled under the overall direction of the FRA Office of Rail Safety Research. The Transportation Systems Center headed the task force supported by Battelle, ENSCO and Arthur D. Little, Inc. A Government-Industry Review Group consisting of representatives from the FRA, AAR, AMTRAK, EMD and Chessie provided guidance on the data analysis activity. Several review meetings were held at which interim results and future plans were discussed with the Review Group for comment and guidance. Figure 4-2 shows the data reduction and analysis organization. Figure 4-3 shows the manner in which these groups interacted with the data analysis process.

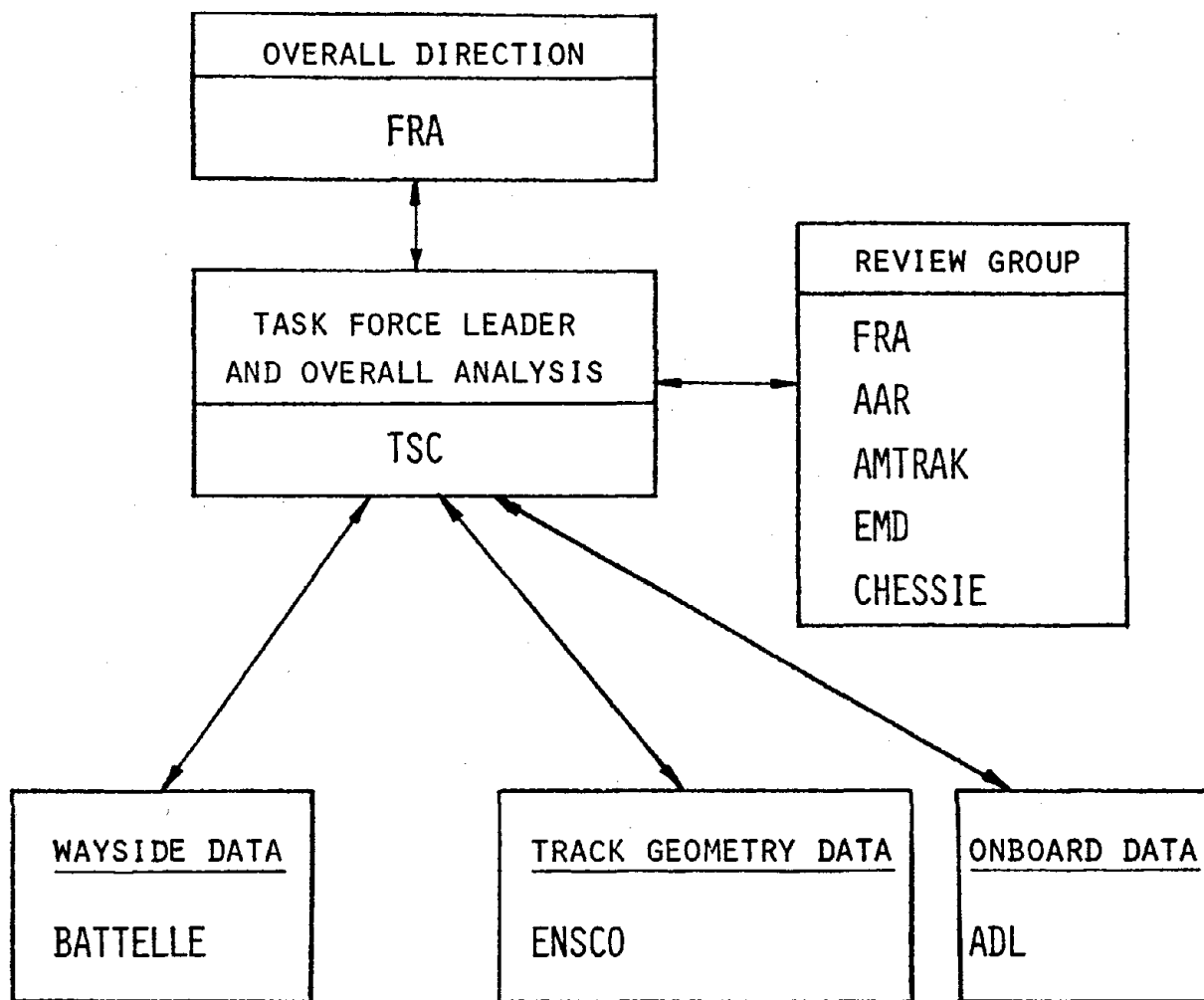


FIGURE 4-2 ORGANIZATIONAL FLOW FOR DATA REDUCTION AND ANALYSIS OF THE SDP-40F AND E-8 LOCOMOTIVE TESTS CONDUCTED ON CHESSIE SYSTEM TRACK

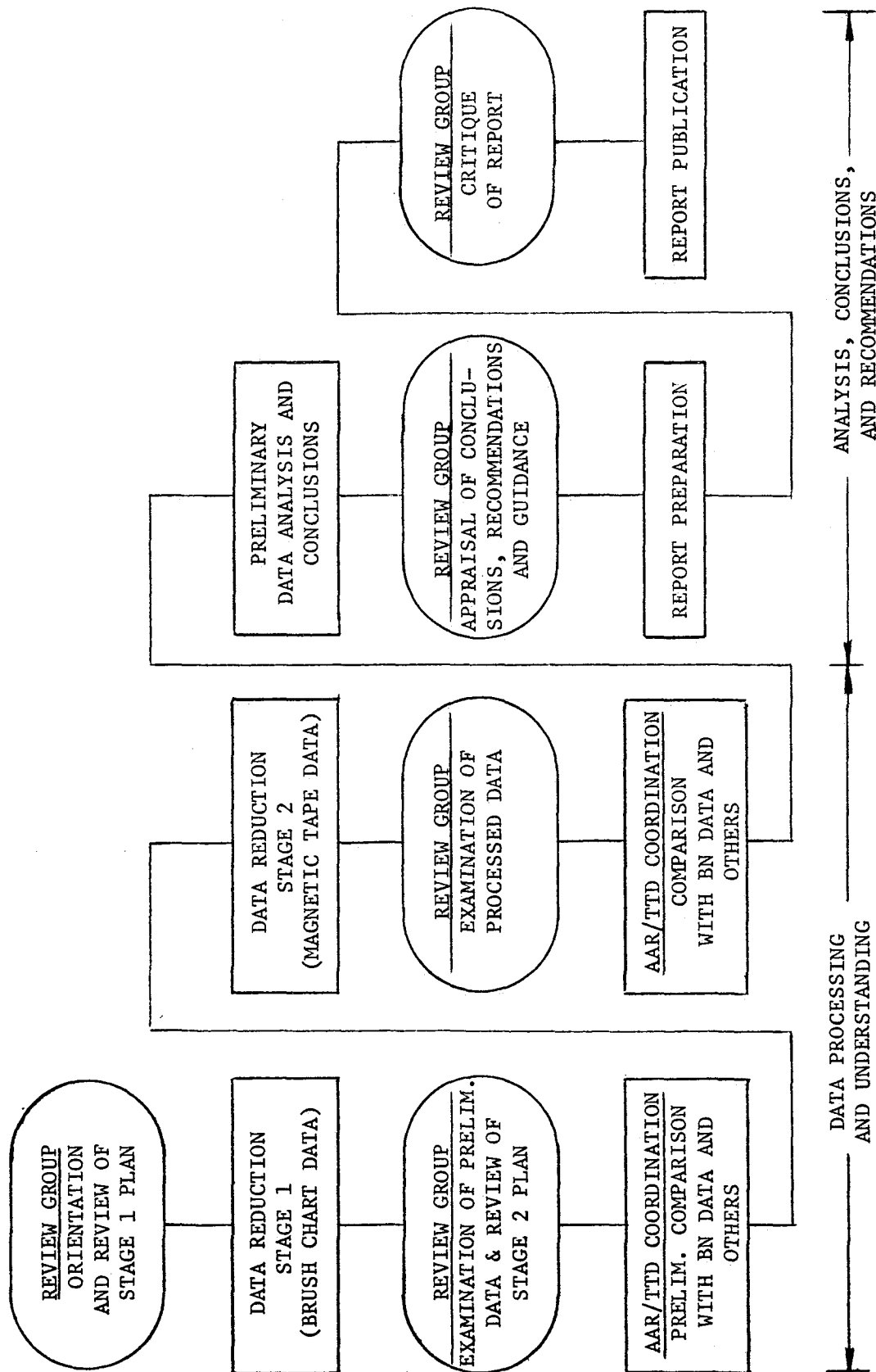


FIGURE 4-3 FRA/TSC DATA REDUCTION AND ANALYSIS SEQUENCE FOR THE SDP-40F AND E-8 LOCOMOTIVE TESTS

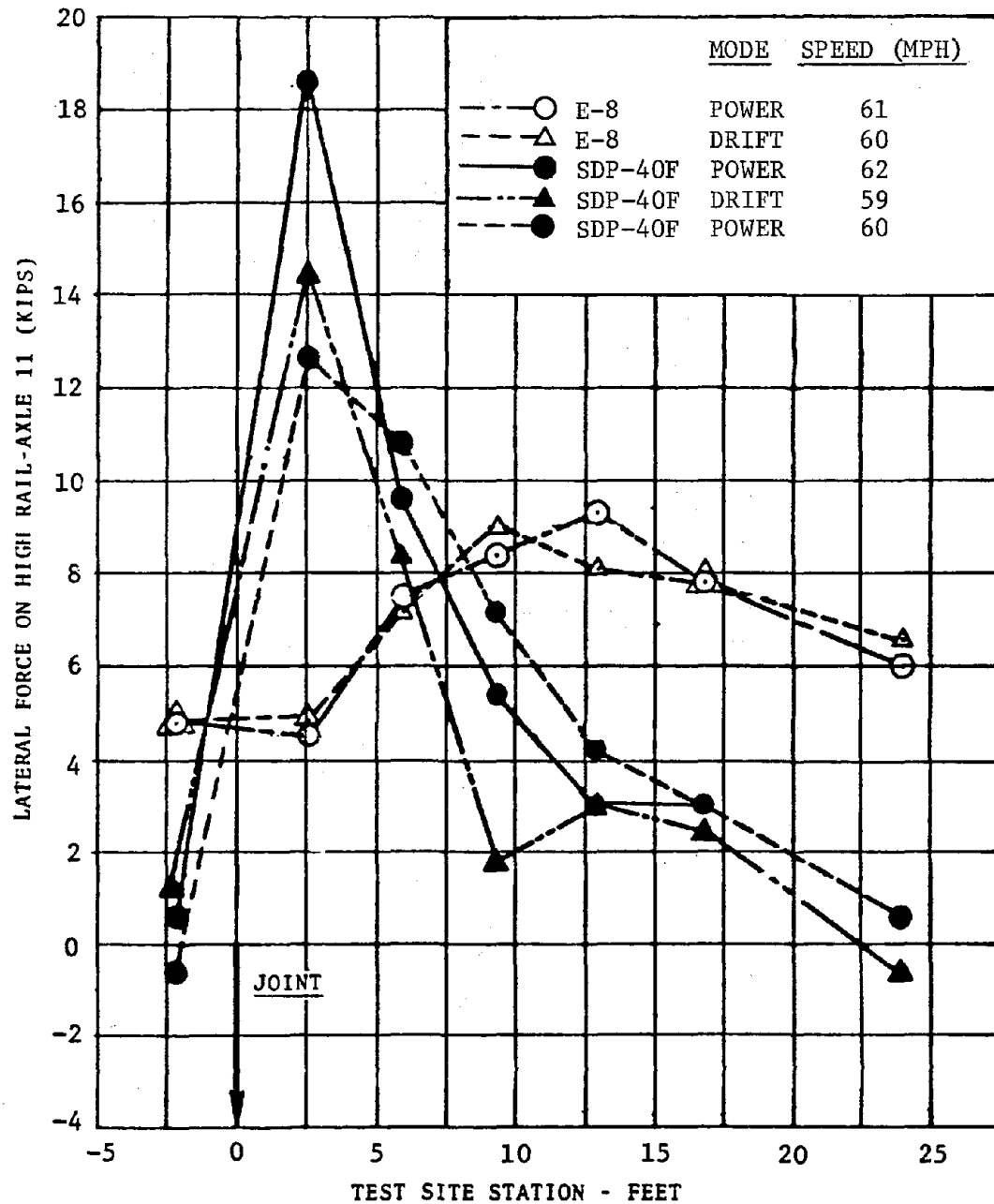


FIGURE 5-7 COMPARISON OF E-8 AND SDP-40F AXLE 11 LATERAL FORCE TRACES UNDER POWER AND DRIFT NEAR 60 MPH (WAYSIDE DATA)

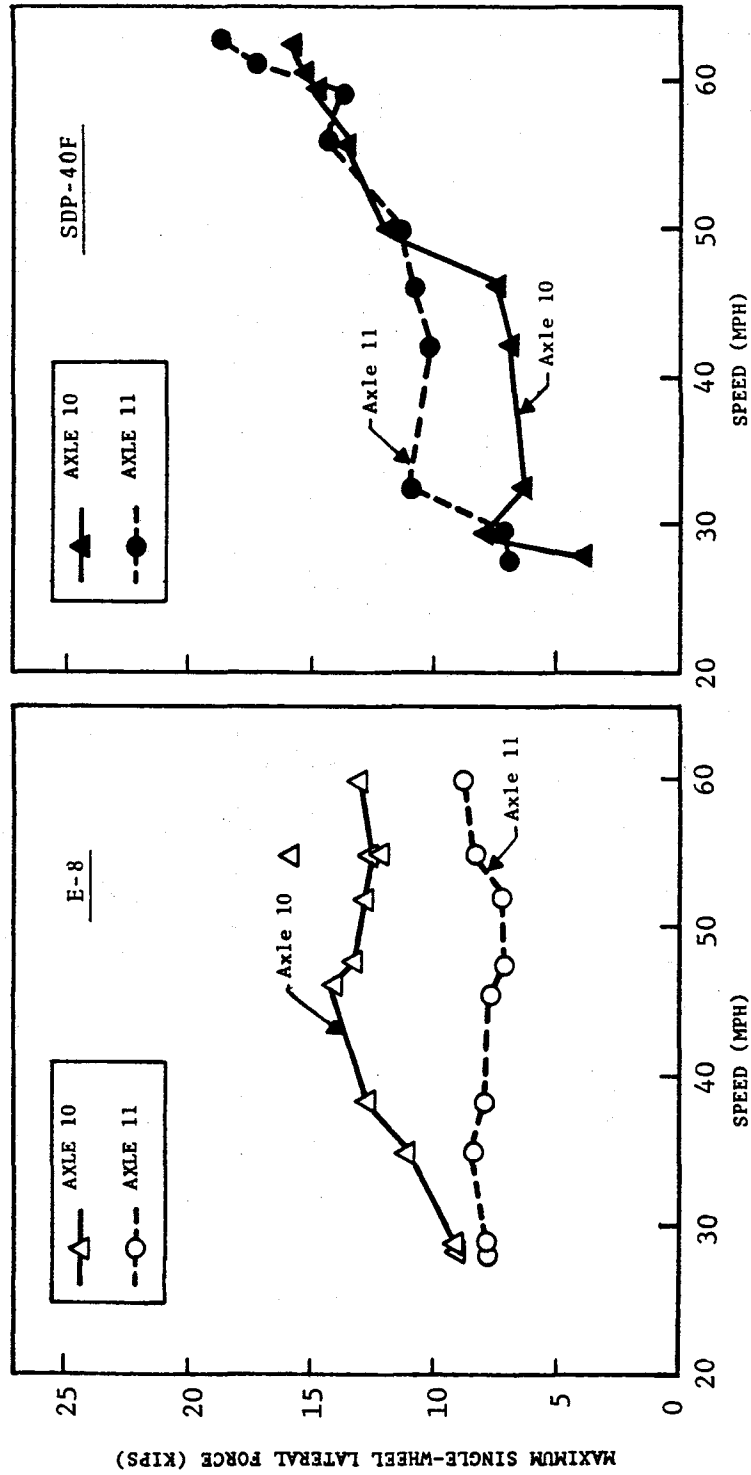


FIGURE 5-8 MAXIMUM SINGLE-WHEEL LATERAL FORCE FOR AXLES 10 AND 11, E-8 AND SDP-40F (BASELINE RUNS, WAYSIDE DATA)

are much less than the corresponding axle 10 lateral force throughout the entire speed range. For the SDP-40F, the axle 11 maximum lateral force is comparable to the corresponding axle 10 maximum lateral force. Both these axle forces tend to rise more rapidly at higher speeds. A comparison of the middle axle maximum lateral loads for all middle axles for the E-8 and SDP-40F is given in Figures 5-9 and 5-10. The E-8 middle axles have a relatively flat response throughout the entire speed range, and their maximum lateral loads are much less than their lead axle values. The SDP-40F middle axle forces are generally much greater than the corresponding E-8 middle axle forces and can be comparable to their own lead axle forces. At 60 mph, the highest SDP-40F middle axle force is 75% greater than the highest E-8 middle axle force.

The maximum lateral force and maximum L/V of the trailing axle of each truck are shown in Figure 5-11. The forces are uniformly low and not sensitive to speed within the tested range. These low values of L_{\max} and $(L/V)_{\max}$ indicate that the trailing axles of the trailing trucks do not contribute significantly to truck loads on either locomotive for the speed range and track geometry investigated.

Truck Loads (Instrumented Site)

The distribution of wayside gages and the relative size of the truck base (14 feet) compared to the test site (26 feet) allows the near simultaneous measurement of lateral forces on the high rail on all three axles of the same truck at only three instances in time for each run. These three observations provide only a sample of a cycle of truck load variations. Since the data shows that the trailing axle in each truck produces consistently low lateral forces throughout the test site, it was decided to evaluate the truck force on the high rail using the lead and middle axle loads and adding only a constant of 3 kips to approximately account for the contribution of the trailing axle. The lead and middle axle forces were estimated continuously by linear interpolation of the data points within the 26-foot test site. The advantage of using only two axles to estimate the truck force on the high rail is that it permits the first truck force measurement to be obtained after only 7 feet of penetration into the instrumented region.

Variations in truck lateral forces with spatial position at the test site are shown in Figure 5-12 for the E-8, and Figure 5-13 for the SDP-40F. For both the E-8 and the

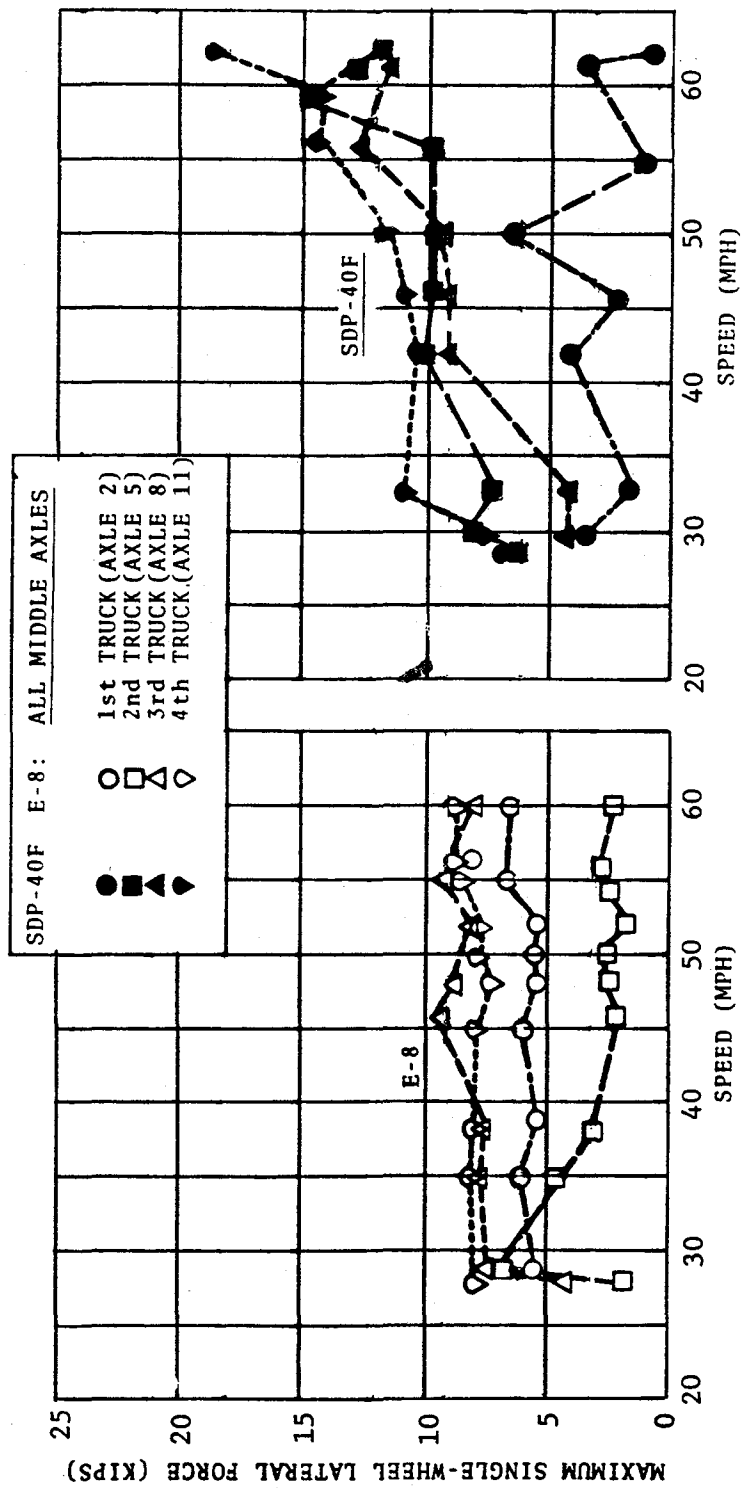


FIGURE 5-9 MAXIMUM SINGLE-WHEEL LATERAL FORCE VERSUS SPEED FOR MIDDLE AXLE IN EACH TRUCK OF THE E-8 AND SDP-40F CONSISTS (BASELINE RUNS, WAYSIDE DATA)

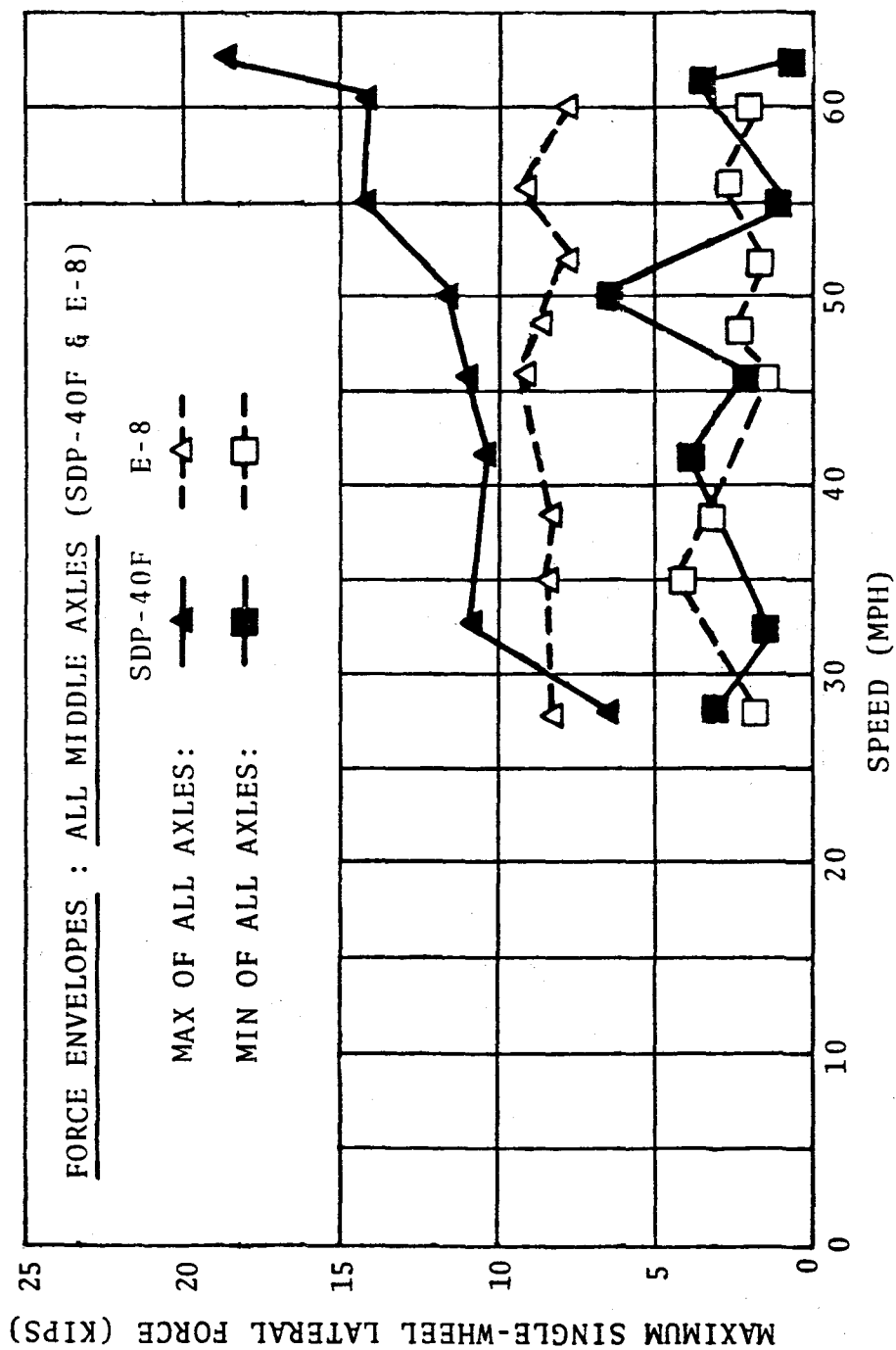


FIGURE 5-10 SDP-40F AND E-8 ENVELOPES OF MAXIMUM SINGLE-WHEEL LATERAL FORCE VERSUS SPEED FOR ALL MIDDLE AXLES (BASELINE RUNS, WAYSIDE DATA)

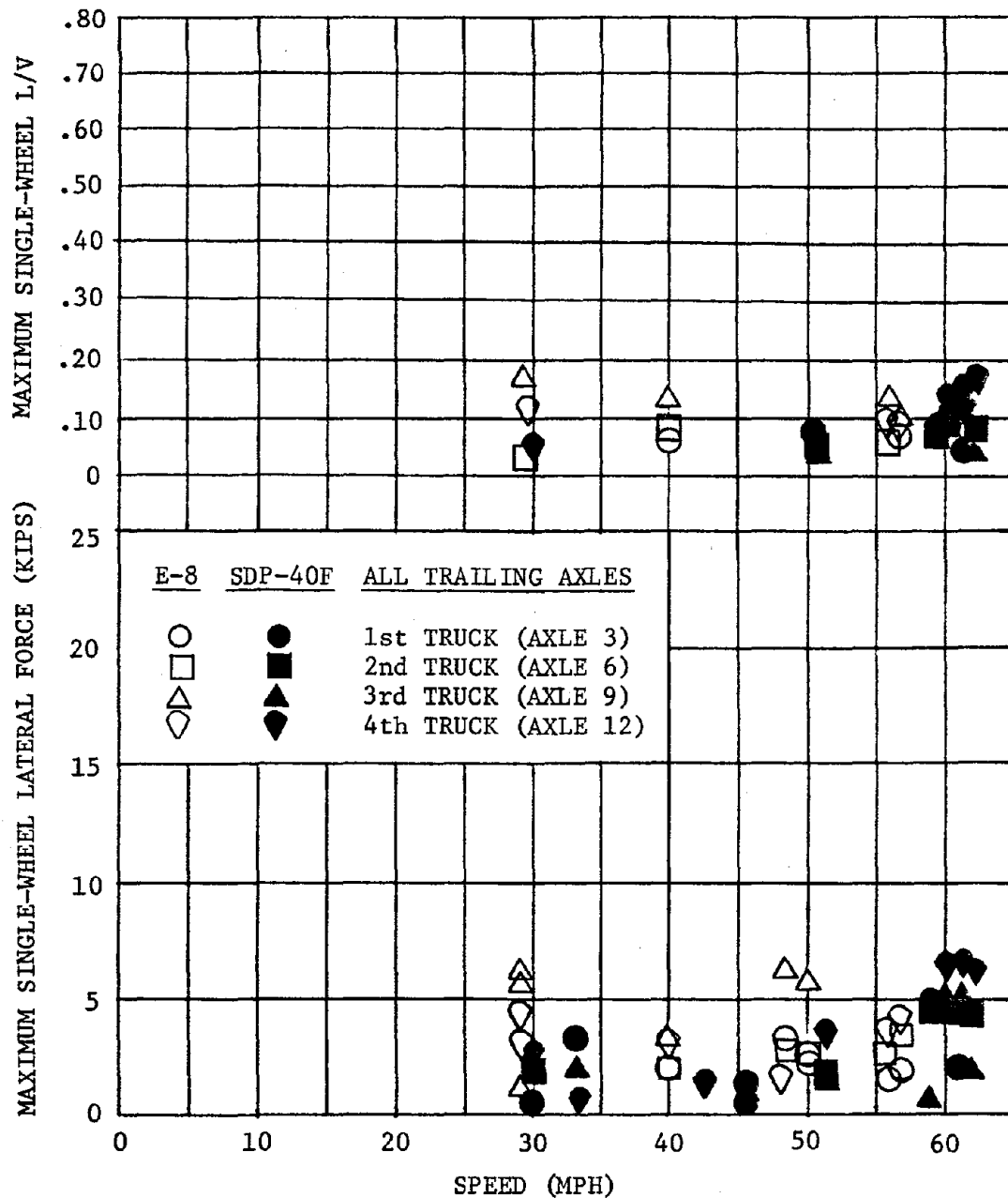


FIGURE 5-11 MAXIMUM SINGLE-WHEEL LATERAL FORCE AND L/V VERSUS SPEED FOR TRAILING AXLE IN EACH TRUCK OF THE E-8 AND SDP-40F CONSISTS (BASELINE RUNS, WAYSIDE DATA)

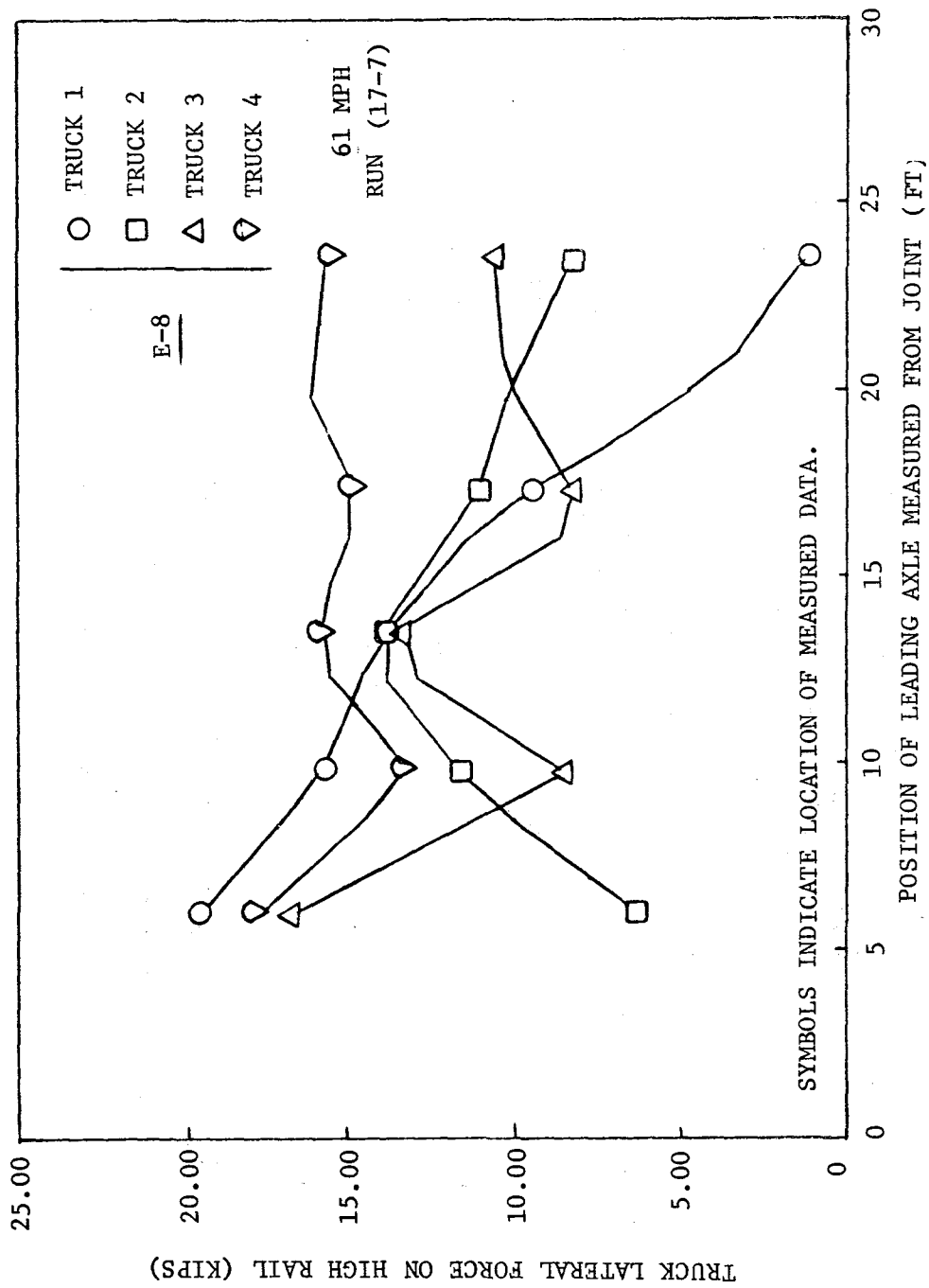


FIGURE 5-12 E-8 TRUCK LATERAL FORCES ON HIGH RAIL (BASELINE RUNS, INTERPOLATED WAYSIDE DATA)

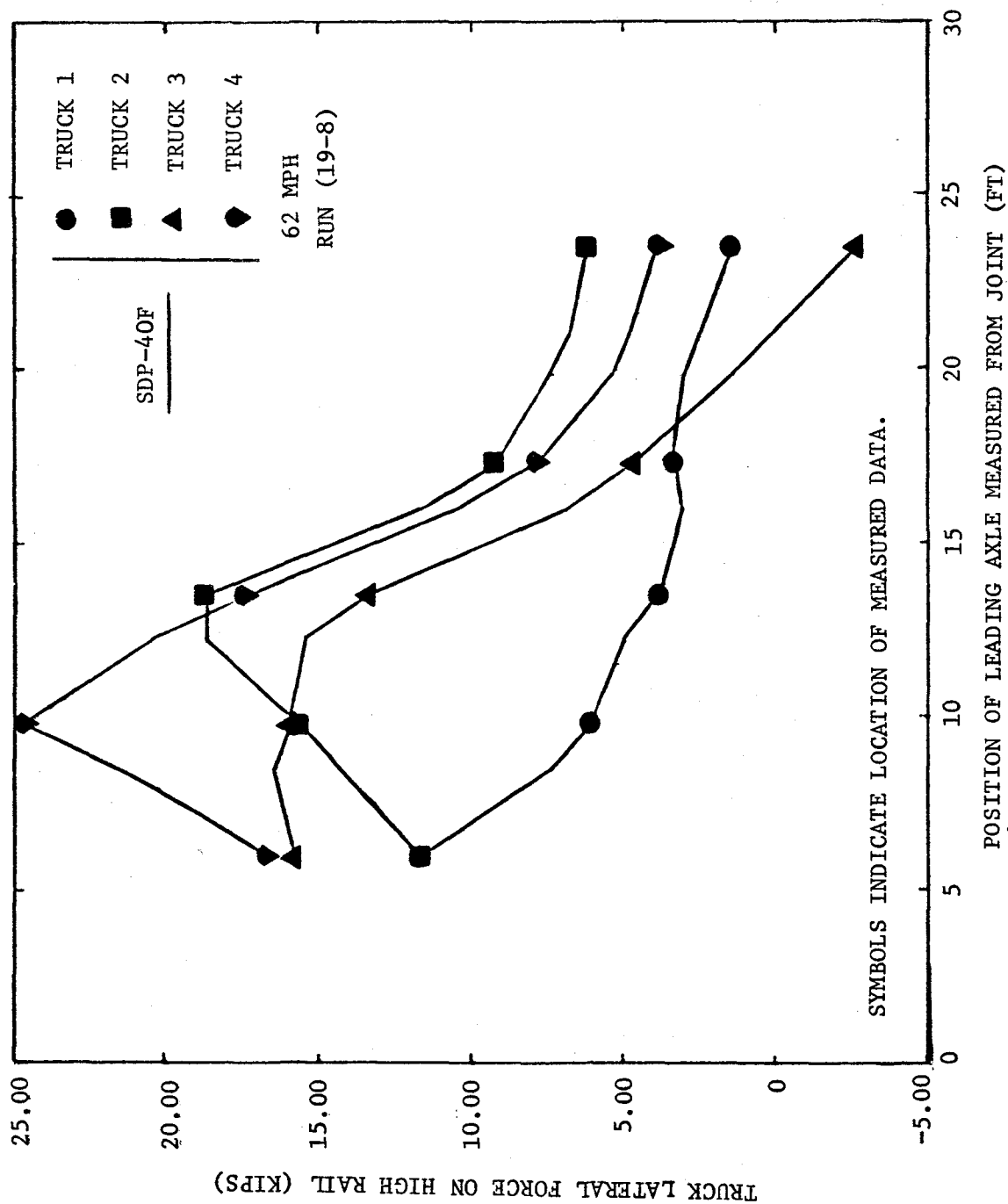


FIGURE 5-13 SDP-40F TRUCK LATERAL FORCES ON HIGH RAIL (BASELINE RUNS, INTERPOLATED WAYSIDE DATA)

SDP-40F locomotives, trucks 3 and 4 of the trailing locomotive tend to have high lateral forces. Truck 1 of the E-8 also encounters force levels comparable to trucks 3 and 4 at speeds around 60 mph. For both the E-8 and SDP-40F, the spatial force traces in Figures 5-12 and 5-13 show that the truck loads tend to decrease as the first two truck axles move away from the joint (position 0 in the figures). In addition, the spatial force trace for the SDP-40F trucks often have peaks when either the lead or middle truck axles are in the vicinity of the joint.

For trucks 3 and 4, the variation in truck force with speed tends to parallel the axle force trends, as shown in Figures 5-14 and 5-15. The lines in these figures indicate the upper boundary of the data points, which show substantial scatter due to the inherent limitations in the truck force data as described above. The E-8 truck lateral loads are greater than, or comparable to, the SDP-40F values below about 45 mph. Above 45 mph, the SDP-40F truck loads rise faster than the E-8 truck loads. At 60 mph, these SDP-40F values are about 40% greater than E-8 values.

There is an important limitation on the high rail truck loads comparison shown in Figures 5-14 and 5-15. The maximum values plotted represent the maximums obtained only in the region where simultaneous loads measurements exist for both lead and middle axles. Figure 5-13 indicates that this region probably does contain the true maximum of the SDP-40F truck 4 lateral load. However, the lateral load for truck 3 is still rising at the initial location of data (rail position = 6 ft.). The maximum truck 3 lateral loads apparently occur when the truck is farther up the track from the instrumented site. This is also true for the E-8 truck 3 and 4 lateral loads. The maximum truck loads for both the E-8 and SDP-40F were estimated by various methods of extrapolation of the middle axle force data beyond the first gage location (see Figure 3-8). These included linearly extrapolating the axle force between gages 1 and 2 using the same value as that at gage 1, and extrapolating beyond gage 1 using the negative slope of the axle forces between gages 1 and 2. The different extrapolations produced somewhat different maximum values for the truck loads at some speeds. However, the relative trend in the force vs. speed characteristic for the E-8 and SDP-40F remains similar. Therefore, even though the maximum load summary in Figures 5-14 and 5-15, which are based on only the region for which data is actually available, may not contain the maximum for either the E-8 or SDP-40F truck lateral loads, these figures can be used in a qualitative sense to provide an indication of the type of truck loads to expect, and to illustrate that

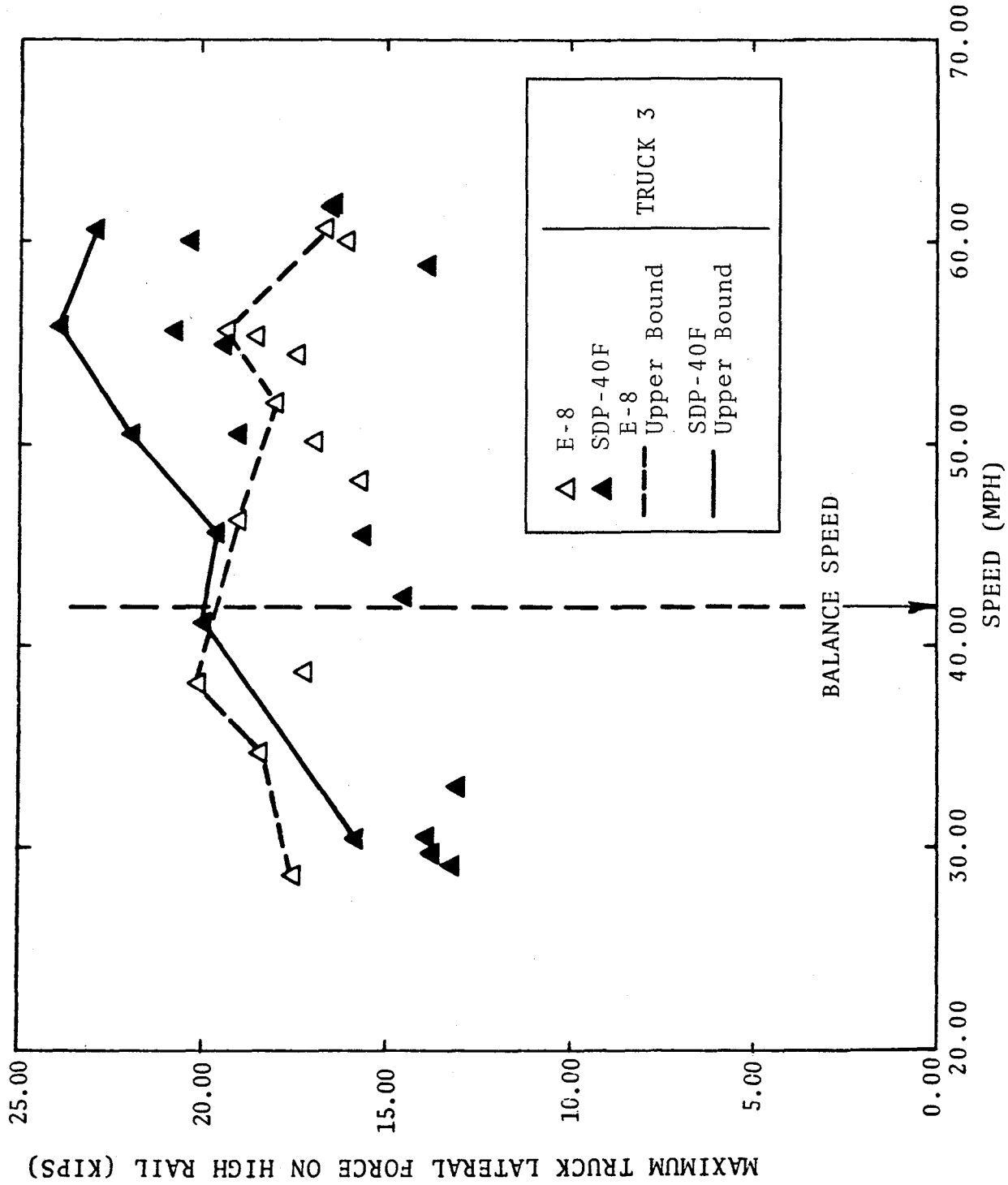


FIGURE 5-14 COMPARISON OF E-8 AND SDP-40F MAXIMUM LATERAL FORCE ON HIGH RAIL FOR TRUCK 3 (BASELINE RUNS, INTERPOLATED WAYSIDE DATA)

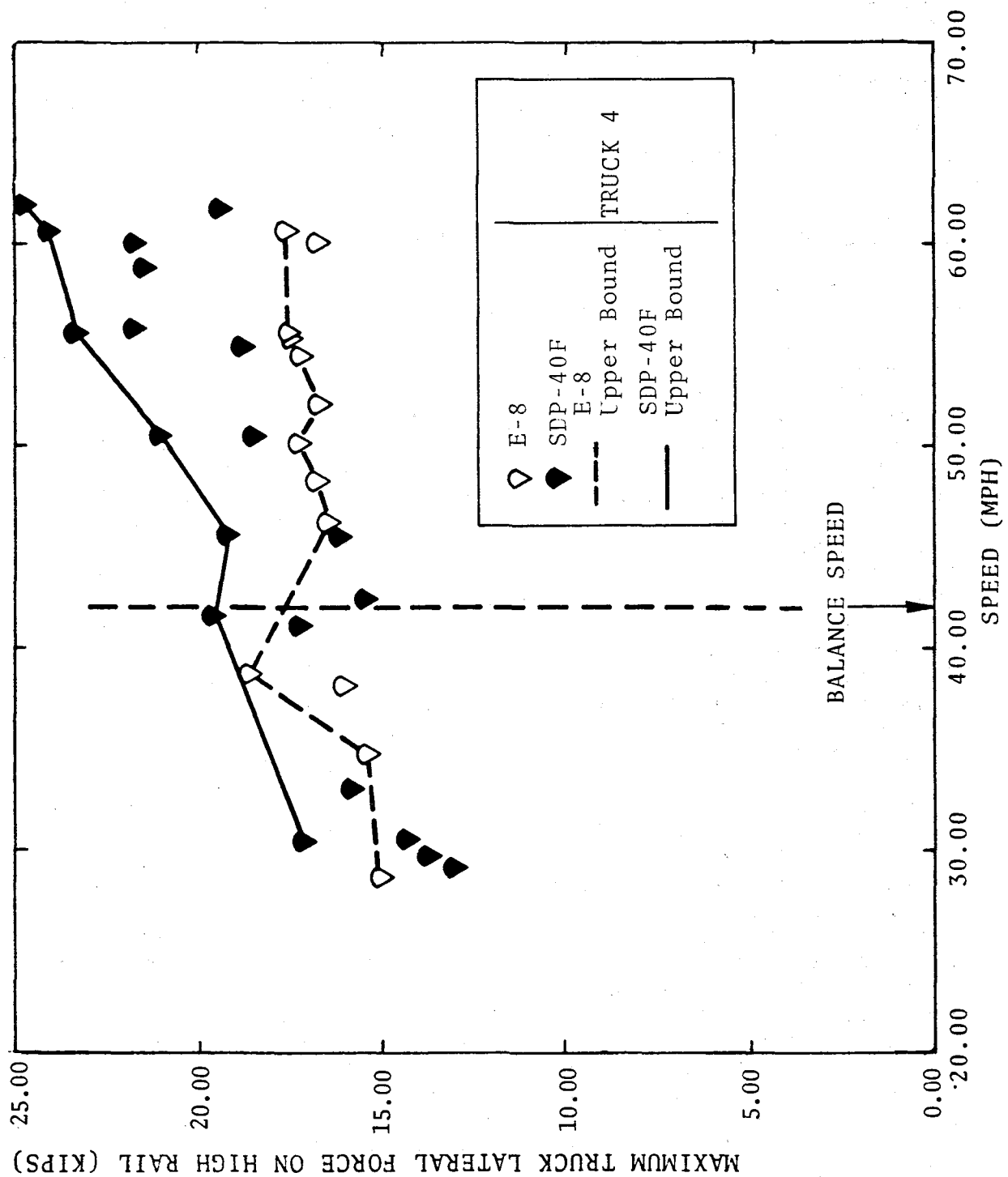


FIGURE 5-15 COMPARISON OF E-8 AND SDP-40F MAXIMUM LATERAL FORCE ON HIGH RAIL FOR TRUCK 4 (BASELINE RUNS, INTERPOLATED WAYSIDE DATA)

the variation in truck force with speed tends to parallel the axle force trends. The additional weight of the SDP-40F compared to the E-8 (395,000 lbs. vs. 345,000 lbs.) can be expected to result in higher lateral truck loads. On the other hand, the particular track geometry variations existing at the test site may also explain some of the truck loads differences among locomotives since one locomotive may exhibit greater dynamic response to these particular geometry variations than the other locomotive.

Instrumented Axle Loads (Survey and Repeat Runs)

The preceding lateral force test results for wheels and trucks were obtained from repeated runs at various speeds through the test site. The site was a 2°06' curve with a balance speed of 42 mph. The results suggest that the SDP-40F wheel and truck lateral loads increase rapidly at speeds above the balance speed, whereas the E-8 lateral loads appear to level off above the balance speed. In order to determine whether this was just a coincidence or whether in fact deviation from balance speed and not absolute speed was the more critical factor in lateral load levels, a second approach to analyzing the effects of speed was developed. This approach used the onboard data on axle 10 lateral wheel loads collected during the survey runs for each locomotive. Twenty-five curves, with curvatures between 2° and 3°, and having various balance speeds, were extracted from the data for further analysis. The locomotive speeds were nearly constant in each curve but, from curve to curve, speed varied from a low of 40 mph to a maximum of 62 mph for both locomotives.

Of course, speed was not the only variable which might have influenced the lateral loads during the survey runs. Power modes were different, but, as will be shown later, the effects of different operating modes on lateral loads were negligible. Track geometry irregularities also varied from curve to curve, with large effects on the lateral forces which could not be neglected. Therefore, some method had to be found to separate the effects of speed from track geometry. Appendix E describes the statistical technique (called regression analysis) which was developed to estimate the separate influences of speed and track geometry. To statistically characterize the axle 10 lateral response through each curve, a new measure called the 95th percentile lateral load (which will be referred to as "L₉₅") was introduced. This is the load which the onboard data indicates is exceeded only 5% of the time during the passage through the curve. Figures 5-16 and 5-17, respectively,

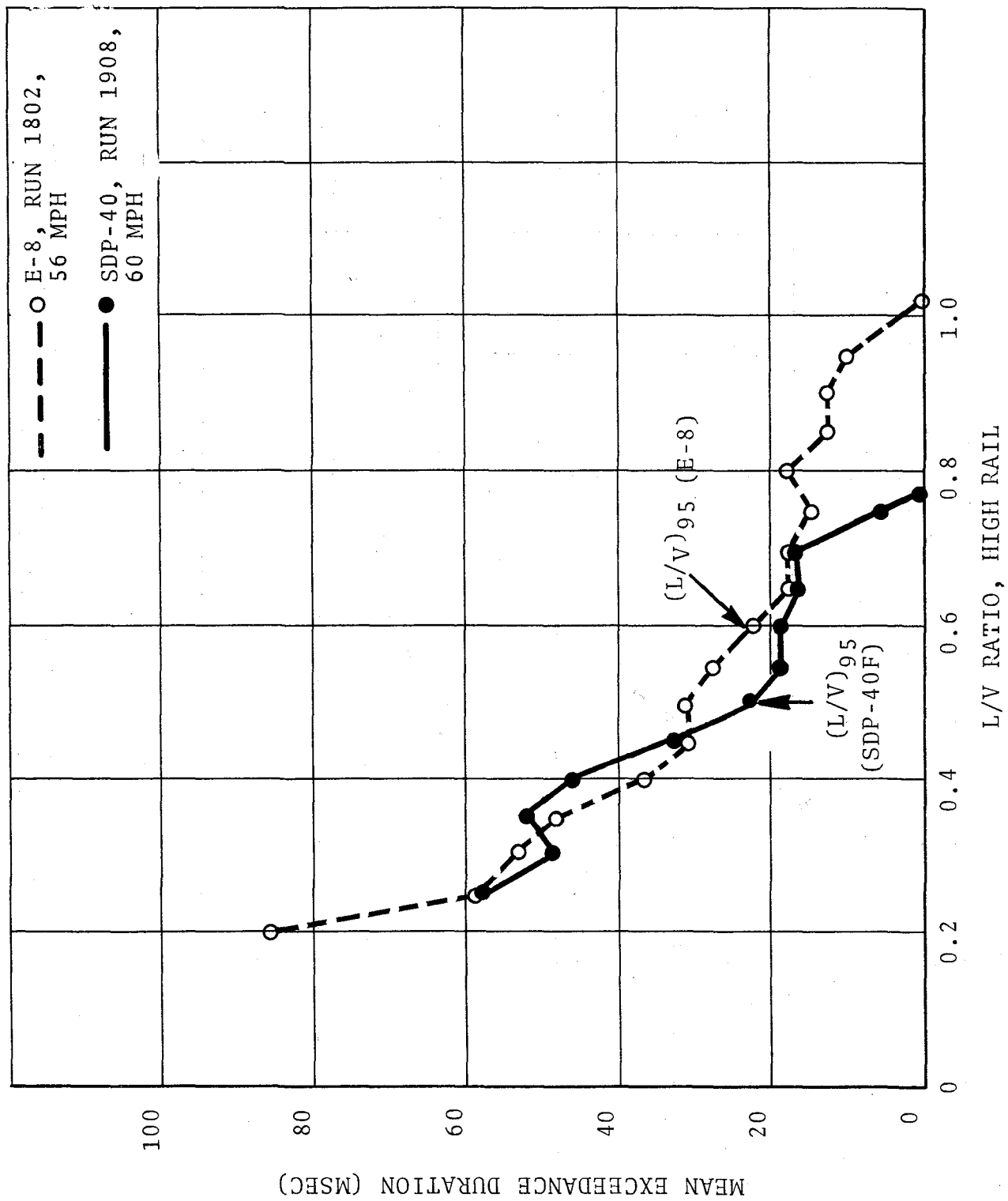


FIGURE 5-16 MEAN EXCEEDANCE TIME VS. L/V RATIO THRESHOLD FOR AXLE 10 IN THE TEST CURVE (ONBOARD DATA, NOMINAL CONFIGURATION)

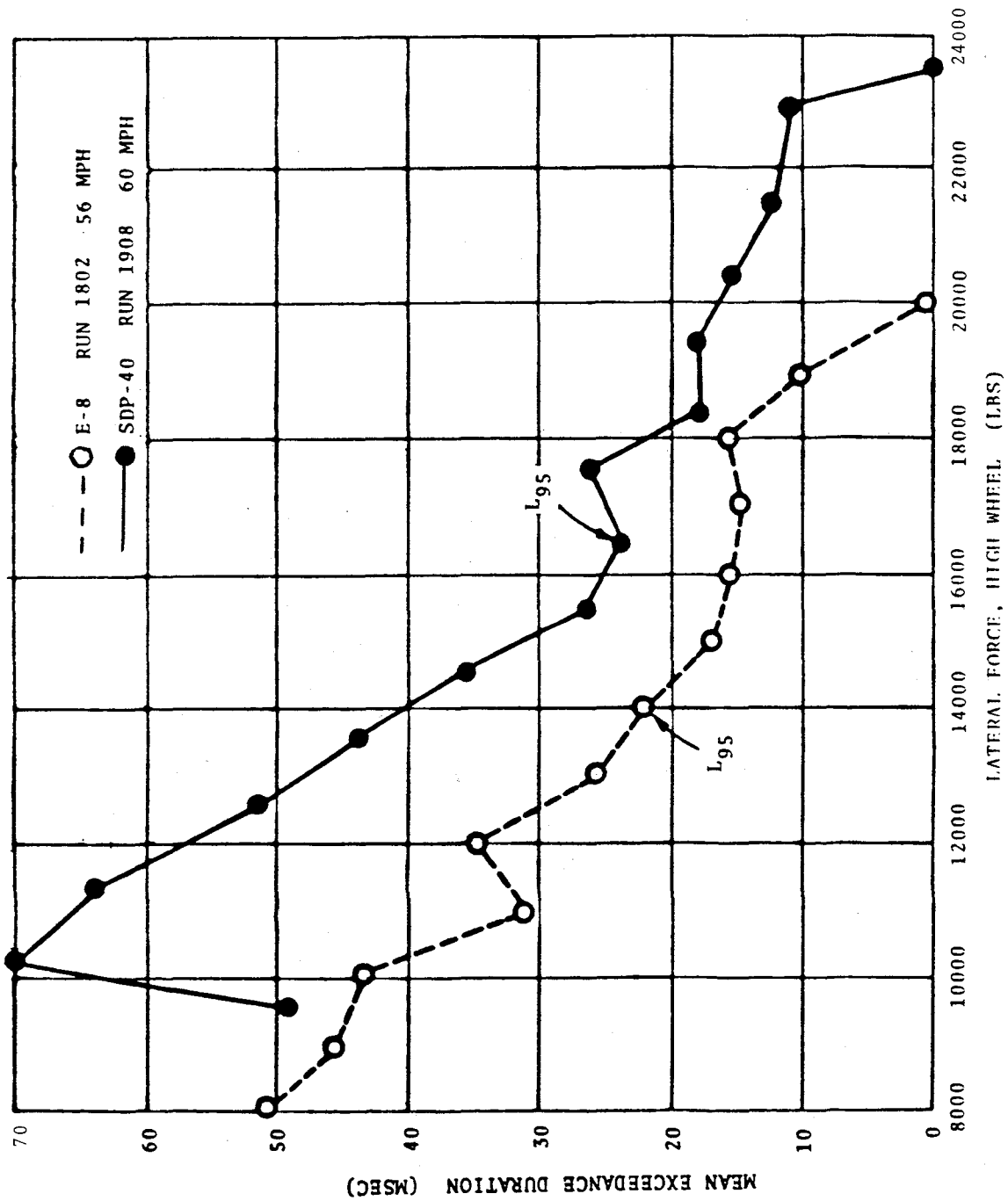


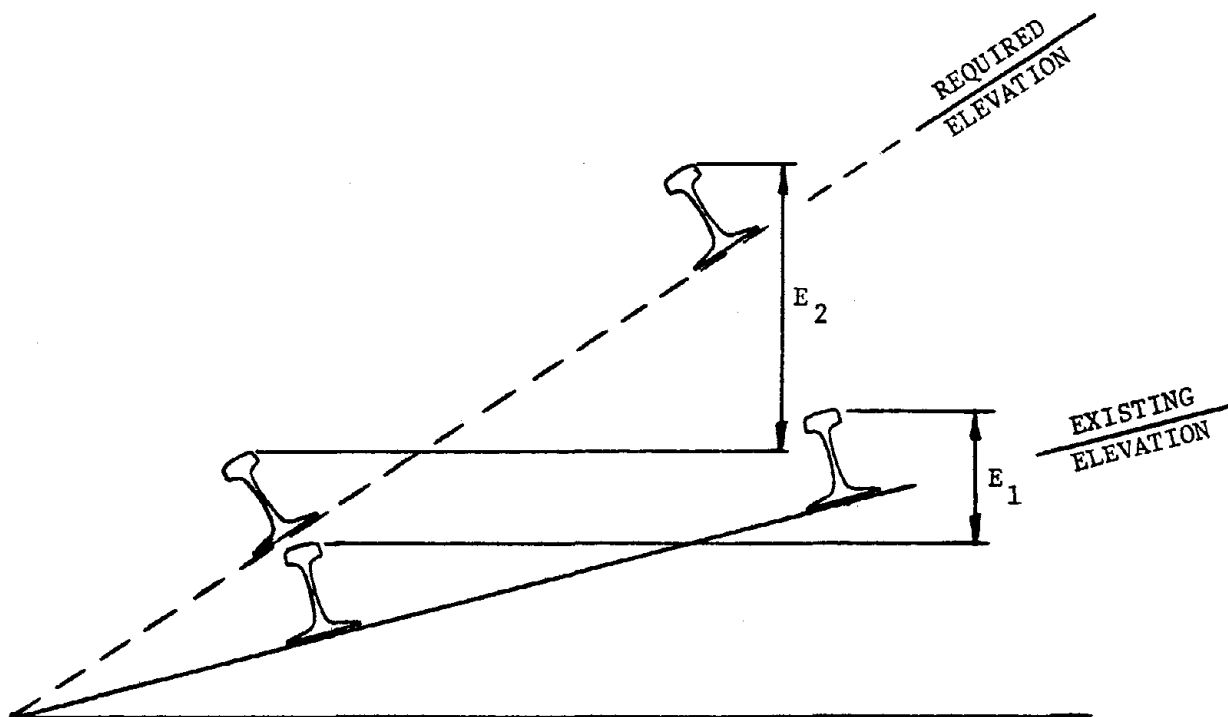
FIGURE 5-17 MEAN EXCEEDANCE TIME VS. LATERAL FORCE THRESHOLD
IN TEST CURVE (ONBOARD DATA, NOMINAL CONFIGURATION)

show the typical mean exceedance duration of L and L/V at various force levels. The average time duration for $L_{.95}$ and $(L/V)_{.95}$ for these two runs is about 22 m/sec at 60 mph. The advantages of using the 95th percentile lateral load are discussed in detail in Appendix D.

The results of this regression analysis are described in more detail in the next section on track geometry effects. However, the results of this analysis dealing with the effects of speed will be described here. The regression analysis involved trying a variety of different estimating equations for $L_{.95}$. The results showed clearly that the difference in actual speed in comparison with the curve balance speed, was an excellent estimator of the influence of speed on lateral loads at speeds above the balance speed. To describe this speed difference, a parameter known as ΔE , the amount of curve underbalance, was introduced. Underbalance is a measure of how fast the vehicle is going above the design (balance) speed of the curve. It is measured in inches, and refers to the amount of additional superelevation (i.e., additional curve banking) that would be required to balance the outward centrifugal forces on the vehicle at its current speed. FRA Track Safety Standards allow exceeding the curve design speed by an amount equivalent to 3 inches of underbalance. Figure 5-18 illustrates the definition of underbalance.

The use of underbalance, ΔE , in the estimating equations for lateral loads provided a clear trend for the two locomotives, as illustrated in Figure 5-19. That portion of the 95th percentile lateral loads encountered in each of the 25 survey curves which could be "attributed" to underbalance is shown in this figure. The data points represent for each curve the remainder of the actual measured 95th percentile lateral load after subtracting the contribution due to track geometry as predicted by the regression equation. As can be seen, $L_{.95}$ for the SDP-40F axle 10 shows a strong correlation with underbalance (ΔE), whereas the E-8 axle 10 shows a flat response for the range of underbalance observed. These results from the regression analysis of 25 survey run curves therefore suggest that, within the range of test conditions, the characteristic lead axle trends observed at the test site are indeed general, and are a function of underbalance rather than absolute speed.

As a final confirmation of this conclusion, axle 10 data was analyzed from repeat runs over two curves in the test zone having approximately the same geometry, but with different balance speeds. Figure 5-20 shows the effect of speed on the actual measured values of $L_{.95}$ and $(L/V)_{.95}$ for axle 10



$$\Delta E = E_2 - E_1, (+ = \text{UNDERBALANCE})$$

E_1 = EXISTING ELEVATION

E_2 = ELEVATION REQUIRED TO ACHIEVE BALANCE AT
ACTUAL TRAIN SPEED

FIGURE 5-18 DEFINITION OF UNDERBALANCE

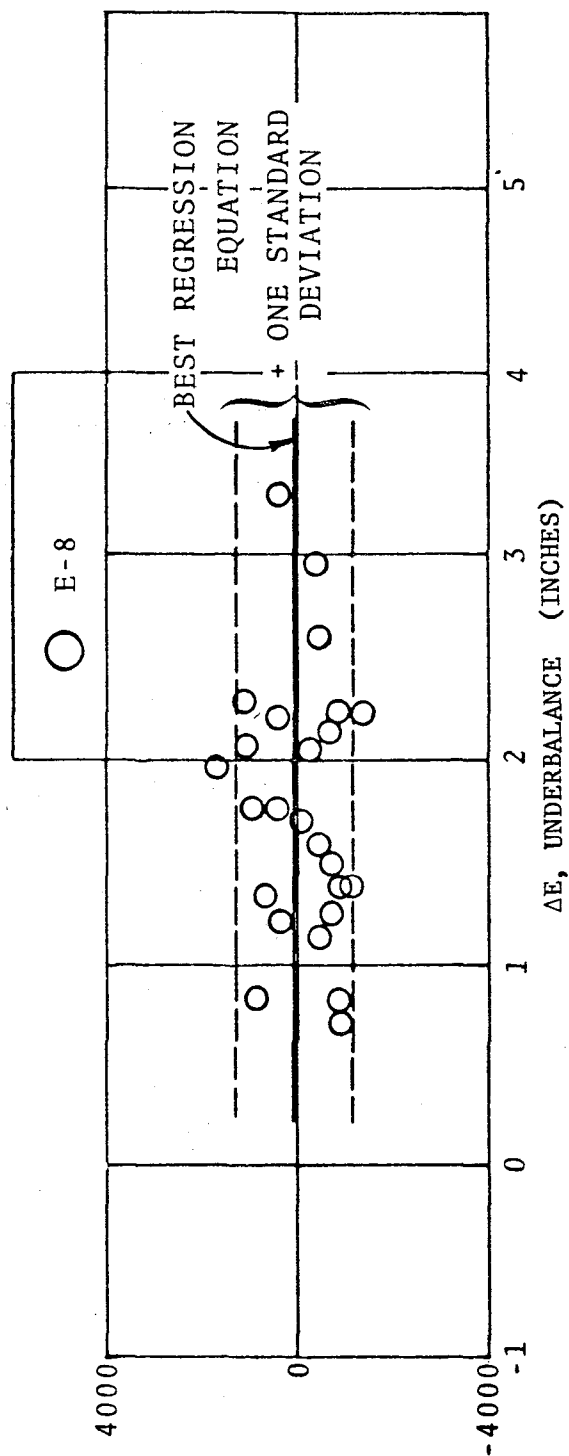
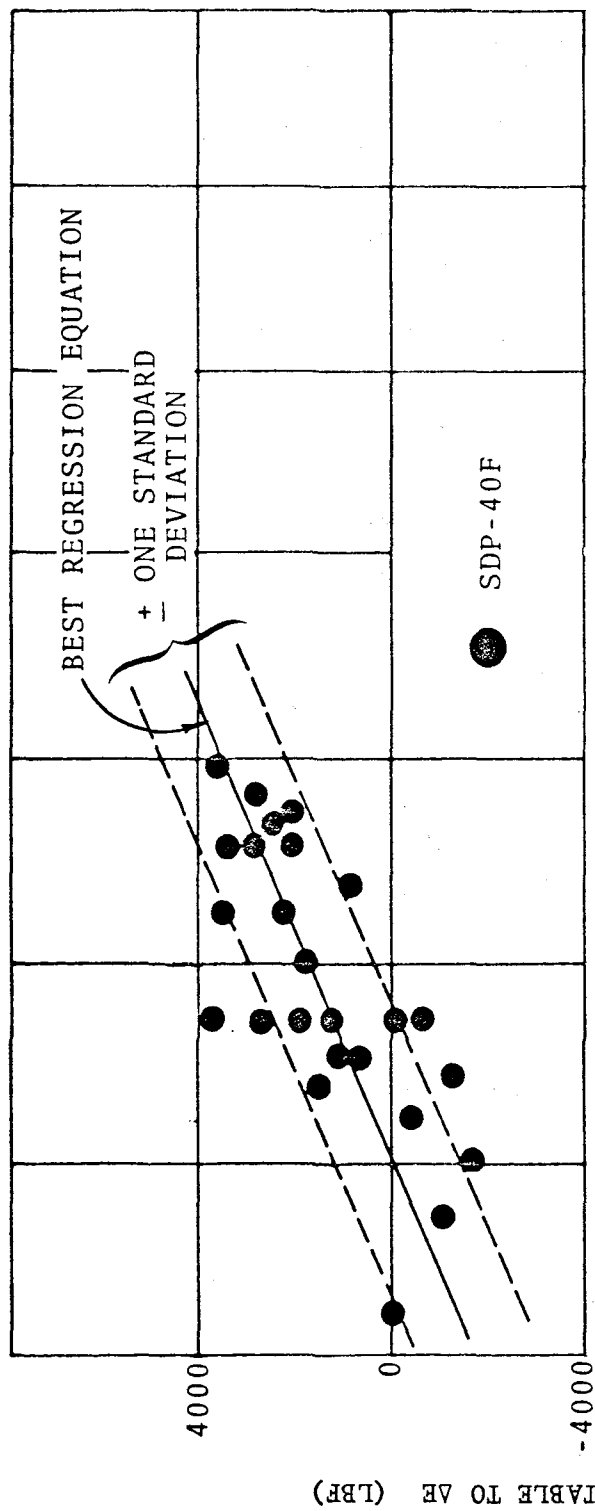


FIGURE 5-19 INFLUENCE OF UNDERBALANCE ON THE SDP-40F AND E-8 L_{95} FORCES FOR AXLE 10 (SURVEY RUN DATA)

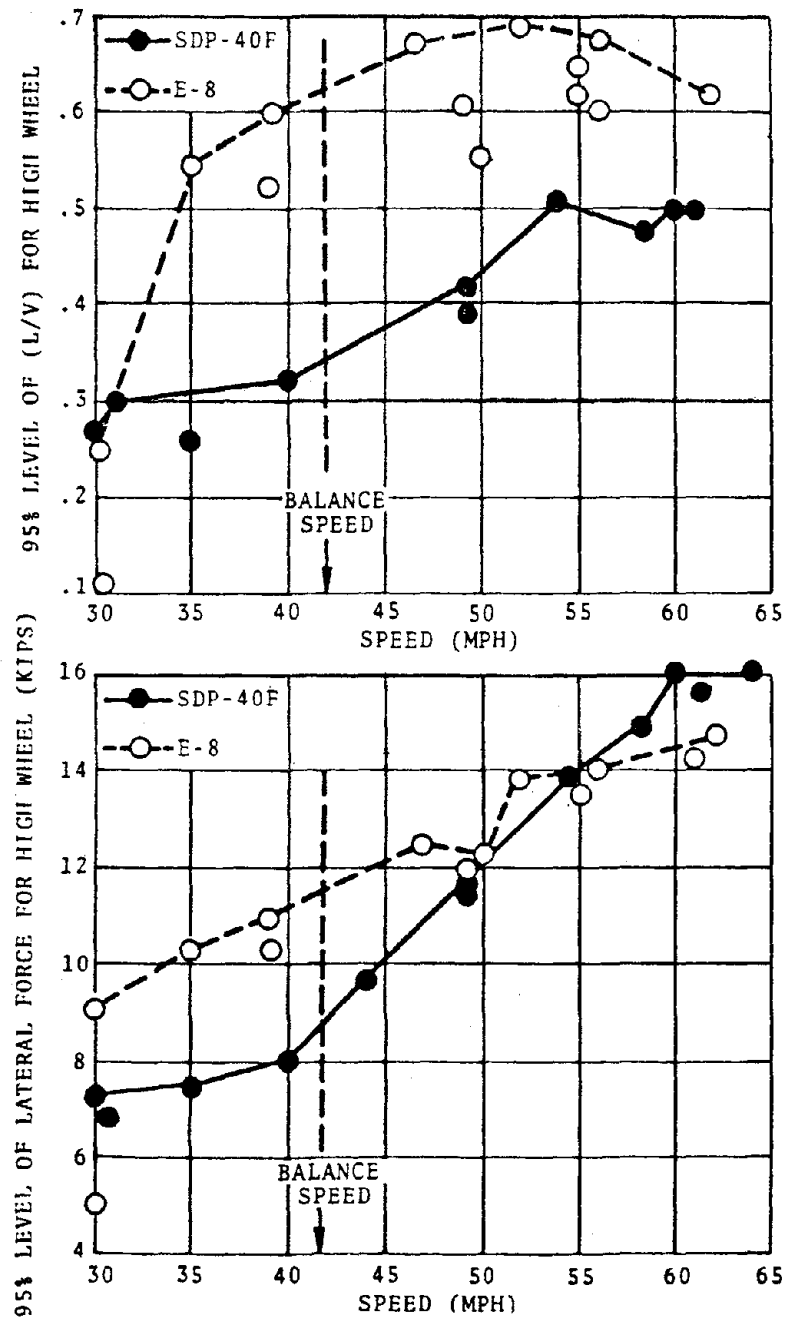


FIGURE 5-20 COMPARISON OF AXLE $10 L_{95}$ AND $(L/V)_{95}$ FOR E-8 AND SDP-40F VERSUS SPEED IN TEST CURVE (BASELINE RUNS, ONBOARD DATA)

through the test curve. The balance speed is 42 mph. Figure 5-21 shows the same information for the curve at milepost 257.2, for which the balance speed is 10 mph greater (52 mph). Comparison of these two figures indicates the same trends previously obtained both at the test site and from the regression analysis of the 25 survey run curves.

Therefore, within the range of the following observed test conditions:

1. Class 3 bolted rail;
2. 2° to 3° curves;
3. Underbalance up to 3"; and
4. Speed range from 30 to 62 mph;

and based upon the following data:

1. A linear regression analysis of the axle 10 data from 25 survey run curves;
2. Onboard repeat run data for axle 10 through two different curves with balance speeds 10 mph apart;
3. Wayside repeat run data at the test site for each lead axle; and
4. Wayside trend data at the test site for each locomotive truck;

it appears that, in general, for the observed range of operating conditions:

1. The E-8 and SDP-40F characteristic truck and lead axle responses are a function of amount of underbalance rather than absolute speed.
2. The SDP-40F is much more sensitive than the E-8 to operation above balance speed.
3. Below balance speed, the SDP-40F truck and lead axle forces are either comparable to or less than those of the E-8.
4. Above balance speed, the SDP-40F truck and lead axle forces begin to increase very rapidly and can become significantly greater than those of the E-8.

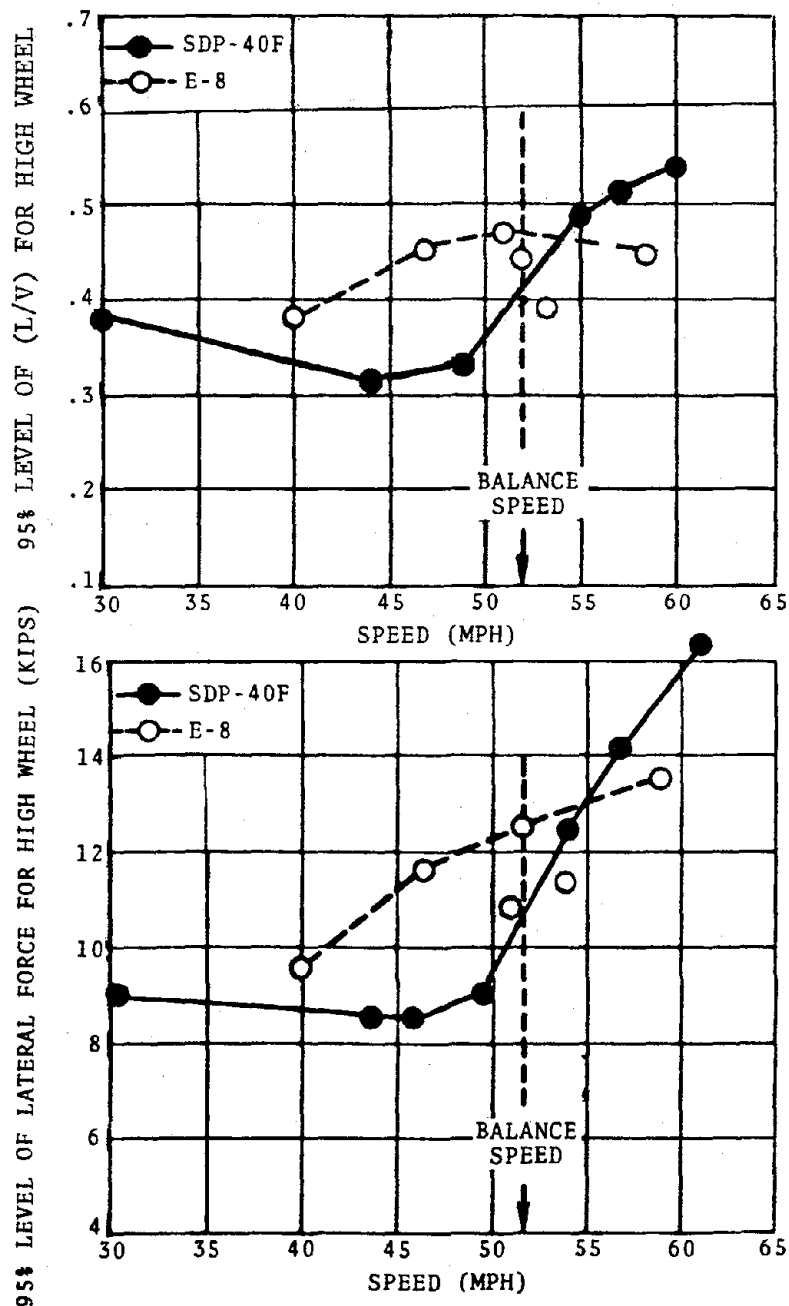


FIGURE 5-21 COMPARISON OF AXLE 10 L_{95} AND $(L/V)_{95}$ FOR E-8 AND SDP-40F VERSUS SPEED IN CURVE AT MP 257.2 (BASELINE RUNS, ONBOARD DATA)

Why should the SDP-40F exhibit a response to speeds above balance speed that is different from that of the E-8? Unfortunately, the complexity of the locomotive/track dynamic system and the lack of sufficiently detailed explanatory models makes this question unanswerable at the present time. Model development activities currently being sponsored by FRA should satisfy this need.

5.1.2 Effect of Track Geometry

The complex dynamic interaction between a rail vehicle and the track make isolation of any one contributing effect quite difficult. In order to isolate the influence that track geometry exerts on the E-8 and SDP-40F dynamic response, it would have been desirable to hold all other parameters constant while performing test runs over differing components of track geometries. Within the limits of this test project, such a series of tests was not feasible; however, the survey runs have provided a reasonable approximation to this "ideal" test series. In these runs, the number of major variables affecting the baseline locomotive configuration's dynamic response have been limited to speed and track geometry. A method was found which could successfully separate from the data the individual effects of speed and the more important components of track geometry. This method, called regression analysis, and its application to the survey run data, are described in detail in Appendix E. The remainder of this section will describe the results of this analysis.

Regression equations developed for axle 10 from a statistical regression analysis of 25 curves between 2° and 3° of the survey runs are presented in Figure 5-22. For the E-8, these equations relate L_{95} to the standard deviation of curvature and the square of the standard deviation of gage in each test curve. Due to the fact that the tested E-8 had an unbalanced weight distribution between its left and right sides, a correction factor for left and right-hand curves was also extracted from the regression analysis. For the SDP-40F, the regression equations include the variables of mean curvature and underbalance as well as curvature and gage deviations.

Although alignment does not appear explicitly in these equations, this is only because the track geometry cars did not have an alignment measuring capability. However, the measurements of curvature and gage variation are implicit measures of track alignment. As discussed in Appendix B, σ_c (the curvature deviation) is a measure of the longer

$$\text{SDP-40F } L_{95} = 4100 + 400(\bar{C}) + 17,300(\sigma_c) + 40,100(\sigma_G^2) + 1800(\Delta E) \quad R^2 = 0.8 \\ S_e = 1200 \text{ (LBF)}$$

$$\text{E-8 } L_{95} = 7700 + 9400(\sigma_c) + 74,700(\sigma_G^2) \begin{bmatrix} + 600 \text{ FOR LEFT CURVE} \\ - 600 \text{ FOR RIGHT CURVE} \end{bmatrix} \quad R^2 = 0.8 \\ S_e = 900 \text{ (LBF)}$$

TYPE AND RANGE OF TRACK DESCRIPTORS USED IN REGRESSION ANALYSIS		\bar{C}	σ_c	σ_G^2	ΔE	R or L
	MIN	2°	.13°	.01 in ²	0 in	-1 or
	MAX	3°	.32°	.073 in ²	3 in	+1

<u>SDP-40F</u>	CONSTANT	\bar{C}	σ_c	σ_G^2	ΔE	R or L	TOTAL (L_{95})
COEFFICIENT FROM REGRESSION ANALYSIS	4,100	400	17,300	40,100	1,800	--	
MIN. VALUE, LBF	4,100	800	2,200	400	0	--	7,500
MAX. VALUE, LBF	4,100	1,200	5,500	2,900	5,400	--	19,200

<u>E-8</u>	CONSTANT	\bar{C}	σ_c	σ_G^2	ΔE	R or L	TOTAL (L_{95})
COEFFICIENT FROM REGRESSION ANALYSIS	7,700	-	9,400	74,700	--	600	
MIN. VALUE, LBF	7,700	-	1,200	700	--	-600	9,100
MAX. VALUE, LBF	7,700	-	3,000	5,500	--	+600	16,800

NOTATION:

- \bar{C} - MEAN CURVATURE, DEGREES
 σ_c - STANDARD DEVIATION OF CURVATURE, DEGREES
 σ_G^2 - STANDARD DEVIATION OF GAGE, INCHES
 ΔE - UNDERBALANCE, INCHES
 R or L - RIGHT OR LEFT DIRECTION OF CURVE IN DIRECTION OF LOCOMOTIVE TRAVEL

FIGURE 5-22 INFLUENCE OF VARIOUS TRACK DESCRIPTORS IN EQUATION FOR L_{95} on AXLE 10 OF SDP-40F AND E-8 BASED ON RESULTS OF REGRESSION ANALYSIS

wavelength alignment variations (>80 feet), while σ_G (the gage deviation) is related more to the high rail alignment variations occurring from joint to joint. Other track geometry parameters such as crosslevel deviations and deviations on high rail profile were found to have little correlation with the lateral loads (crosslevel deviations, however, did have a strong effect on L/V ratios).

Two techniques were used to test the accuracy or predictive power of these equations. The first was the standard statistical test of determining the value of R^2 , the coefficient of determination, and the "standard error," S_e . R^2 is a measure of the percentage decrease in data scatter obtained by the regression technique. If $R^2 = 1.0$, then the data points are predicted exactly by the regression equation, and there is no residual scatter in the data. If $R^2 = 0$, the equation exhibits no ability to reduce the data scatter. The standard error is a measure of the magnitude of the residual scatter. In effect, it provides an estimate of the width of a "scatterband" around the predictions of the regression equation. Suppose that for a certain combination of values of the track geometry descriptors, the predicted value of L_{95} is L_{95} . Then, for a Gaussian scatter distribution, the probability that additional measurements of L_{95} for other curves with the same track geometry will fall between $(L_{95} - S_e)$ and $(L_{95} + S_e)$ is 0.68, or 68%.* Similarly, the probability that additional observations will fall between $(L_{95} - 2 S_e)$ and $(L_{95} + 2 S_e)$ is 0.95, or 95%. If S_e is small compared to L_{95} , then one can be reasonably confident about the predicted values. The values of R^2 and S_e obtained for the equations in Figure 5-22 are also shown in that same figure. These values demonstrate a high degree of accuracy in the predictions provided by these equations.

The second test of the validity of these equations was to use them to predict the values of L_{95} anticipated in runs through the test curve at milepost 257.5. The data from the test curve had not been used in the development of the prediction equations. The ability of the regression equations to predict the values of L_{95} for the SDP-40F and E-8 for various speed runs through the test curve is shown

*In our particular case, 80% of the survey run data falls between $\pm 1 S_e$ of the predicted values obtained from the linear regression equations that have been developed, providing an even greater confidence level.

in Figures 5-23 and 5-24, respectively. The values used in the prediction equations for the test site were:

$$\bar{c} = 2^{\circ}06'$$

$$\sigma_G = 0.2 \text{ inches}$$

$$\sigma_c = 0.3^{\circ}$$

$$\Delta E = 0 \text{ to } 3 \text{ inches (corresponding to 42 to 62 mph)}$$

The accuracy of the predictions is apparent. Based on these two checks, the use of the regression equations to describe the influence of track geometry (and speed) seems justified.

The regression equations were used to prepare Figures 5-25 through 5-29. These figures show the predicted values of L_{95} for four categories of track geometry described in Table 5-1. The analysis was performed for a 2.5° curve and a locomotive speed corresponding to $3.0''$ of ΔE , which is the maximum allowable overspeed as specified in the FRA Track Safety Standards. The four track geometry categories correspond to the range of track quality variations encountered in the survey runs. "Poor" curvature and gage represent the worst variations observed in these runs. As can be seen from the bar chart, in going from the best observed track geometry to the poorest (all nominally Class 3), L_{95} track forces can increase by as much as 80 percent. The equations made it possible to estimate the portions of L_{95} due to speed, curvature, curvature variation and gage variation for each combination. The E-8 is more sensitive to gage variations (i.e., typically short wavelength alignment irregularities), while the SDP-40F is more sensitive to overspeed and curvature variations (i.e., long wavelength alignment irregularities).

Figures 5-26 through 5-29 show the values of L_{95} predicted by the equations for the two locomotives as a function of underbalance and various track conditions. For the range of track quality observed, axle 10 of the SDP-40F will consistently have lower lateral forces than those of the E-8 when below balance speed. The crossing point ranges from about $1/2$ to 3 inches of underbalance, depending upon track quality, and is most significantly affected by the amplitude of the short wavelength lateral irregularities. When the amplitude of these irregularities is large, the E-8 axle 10 will remain higher than the SDP-40F through most of the speed regime. Note that this conclusion is not necessarily

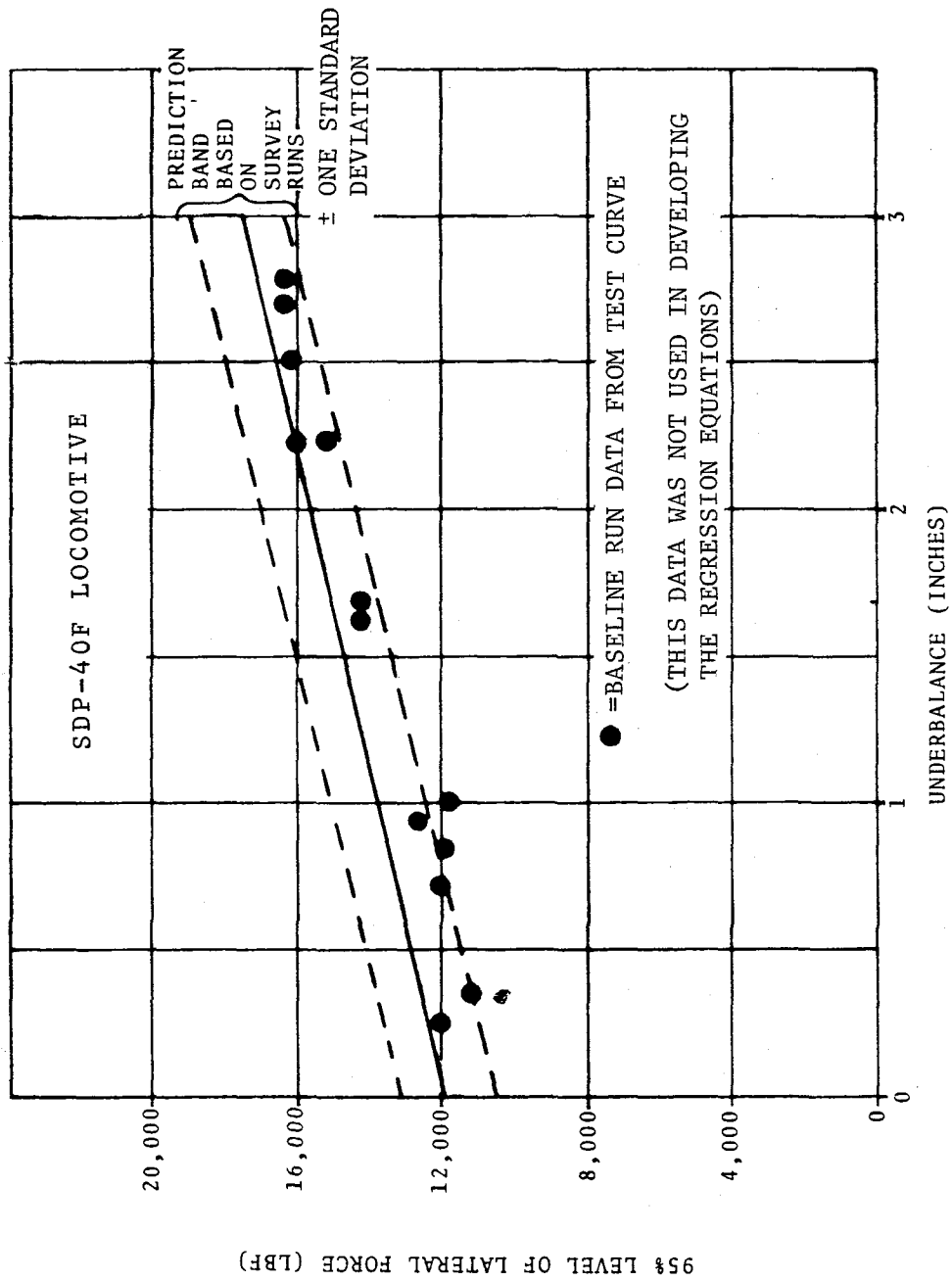


FIGURE 5-23 COMPARISON OF PREDICTED SDP-40F AXLE 10 RESPONSE FROM REGRESSION ANALYSIS WITH BASELINE RUN DATA, IN TEST CURVE, AS A FUNCTION OF UNDERBALANCE

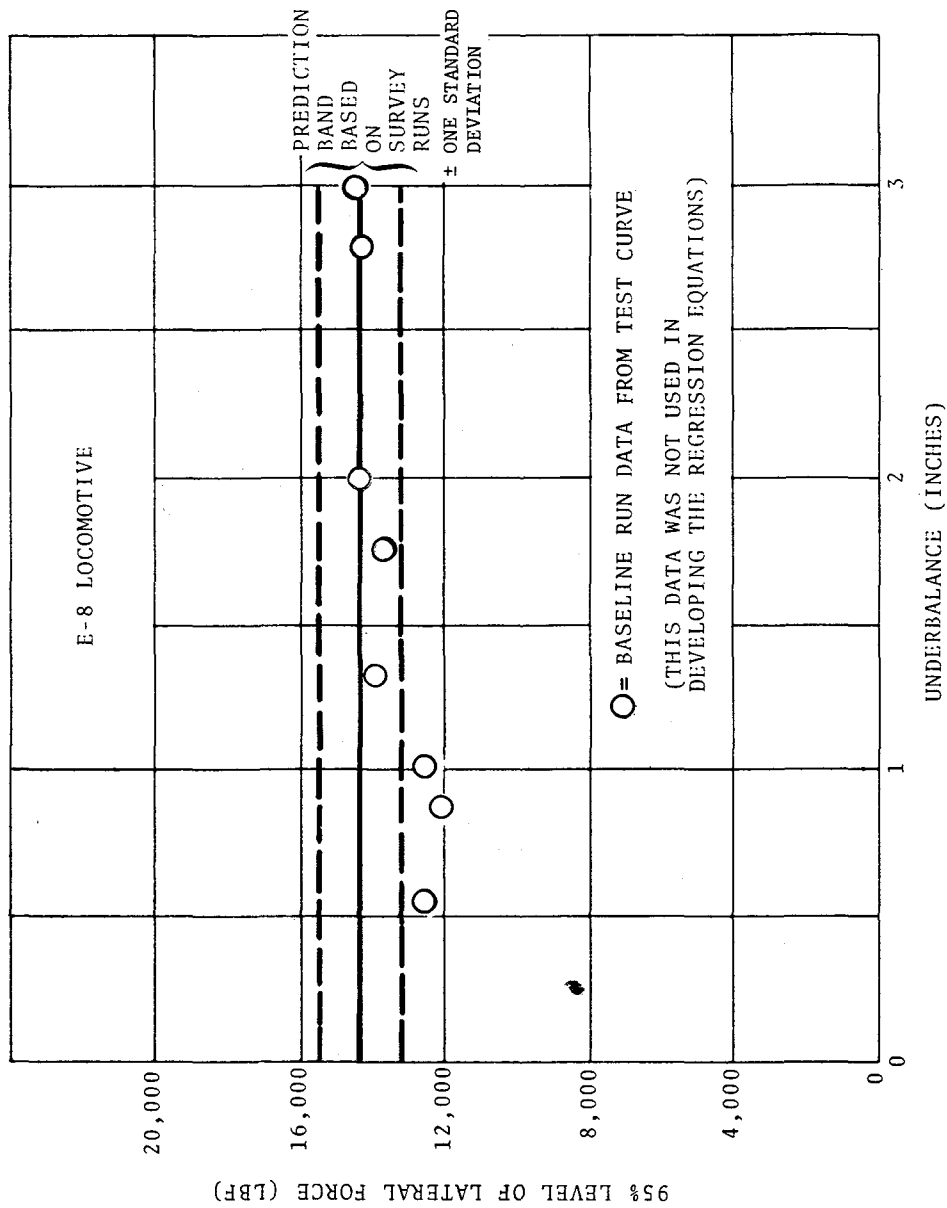
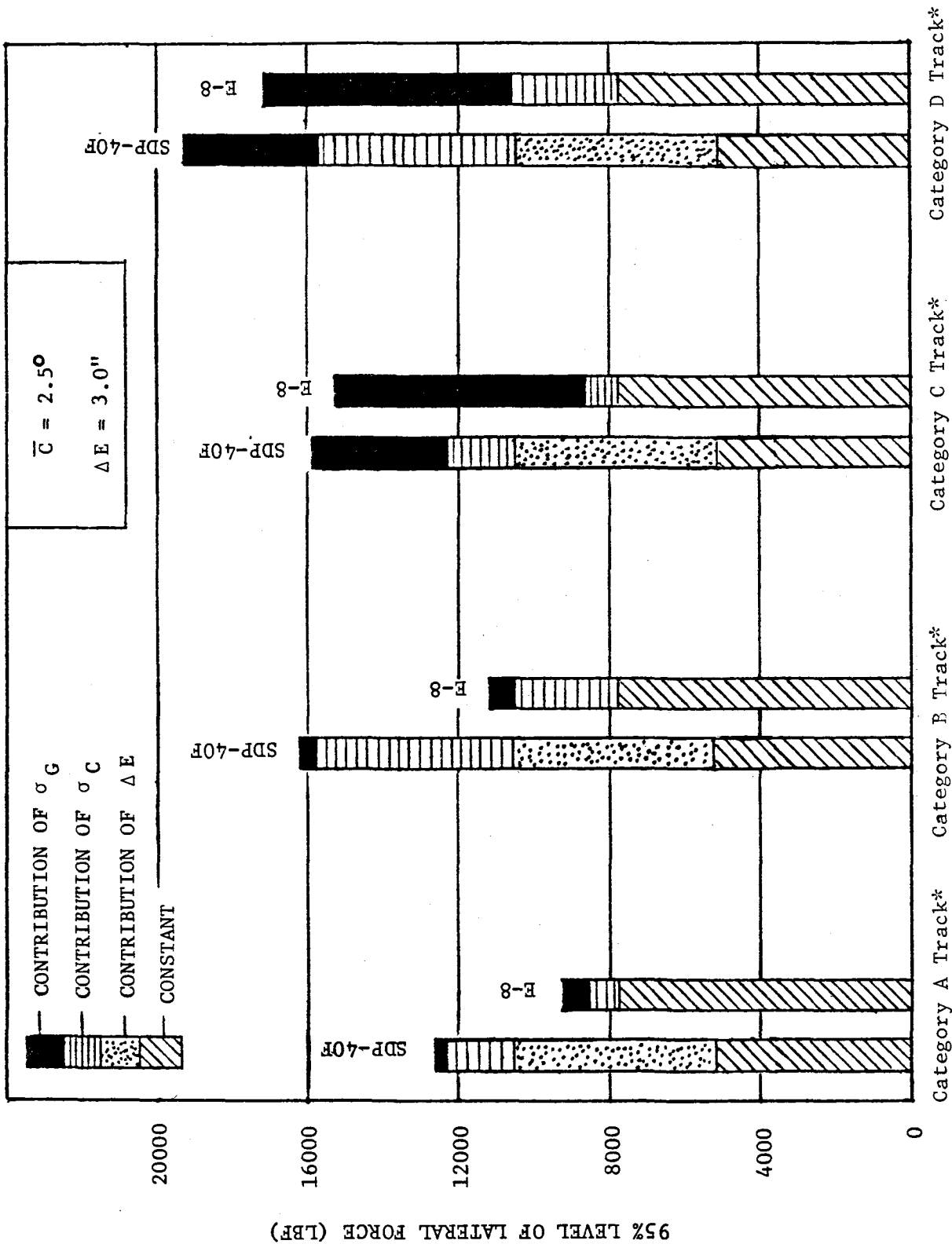


FIGURE 5-24 COMPARISON OF PREDICTED E-8 AXLE 10 RESPONSE FROM REGRESSION ANALYSIS WITH BASELINE RUN DATA, IN TEST CURVE, AS A FUNCTION OF UNDERBALANCE



*See Table 5-1 for definition of categories of track.

FIGURE 5-25 COMPARISON OF AXLE 10 SENSITIVITY PREDICTIONS FOR E-3 AND SDP-40F FROM STATISTICAL REGRESSION ANALYSIS

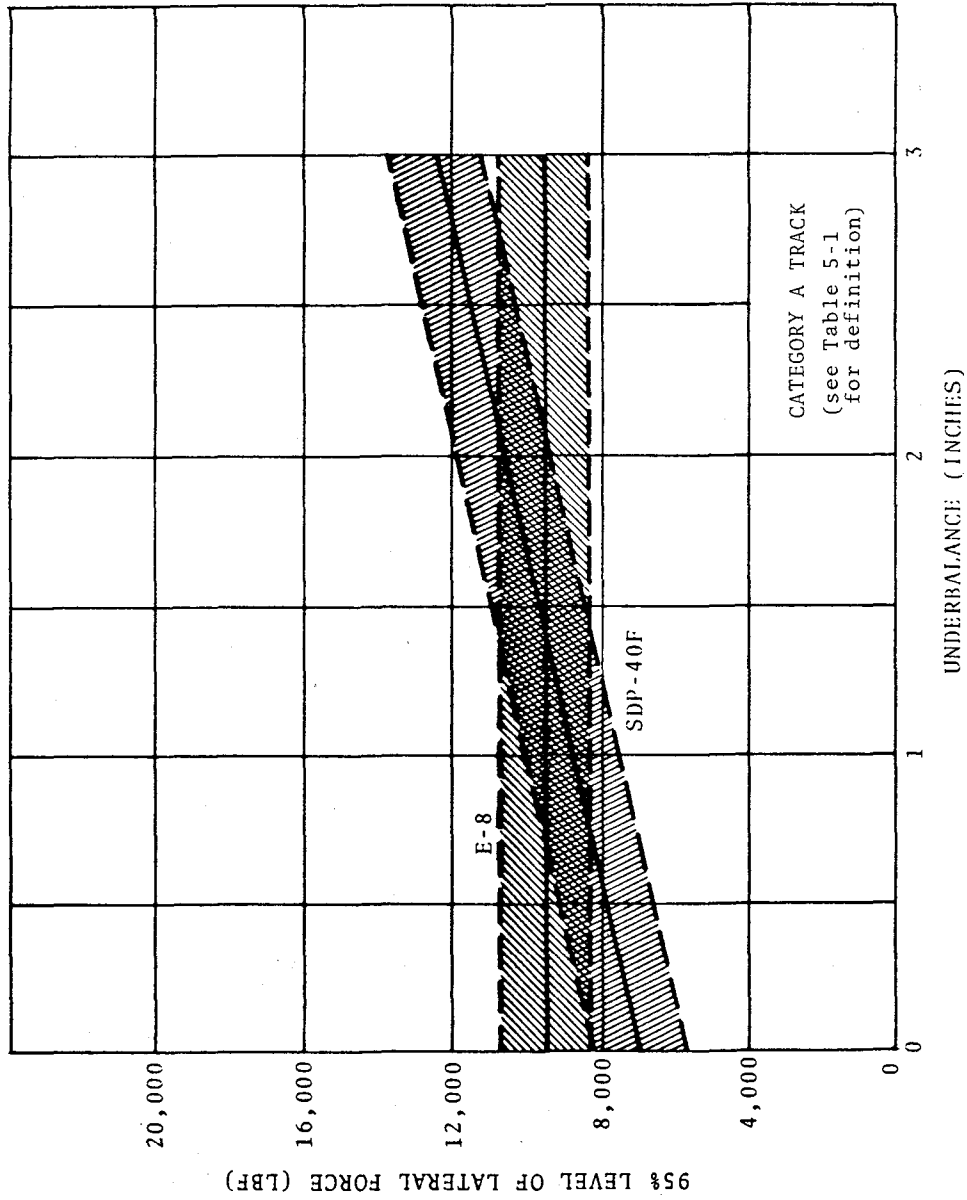


FIGURE 5-26 REGRESSION ANALYSIS PREDICTION FOR L_{95} OF AXLE 10 FOR E-8 AND SDP-40F, AS A FUNCTION OF UNDERBALANCE, FOR CATEGORY A TRACK

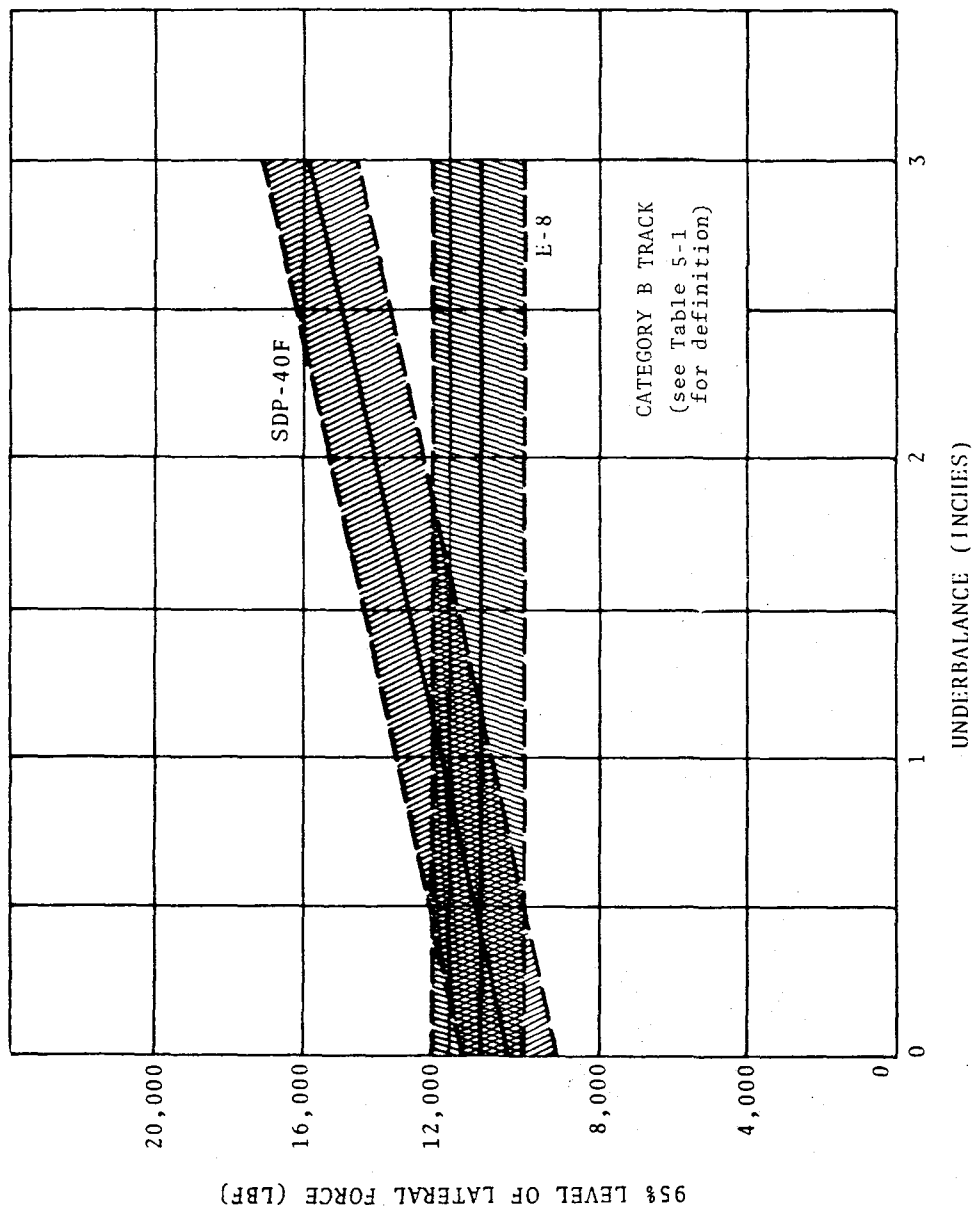


FIGURE 5-27 REGRESSION ANALYSIS PREDICTION FOR L95 OF AXLE 10 FOR E-8 AND SDP-40F, AS A FUNCTION OF UNDERBALANCE, FOR CATEGORY B TRACK

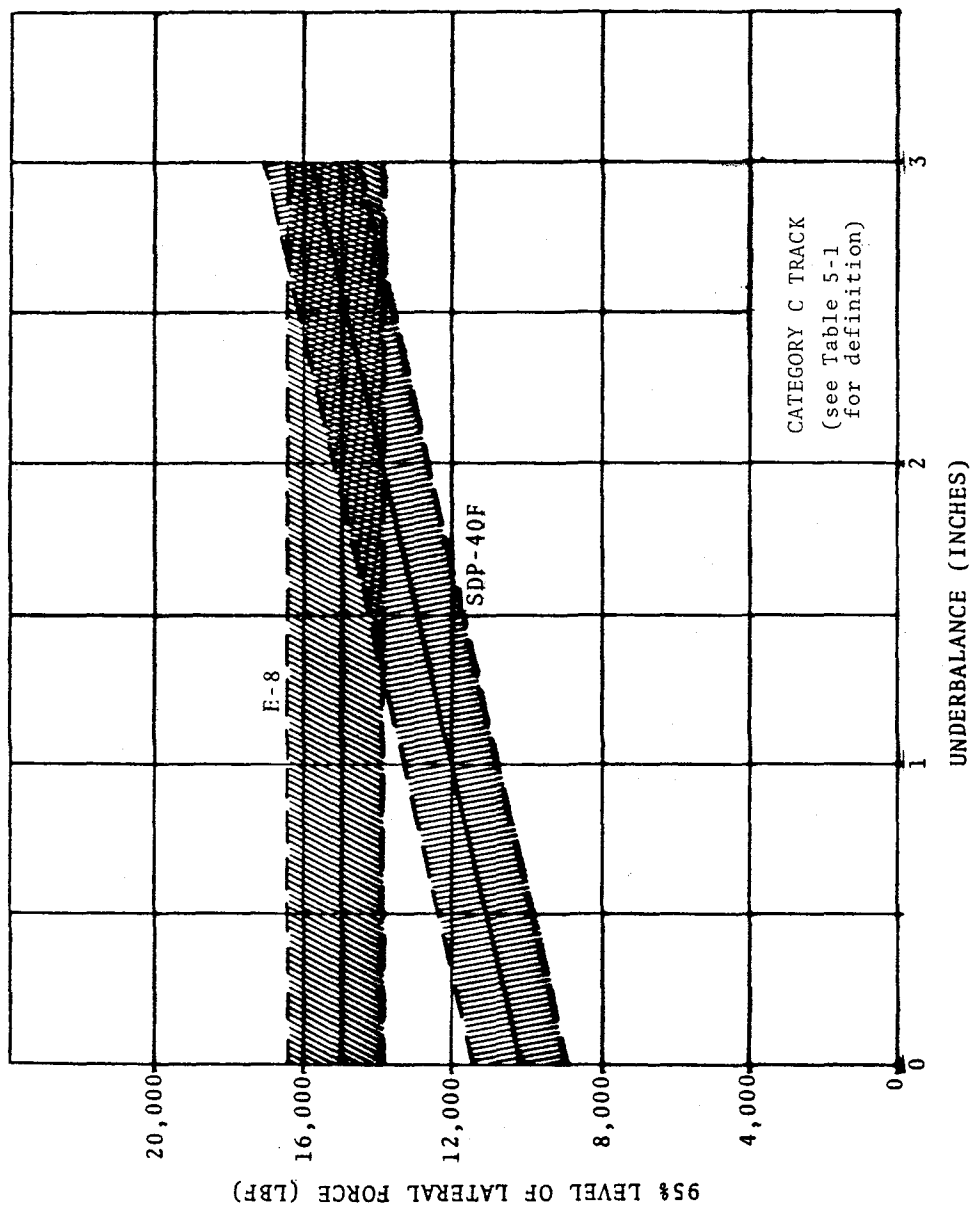


FIGURE 5-28 REGRESSION ANALYSIS PREDICTION FOR L₉₅ OF AXLE 10 FOR E-8 AND SDP-40F, AS A FUNCTION OF UNDERBALANCE, FOR CATEGORY C TRACK

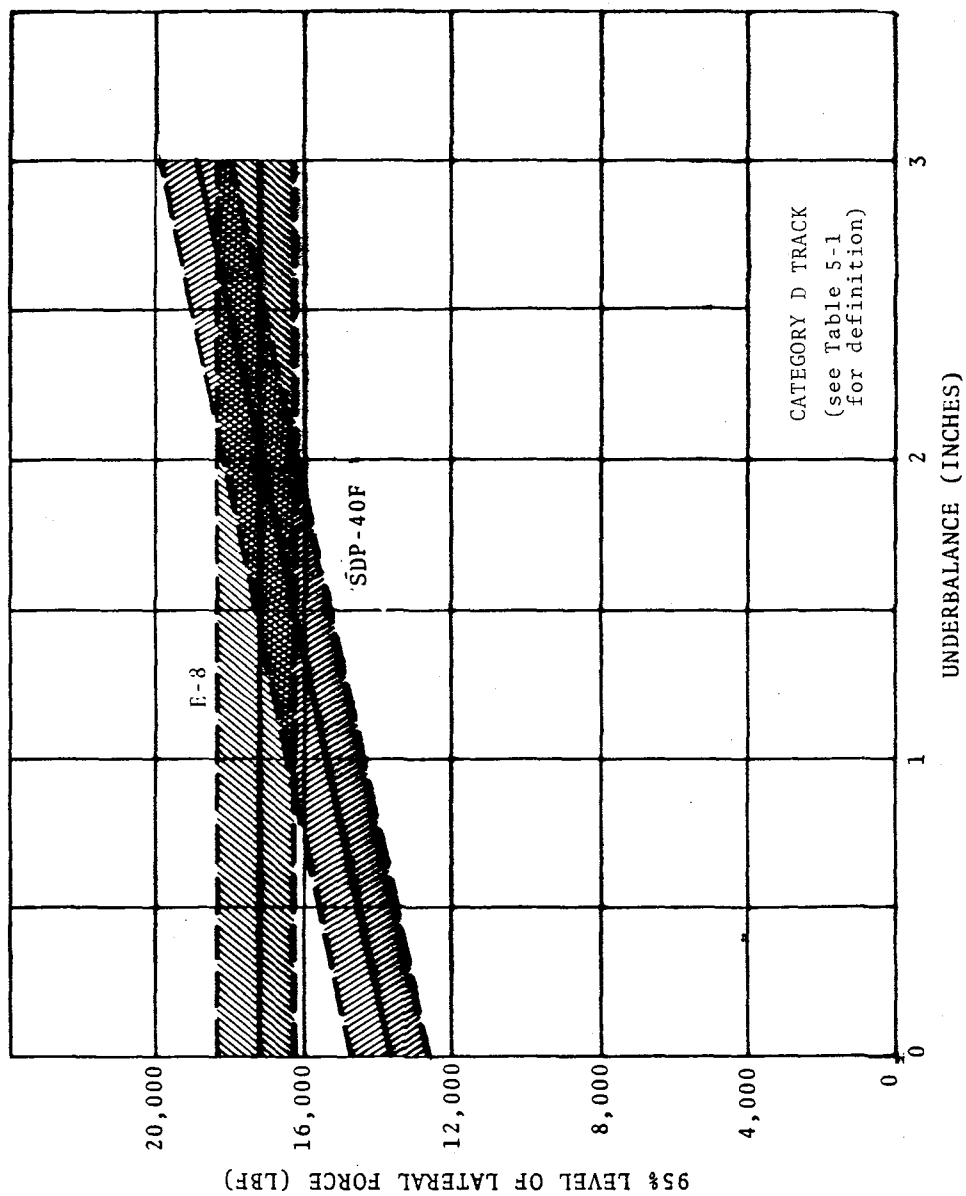


FIGURE 5-29 REGRESSION ANALYSIS PREDICTION FOR L_{95} OF AXLE 10 FOR E-8 AND SDP-40F, AS A FUNCTION OF UNDERBALANCE, FOR CATEGORY D TRACK

TABLE 5-1 SUMMARY OF TRACK GEOMETRY CHARACTERISTICS
USED IN PREPARING FIGS. 5-25 THROUGH 5-29

Track Geometry Categories (1) *	Long Wavelength Lateral Irregularities ("Curvature" Variation) (2) *	Short Wavelength Lateral Irregularities ("Gage" Variation) (3) *
A	Small ($\sigma_C = 0.1^\circ$)	Small ($\sigma_G = 0.1''$)
B	Large ($\sigma_C = 0.3^\circ$)	Small ($\sigma_G = 0.1''$)
C	Small ($\sigma_C = 0.1^\circ$)	Large ($\sigma_G = 0.3''$)
D	Large ($\sigma_C = 0.3^\circ$)	Large ($\sigma_G = 0.3''$)

* NOTES:

- (1) Combinations of track irregularities used in preparing Figs. 5-25 through 5-29.
- (2) Corresponds to long wavelength alignment deviations (≥ 2 rail lengths). The magnitudes for σ_C correspond to the upper and lower bounds observed in the survey runs.
- (3) Corresponds to short wavelength alignment deviations (≥ 1 rail length dominated by high rail alignment variations occurring from joint to joint) and/or rapid change in gage ($> 1/2$ rail length). The magnitudes for σ_G correspond to the upper and lower bounds observed in the survey runs.

valid for truck lateral loads on the high rail because of the higher SDP-40F middle axle loads. Also, it should be remembered that, as shown at the test site, axle 10 of the SDP-40F was typically the lowest responding lead axle, while for the E-8, axle 10 was typically its highest responding axle.

This same regression technique was applied to data on vertical loads, V , and lateral to vertical load ratio, L/V . Since high values of L/V , corresponding to low values of V , are more critical in derailment processes, the 95th percentile level of L/V and the 5th percentile level of V were used. The results of the regression analyses for these two variables are presented in Figures 5-30 and 5-31.

For V_5 , from Figure 5-30, the ΔE effect is small for both locomotives, and less than 10% of the constant term in the equation. No other track parameters appear to have a significant effect on V_5 for the range of crosslevel and profile observed in the survey runs. For $(L/V)_{95}$, from Figure 5-31 the ΔE effect is quite large for the SDP-40F, but quite small for the E-8. In addition, the correlation coefficients are relatively low. This is probably due to the 4 per revolution sample and hold procedure for V , whereas L was obtained continuously. This effect was confirmed by the large scatter seen in L/V in the repeat runs.

Because of the importance of gage variations on lateral loads, some insight into the sources of these variations would be useful. One possible mechanism which should explain the coincidence of the maximum gage variations and peak lateral wheel loads at the high rail joints is shown in Figure 5-32. Localized rail alignment change can develop at the high rail joint due to the repeated application of curving forces on the high rail. The relationship between high rail joints and gage variation is shown in Figure 5-33 based on data obtained from track geometry car measurements. The ALD markers are located at the joints. There, signals indicate that the local maximums in gage variation occur at the high rail joints. Half-rail length gage changes on the order of 0.8 to 1.0 inches within 19 feet were not uncommon in this 4-mile test zone. As can be seen in Figure 5-34, peak wheel forces occur immediately after joints on the high rail (within $1/4$ rail length), while mid-rail sections typically have very low forces. These peak lateral forces increase with speed and, at posted speeds, are commonly 2 to 4 times higher than the steady state curving force, which is

$$\text{SDP-40F } V_5 = 23,600 + 700(\Delta E) \begin{bmatrix} + 700 \text{ FOR RIGHT CURVE} \\ - 700 \text{ FOR LEFT CURVE} \end{bmatrix} \quad \begin{matrix} R^2 = 0.65 \\ S_e = 800 \text{ (LBF)} \end{matrix}$$

$$\text{E-8 } V_5 = 18,900 + 600(\Delta E) \begin{bmatrix} + 3200 \text{ FOR RIGHT CURVE} \\ - 3200 \text{ FOR LEFT CURVE} \end{bmatrix} \quad \begin{matrix} R^2 = 0.94 \\ S_e = 900 \text{ (LBF)} \end{matrix}$$

TYPE AND RANGE OF TRACK DESCRIPTORS USED IN REGRESSION ANALYSIS	ΔE R or L	
	MIN	0 in -1 or
	MAX	3 in +1

<u>SDP-40F</u>	CONSTANT	ΔE	R or L	TOTAL (V_5)
COEFFICIENT FROM REGRESSION ANALYSIS	23,600	700	700	
MIN. VALUE, LBF	23,600	0	-700	22,900
MAX. VALUE, LBF	23,600	2100	+700	26,400

<u>E-8</u>	CONSTANT	ΔE	R or L	TOTAL (V_5)
COEFFICIENT FROM REGRESSION ANALYSIS	18,900	600	3200	
MIN. VALUE, LBF	18,900	0	-3200	15,700
MAX. VALUE, LBF	18,900	1800	+3200	23,900

NOTATION:

ΔE - UNDERBALANCE, INCHES

R or L - RIGHT OR LEFT DIRECTION OF CURVE IN DIRECTION OF
LOCOMOTIVE TRAVEL

FIGURE 5-30 INFLUENCE OF VARIOUS TRACK DESCRIPTORS IN EQUATION FOR V_5
ON AXLE 10 OF SDP-40F AND E-8 BASED ON RESULTS OF REGRESSION ANALYSIS

$$\text{SDP-40F } (L/V)_{95} = 0.14 + 0.53(\sigma_c) + 0.10(\Delta E) \begin{bmatrix} + 0.05 \text{ FOR RIGHT CURVE} \\ - 0.05 \text{ FOR LEFT CURVE} \end{bmatrix} \quad \begin{matrix} R^2 = 0.6 \\ S_e = 0.08 \end{matrix}$$

$$\text{E-8 } (L/V)_{95} = 0.32 + 4.34(\sigma_c \sigma_{XE}) \quad \begin{matrix} R^2 = 0.22 \\ S_e = 0.21 \end{matrix}$$

TYPE AND RANGE OF TRACK DESCRIPTORS USED IN REGRESSION ANALYSIS	σ_c	ΔE	σ_{XE}	$\sigma_c \sigma_{XE}$	R or L
MIN	.13°	0 in	.15 in	0.02° in	-1 or
MAX	.32°	3 in	.56 in	0.18° in	+1

<u>SDP-40F</u>	CONSTANT	σ_c	ΔE	$\sigma_c \sigma_{XE}$	R or L	TOTAL $(L/V)_{95}$
COEFFICIENT FROM REGRESSION ANALYSIS	0.14	0.53	0.10	-	0.05	
MIN. VALUE, LBF	0.14	0.07	0	-	-0.05	0.16
MAX. VALUE, LBF	0.14	0.17	0.3	-	+0.05	0.66

<u>E-8</u>	CONSTANT	σ_c	ΔE	$\sigma_c \sigma_{XE}$	R or L	TOTAL $(L/V)_{95}$
COEFFICIENT FROM REGRESSION ANALYSIS	0.32	-	-	4.34	-	
MIN. VALUE, LBF	0.32	-	-	0.09	-	0.41
MAX. VALUE, LBF	0.32	-	-	0.78	-	1.10

NOTATION:

- σ_c - STANDARD DEVIATION OF CURVATURE, DEGREES
- ΔE - UNDERBALANCE, INCHES
- σ_{XE} - STANDARD DEVIATION OF CROSS ELEVATION, INCHES
- R or L - RIGHT OR LEFT DIRECTION OF CURVE IN DIRECTION OF LOCOMOTIVE TRAVEL

FIGURE 5-31 INFLUENCE OF VARIOUS TRACK DESCRIPTORS IN EQUATION FOR $(L/V)_{95}$ ON AXLE 10 OF SDP-40F AND E-8 BASED ON RESULTS OF REGRESSION ANALYSIS

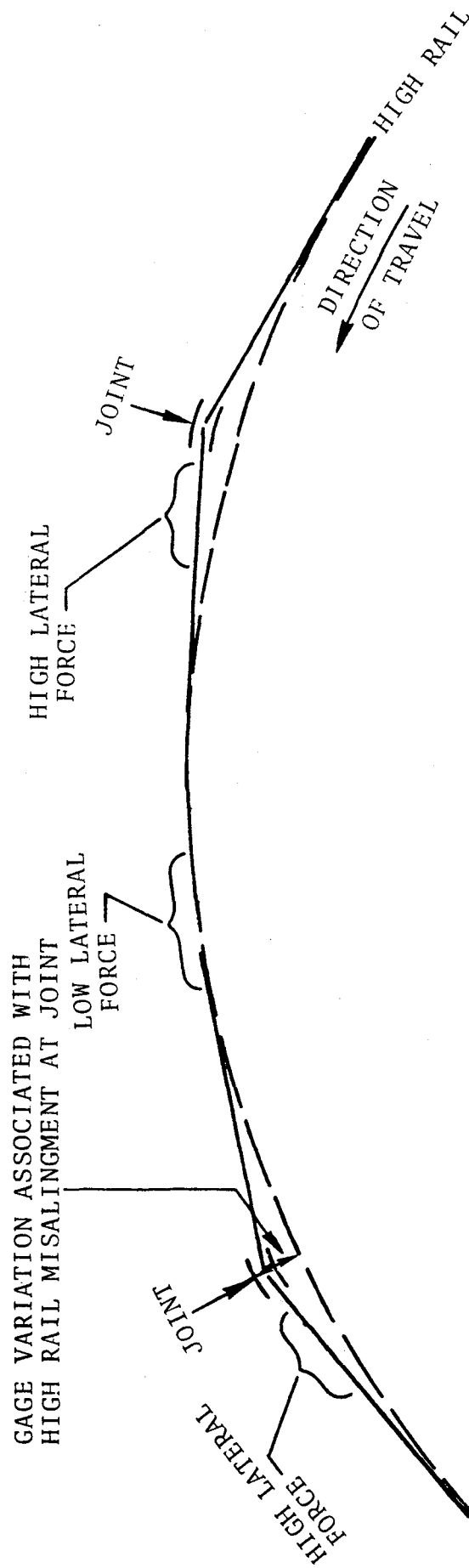


FIGURE 5-32 POSSIBLE MECHANISM EXPLAINING COINCIDENCE OF PEAK LATERAL LOADS AND PEAK GAGE VARIATIONS NEAR HIGH RAIL JOINTS

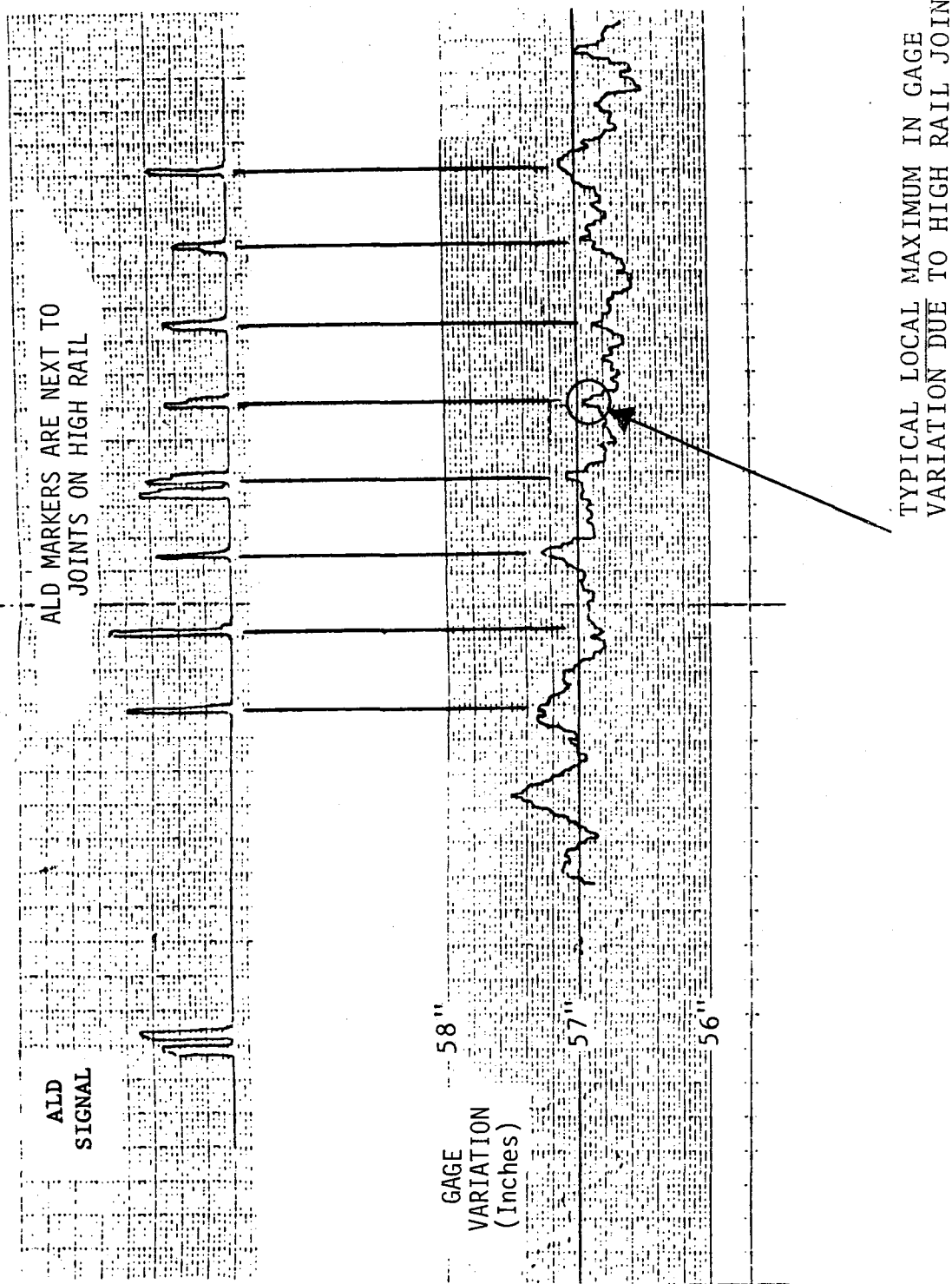


FIGURE 5-33 BRUSH CHART RECORDING SHOWING VERIFICATION OF GAGE VARIATION WITH RESPECT TO HIGH RAIL JOINT LOCATIONS

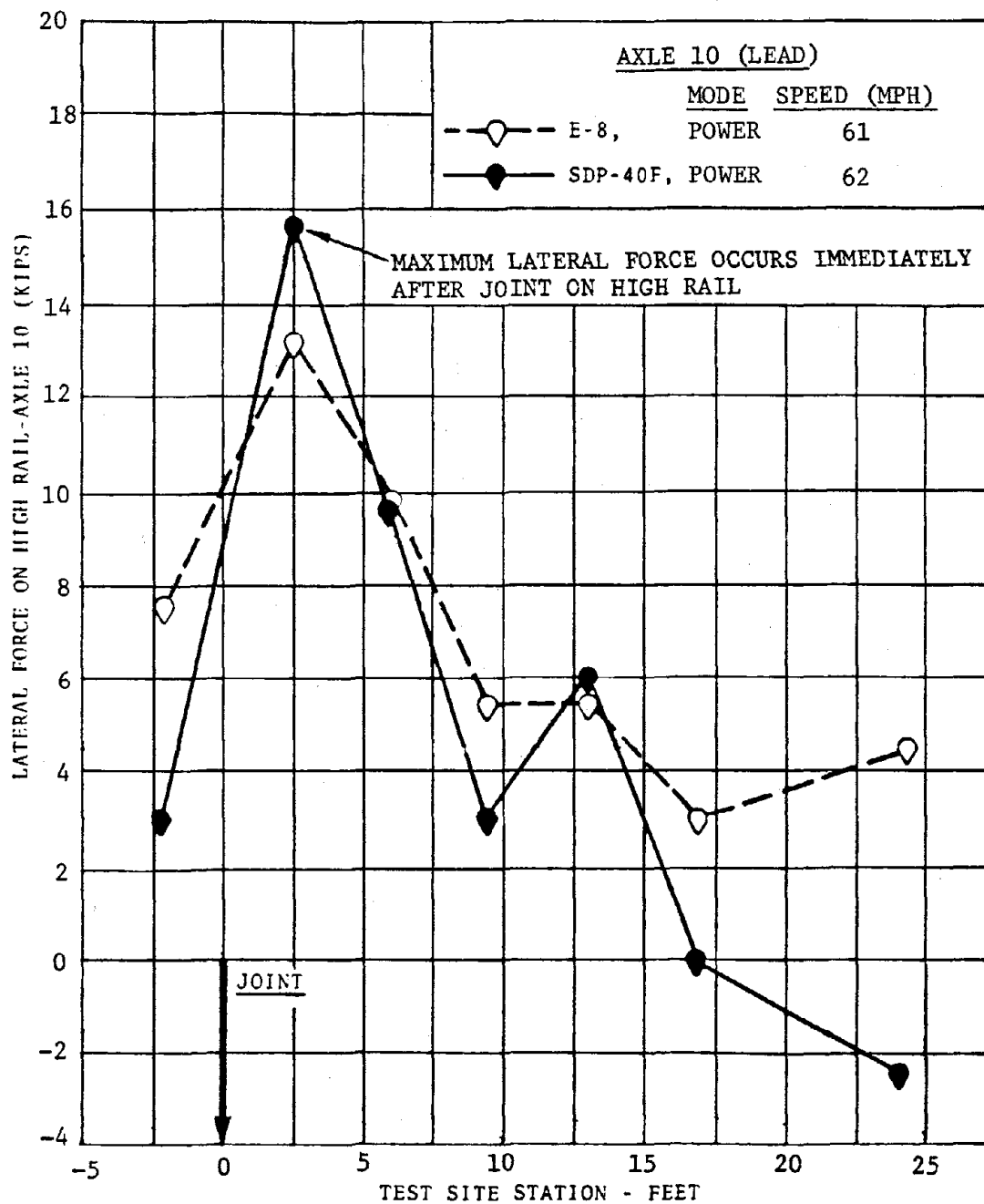


FIGURE 5-34. TYPICAL AXLE 10 LATERAL FORCE TRACES AT TEST SITE, E-8 AND SDP-40F NEAR 60 MPH (WAYSIDE DATA)

on the order of 6 to 7 kips.* These peak forces appear to be in response to the rapid change in gage (from increasing to decreasing) that generally occurs in the immediate vicinity of a joint on the high rail and which appears to be due to local high rail misalignment.

Curvature variations are also an important parameter in determining lateral load. Track curvature variations are related to the longer wavelength alignment irregularities (>80 ft.). There are many sources for these longer wavelength irregularities, most being related to weakening of the overall track structure.

The success of the regression equations in predicting the effects of track geometry variations and speed on lateral wheel loads of axle 10 is most promising. Additional analyses of the Chessie data could lead to a set of prediction equations with applicability over a broader range of curvatures. It must be kept in mind, however, that there was a substantial difference in the regression equations for the SDP-40F and the E-8, indicating that neither of these equations is probably suitable for predicting lateral wheel forces on other locomotives and track and operating conditions beyond the range indicated previously. Only similar testing of each locomotive could provide such predictive abilities in the near term. In the longer term, the development of comprehensive validated analytical models applicable to a broad range of locomotive configurations may provide a more convenient means of predicting locomotive dynamic response under various operating conditions.

5.1.3 Effect of Rail Surface Condition

Rail surface condition (wet, sanded, dry) appears to be one of the most significant parameters affecting lateral dynamic curving force. The results of a series of runs around 30 mph at the test curve, the only set for which the exact condition of the rail surface was known, are shown in Figures 5-35 and 5-36. Sanding caused L and L/V maximums twice as high as under dry conditions, while wet (with no sand) substantially reduced all L and L/V dynamic activity and produced lateral loads half those under dry conditions.

*K.R. Smith, "Locomotive Truck Curving Model," Track/Train Dynamics Interaction Conference, 2nd; December 1974, Proceedings, Vol. II, pp. 371-384.

SAND
NO SHOCKS
RUN 23-3
31 MPH
IN TEST CURVE

WET
NO SHOCKS
RUN 22-13
33 MPH
IN TEST CURVE

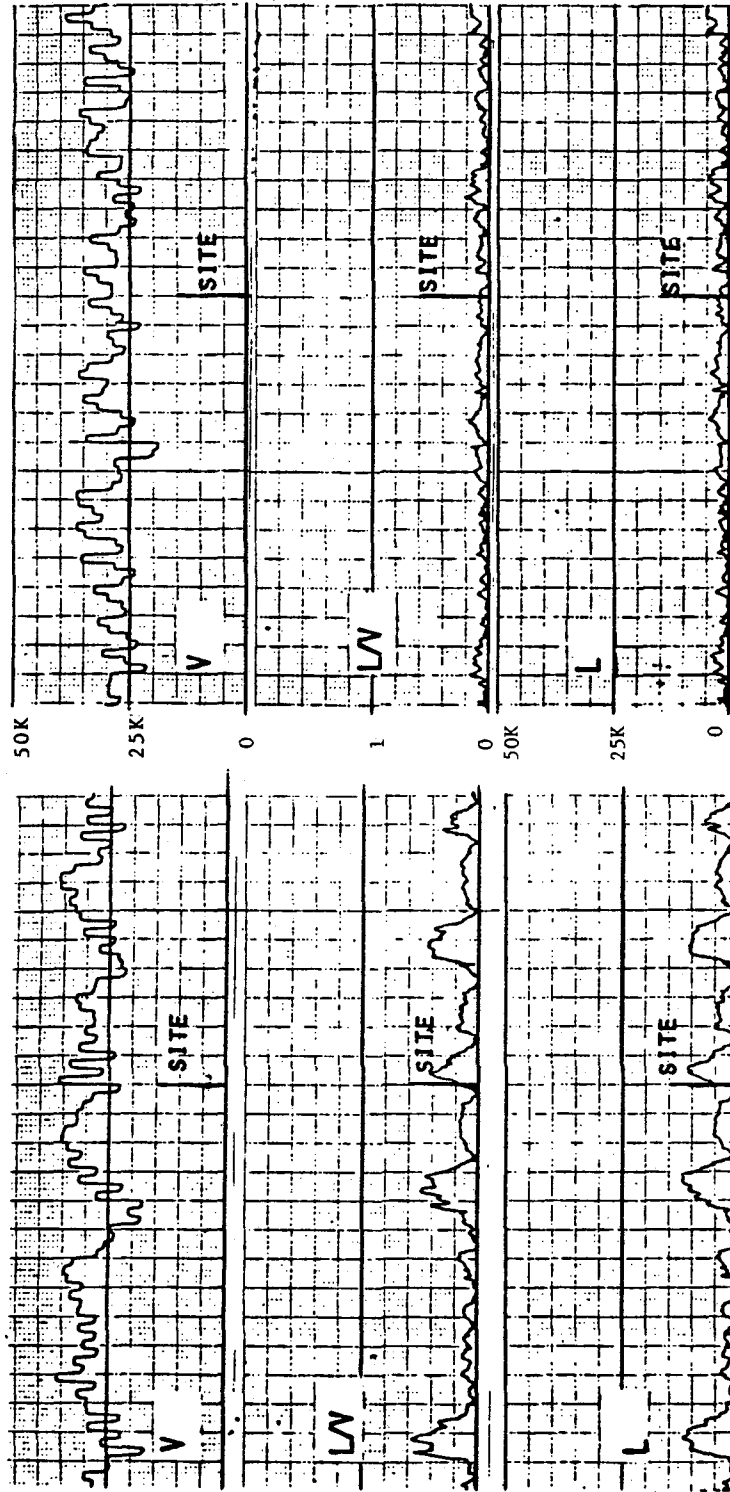


FIGURE 5-35 EFFECT OF WET AND SANDED RAIL SURFACE CONDITIONS ON PERFORMANCE OF AXLE 10 OF SDP-40F IN TEST CURVE (POWER MODE, ONBOARD DATA)

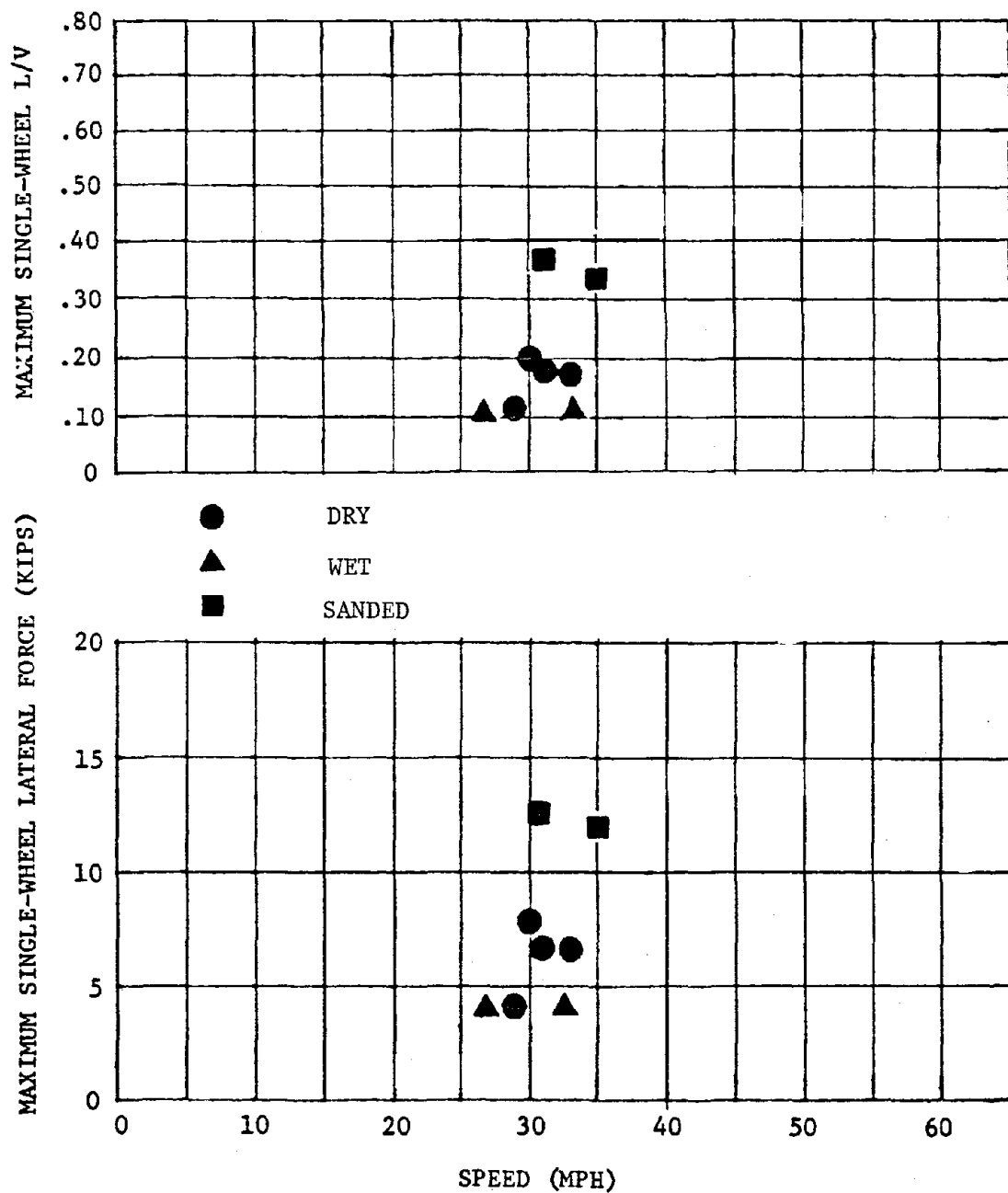


FIGURE 5-36 EFFECT OF WET AND SANDED RAIL SURFACE CONDITIONS ON PERFORMANCE OF AXLE 10 OF SDP-40F AT TEST SITE (WAYSIDE DATA)

However, if the rail was wet and sand was present, then the sand dominated. As the sanding or wetness was diminished during repeated runs over the same section of track, the loads tended to return to the nominal values. It is not known whether the large effect of sanding persists at higher speeds.

What mechanism might explain the relationship between the presence of sand on the rails and large lateral loads? In many previous tests it has not been uncommon for hunting oscillations to vanish as a result of rail lubrication. This occurs because the friction force between the wheel and the rail is the driving force in the lateral direction that produces the hunting phenomenon and wheel climb. Wheel climb is a basic mode of derailment associated with the wheel rolling over the head of the rail. Friction acts to sustain this rolling motion of the wheel in the direction of rolling even though track alignment is forcing the wheel around a curve.

This data is far from a complete definition of the effects of surface condition, in general, and sanding, in particular. It is clear that significant changes in force characteristics occur when rail surface conditions are changed. Further investigation of this phenomenon is warranted in future tests.

5.1.4 Effect of Operating Modes

Operating modes tested for the E-8 were power, drift, and power (train) brake. For the SDP-40F, an additional operating mode, dynamic braking, was tested also. The axle 10 response at the test site is shown in Figure 5-37. Based on these results, it appears that for short consists, characteristic of passenger service, operating mode has no significant effect on the magnitude of the wheel/rail forces generated by either the E-8 or the SDP-40F (although there is an apparent reduction in lateral force due to dynamic braking on the SDP-40F at 60 mph, this data point is considered questionable).

5.2 SDP-40F CONFIGURATION CHANGES

This section presents the results of tests to determine how various changes to the SDP-40F baseline configuration affected its dynamic response. The changes tested included:

1. Vertical primary damping,

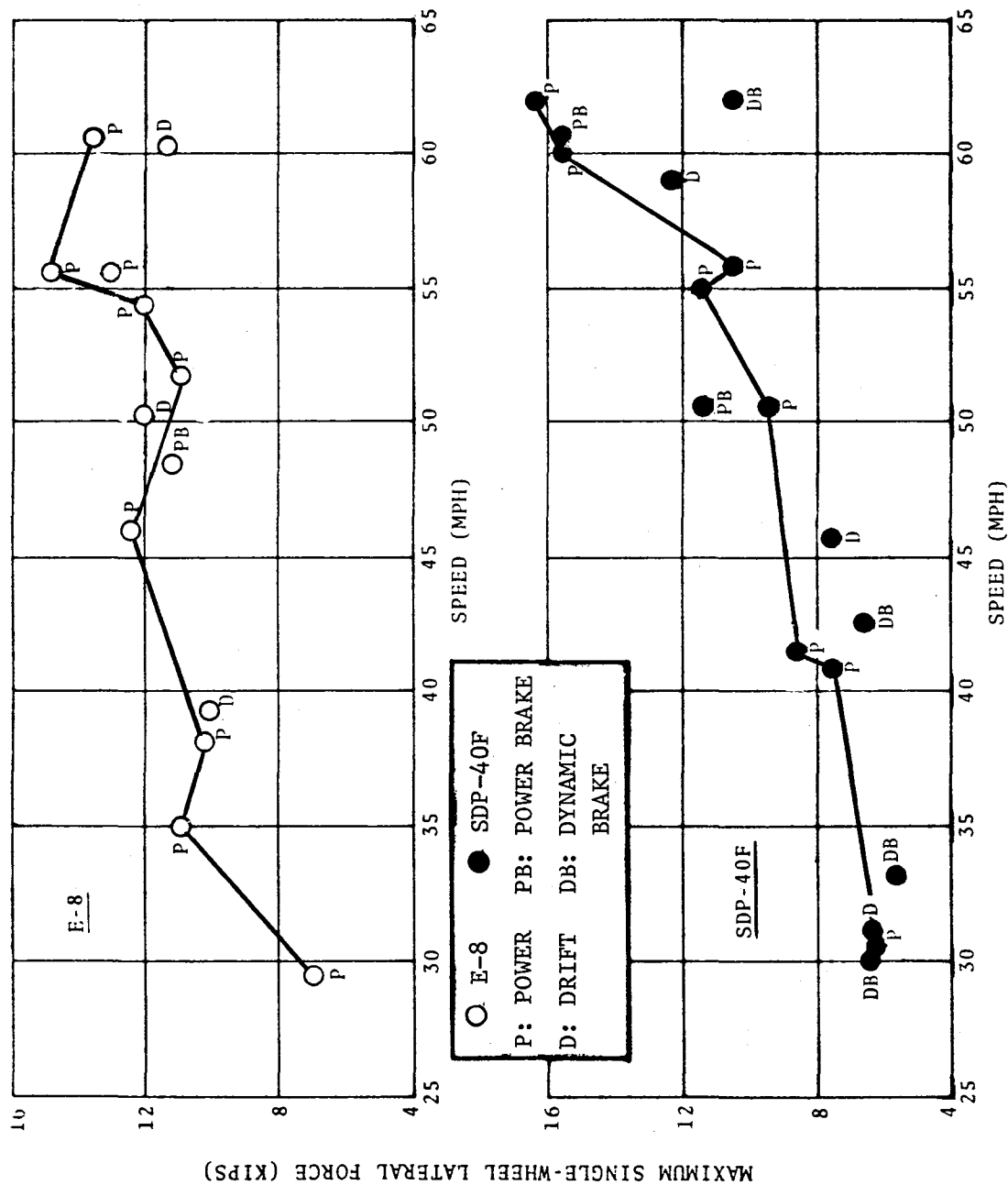


FIGURE 5-37 EFFECT OF OPERATING MODE ON AXLE 10 MAXIMUM LATERAL FORCE FOR E-8 AND SDP-40F AT THE TEST SITE (BASELINE RUNS, ONBOARD DATA)

2. Wheel diameter mismatch, and
3. Lateral axle clearance.

These particular configuration changes were selected to represent various locomotive component wear conditions or design modifications which might have a significant influence on the dynamic response. Configuration changes on the E-8 locomotive were not investigated.

5.2.1 Vertical Primary Damping

Several series of runs were made to study the effects of variations in vertical primary damping on locomotive response. These runs involved standard shocks (1200/400), heavy-duty shocks (1800/1800), and no shocks with estimated damping values of 25 and 100 lbs-sec/inch per shock, respectively. As shown in Figure 5-38, the standard shocks have a small effect on reducing the root mean square (RMS) primary spring deflection of the locomotive on curves. From the one data point close to 50 mph, the heavy shocks appear to reduce the primary spring deflection by approximately 15 percent. The SDP-40F tested had not yet been retrofitted with the softer rubber bolster springs which are being installed on later versions.

The effect of damping variation on the response of the front (hood) end and rear (cab) end of the trailing locomotive at the road crossing near MP 257.5 is shown in Figures 5-39 and 5-40. The SDP-40F has two vertical resonances which are close together and are within the general operating speed range. The first resonance occurs at about 42 mph and corresponds to a bounce mode, while the second resonance occurs at about 50 mph and corresponds to a pitch mode. The standard shocks (1200/400) had only a small effect on attenuating this response. However, the heavy-duty shocks (1800/1800) had a much larger effect, reducing the SDP-40F peak vertical accelerations to the vicinity of the E-8 response, a reduction of about 25% from the standard SDP-40F shock acceleration levels.

Test results of the effects of external shock absorbers on

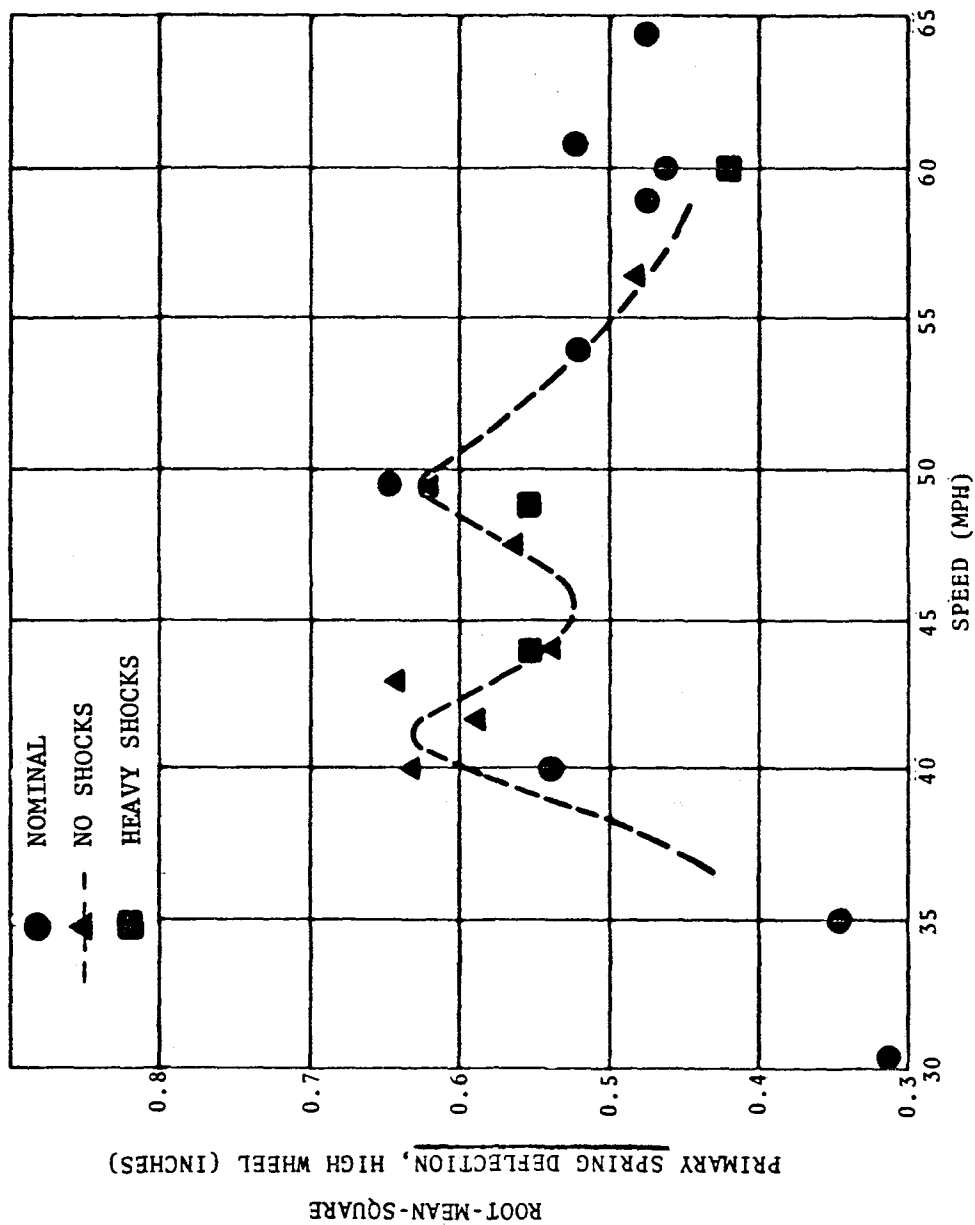


FIGURE 5-38 EFFECT OF VARIATION IN VERTICAL PRIMARY DAMPING ON RMS PRIMARY SPRING DEFLECTION AT HIGH WHEEL OF SDP-40F VERSUS SPEED IN TEST CURVE

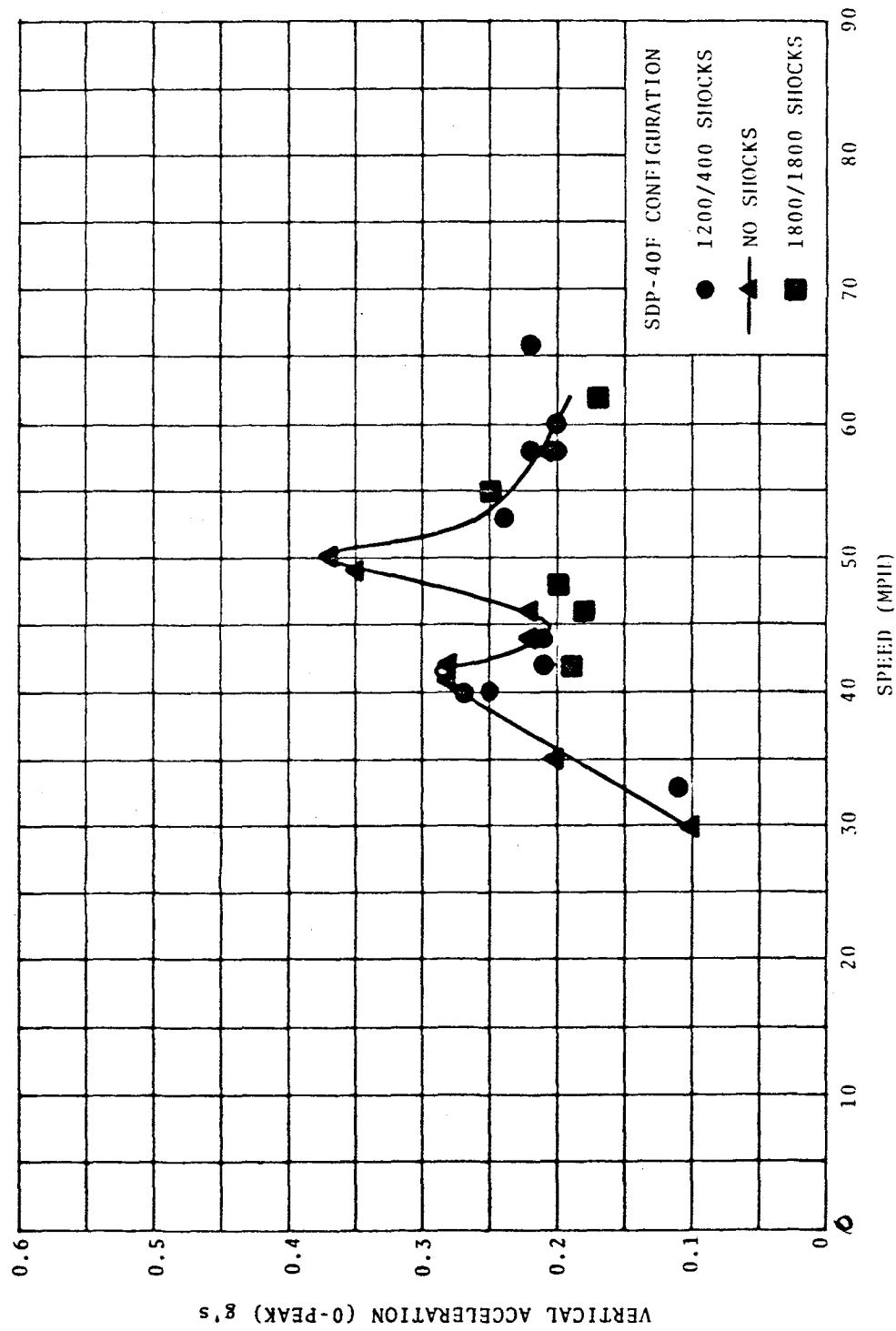


FIGURE 5-39 EFFECT OF VARIATION IN VERTICAL PRIMARY DAMPING ON SDP-40F FRONT HOOD END VERTICAL ACCELERATION (ALL RUNS FOR TRAILING LOCOMOTIVE AT ROAD CROSSING NEAR MP 257.5 IN POWER MODE)

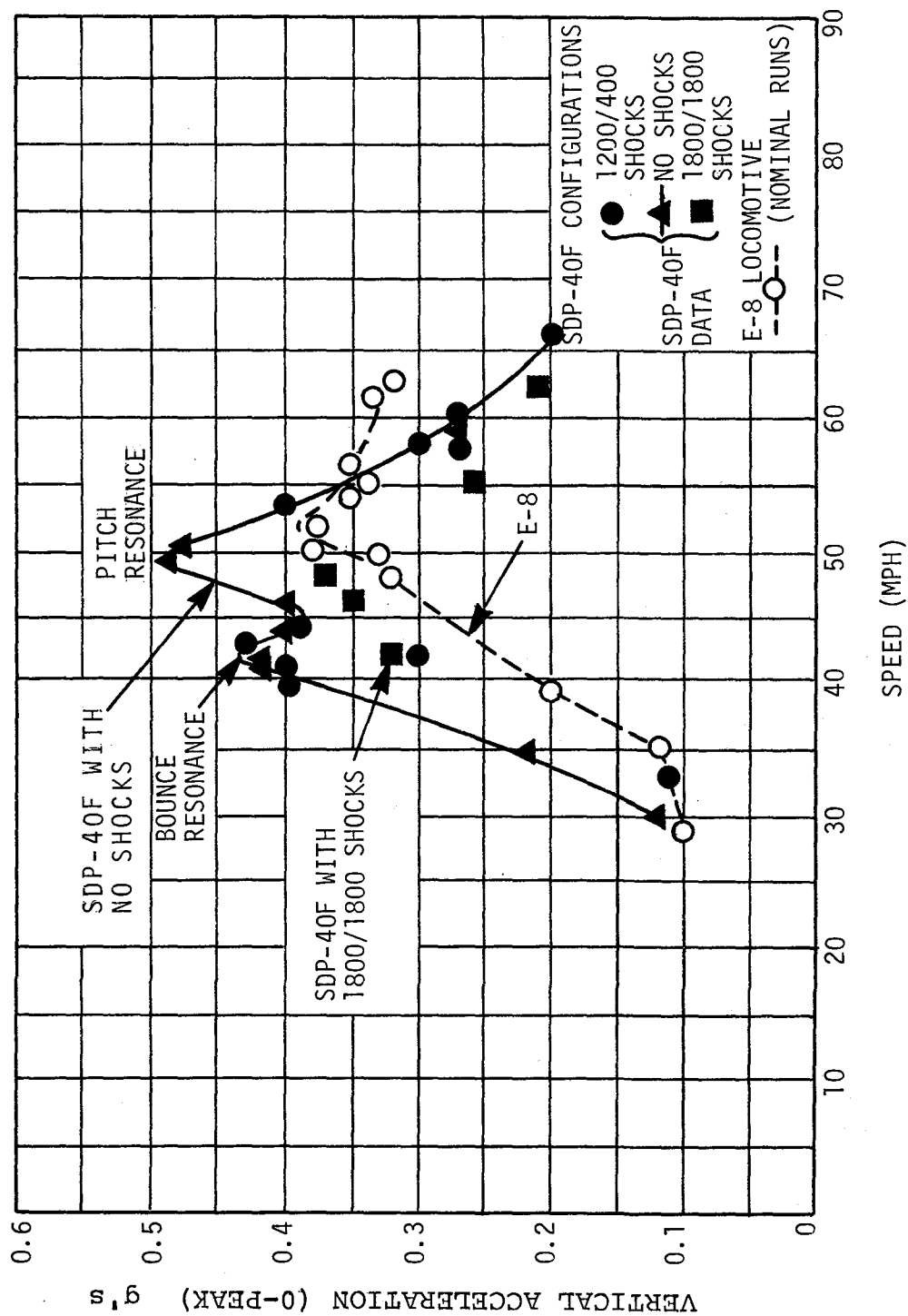


FIGURE 5-40 COMPARISON OF E-8 AND SPD-40F REAR CAB END VERTICAL ACCELERATIONS (ALL RUNS FOR TRAILING LOCOMOTIVE AT ROAD CROSSING NEAR MP 257.5 IN POWER MODE)

HTC truck performance were also obtained from Southern Pacific tests.* These tests indicate, as shown in Figure 5-41, that with a softer secondary vertical suspension system having a 30 percent reduction in stiffness from the standard pad and heavy-duty (1800/1800) shocks, there is a reduction in dynamic loading of the primary suspension, on an average peak-to-peak basis of 25% on both curves and tangents.

In order to confirm some of the trends indicated by the tests and to investigate the consequences of the damping changes further, an analytical simulation model was developed for the vertical response of a six-axle locomotive.** It has been used to examine the effects of parametrically varying the vertical primary damping. See Appendix H for further details of the model. The results of these studies produced verification of the double peak resonance phenomena for the SDP-40F locomotive. A typical result for the rear end acceleration, with SDP-40F parameters, is shown in Figure 5-42 for a track input, based on a 39-foot rectified sine wave with 0.6" peak-to-peak amplitude: The internal truck damping coefficient of 400 lbs-sec/inch was chosen by matching the peak-to-trough acceleration of Figure 5-40 for the no shock case. The values of the external shock damping coefficients were determined by matching either the bounce or pitch resonance peaks, depending on where data was available. As may be seen from Figure 5-42, the no-shock and standard-shock values, 0 and 25 lbs-sec/inch, respectively, predict accelerations which are quite representative of the actual experimental values shown in Figure 5-40.

The analytical model was used to verify that the vertical resonances near 42 and 50 mph were bounce (in phase) and pitch (out of phase) resonances, respectively. Comparison of the vertical displacement as a function of time at the front and rear truck attachment points showed that the displacements were exactly in phase at the lower speed and nearly 180° out of phase at the higher speed. The variation

*"Dynamic Performance of the HTC Suspension System under 6-Axle Locomotives," Southern Pacific Transportation Co., July 1977.

**"Pilot Study of Dynamic Response of 6-Axle Locomotive," U.S. Department of Transportation, Transportation Systems Center, Structures and Mechanics Branch, Cambridge, MA, report in preparation.

REDUCTION IN PEAK-TO-PEAK PRIMARY SUSPENSION DYNAMIC LOADS

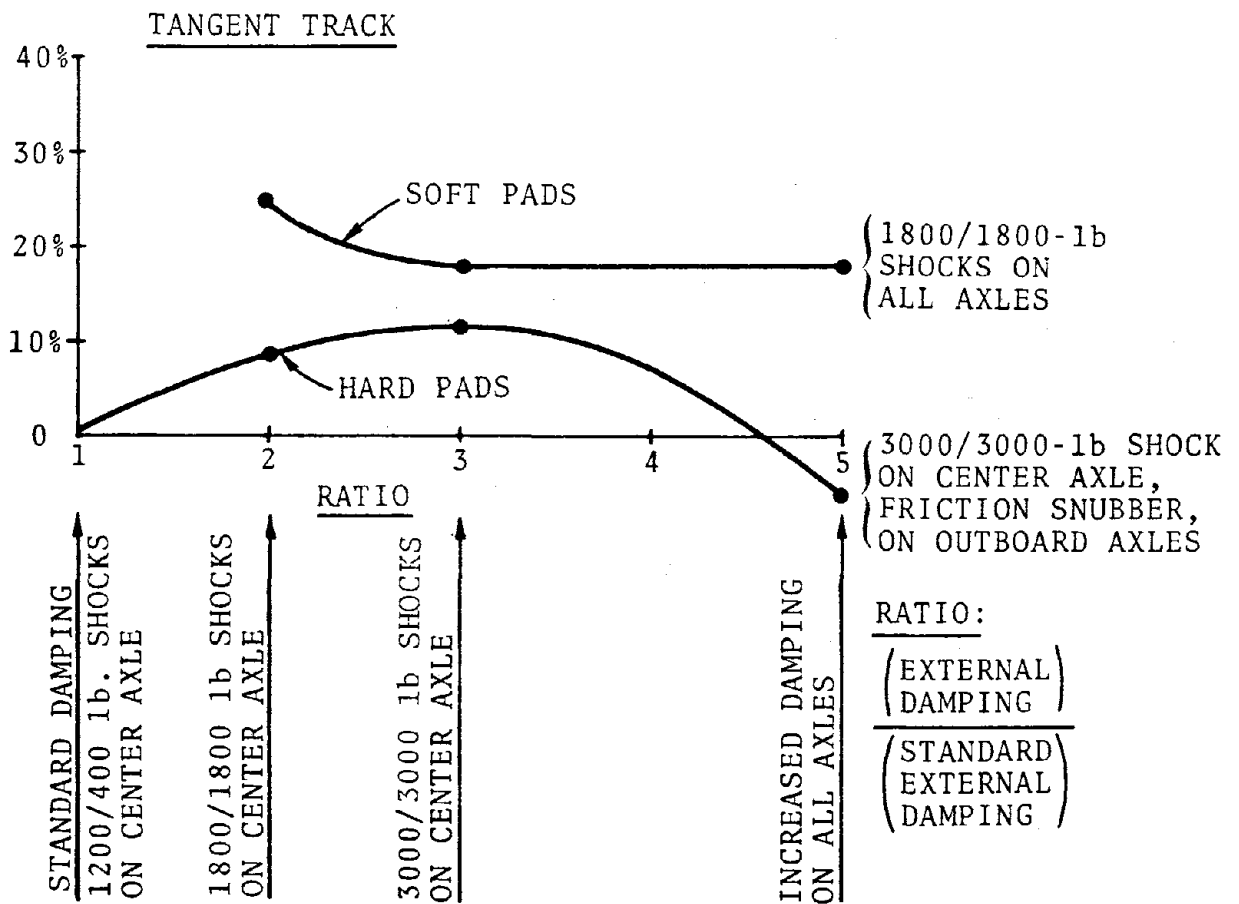
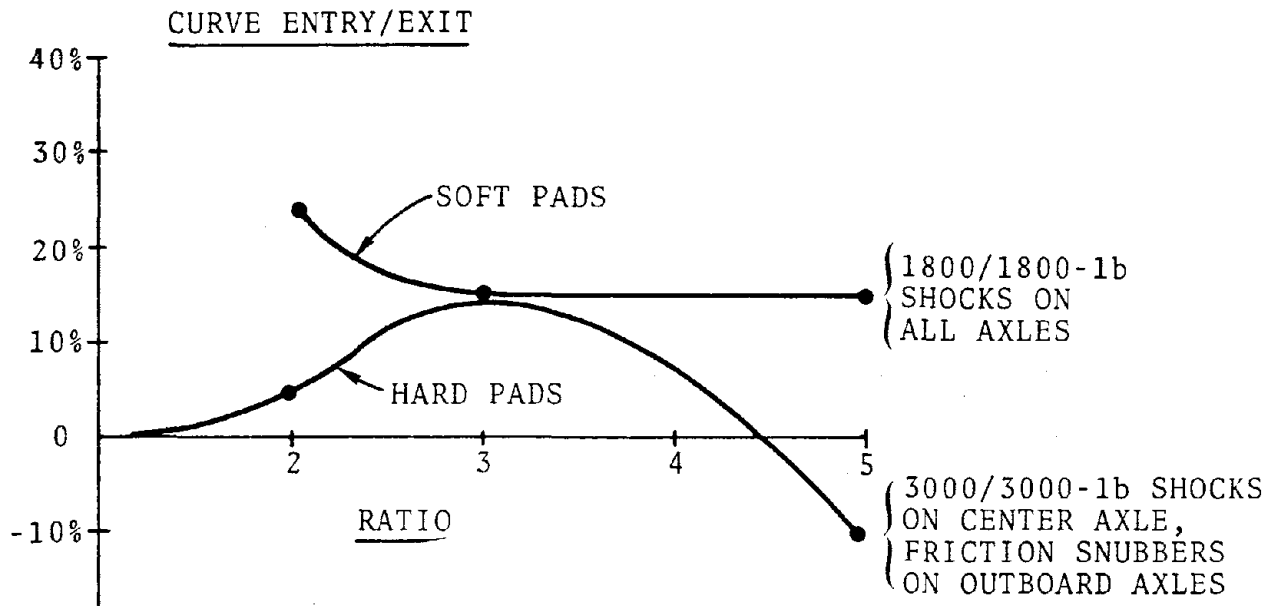


FIGURE 5-41 EFFECT OF SECONDARY SPRING RATE AND PRIMARY DAMPING ON HTC PRIMARY SUSPENSION PERFORMANCE (SP TEST RESULTS)

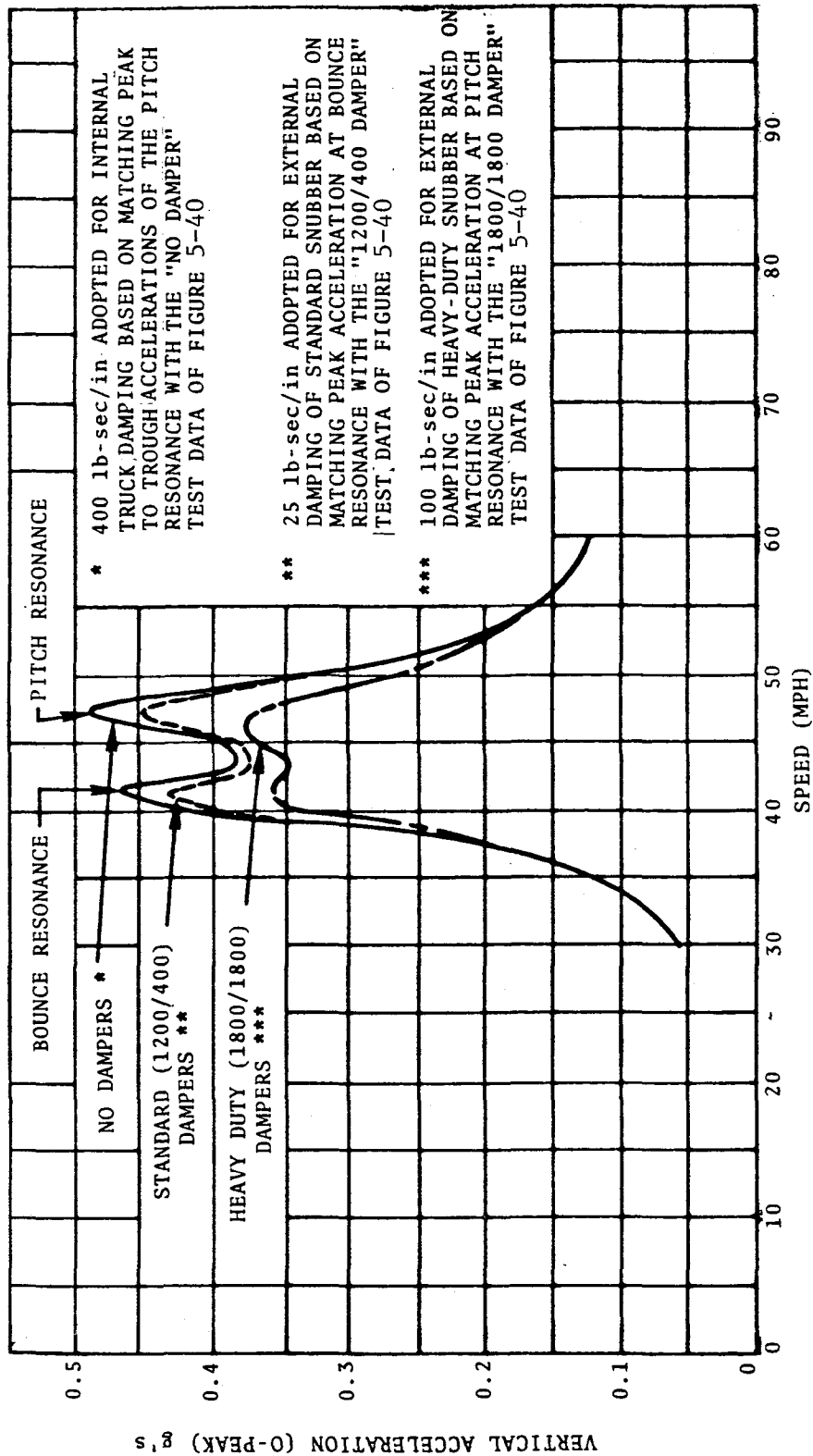


FIGURE 5-42 ANALYTICAL SIMULATION OF EFFECT OF VARIATION IN THE VERTICAL PRIMARY DAMPING ON SDP-40F REAR END VERTICAL ACCELERATIONS (TRACK REPRESENTED AS A .6" AMPLITUDE RECTIFIED SINE WAVE.)

of the rms amplitudes of the vertical displacements and accelerations obtained from the simulation is shown in Table 5-2:

TABLE 5-2 RMS AMPLITUDES OF VERTICAL DISPLACEMENT AND ACCELERATION AT THE FRONT AND REAR TRUCK ATTACHMENT POINTS, 0.6" PEAK-TO-PEAK RECTIFIED SINE WAVE TRACK PERTURBATION

TRUCK ATTACHMENT POINT	VELOCITY			
	41 mph		47 mph	
	DISPLACEMENT (IN)	ACCELERATION (G'S)	DISPLACEMENT (IN)	ACCELERATION (G'S)
Rear	1.37	0.33	1.08	0.36
Front	1.03	0.25	0.362	0.12

These results, along with the phase differences, indicate that although neither mode is a pure pitch or bounce mode, bounce dominates the lower speed mode, and pitch dominates the higher speed mode. In addition, the carbody vertical displacements and accelerations are larger at the rear end than at the front end due to phasing of the track input with the vehicle response.

Experimental wheel unloading data was limited due to the sensing procedure which provided only a sample and hold peak detection every quarter revolution. Therefore, the analytical model was also used to estimate the following dynamic wheel unloading characteristics:

1. Maximum vertical wheel/rail force unloading at the leading wheelset of the trailing truck for all three values of the external shocks.
2. Maximum vertical wheel/rail force unloading at the trailing wheelset of the trailing truck for the standard external shock.
3. Vertical wheel/rail force trace as a function of time at the leading wheelset of the trailing truck for all three values of the external shocks.

In each of these cases, it was convenient to express the vertical wheel/rail force unloading as a ratio (R_u) representing the percent unloading from static conditions:

$$R_u = \frac{F_d}{F_s} \times 100\%$$

where F_d is the dynamic unloading at the wheel/rail interface, and F_s is the corresponding static wheel load. R_u is a function of the periodic input perturbation which is a rectified sine wave. $R_{u,max}$ is the maximum value of R_u within one cycle at the wheelset under consideration.

All simulated data describing R_u and $R_{u,max}$ were calculated for the same set of conditions identified in Figure 5-43. Figure 5-43 shows the percent maximum vertical wheel unloading ($R_{u,max}$) at the leading wheelset of the trailing truck as a function of velocity for the three different cases of external damping. The peak wheel unloading occurs at the bounce resonance (41 mph), and is as much as 40% for the no shock case. As was the case for the carbody vertical accelerations, the standard shocks show only a small effect on reducing this maximum wheel unloading, while the heavy-duty shocks reduce the unloading by about 25% in the resonant range.

Figure 5-44 compares the maximum wheel unloading of the leading and trailing wheelsets of the trailing truck for the standard shock case. The responses are seen to be fairly similar. Figure 5-45 shows a trace of the vertical wheel force at the leading wheelset of the trailing truck as a function of time and distance at 41 mph (the bounce resonance). The force traces are again given for the three different values of the external damping. The displacement of the rectified sine wave perturbation under the wheelset is also shown in Figure 5-45. Note that the greatest vertical unloading occurs about 60 msec (3 feet) after the cusp in the perturbation, with the duration of this minimum force level lasting for an additional 60 msec. The greatest additional loading occurs near the region of the perturbation maximum. This suggests that the spring forces dominate the inertia and damper (shock) forces.

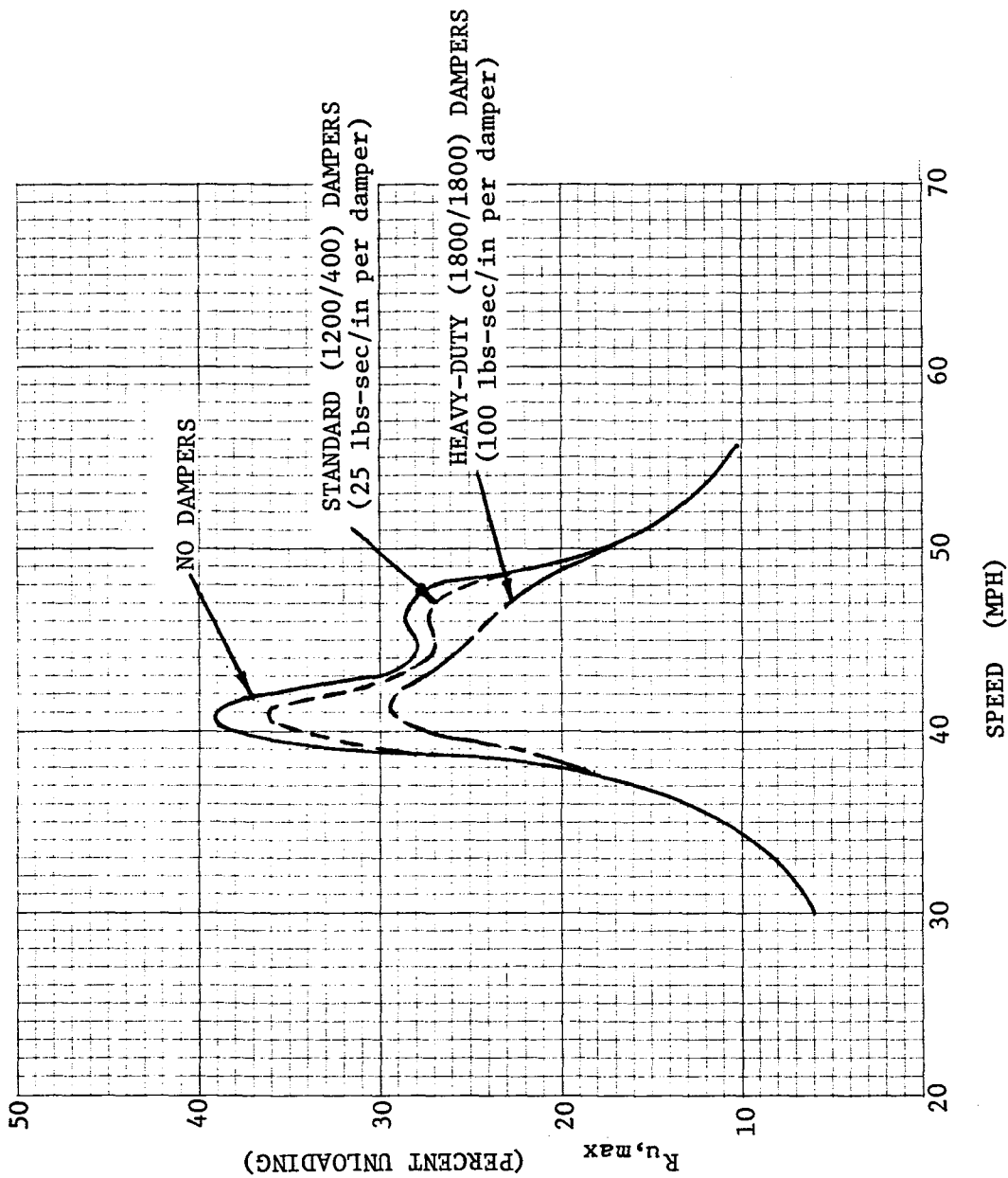


FIGURE 5-43 ANALYTICAL SIMULATION OF EFFECT OF VARIATION IN THE VERTICAL PRIMARY DAMPING ON SDP-40F MAXIMUM WHEEL UNLOADING FOR LEADING WHEELSET OF THE TRAILING TRUCK. (RESPONSE TO TEN-TERM .6" AMPLITUDE RECTIFIED SINE WAVE; INTERNAL TRUCK DAMPING = 400 lbs-sec/in.)

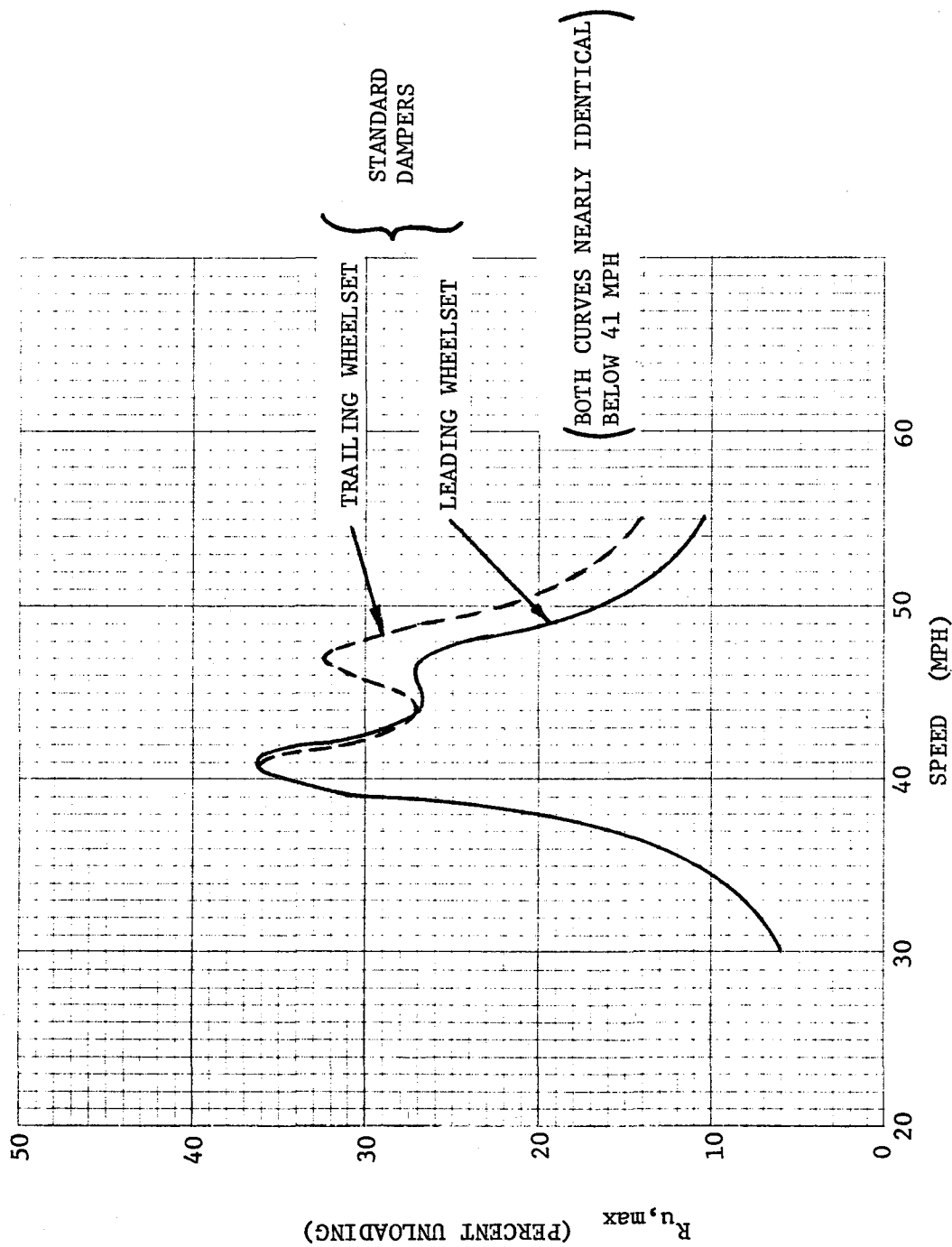


FIGURE 5-44 ANALYTICAL SIMULATION COMPARING THE MAXIMUM WHEEL UNLOADING OF THE LEADING AND TRAILING WHEELSETS OF THE TRAILING SDP-40F TRUCK. (RESPONSE TO TEN-TERM .6" AMPLITUDE RECTIFIED SINE WAVE; INTERNAL TRUCK DAMPING = 400 lbs-sec/in; EXTERNAL DAMPING = 25 lbs-sec/in per damper.)

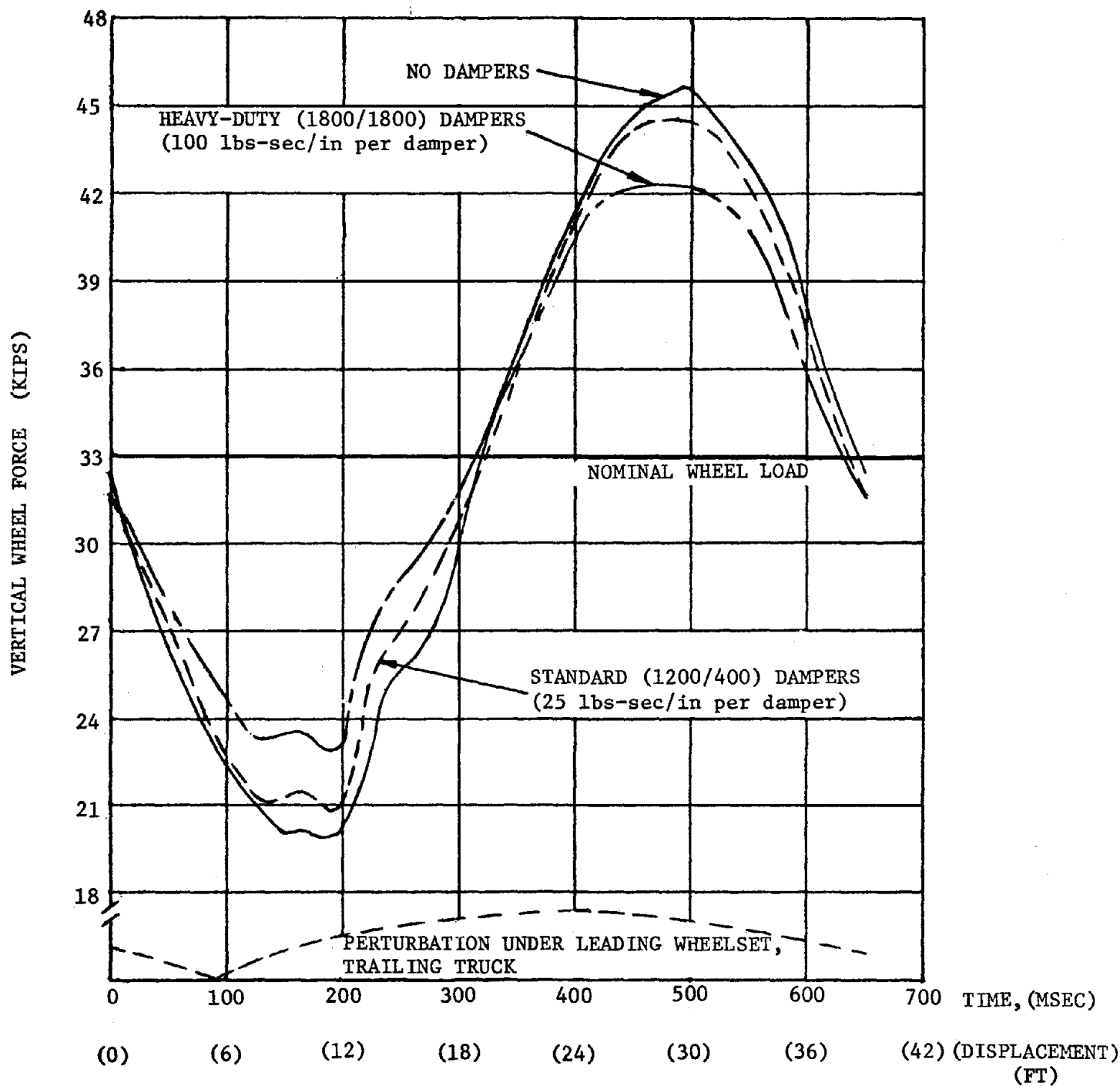


FIGURE 5-45 ANALYTICAL SIMULATION OF EFFECT OF VARIATION IN THE VERTICAL PRIMARY DAMPING ON THE VERTICAL WHEEL FORCE TRACE OF THE LEADING WHEELSET OF THE TRAILING SDP-40F TRUCK AT THE BOUNCE RESONANCE. (SPEED = 41 MPH; STATIC WHEEL LOAD = 33 KIPS; RESPONSE TO TEN-TERM .6" AMPLITUDE RECTIFIED SINE WAVE; INTERNAL TRUCK DAMPING = 400 lbs-sec/in.)

A recent series of tests by the Martin Marrietta Corp.* under contract to the FRA has indicated that secondary suspension stiffness of the HTC trucks used on the SDP-40F increases at low temperatures. This effect may result in additional increases in locomotive vertical accelerations and therefore wheel unloading. EMD reviewed the low temperature characteristics of the HTC rubber springs in early 1977. The data then available indicated an increase in lateral stiffness of about 10% after a short period of operation at 20°F.

5.2.2 Wheel Diameter Mismatch

Wheel diameter mismatch was simulated on the SDP-40F in order to determine the degree of reduced vertical loading that would be achieved by wheels with smaller diameters. Such a condition could occur if one wheelset were more worn than the others. Reduced vertical loads would, in turn, cause the smaller wheels to climb the railhead more readily in the presence of large lateral loads on the same wheels (i.e., high L/V).

Since attention in this test series was concentrated on the trailing truck of the trailing locomotive due to its greater involvement in accidents, the most appropriate place to try the wheels with smaller diameters was the leading axle, where lateral loads were expected to be higher. Unfortunately, this was the location of the instrumented wheelset. Replacing it with worn wheels would eliminate essential onboard instrumentation. Therefore, the smaller diameter wheels were located on the trailing axle.

The effects of smaller diameter wheels on the front axles were approximated by placing 1-1/4" thick metal spacers, or "shims," between the journal box and primary (coil) springs of the middle and rear axles, #11 and #12. This approximates the unloading effect of 2-1/2" smaller diameter wheels on the leading axle.

The onboard test data were analyzed by determining V_s , the 5th percentile vertical wheel load. This parameter indicates the degree of vertical force unloading caused by the smaller wheels. Figure 5-46 shows the effect on axle 10 of shimming the middle and rear axles.

*See Appendix F.

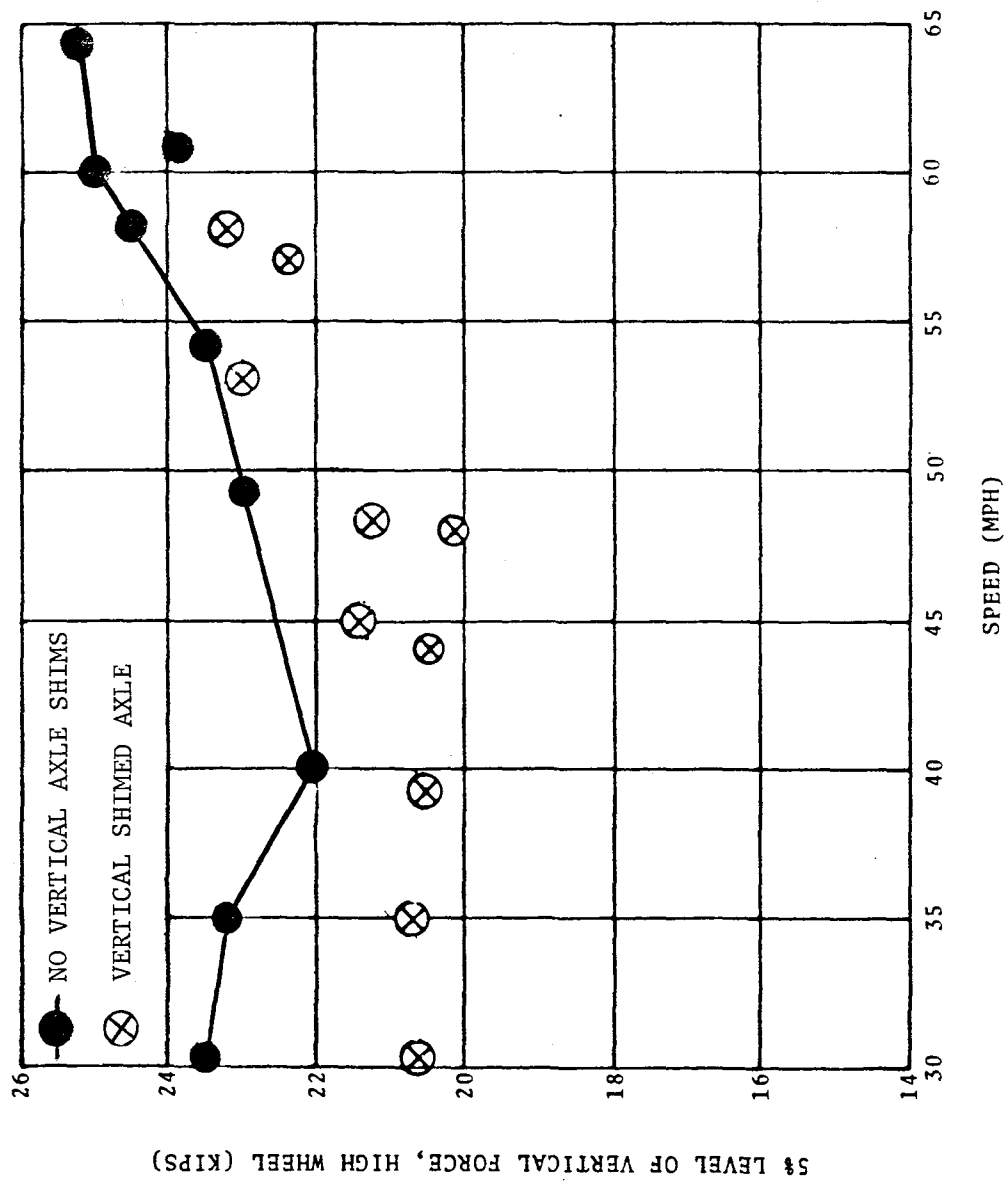


FIGURE 5-46 EFFECT OF SHIMMED AXLES 11 AND 12 ON V₅ RESPONSE OF AXLE 10 OF SDP-40F IN TEST CURVE (ONBOARD⁵ DATA)

Shimming appears to decrease V_s on axle 10 by about 10% below the balance speed and the difference between the shimming and nominal values decreases above balance speed. Another indicator of the unloading effect is $(L/V)_{.5}$, as shown in Figure 5-47. $(L/V)_{.5}$ ratios on axle 10 were about 40% higher than nominal below balance speed for the curve at MP 257.5, while above balance speed, this difference in $(L/V)_{.5}$ dropped to only about 15%. The shimming of the rear axles also significantly increased the vertical response of the front end of the baggage car, as will be discussed in Section 5.3.

However, the 3" wheel diameter mismatch on axle 12 had no significant effect on the forces developed on axles 10 and 11. The $(L/V)_{.5}$ result for axle 10 is shown in Figure 5-48. There was a small unloading effect on axle 12, generally less than 15%, as shown in Figure 5-49.

5.2.3 Lateral Axle Clearance

Metal shims were placed between the journal and the thrust block of each wheel of the trailing locomotive. In this way, the lateral clearance was increased by 1/4" per side. A series of runs was made at speeds between 31 and 61 mph. No significant effect was noted on the lateral axle forces below balance speed, as shown in Figure 5-50. Above balance speed, the increased lateral clearance decreased $L_{.5}$ by about 10-15%.

5.3 BAGGAGE CAR/LOCOMOTIVE INTERACTION

The previous operating experience with the SDP-40F indicated that large motions of the baggage car were occurring under some conditions. It was postulated that these motions were the result of dynamic interaction between the SDP-40F and its trailing baggage car. Therefore, baggage car accelerations and coupler angles were measured as possible indicators of such interactions. In addition, the wayside instrumentation also provided baggage car wheel forces at the test site.

In Figure 5-51, maximum single-wheel lateral force for the lead axle of both trucks of the baggage car is plotted against speed for the repeat runs at the test site. Although the lead axle lateral loads for the trailing truck of the baggage car showed no difference for the E-8 and SDP-40F, there is a significant difference for the leading truck. Maximum lateral loads for the lead axle of the

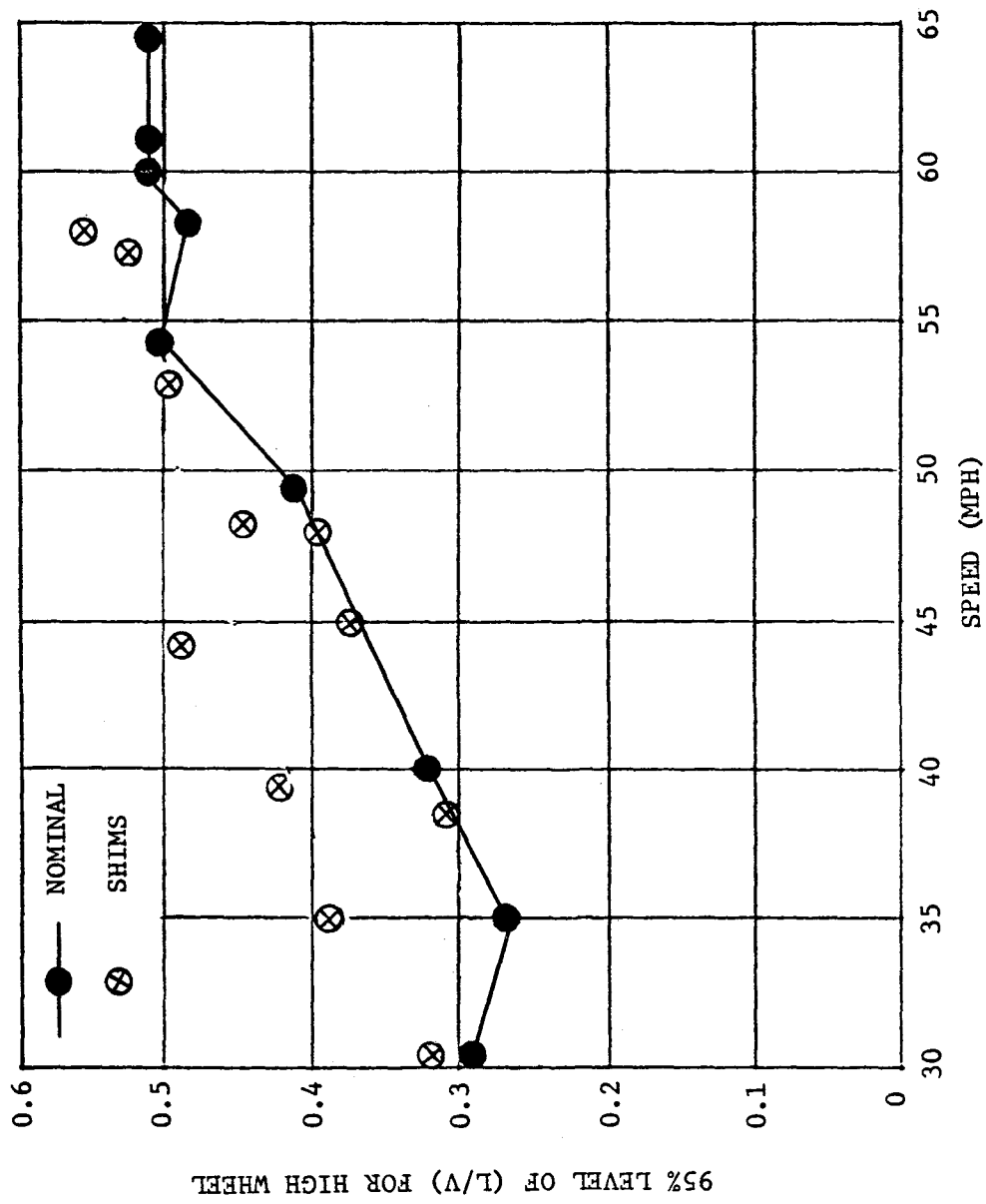


FIGURE 5-47 EFFECT OF SHIMMED AXLES 11 AND 12 ON $(L/V)_{95}$ RESPONSE OF AXLE 10 OF SDP-40F IN TEST CURVE (ONBOARD DATA)

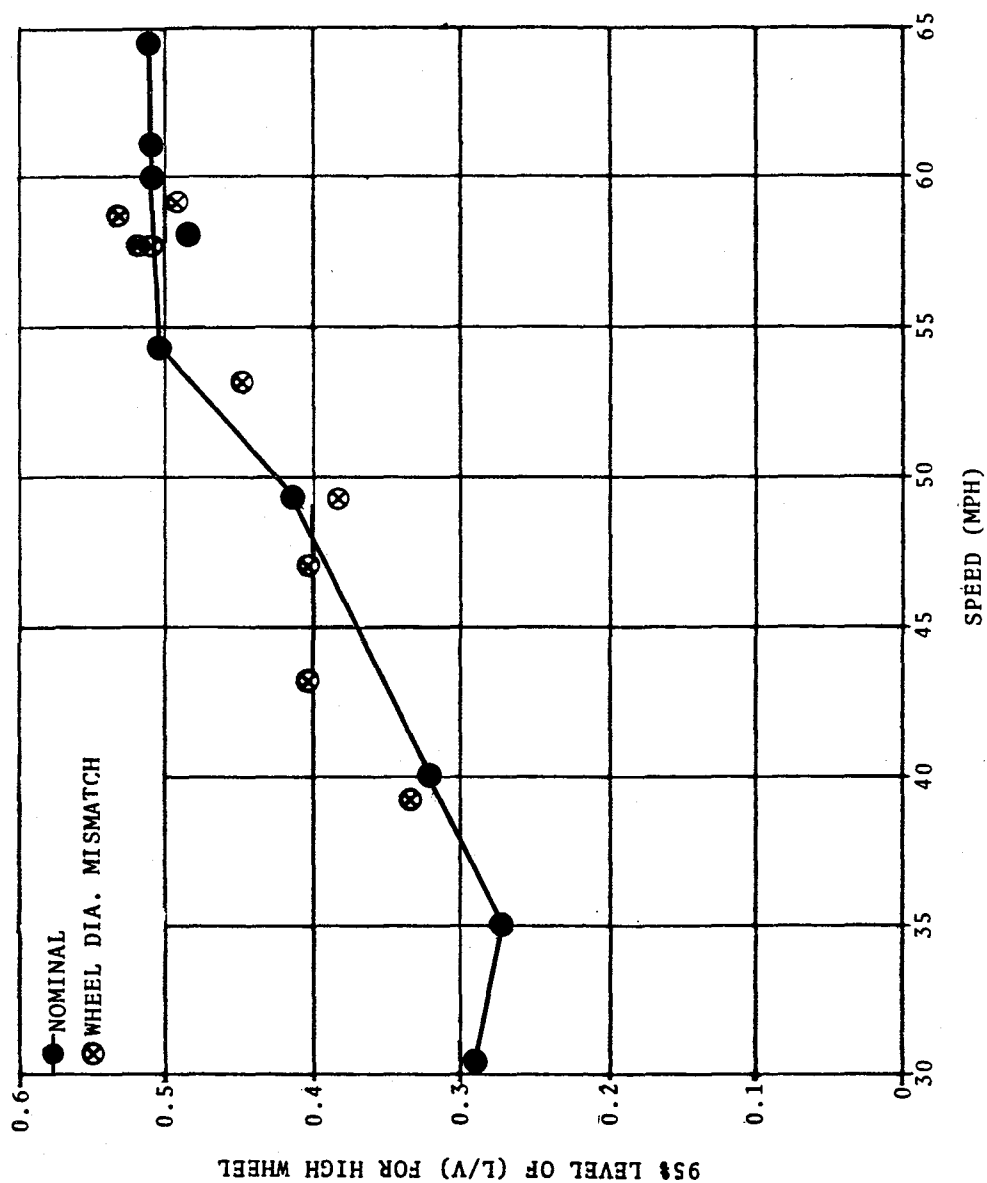


FIGURE 5-48 EFFECT OF AXLE 12 WHEEL DIAMETER MISMATCH ON (L/V)₉₅
RESPONSE OF AXLE 10 SDP-40F IN TEST CURVE (ONBOARD DATA)

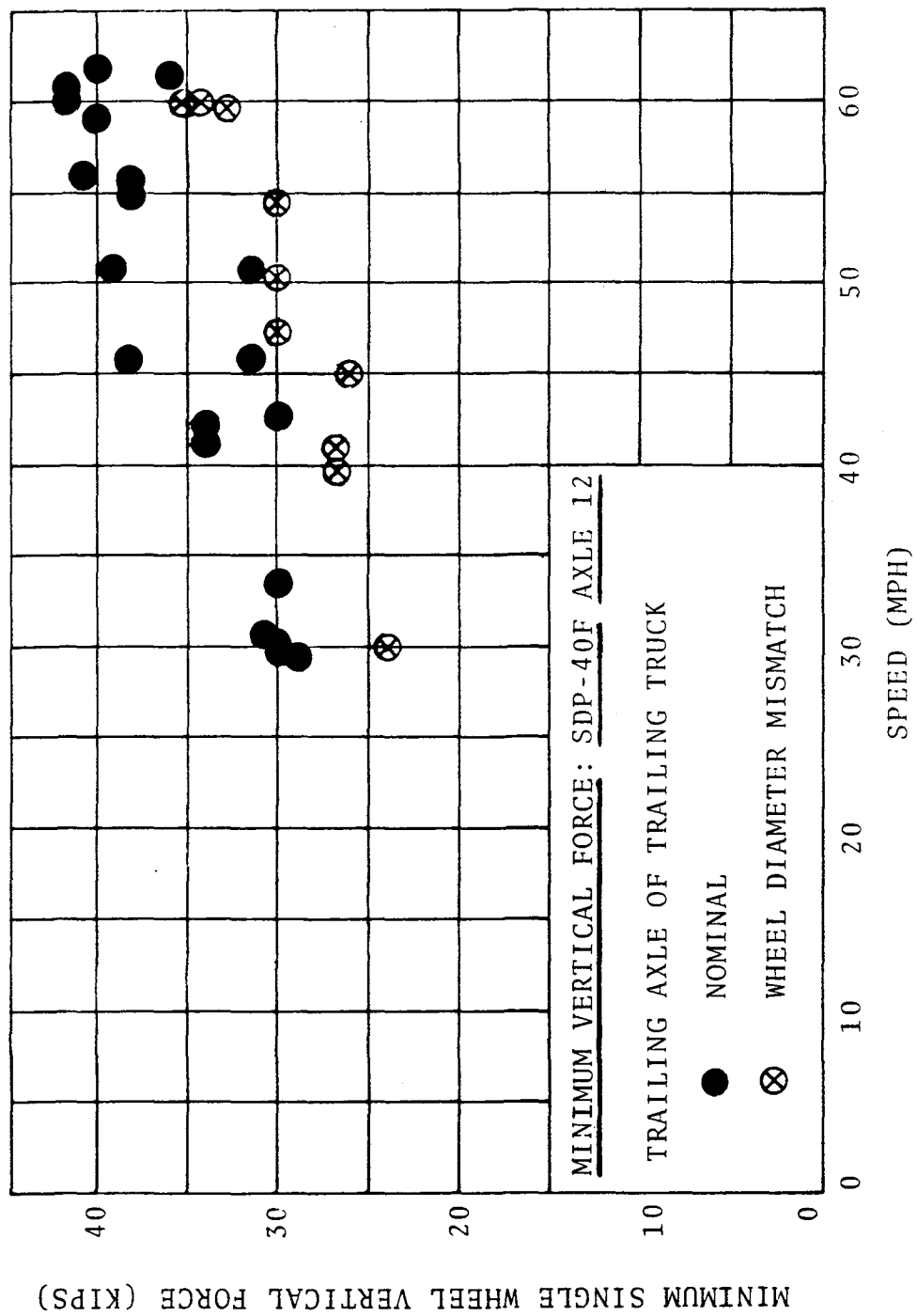


FIGURE 5-49 EFFECT OF WHEEL DIAMETER MISMATCH ON MINIMUM SINGLE-WHEEL VERTICAL FORCE FOR AXLE 12 OF SDP-40F (WAYSIDE DATA)

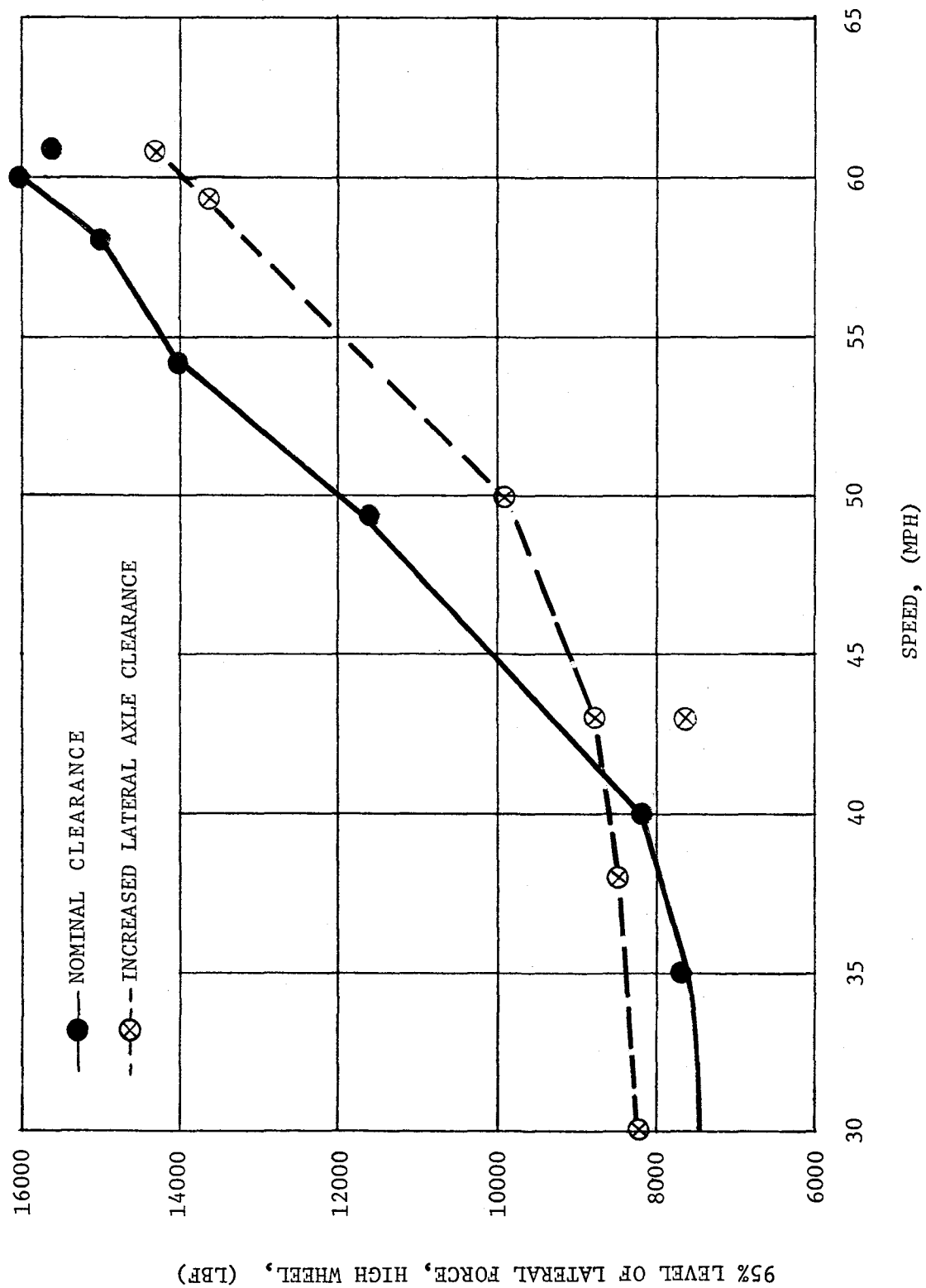


FIGURE 5-50 EFFECT OF INCREASING LATERAL AXLE CLEARANCE OF THE TRAILING TRUCK OF TRAILING LOCOMOTIVE ON L_{95} RESPONSE OF AXLE 10 OF SDP-40F IN TEST CURVE (ONBOARD DATA)

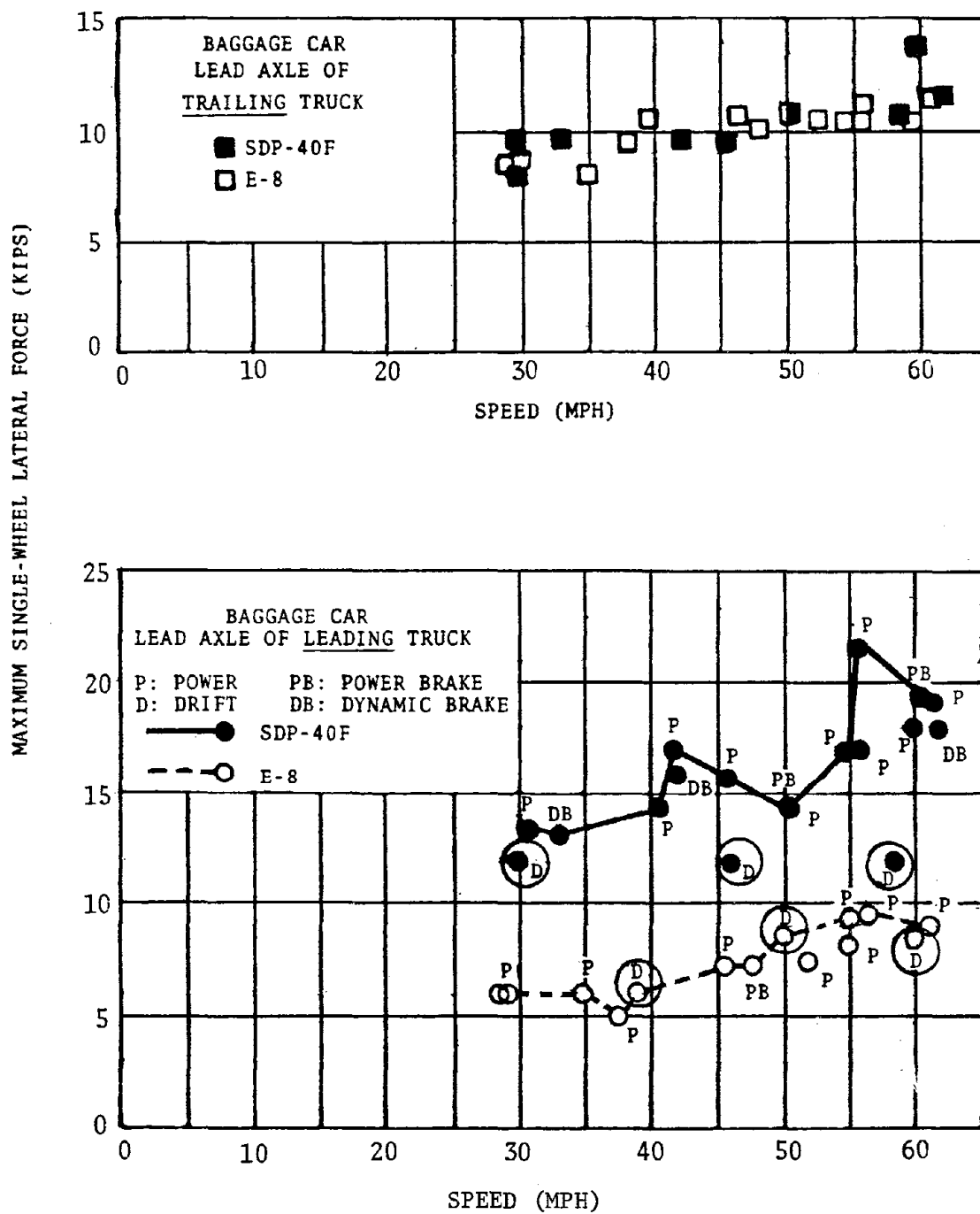


FIGURE 5-51 MAXIMUM SINGLE-WHEEL LATERAL FORCE FOR LEAD AXLES OF E-8 AND SDP-40F BAGGAGE CARS (BASELINE RUNS, WAYSIDE DATA).

leading truck of the SDP-40F baggage car are about twice the corresponding values for the E-8 baggage car. In addition, there are several SDP-40F drift mode data points that are below the other corresponding data points. In the drift mode, there are normally small forces in the mechanical coupling between locomotive and baggage car. The difference between the drift mode data points and the remaining data points indicates some form of locomotive-baggage car interaction. In addition, the SDP-40F coupler has a tendency to have relatively large coupler oscillations extending for a long duration upon entering and exiting curves encountered during the survey runs. For a 2° and a 2°50' curve, coupler oscillations up to $\pm 3^\circ$ lasting for 15 cycles (at 1.1 Hertz) were recorded, as shown in Figure 5-52. There may be some effect of the SDP-40F coupler alignment control at large coupler angles.

Acceleration data for the baggage car also indicated locomotive/baggage car dynamic interaction. In Figure 5-53, lateral acceleration levels are plotted for the trailing SDP-40F locomotive and its baggage car in the test zone. The peak lateral accelerations at the front end of the baggage car were consistently about twice as high as those at the rear end of the baggage car. Vertical acceleration data at the front and rear end of the baggage car at the road crossing near MP 257.5 are given in Figures 5-54 and 5-55. The baggage car containing a 21,000-lb. load has a vertical resonance at 50 mph, which corresponds to the pitch resonance speed of the SDP-40F locomotive, as shown in Figure 5-54. Vertical accelerations at the front end of the baggage car reached .39 g (zero to peak). For the same conditions vertical accelerations over the loaded baggage car rear bolster reached as high as .7g (0 - peak), as shown in Figure 5-55. A second vertical resonance for the baggage car occurs at around 57 mph. At this speed, the front end vertical acceleration of the baggage car remains about the same, while the rear end vertical acceleration decreases by about 20%.

Figures 5-54 and 5-55 also show that changing the values of the primary vertical shock absorbers on both trucks of the trailing locomotive had little effect on the baggage car response in the speed ranges where data for more than one shock configuration was available. On the other hand, shimming axles 11 and 12, the trailing two axles on the trailing locomotive, had a significant effect on the front end vertical acceleration of the SDP-40F baggage car, as shown in Figure 5-56. Placing 1-1/4" shims on the two trailing axles of the trailing truck of the SDP-40F (which raised the SDP-40F coupler by an estimated 1" with respect

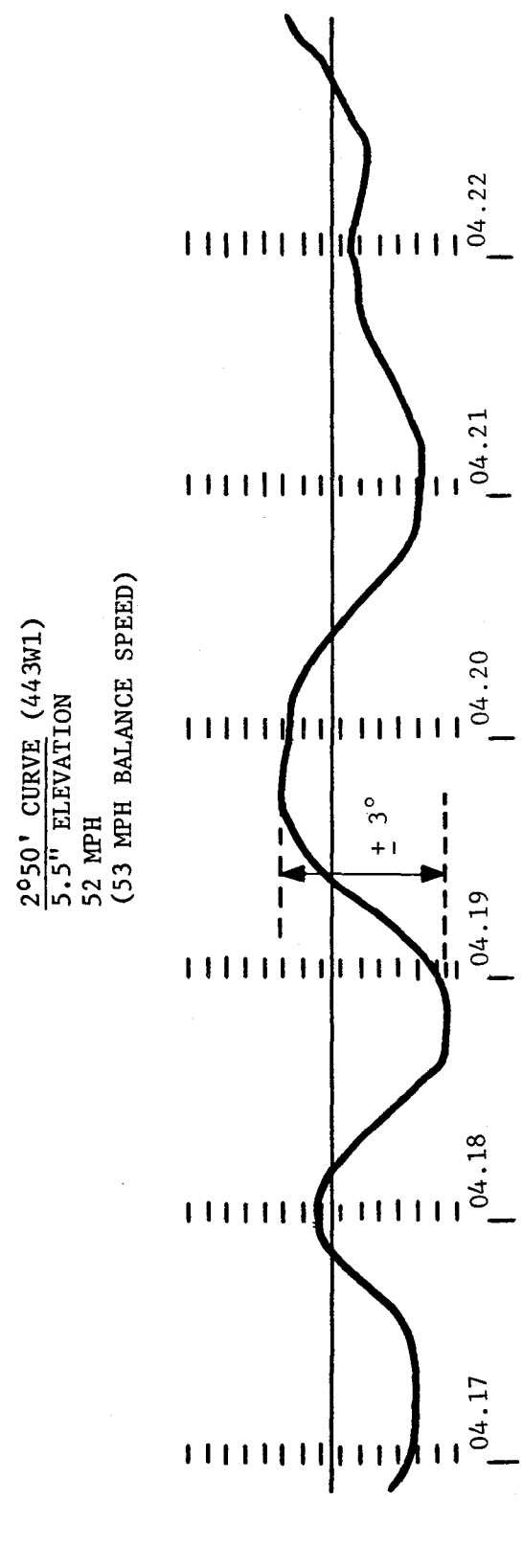
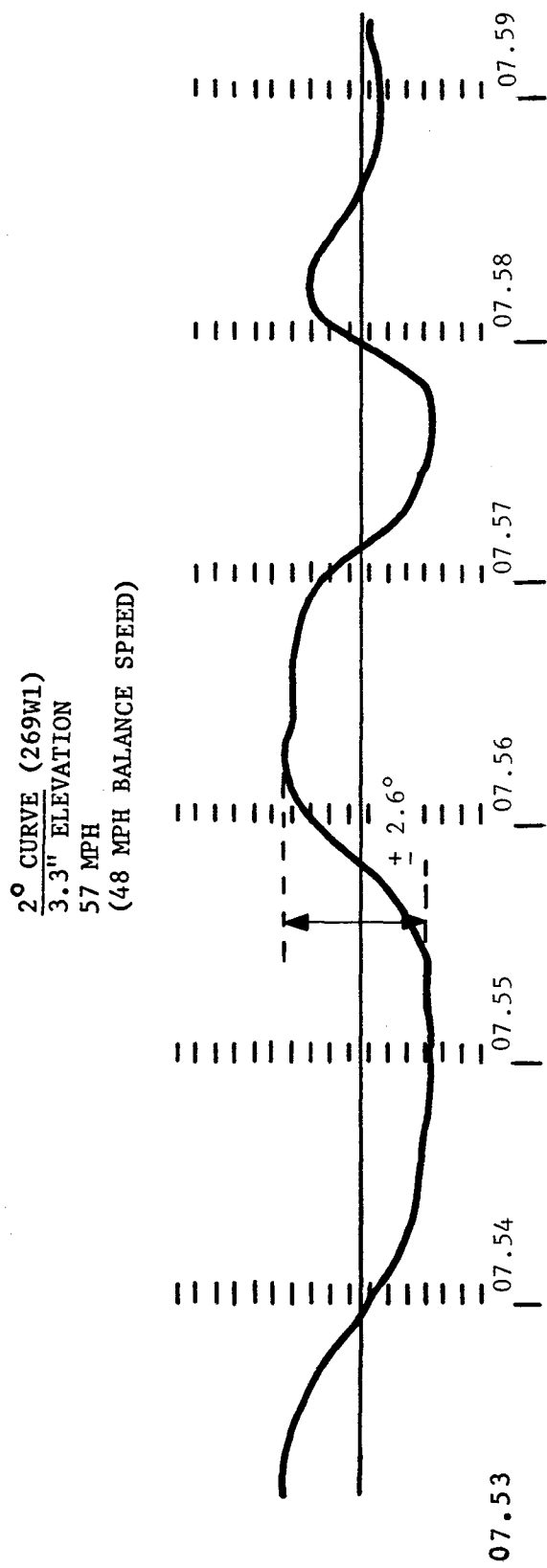


FIGURE 5-52 COUPLER OSCILLATION BETWEEN TRAILING LOCOMOTIVE AND BAGGAGE CAR IN THE SDP-40F CONSIST

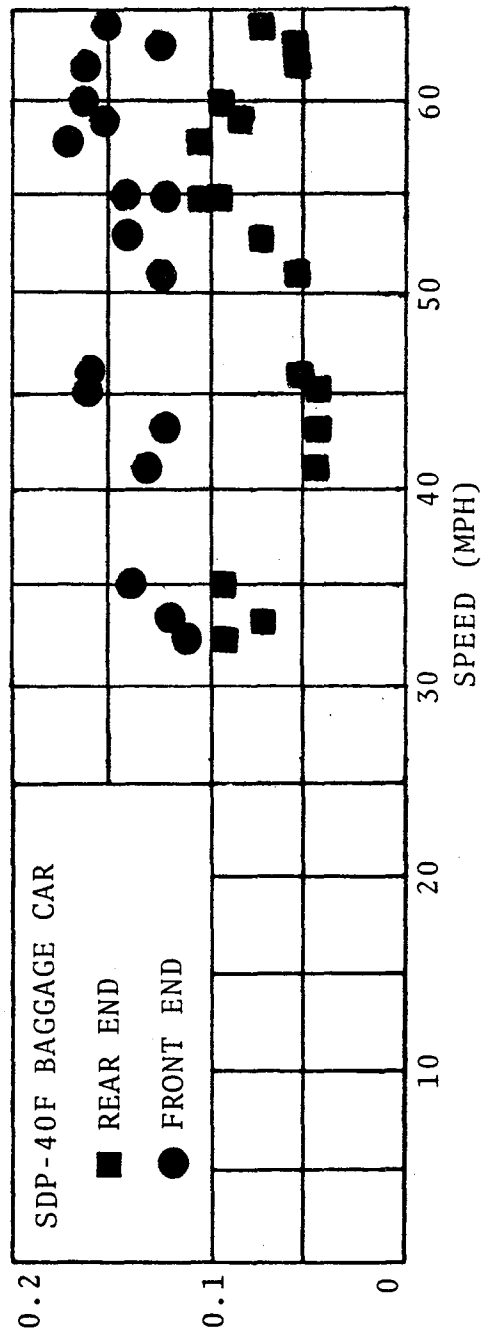
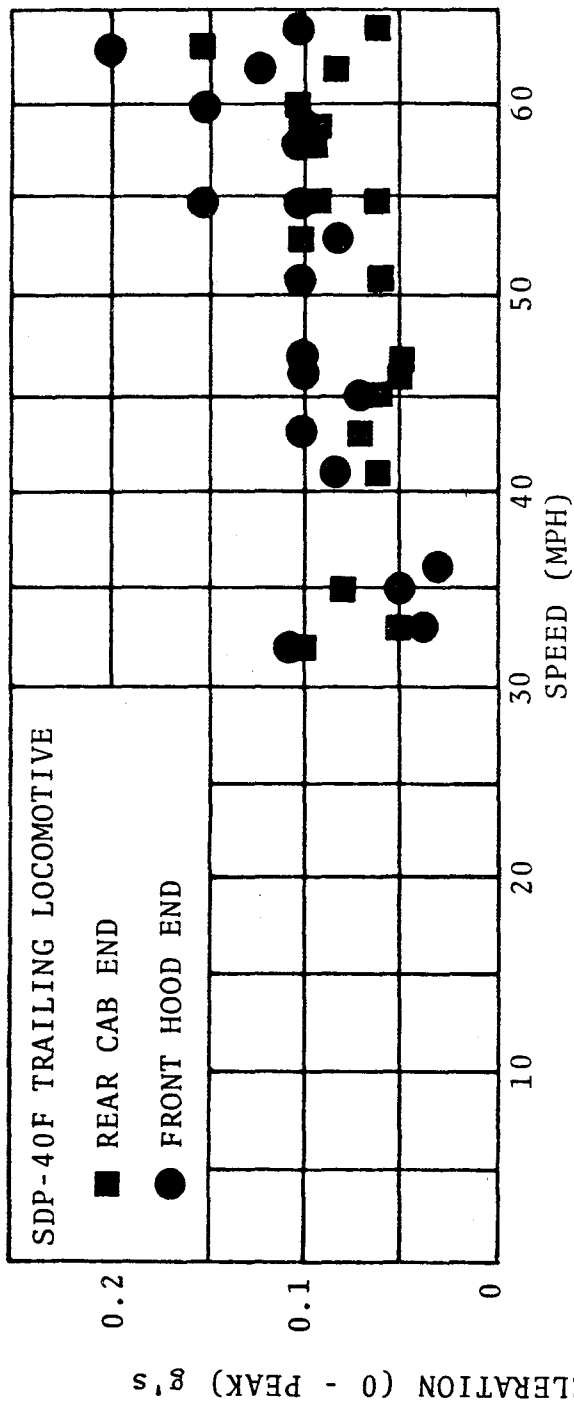


FIGURE 5-53 TRAILING LOCOMOTIVE/BAGGAGE CAR LATERAL ACCELERATION INTERACTION FOR SDP-40F CONSIST VERSUS SPEED (BASELINE RUNS, ONBOARD DATA)

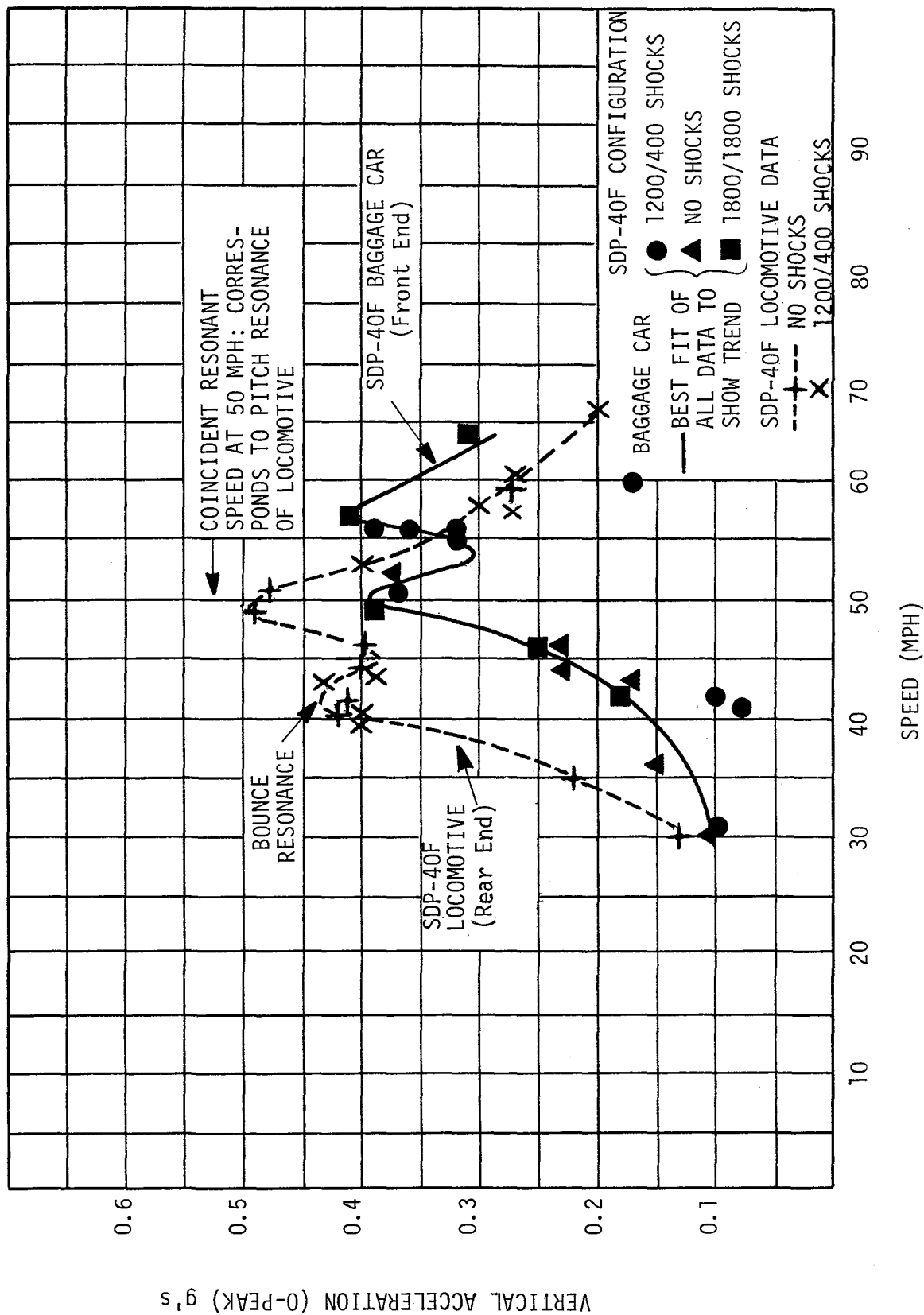


FIGURE 5-54 VERTICAL CARBODY ACCELERATIONS OF SDP-40F LOCOMOTIVE AND BAGGAGE CAR OVER ADJACENT TRUCKS AT ROAD CROSSING NEAR MP 257.5 (POWER MODE)

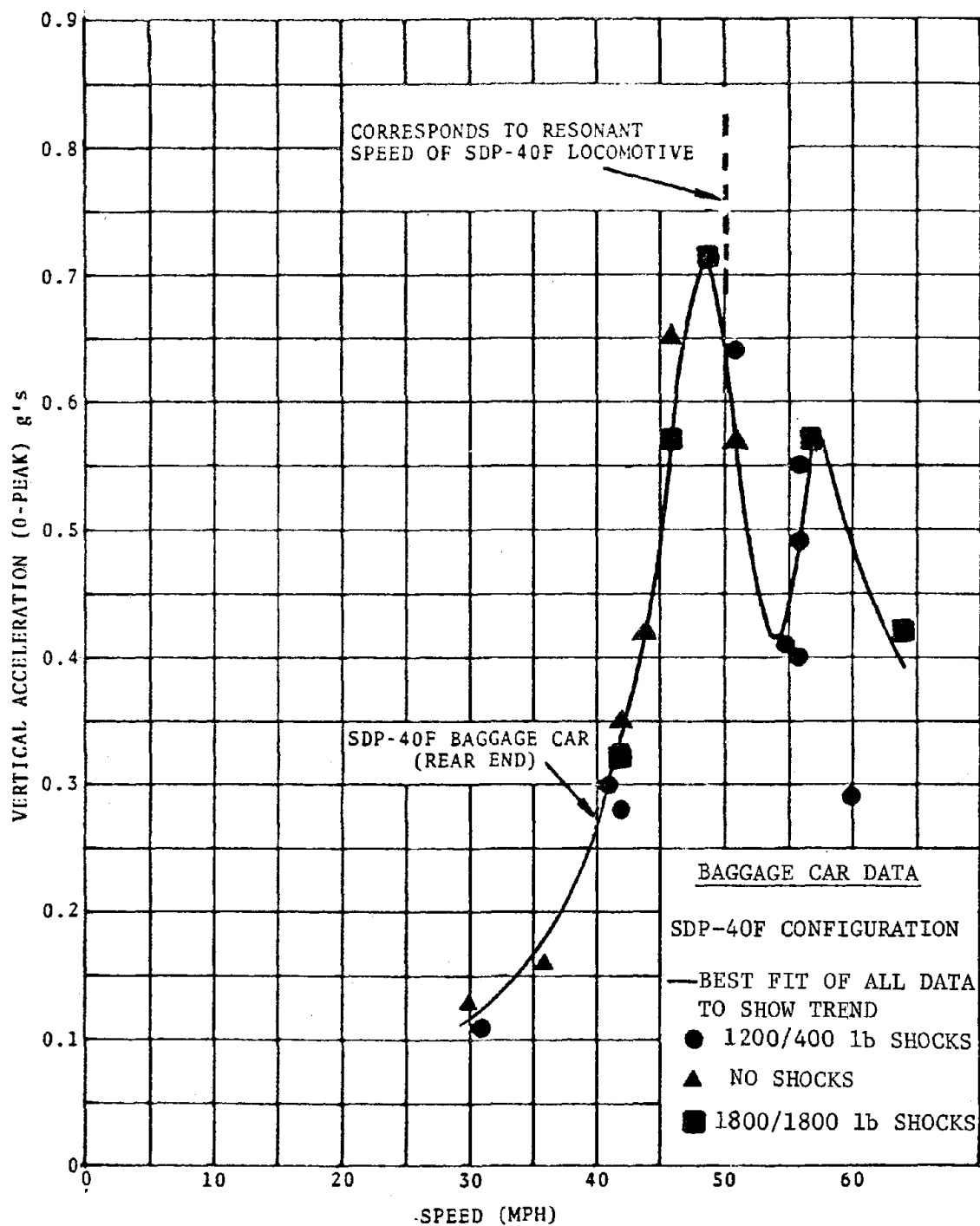


FIGURE 5-55 VERTICAL ACCELERATION OF SDP-40F BAGGAGE CAR REAR END AT ROAD CROSSING NEAR MP 257.5 (POWER MODE)

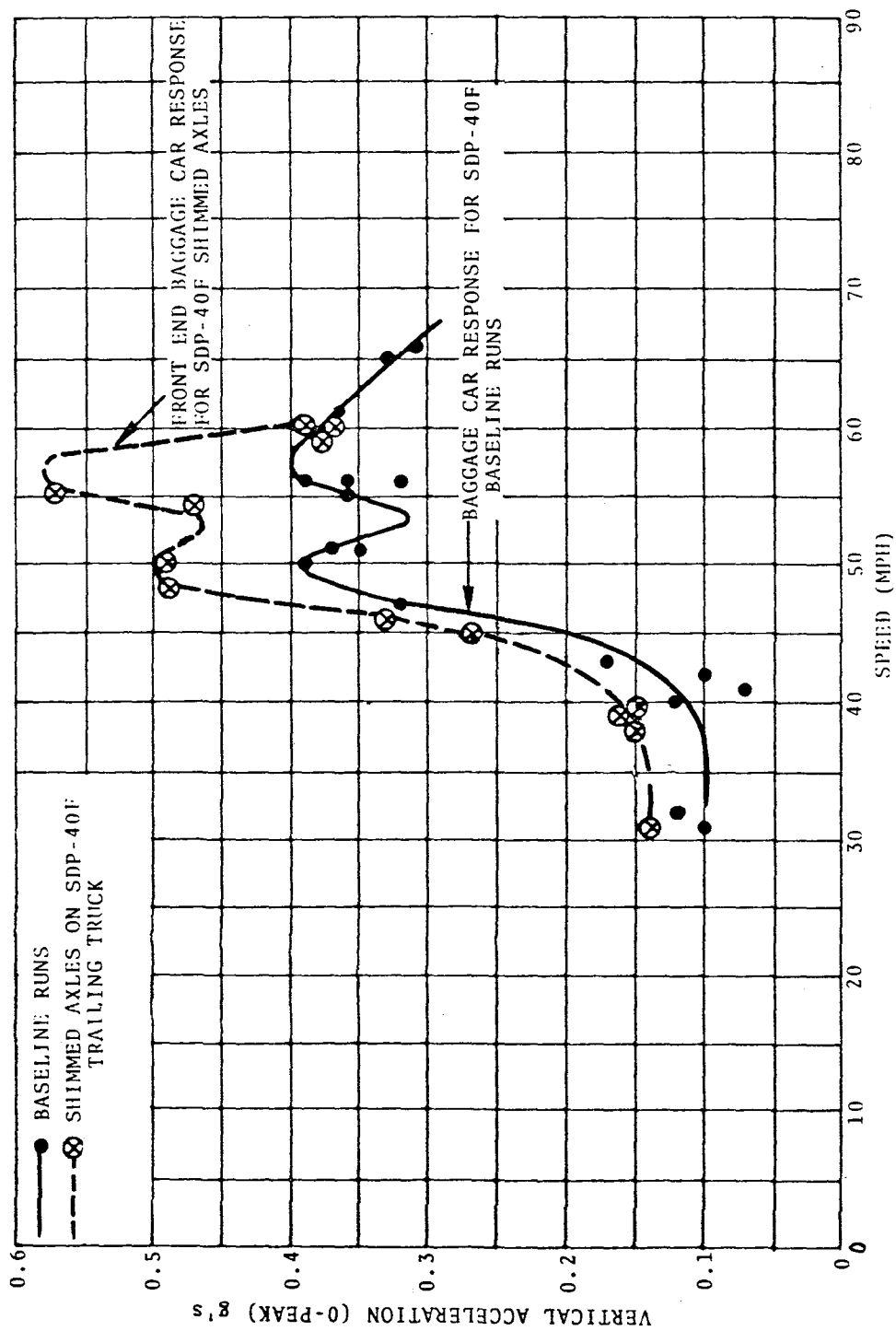


FIGURE 5-56 EFFECT OF SHIMMED AXLES 11 AND 12 OF SDP-40F ON FRONT END VERTICAL ACCELERATION OF THE BAGGAGE CAR AT ROAD CROSSING NEAR MP 257.5

to the baggage car coupler) increased the baggage car front end vertical acceleration by 45% near the resonant speed around 57 mph. The shimming of the two trailing axles of the trailing truck, although intended as a simulation of the presence of worn (smaller diameter) wheels on the lead axle, also produced a vertical displacement of the locomotive coupler relative to the baggage car coupler. Such a mismatch would not result from worn lead axle wheels. The observed increase in baggage car vertical accelerations with the addition of shims to the SDP-40F is most probably associated with the change in locomotive coupler height. This result indicates a need for special concern in maintenance control and train makeup for assuring appropriate vertical coupler alignment between the SDP-40F and the baggage car.

Because of the coupler equipment problems on AMTRAK baggage cars which EMD reported in February 1977, EMD recommended that an "E"-shelf coupler be used in place of the type "F"-interlocking coupler on SDP-40F locomotives. The "E"-shelf coupler would be more tolerant of vertical coupler mismatching and would minimize the transmission of vertical coupler loads between locomotive and baggage car, while still preventing coupler override.

Figure 5-54 also shows the proximity in maximum vertical acceleration response speeds of locomotive and baggage car. These resonant speeds vary depending on the baggage car load and the weight of fuel and water in the locomotive. This creates a potential overlap of resonant speeds and can contribute to a stronger vertical interaction between locomotive and baggage car, especially when coupler misalignments may exist.

5.4 FUTURE IMPLICATIONS

The results of a testing program of this scope have several kinds of implications for the future:

1. For the railroads and how they choose to operate the SDP-40F in the future.
2. For the locomotive builders and how future locomotives are designed.
3. For the railroads, the locomotive manufacturers and the Federal Railroad Administration and how new locomotives should be tested and accepted for service in the future.

This report will not attempt to develop the implications for future locomotive operations and/or design. There are many factors other than these test results which enter into such decisions and these are beyond the scope of this report. However, this test series has provided some clear implications and lessons regarding future rail vehicle testing. The most important of these are summarized in the remainder of this section.

1. Vehicle Acceptance Testing

The results of these comparative locomotive tests on Chessie System track show significant differences in the sensitivity of the SDP-40F and E-8 locomotives to track geometry inputs and operational conditions. These tests performed after the fact of a perceived safety problem, demonstrate the need for before-the-fact guidelines for safety acceptance of new or modified locomotives. The purchasing railroad and the locomotive builder have traditionally negotiated specifications for equipment with particular structural or mechanical features such as weight, tractive force, and compatibility, but the aspect of the dynamic response of locomotives is rarely addressed in detail. To fill this void, consideration should be given to developing a methodology for testing the dynamic performance of locomotives before they are permitted in general service. Development of such a locomotive acceptance testing procedure would be beneficial to both manufacturers and users of railroad equipment.

2. Permanent Test Facility

It is difficult to predict whether the need for testing of this type will be continuous. However, if only two or three such tests are forecast, a test facility would probably represent the most cost-effective approach. Wayside instrumentation could be permanently installed and amortized over several test series. Provisions could be made for controlled introduction of track geometry perturbations. Data reduction processes could be standardized. Logistical support could be established and routinized. A learning process could begin through repeated use of the same personnel and equipment.



6. REVIEW GROUP COMMENTS, OPINIONS AND VIEWPOINTS

This section provides the observations, comments, and dissenting opinions resulting from a review of the draft of this report by the Review Group. This group was composed of technical railroad safety experts who worked interactively over a period of more than a year, as outlined on pages 4-8 and 4-9. As part of the process, the group members had recurring opportunity to review the work and to make valuable contributions to various aspects of the undertaking. Each group member reviewed the draft of the report and was invited to submit any comments or criticisms for inclusion in this section of the final publication with the understanding that the authors would provide accompanying remarks. Only EMD offered written comments. The entire text of their submittal has been included with remarks by the authors inserted after each of the comments.

EMD Comments

"Tests of the AMTRAK SDP-40F Train Consist Conducted on Chessie System Track"

As the manufacturer of the SDP-40F locomotive, we have been vitally interested in determining the causes of derailments of Amtrak trains pulled by SDP-40F's. Accordingly, we have conducted extensive tests to evaluate the performance of SDP-40F and other locomotives and have actively participated in joint tests and studies designed to examine train-track interaction. EMD supported the tests on the Chessie System because we felt that more light could be shed on the dynamic interaction between locomotives and adjacent baggage cars and on the dynamic interaction between vehicles and the track on the Chessie. To aid this effort, we provided our test car and instrumentation, participated in the acquisition of the data, and participated as a member of the Review Group.

We would like to add the following comments to the report of these tests on the Chessie System:

1. We have not seen statistics developed, in this report or elsewhere, that demonstrate that the SDP-40F locomotive experiences a higher or lower number of derailments than other locomotives operating under similar conditions. There have been no statistics produced regarding E locomotive operation in the 1940's

to the 1960's when these locomotives were the predominant passenger locomotive in the U.S.A. Furthermore, we are not aware of any adequate statistics available to compare the use of SDP-40F locomotives with E or any other locomotives in the 1970's - a period of changing track conditions in some operations - when the SDP-40F's were the predominant Amtrak passenger locomotive.

Available statistics comparing the SDP-40F with other 6-axle locomotives in lower speed freight service indicate that the derailment rates (in million miles per derailment) are similar in the same time periods.

Appendix A of the report shows statistics for trains derailed with SDP-40F units - whether the locomotives were involved or not. Using train derailment statistics (and such statistics are not necessarily relevant to locomotive derailments), the available data suggests that SDP-40F-powered trains have a derailment rate similar to or more favorable than the Amtrak trains powered by other locomotives.

Authors' Remarks:

As EMD states, one of the reasons for these extensive tests were "that more light could be shed on the dynamic interaction between locomotives and adjacent baggage cars and on the dynamic interaction between these vehicles and the track---". We agree that historical statistical data cannot adequately distinguish the changing conditions described and is not applicable for comparing the relative dynamic performance of locomotive consists used under an undocumented variety of different operating, track, maintenance, and environmental conditions. However, in this case, various safety interests expressed concern about the derailment record of the SDP-40F consist which resulted in this and other test programs. The Chessie Test used a direct experimental approach and, for the first time, quantitatively measured and analyzed dynamic wheel/rail interactive forces utilizing both onboard and wayside instrumentation on two similar consists--the SDP-40F being investigated and the predecessor baseline E-8 under the same set of identical real world conditions. This effectively allowed comparison of the SDP-40F consist with a previously recognized standard.

2. The tests on the Chessie System represent an extensive effort, within a limited scope, to study locomotive-

train-track interaction relative to passenger train derailments. The data provides some new and valuable insights into locomotive and baggage car responses and vehicle-track interaction. The tests identified, and, to some extent, quantified several variables which might, in combination, cause a derailment.

We are in strong agreement with the observations in the report that the levels of wheel-rail loads measured in the tests are not considered excessive and that, in general, a combination of track conditions, vehicle configurations and maintenance, and operations is required for a derailment to occur (Executive Brief, page 1-6, Item 7). Furthermore, we support the approach that the findings can be used to develop recommendations to help minimize the contribution of each vehicle, track, and operations variable that was tested.

Authors' Remarks:

These tests not only facilitated "recommendations to help minimize the contribution of each vehicle, track and operations variable that was tested", but produced better measurement devices, improved analytical techniques, predictive capabilities and developed a systems methodology to deal with the "combinations" often involved in derailments. The consistency of the data collected together with the analytical procedures employed generated meaningful comparative trends which established the power of the approach in dealing with such difficult but characteristic safety problems which are inevitably rare events.

3. While the tests on the Chessie System were very comprehensive within the scope of the test program conducted, the scope itself turned out to be relatively narrow with respect to range of track conditions and with respect to locomotive design configurations and maintenance. Of course, any test or series of tests is inherently limited. However, the scope of these tests was further restricted by the objective of concentrating on the test data "where the performance of the SDP-40F consist exhibited unfavorable trends in comparison to the E-8 baseline case." Consequently, the report gives a one-sided picture of the SDP-40F-E-8 comparison.

A primary test site was selected to maximize the SDP-40F locomotive response with respect to the E-8

locomotive response, even though the response levels were relatively low at this location. Based on our experience in testing SDP-40F, E-8, and other locomotives, the lateral loads shown in the report (maximum or 95th percentile levels) are relatively low and are well below levels believed to be of concern from a derailment standpoint. For examples, the "severe case" L_{95} load in Figure 1-1 reaches only 16,000 lbs, and the maximum total truck lateral load shown in Figure 1-3 reaches only 25,000 lbs. These responses resulted from a particular set of track conditions selected and they are not representative of the wider range of responses observed in other tests. The regression analysis of 25 curves on "typical Class 3" track represents a somewhat larger range of track conditions and the results are an illustration of how either the SDP-40F or the E-8 may exhibit higher responses.

With regard to locomotive design configurations, the testing was limited to an SDP-40F locomotive weighing 396,000 lbs. and an E-8 locomotive weighing 345,000 lbs. The findings do not compare the SDP-40F to other heavy 6-axle locomotives or compare the HT-C truck to other 3-axle, 3-motor truck designs.

The tests also did not, in depth, address locomotive design and maintenance variations such as those relating to middle axle lateral loads of 3-axle trucks. In these tests, middle axle data is available for only the joint that was selected for wayside instrumentation. While this joint consistently produced relatively low middle axle loads on the E-8 locomotive, other tests have demonstrated that middle axle lateral loads can be relatively low or relatively high for both SDP-40F and E-8 locomotives (see Item 4 below for an example). Based on our testing and mathematical modeling, it appears that middle axle lateral loads are influenced by a number of variables, including lateral axle clearance, lateral wheel-rail clearance, unsprung mass, rail geometry, rail stiffness, and wheel profile. Although differences in several of these variables existed between the two locomotives tested, only one of these variables was investigated.

Authors' Remarks:

The scope of these tests and subsequent analysis was significantly more extensive than that of previous tests in many respects. Continuous measurement of wheel/rail forces on axles of both the SDP-40F and E-8 locomotives over hundreds of miles of trackage with concurrent track geometry recording produced a massive "bank" of unique and valid data. For the first time, albeit mostly limited to one axle on each locomotive, the historical dilemma of how to determine what constitutes (1) a "level" of wheel/rail force for concern and (2) a representative curved track segment, was addressable. Various force trend lines were produced for each of the two instrumented locomotives based on data from a number of track curves. These trends, when plotted, very definitely indicated where the forces associated with the locomotive under investigation differed from the baseline standard and substantiated that the primary test site was representative. In addition, the track geometry data provided regression analysis variables to tie-in track variations for evaluating and predicting performance. The comparative trends described in the report are a vastly improved basis for resolving many of the statistical evaluation problems encountered in the past.

The purpose of the Chessie Test was not to provide a general comparison of the E-8 and SDP-40F locomotives, but rather to use the E-8 as a basis of comparison to help identify what conditions or combination of conditions might cause the SDP-40F to exhibit unfavorable dynamic response. As such, test conditions and test variables were selected which represented the particular range of track and vehicle conditions characteristic of the earlier AMTRAK derailments of the SDP-40F consists. Vehicle configuration changes concentrated on those which had been agreed upon with the Review Group as possibly contributing to prior derailments.

Subsequent to these tests, an additional series of SDP-40F and E-8 consist tests were conducted at the Transportation Test Center in Pueblo, Colorado as part of a broader test program on rail/vehicle interaction. These tests will provide additional continuous and simultaneous wheel/rail force data for all three axles of the trailing truck of locomotives over a broader speed range than the Chessie Test and over precisely controlled rail geometry perturbations. The results of these tests, to be published at a later date, will expand the range of test variables for these two locomotives and other rail vehicles.

4. In the absence of finding a specific cause for the derailments of SDP-40F-powered trains, the report focuses on certain locomotive response trends that were observed. Although examination of trends can be helpful in studying vehicle-track interaction phenomena, we strongly disagree with the assumption stated on page 1-3 of the Executive Brief:

".....this approach.....assumes that extrapolation of comparative trends is justified."

The approach of taking data from lower level locomotive responses and extrapolating to higher level responses generally is not justified. It is not valid to assume that comparative trends can be extrapolated to higher level track inputs or to higher speeds. This can be illustrated in two ways within the context of comparative SDP-40F-E8 testing that has been performed:

- A. Consider the example of Figure 1-1 in the Executive Brief. If the test data was only available up to speeds of 45 or 50 mph, extrapolation of this data would suggest that the E-8 lateral loads continue to exceed the SDP-40F loads at higher speeds. Obviously, the data obtained at higher speeds on this site contradicts such an extrapolation.
- B. Consider the lead and middle axle data of Figures 1-2 and 1-4 in the Executive Brief. This wayside L_{max} data is reproduced in Figure 6-1 below and is compared to the corresponding axle 10 and 11 (trailing truck of a two-locomotive consist) data from the SDP-40F-E8 testing in 1976 on another railroad.

In these tests at a site on the Illinois Central Gulf Railroad, the track perturbations produced higher lateral loads than at the site that was selected for the Chessie Test. At the ICG site, both the SDP-40F and E-8 locomotives exhibited lead axle and middle axle lateral loads in the range of 25,000-30,000 lbs. At these higher level responses, the SDP-40F and E-8 lateral loads were very similar. These results cannot be extrapolated from the data reported from the tests on the Chessie. (The ICG data shown here was obtained from wayside instrumentation which was applied, calibrated, and corrected the same as described in the report on the Chessie Test.)

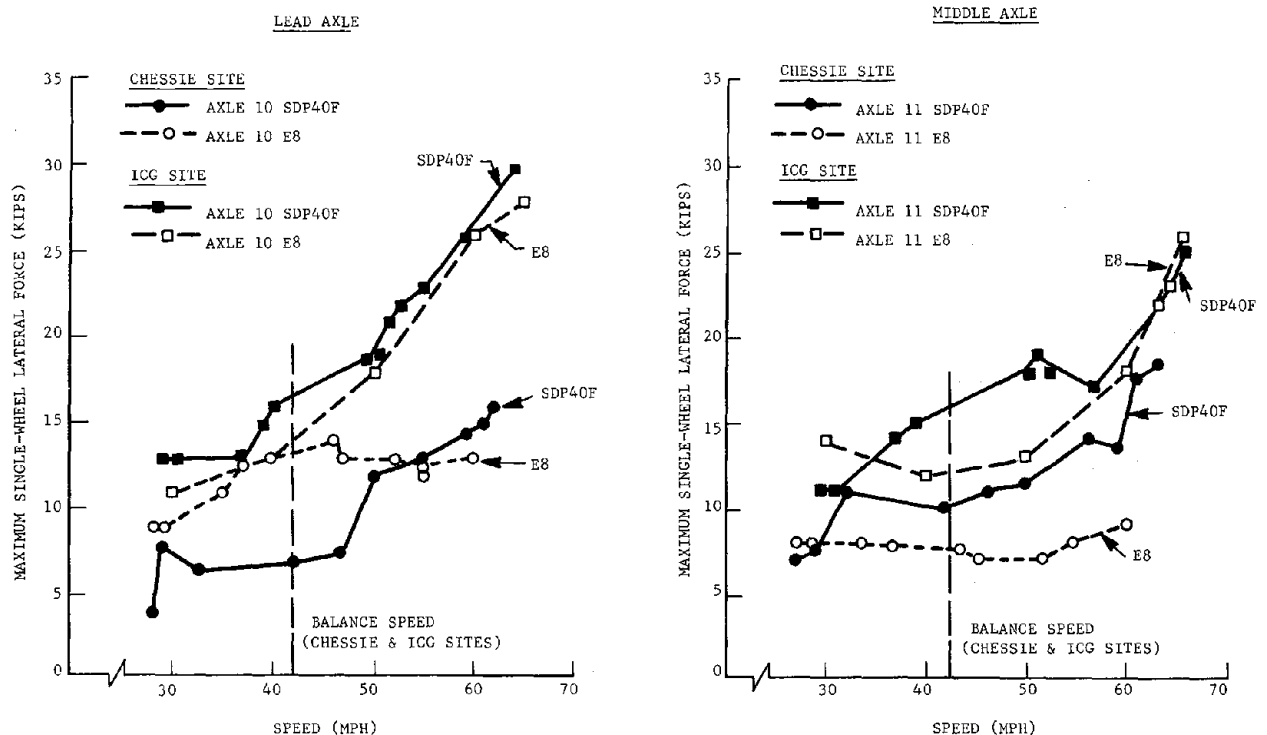


FIGURE 6-1 COMPARISON OF LEAD AND MIDDLE AXLE WHEEL LOADS IN CHESSIE & ICG TESTS (WAYSIDE DATA FROM BASELINE RUNS IN BOTH TESTS)

Since it is generally not valid to extrapolate trends from lower level locomotive responses to higher level responses, caution should be exercised in using the comparative data to predict differences at higher levels.

Authors' Remarks:

We recognize that "caution should be exercised in using comparative data to predict differences at higher levels". However, the reproducible trends developed can be supplemented with available knowledge of dynamic curving tendencies and mechanisms to rationally support predictions of force behavior for other than the precise speeds and conditions tested. In fact, most tests because of cost considerations are limited and thus depend to some extent on inferences made from comparative trends.

In relating one series of tests to another, the comparisons should be made on a common basis. In the present report, results from the Chessie Test indicate that the trend of $L_{0.5}$ through a complete curve is a more effective descriptor than L_{max} in characterizing the general performance of the vehicle. Indeed, in Appendix D of the report, it was shown that the trends obtained by looking only at L_{max} at a specific location on the track could be very different from location to location, depending upon the specific track geometry at that location. The purpose of the regression analysis, therefore, was to extract the characteristic behavior of the vehicle through a representative sample of curves (including curves where L_{max} exceeded 35 kips), and to identify conditions under which the SDP-40F loads would be different from or similar to those of the E-8. Since the ICG data supplied by EMD is based only on L_{max} at a specific location, it should not be compared directly with $L_{0.5}$. In addition, the supplied ICG data does not specify the track geometry and test conditions at the wayside test site. Therefore, meaningful comparison with the L_{max} data obtained at the ICG tests and the trends obtained at the Chessie test site is difficult.

The ultimate proof of the efficacy of any extrapolation to higher force levels and/or speeds is actual test results covering the extended conditions. Preliminary indications are that the results of subsequent tests conducted at the Pueblo Transportation Test Center will confirm the types of track and operating conditions under which significantly higher single wheel and total truck lateral force level differentials are experienced by the SDP-40F locomotive.

5. Although present FRA track safety standards allow operation up to 3 inches unbalance on curves, we believe that maximum unbalance should, in general, be more restricted on the lower classes of track in recognition of the track geometry and strength deviations permitted. The 3-inch unbalance rule applies generally to all rail vehicles, although there are restrictions in effect for certain cars with high centers of gravity. Lower classes of track permit larger geometry deviations such as alignment and cross-level and allow lower structural integrity of the crossties and fasteners. Consequently, operation at a specific unbalance provides a greater margin of safety on Class 5 track than on Class 3 track, for example. It is reasonable, then, that maximum allowable unbalance be reduced as the class of track is reduced. On the lower FRA classes of track, maximum unbalance of less than 3 inches is appropriate for rolling stock

with heavy axle loads and/or high centers of gravity. The SDP-40F is just one example of vehicles that are in this category.

Authors' Remarks:

The important consideration is the level of dynamic lateral force (or ratios) exerted between the particular vehicle and the track. We agree that for the same force levels, "stronger" track will be better able to resist rail spreading and overturning. Logically, distinctions as to vehicle, class of track and maximum speed limits are in order as suggested. Recommendations in the report support the construction of a dedicated test facility which could be utilized by the industry to quantify and establish appropriate categories.

6. The importance of quantifying the time duration of wheel-rail loads has been more fully recognized in recent tests, and we recommend that rail vehicle response descriptors for specific time durations be considered in future tests and in research aimed at developing derailment criteria. Our analysis of the locomotive response on the specific Chessie test curve has utilized such descriptors. Figure 6-2 shows the specific time durations of lateral wheel-rail loads and L/V ratios from the instrumented wheelsets at the maximum test speeds. This data was developed not from just the instrumented joint in the curve but from all of the track perturbations in the curve. In the 60-62 mph runs, the SDP-40F generated lead axle lateral loads 1000-4000 lbs. higher than the E-8 at specific time durations in the range of 20 msec (milliseconds) to 100 msec. Comparing wheel LV ratios, the E-8 generated levels about 50% higher than the SDP-40F in the 30-40 msec range and generated equivalent levels for time durations above 80 msec. For reference, the L/V data is compared to EMD's predicted wheel L/V vs. time duration relationship for wheel climb.

The $L_{0.5}$, V_5 and $L/V_{0.5}$ descriptors utilized in the Chessie Test have some definite merits for analyzing vehicle responses. Looking at the load or L/V that is exceeded 5% of the time helps to reduce the data scatter sometimes associated with peak values.

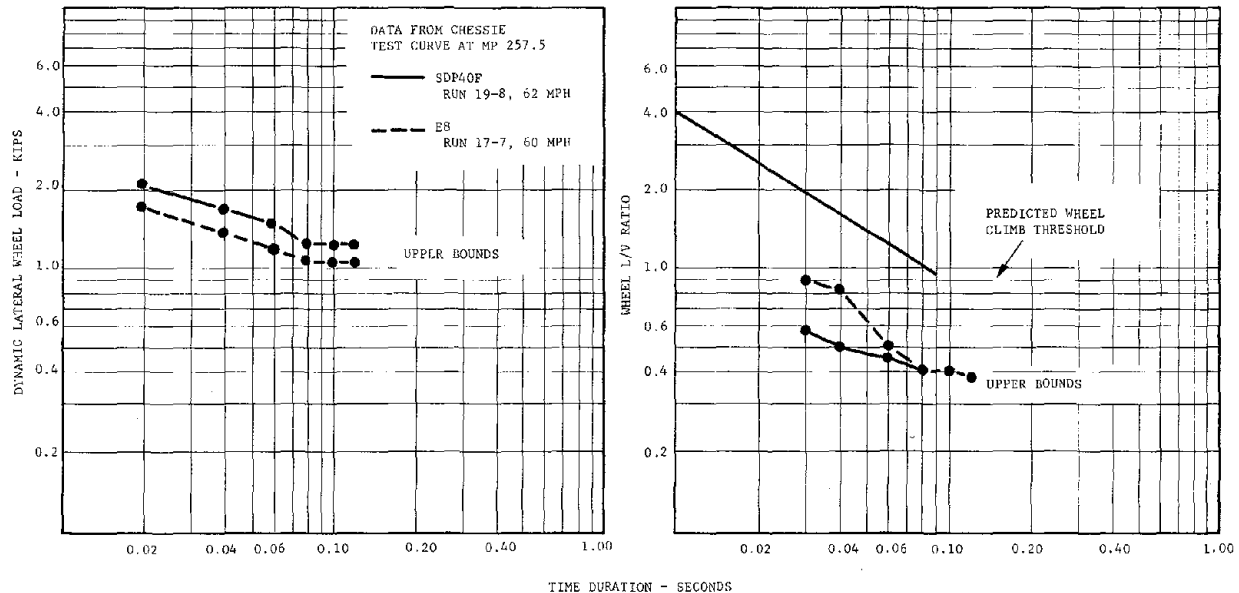


FIGURE 6-2 COMPARISON OF LEAD AXLE WHEEL LOADS & L/V RATIOS IN CHESSIE TEST

However, this 95th percentile level can be raised or lowered depending on the length of the test zone chosen for analysis. Also, this 95th percentile level is not definitive with regard to the time duration characteristics and energy content of the highest responses in the test zone. Within the L_{95} time range of about 20-40 msec (as described in Appendix D of the report), there can be significant changes in locomotive response levels. Although we do not take exception to the 95th percentile data in the report, primarily because it is generally of relatively low levels, we recommend using descriptors associated with specific time durations in comparing locomotive responses and in developing derailment criteria.

Authors' Remarks:

As mentioned, the importance of incorporation of time duration representations of wheel/rail loads is well recognized. The data exhibited in Figure 6-2 of the EMD comment illustrates very well the type of comparisons that can be made by extracting information from the data bank as dictated by the needs of the technique. We feel that this

method of data reduction complements the L_{95} , V_5 and L/V_{95} descriptors utilized, and a limited application to this case revealed no significant differences in essential findings. Performances of the two consists tested were very reproducible at the 95th percentile level because the various test zones were carefully selected within the confines of each curve and under these conditions the percentile approach has definite advantages in concisely depicting comparative force trends.

The report recommends further work to develop and validate more absolute derailment criteria and it appears that generation and analysis of time duration-oriented force data in this respect is very desirable. The data bank is available for such purposes.

7. Table 1-1 of the Executive Brief states that "wheel climb was never designated as the mechanism of the derailment." We would concur that it is unlikely that individual wheel climb was the derailment mode for locomotives which have a high vertical wheel load. However, it is possible that individual wheel climb could have been involved in the 9 derailments listed in which the locomotive did not derail. It is also possible that wheel climb of the baggage car was involved in some of the locomotive-baggage car derailments. The wheel climb mode should not be overlooked; and data which is related to wheel climb (e.g., wheel L/V) should be considered, especially for vehicles such as the baggage car with light wheel loads.

Authors' Remarks:

As EMD Figure 6-2 indicates, wheel load L/V ratios were collected and analyzed for the onboard instrumented axles of both the SDP-40F and E-8 locomotives. Various summaries of locomotive L/V_{95} ratios are included in the report, together with some L/V_{max} exhibits generated from the instrumented wayside site. Baggage car L/V ratios were only available from the wayside instrumentation and were not utilized to any extent in the development of baggage car-related recommendations. Rather, the continuous onboard lateral and vertical acceleration measurements provided the preponderance of comparisons concerning baggage car performance.

BIBLIOGRAPHY

Abbott, P.W. Track/Train Dynamics Test Results: Flexicoil Truck Static Test, Vol. I. Martin Marietta Corp., Denver Division. MCR-77-100, June 1977.

Abbott, P.W. Track/Train Dynamics Test Results: HTC Truck Static Test, Vol. I. Martin Marietta Corp., Denver Division. MCR-77-100, March 1977.

Ahlbeck, D.R., Dean, F.E., and Harrison, H.D. An Evaluation of the SDP-40F Derailment Problem. Battelle Columbus Laboratories. Summary Report to National Railroad Passenger Corp., February 18, 1977.

Association of American Railroads. Track-Train Dynamics Staff. AMTRAK Locomotive Equipment Evaluation Program Recommendation for Improvement, February 1977.

"CN Seeks More Stable Track." Progressive Railroading. Vol. 16, No. 2, March 1973, pp. 62-66.

Dokainish, M.A., Siddall, J.N., Elmaraghy, W. "On the Effect of Track Irregularities on the Dynamic Response of Railway Vehicles." ASME Transactions. Vol. 96, No. 4, November 1974, pp. 1147-58.

"Dynamic Characteristics of Several Elastomeric Suspension Elements Used on Locomotives." Report No. NCR 78-622.

Elkins, J.A. and Gostling, R.J. "A General Quasi-Static Curving Theory for Railway Vehicles." British Railways Research and Development Division. Presented to IUTAM Symposium, Vienna, September 1977.

Ellsworth, D.H. Locomotive Derailment Study: Pt. 1, Analysis of 4-Year Locomotive Derailment Sample. Chesapeake and Ohio Railway, Technical Report 71-120, September 1971.

ENSCO, Inc. Engineering Test and Analysis Division. SDP-40F/E-8 Test Results Report: Dynamic Performance Testing, Vols. 1 & 2. Prepared for Federal Railroad Administration, September 1977.

ENSCO, Inc. SDP-40F Test Series conducted between March 16 and April 13, 1976, on the ICG Railroad: Summary of Comments and Conclusions. Prepared for AMTRAK, May 1976.

BIBLIOGRAPHY (Cont'd)

ENSCO, Inc. Presentation of SDP-40F Test Results on June 3, 1976: AMTRAK, ENSCO, EMD, BATTELLE.

Garg, V.K. and Mels, K.D. "Comparative Study of Locomotive Lateral Stability Models," in Railroad Engineering Conference, October 1975 Proceedings, pp. 123-129. PB 252968.

Garg, V.K. and Mels, K.D. Lateral Stability of a 6-Axle Locomotive. Presented at IEEE-ASME Joint Railroad Conference, San Francisco, April 1975. ASME 75-RT-7.

Garg, V.K., Hawthorne, K.L., Chang, E.H., and Hartmann, P.W. Development of a Simulation Methodology for Optimizing Locomotive Suspension Systems. American Society of Mechanical Engineers. ASME 77-RT-6, 1977.

Gilchrist, A.G. "Interaction Between Vehicle and Track." British Railways, Research and Development Division. Presented at AIT Symposium on Railway Dynamics, May 1977.

International Union of Railways. Constructional Arrangements for Improving the Riding Stability and the Guiding Quality of Electric and Diesel Engined Locomotives and Vehicles: Report on Tests Made on the Locomotive 1141-04 of the Austrian Federal Railways. No. BIO/RPI/E, 1957.

Klinke, W.R., Swenson, C.A. "Tracking and Ride Performance of Electromotive 6-Axle Locomotives," in Railroad Engineering Conference, Pueblo, October 1976, Proceedings: "Railroading Challenges in America's 3rd Century, Improved Reliability and Safety," FRA/ORD-77/13, pp. 106-188.

Koffman, J.L., Fairweather, D.M.S. "Some Problems of Railway Operation at High Axle Loads." Rail Engineering International, Vol. 5, No. 4., June 1975.

Lind, E.F. "National Research Program on Track-Train Dynamics," in Railroad Engineering Conference, September 1972, Proceedings: "Advancing Freight Car Design to Meet the Changing Environment of Modern Train Operations."

Magee, G.M. Measurements of Vertical and Lateral Forces on Both Rails of a 6 Degree Reverse Curve Under Different Types of 6-Axle and 4-Axle Diesel Locomotives. Association of American Railroads, March 1967.

BIBLIOGRAPHY (Cont'd)

Marta, H.A., Mels, K.D., Itami, G.S. Design Features and Performance Characteristics of the High Traction, 3-Axle Truck. American Society of Mechanical Engineers reprint.

Marta, Henry A. and Mels, Kenneth D. Tracking and Ride Performance of EMD-2 6-Axle Locomotives. General Motors Corp., Electro-Motive Division. Presented at Railway Fuel and Operating Officers Assoc. Convention, September 1976.

National Transportation Safety Board. Railroad Accident Report: Derailment of AMTRAK Train on Burlington Northern Railroad Near Ralston, Nebraska, December 16, 1976. NTSB-RAR-77-8, October 1977.

National Transportation Safety Board. Railroad Accident Report: Derailment of AMTRAK Train on Louisville and Nashville Railroad, New Castle, Alabama, January 16, 1977. NTSB-RAR-77-9, October 1977.

National Transportation Safety Board. Railroad Accident Report: Derailment of AMTRAK Train on Louisville and Nashville Railroad, Pulaski, Tenn., October 1, 1975. May 1976. PB 254965.

National Transportation Safety Board. Safety Recommendation R-77-1 and 2, Issued February 3, 1977; revised April 4, 1977.

Noble, S.L. et al. Analysis of Track Forces Generated by SDP-40F and E-8 Locomotives at Farina and Dongola, Ill. Battelle Columbus Laboratories. Summary Report to National Railroad Passenger Corp., May 1976.

"Pilot Study of Dynamic Response of 6-Axle Locomotive." U.S. Department of Transportation, Transportation Systems Center, Structures and Mechanics Branch, Cambridge, MA, report in preparation.

Reich, O. and Villa, V. Contribution Towards the Study of the Horizontal and Vertical Running Qualities of 6-Axle Motive-Power Unit. (Beitrag zur horizontalen und vertikalen Laufgutuntersuchung 6-achsiger Triebfahrzeuge) Hochschule F, Verkehrs F List Wissenschaft Zeitschr. N. 3, 1972.

BIBLIOGRAPHY (Cont'd)

Schmidt, J.J. Suitability of 6-Axle Locomotives for CO-BO Service; the Interaction with Track Structure. Chesapeake and Ohio Railway Research Report, February 1966.

Siddall, J.N., Dikainish, M.A., Elmaraghy, W.H. Vibrations of Railway Vehicles. Canadian Congress of Applied Mechanics, 4th Proceedings.

Scott, J.F., Blevins, W.G., and Wilson, J.T. Technical Studies to Evaluate the Influence of Operational Factors on Track Loading. ASME Winter Annual Meeting, 1972, 72-WA-RT-11.

"Six-Axle 10,600 HP Locomotive Selected for Gotthard Route." Railway Gazette International. Vol. 129, No. 6, June 1973, pp. 220-223.

Smith, K.R. and Yoshino, R.T. AAR-AMTRAK-EMD-FRA Testing of SDP-40F and E-8 Locomotives of the Chessie System. General Motors Corp. Electro-Motive Division. Final Report No. 898-77-199, October 1977.

Southern Pacific Transportation Co., Technical Research and Development Dept. Dynamic Performance of the HTC Suspension System under 6-Axle Locomotives, July 1977.

Swiss Locomotive and Machine Works, Winterthur. Mechanical Design of the High Performance Locomotive Type Re 6/6 of the Swiss Federal Railway (SBB), July 1974.

"Track Gage and Flangeway Widths for Operation of Diesel Power on Curved Track." American Railway Engineering Association Bulletin. Vol. 59, 1958, pp. 101-174.

Track/Train Dynamics Interaction Conference, 2nd, December 1974, Proceedings, Vols. 1 and 2.

Way, G.H. The Nature, Magnitude and Frequency of Loads and Forces Applied to Railroad Roadbed. Chesapeake and Ohio Railway, Technical Report, May 1967.

Yoshino, R.T. and Smith, K.R. AMTRAK SDP-40F Derailment Tests on the Burlington Northern Railroad. General Motors Corp. Electro-Motive Division. Report No. 898-77-200, December 1977.

APPENDIX A

DERAILMENTS OF SDP-40F CONSISTS

AMTRAK SDP-40F powered trains, in service since mid-1973, had been involved in 21 derailments by early 1978. Complete data on the unit-miles travelled by these locomotives during that period of time are not available. For a three-year segment of this period, mileage estimates range from a low of 50 million miles to a maximum of 150 million miles. The most reasonable estimate appears to be that the SDP-40F fleet accounted for about 70% of AMTRAK's annual mileage, leading to an estimate for the three years of 90 million miles. Using this estimate, one obtains a derailment rate of 4.5 million miles per derailment. The low and high estimates would be 2.5 million miles per derailment and 7.5 million miles per derailment, respectively.

Table A-1 contains a brief summary of the 21 derailments involving an SDP-40F consist up to January 1978. Table A-2 contains more detailed information on 15 of the 21 derailments. Figure A-1 shows some of the information contained in Table A-2 in the form of histograms.

The data in Tables A-1 and A-2 indicate that:

- There were approximately 7 derailments per year, on the average (20 derailments in 3 years). In 1973, the rate was zero, due to the limited number of SDP-40F locomotives in service. In 1974, there were 9 derailments, one of which is not listed because of unavailable data. In 1975, there were 3 derailments. In 1976, there were 7 derailments.
- The derailments occurred on six different railroads.
- Of the 21 derailments:
 - twelve were derailments of an SDP-40F;
 - fifteen were derailments of either an SDP-40F or the car following an SDP-40F in the consist;
 - five were derailments in which the baggage car was the first vehicle derailed; and
 - the train length varied from 1 locomotive + 5 cars to 2 locomotives + 20 cars.

TABLE A-1 DERAILMENTS OF SDP-40F CONSISTS

Study does not include derailments where train speed was known to be less than 20 mph or derailments caused by collision or vandalism.

EY:  LOCO  CAR  DERAILED  BAGGAGE CAR












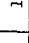
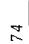
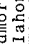

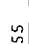
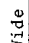
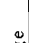
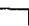











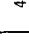
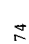
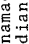

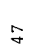
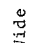
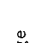
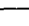












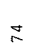
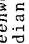

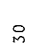
















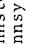
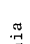
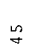
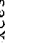
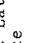
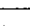











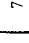

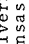


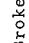
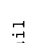












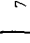
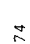
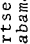

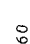
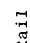
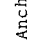
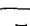






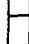




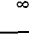
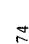
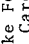
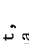
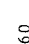
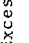
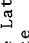
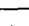
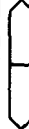
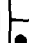
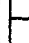









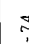
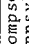
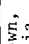

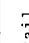
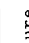
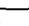
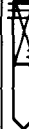
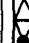









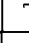
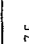
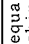

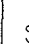
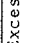
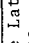
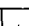


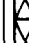






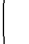

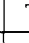
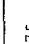
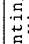

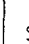
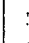

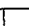





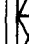



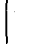

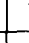

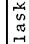




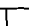











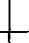

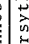




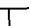

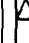

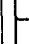
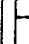






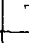

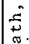

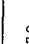
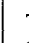
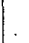
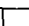
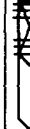



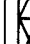






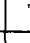
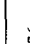


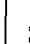

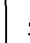
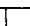
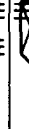










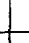

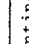




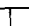
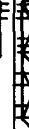










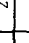

DERAIL- MENT NO.																					DATE	PLACE	SPEED MPH	REPORTED CAUSE
1																					1-14-74	Ardmore, Oklahoma	55	Wide Gauge
2																					4-30-74	Winamac, Indiana	47	Wide Gauge
3																					6-17-74	Greenwood, Indiana	30	o
4																					7-5-74	Johnstown, Pennsylvania	45	Excessive Lateral Force
5																					7-5-74	Malvern, Kansas	70	Broken Rail
6																					7-16-74	Hartselle, Alabama	60	Rail Not Anchored
7																					8-12-74	Wake Forest, N. Carolina	60	Excessive Lateral Force
8																					12-28-74	Thompsonstown, Pennsylvania	55	Rail Failure
9																					1-11-75	Plequa, Washington	60	Excessive Lateral Force
10																					1-31-75	Huntington, W. Virginia	48	Rail Rollover
11																					10-1-75	Pulaski, Tennessee	60	o
12																					1-6-76	Forsythe, Montana	70	Wide Gauge
13																					1-24-76	Heath, Ohio	70	Broken Frog
14																					1-30-76	Shandon, Ohio	50	Spread Rail
15																					2-13-76	Huntington, W. Virginia	60	Spread Rail
16																								

TABLE A-2 SUMMARY OF DATA FROM ACCIDENT REPORT FORMS

PARAMETER	DATE	RAILROAD	(NAME)	ATSF	PC	ATSF	PC	L & N	SCL	SP	PC	BN	C & O	L & N	BN	PC	C & O	1-30-76	2-13-76
SPEED			(MPH)	55	47	70	45	60	60	60	55	60	48	60	70	70	50	60	
DIRECTION			(1)	B/W	/W	-/E	B/E	B/N	B/S	B/W	E/E	B/W	-/E		B/E	W/W		-/W	
TONNAGE			(TONS)	640						1331			640				400		
CURVATURE			(DEG)	3°	1°	1°	2°	2°	3°	2°	2°	3°	2°	3°	3°	T	4°	2°	
GRADE			(% ASCEND. DES)	.39A	.22D		LEV	.2D	.66D	1.0D	.02A	.04D			.5D	LEV		.14A	
TERRAIN			(2)	L	L		L	R	L	R-H	M	H			R	R		H	
TRACK CLASS			(FRA CL)	3	3	5	3	4	4	4	3	2-3	3	3-4	3	4	3-4	4	
AGE			(YR)	9	9	9	22	16	23	3	12	25	30	8	10		2		
DENSITY			(GROSS TONS IN MILLIONS)										25.9	35.2			6.1	20.9	
RAIL LENGTH			(FT, W-WELDED)	1440	W	W	39	W	39	W	35	39	39	39	W	W	W	W	
RAIL WEIGHT			(LB/FT)	131	131	136	140	132	132	136	152	132	131	131	132	122	122	122	
TIE PLATES			(3)	D	D	D	D	D	D	D	D	D	S	D	D	D	D	D	
SPIKES			(4)	2/2	1/2	2/2	2/3	R/2	(9)	2/2	2/2	2/2	0/2	0/2	2/2	0/2	0/2	0/2	
ANCHORS			(5)	26	24	12	8	28	20	32+	12	32	9	46	42	42	42	42	
BALLAST			(6)	#5/8	SL/12	SL/-	ST/12	SL/16	CR/6	CR/10	CR/18	CR/12	ST/18	ST/24	CR/18	ST/24	ST/20	ST/20	
DEFECTIVE TIES/SPIKES			(7)	0/0	LOOSE		6/0	3/12	6/24	6/20	0/0	8/16	0/0	POOR	4/-	4/8	3/6	3/6	
BROKEN RAIL				NO	YES	YES	NO	NO	NO	NO	YES	NO	NO	NO	NO	NO	NO	NO	
GAGE IRREG.			(IN)	2 1/2	2 1/2		1/2	1/4	1	4/12	1 1/4	1 1/4	1/18	1/18	1 1/8	5/8	3/8	3/8	
X-LEV. IRREG			(IN)	1/2			5/8	1/4	1		2 3/4	1	1 1/8	1 1/8	1/2	3/4	1/4	1/4	
LOCO. MODEL			(NO.)	SDP-40F	SDP-40F	SDP-40F	SDP-40F	SDP-40F	SDP-40F	SDP-40F	SDP-40F	SDP-40F	SDP-40F	SDP-40F	SDP-40F	SDP-40F	SDP-40F	SDP-40F	
AGE			(YR)																
1 ST CAR			(TYPE)	BAG	BAG	BAG	BAG	BAG	BAG	BAG	BAG	BAG	BAG	BAG	BAG	BAG	BAG	BAG	
WEATHER			(8)	F	CL	F	C	CL	C	CL	CL	R	R	C	S	C	R	R	
TEMPERATURE			(°F)	45				89				39	40	68	2		50	50	

- (1) TIMETABLE: NORMAL USE/INCIDENT USE
BOTH, NORTH, EAST, SOUTH, WEST
2 = #2 TRACK, 3 = #3 TRACK, ETC.

(2) LEVEL, ROLLING, HILLY, MOUNTAINOUS

(3) SINGLE, SHOULDER, DOUBLE SHOULDER
- (4) NO. PLATE-HOLDING/NO. RAIL-HOLDING
SPIKES PER TIE PLATE

(5) AVERAGE NUMBER PER 39 FT

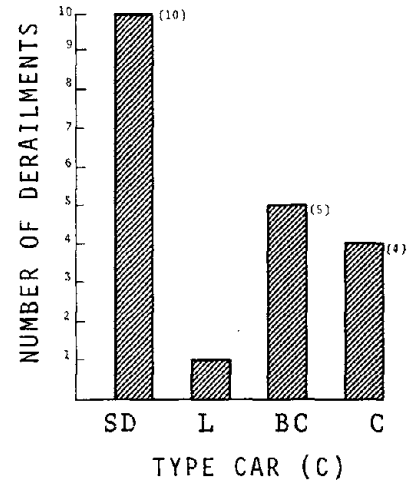
(6) TYPE/DEPTH
SLAG, STONE, CRUSHED ROCK, GRAVEL
- (7) NUMBER DEFECTIVE TIES/SPIKES
PER 39 FT

(8) RAIL, SNOW, CLOUDY, CLEAR, FILL

(9) RANDOM

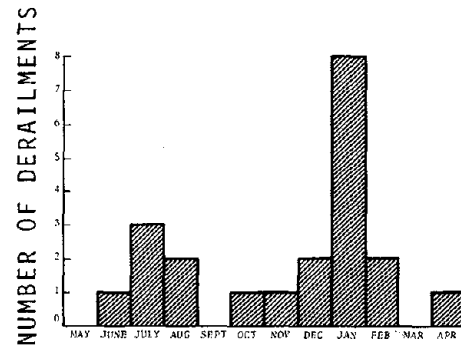
FREQUENCY VS FIRST CAR DERAILMENT

<u>First Car Derailed</u>	<u>C</u>	<u>Frequency</u>
SDP-40F	SD	10
Locomotive other than SDP-40F	L	1
Baggage Car	BC	5
Passenger Coach	C	4



FREQUENCY VS MONTH 21 DERAILMENTS FROM MID-1973 to NOV. 1978

<u>MONTH</u>	<u>SDP-40F</u>
May	0
June	1
July	3
Aug	2
Sept	0
Oct	1
Nov	1
Dec	2
Jan	8
Feb	2
Mar	0
Apr	1
	<u>21</u>



FREQUENCY VS. CURVATURE

<u>CURVATURE (°)</u>	<u>C</u>	<u>SDP-40F</u>
Tangent	T	1
1 - 1.9	1	2
2 - 2.9	2	6
3 - 3.9	3	5
4+	4+	1

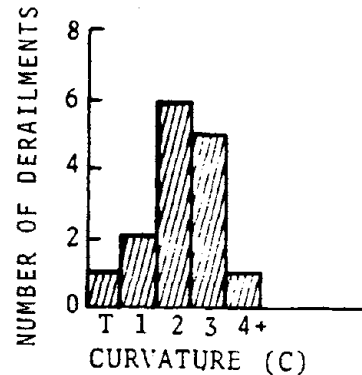
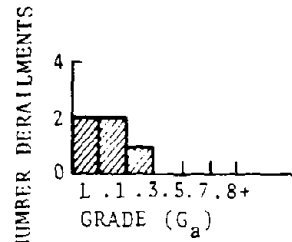


FIGURE A-1 KEY PARAMETER HISTOGRAMS (1 of 3)

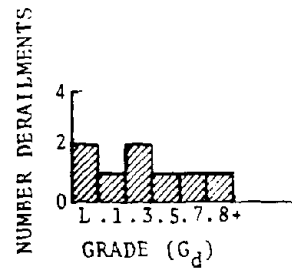
FREQUENCY VS. GRADE (ASCENDING)

<u>GRADE (%)</u>	<u>G_a</u>	<u>SDP-40F</u>
Level	L	2
.01 - .19	.1	2
.20 - .39	.3	1
.40 - .59	.5	0
.60 - .79	.7	0
.80+	.8+	0
Unknown		<u>4</u>
		9



FREQUENCY VS. GRADE (DESCENDING)

<u>GRADE (%)</u>	<u>G_d</u>	<u>SDP-40F</u>
Level	L	2
.01 - .19	.1	1
.20 - .39	.3	2
.40 - .59	.5	1
.60 - .79	.7	1
.80+	.8+	<u>1</u>
		8



FREQUENCY VS. TYPE RAIL

<u>TYPE RAIL</u>	<u>T</u>	<u>SDP-40F</u>
Jointed	J	5
Welded	W	8
Unknown		<u>2</u>
		15

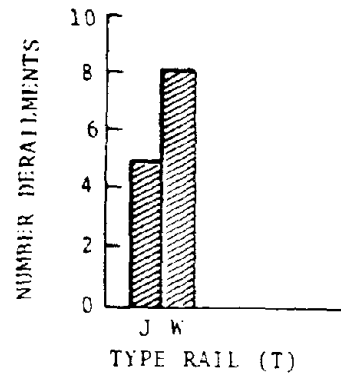
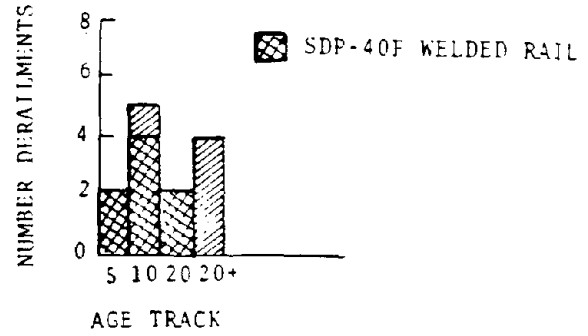


FIGURE A-1 KEY PARAMETER HISTOGRAMS (2 of 3)

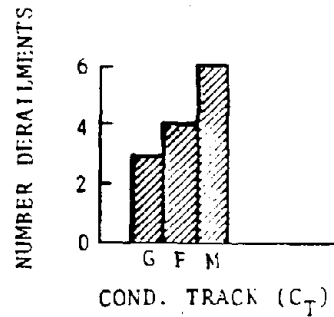
FREQUENCY VS. AGE OF TRACK

AGE (YR)	TOTAL	WELDED RAIL TRACK
0 - 5	2	2
6 - 10	5	4
11 - 20	2	2
20+	4	0
Unknown	2	0
	15	8



FREQUENCY VS. CONDITION OF TRACK

NO. TIES DEFECTIVE	C _T	SDP-40F
< 3	Good	3
3 - 5	Fair	4
6+	Minimum	6
Unknown		2
		15



FREQUENCY VS. SPEED

SPEED (MPS)	S	SDP40
< 40	40	0
41 - 45	45	1
46 - 50	50	3
51 - 55	55	1
55 - 60	60	7
> 60	60+	3
		15

@ CURVATURE $\geq 2^\circ$	S	SDP40
	40	0
	45	1
	50	2
	55	1
	60	7
	60+	1
		12

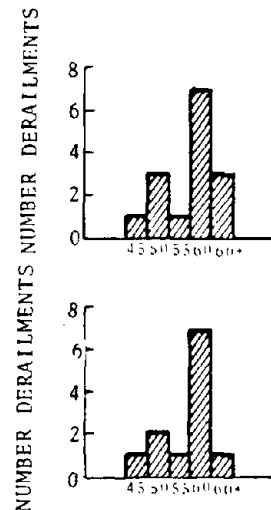


FIGURE A-1 KEY PARAMETER HISTOGRAMS (3 of 3)

- Of the 12 derailments in which an SDP-40F derailed:
 - all 12 were derailments of the trailing axle of the rearmost unit;
 - ten were derailments of the entire trailing truck of the rearmost unit;
 - all 12 were also derailments of the baggage car;
 - the train speed varied from 42 mph to 60 mph; and
 - all occurred on curves ranging from 1° to 5°.
- For the 16 derailments in which either an SDP-40F or the adjacent (baggage) car derailed:
 - the derailment speed varied from 40 mph to 70 mph; and
 - all occurred on curves ranging from 1° to 5°.
- For the 5 derailments in which neither an SDP-40F nor the adjacent (baggage) car derailed:
 - the train length varied from 2 locomotives + 9 cars to 3 locomotives + 18 cars;
 - the speed varied from 30 mph to 70 mph; and
 - the derailments occurred on both curves and tangents.
- Of the 15 derailments for which details were available, three occurred while it was raining, and one while it was snowing. The remaining 11 apparently occurred during dry weather. The temperature varied from 2°F to 89°F.

The histograms of Figure A-1 indicate that:

- Six of the 15 derailments occurred on curves of 2° to 3°, and 11 on curves between 2° and 4°;
- Grade was apparently unimportant: 3 occurred on ascending grades, 6 on descending grades, 2 on level track (the grade of 4 of them is unknown at present);
- Derailments occurred on both jointed and welded rail with approximately equal frequency;

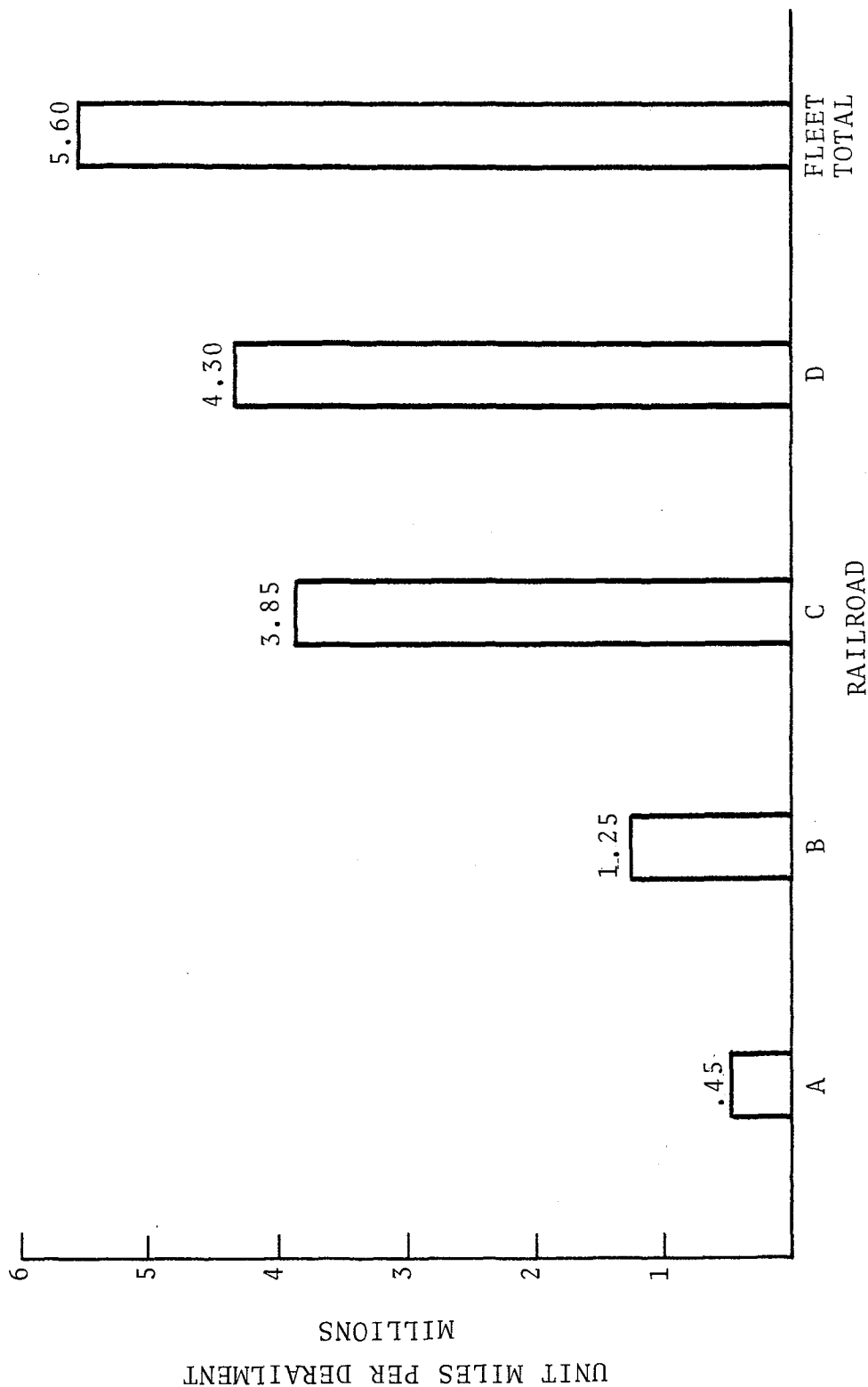
- The age of the track was apparently unimportant;
- The condition of the track (as defined by the number of defective ties per 39 ft.) seemed to have a minor significance;
- Fourteen of the 15 derailments occurred at speeds over 45 mph; and
- An unusually large number of derailments occurred in January (8 of 21) and an additional 5 in other cold weather months indicating a possible cold temperature influence.

Additional information obtained from EMD shown in Figure A-2 indicates a large variation in derailments of SDP-40F consists among railroads. This may be the result of varying track conditions or operating practices among these railroads.

Overall Conclusions

- Derailments generally occur on curves and at speeds of over 45 mph. It seems to be immaterial whether the track is welded or jointed, whether the grade is ascending, descending or level, and what the age of the track is; the frequency of defective ties (no. per 39 ft.) seems to play a minor role.

TRAINS OPERATED BY SDP-40F UNITS FROM JAN. 1975 THRU JAN. 1977



NOTE: The Balance of Eight Other Railroads Using SDP-40F Units Did Not Have Any Derailments in the Same Period

FIGURE A-2 LOCOMOTIVE UNIT-MILES PER DERAILMENT

APPENDIX B

TRACK GEOMETRY DATA ANALYSIS

B.1 INTRODUCTION

The purpose of the measurement analysis of track geometry data during the Chessie Test was to establish which type of track geometry characteristics excite locomotive dynamic response. To achieve this objective, the FRA track geometry survey cars were operated in consist with the E-8 locomotive during the survey run tests. Within the selected test zones, data from both the E-8 locomotive and the track survey cars were recorded on digital tape.

Forty-five curves with 2° to 3° of curvature were selected for analysis. Track geometry and locomotive dynamic data taken from the bodies of these curves were processed statistically. The parameters which were evaluated and the statistical descriptors used will be discussed in the following section.

B.2 PRIMARY PARAMETERS

The FRA track geometry survey cars measured the following parameters during the Chessie Test:

- Gage - distance between the inside faces of each railhead measured across the track at points 5/8 of an inch below the top of the railhead (inches) (Figure B-1).
- Crosslevel - the elevation of the left rail surface minus the elevation of the right rail surface (inches) (Figure B-2).
- Profile - (right and left) the vertical 62-foot mid-chord offset (MCO) of the rail surface (Figure B-3).
- Curvature - track curvature in degrees subtended by 100 feet of track. Calculated from the measured path of the trucks through a given curve (Figure B-4).

Of particular interest to this test are the measurements of gage and curvature. A strong relationship between variations in high rail alignment and lateral wheel/rail forces in curves was observed during the preliminary data analysis.

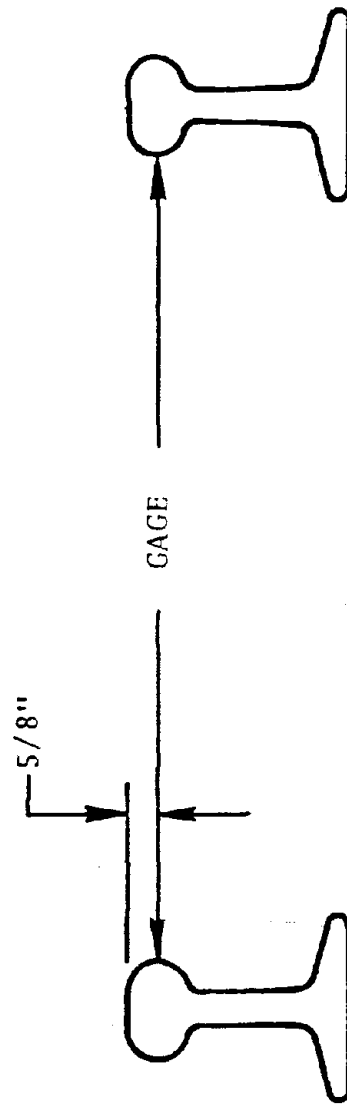


FIGURE B-1 GAGE MEASUREMENT

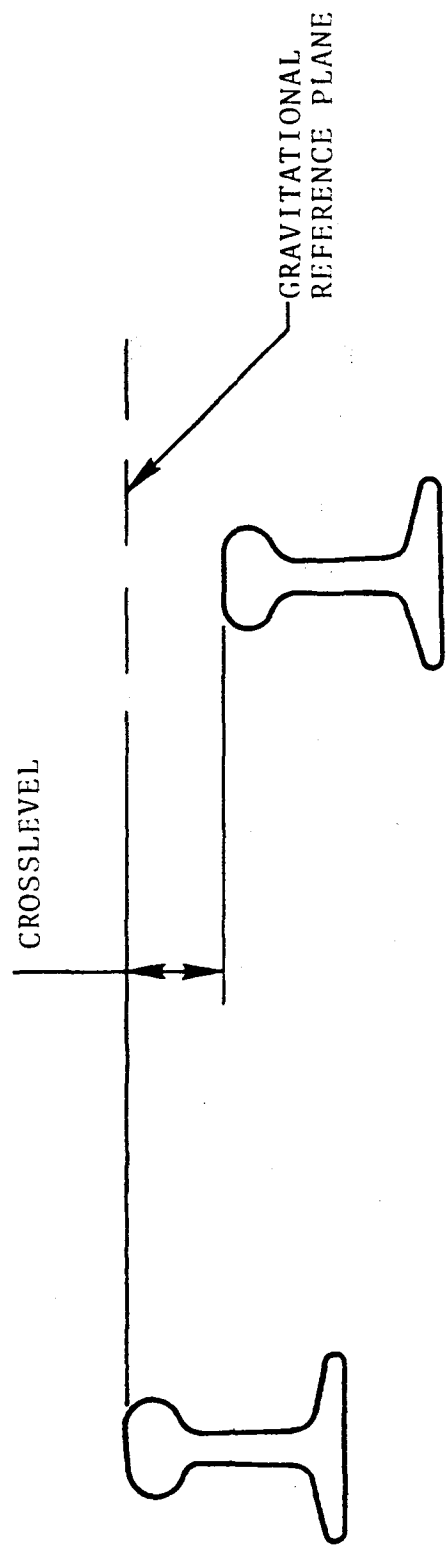


FIGURE B-2 CROSSLEVEL MEASUREMENT

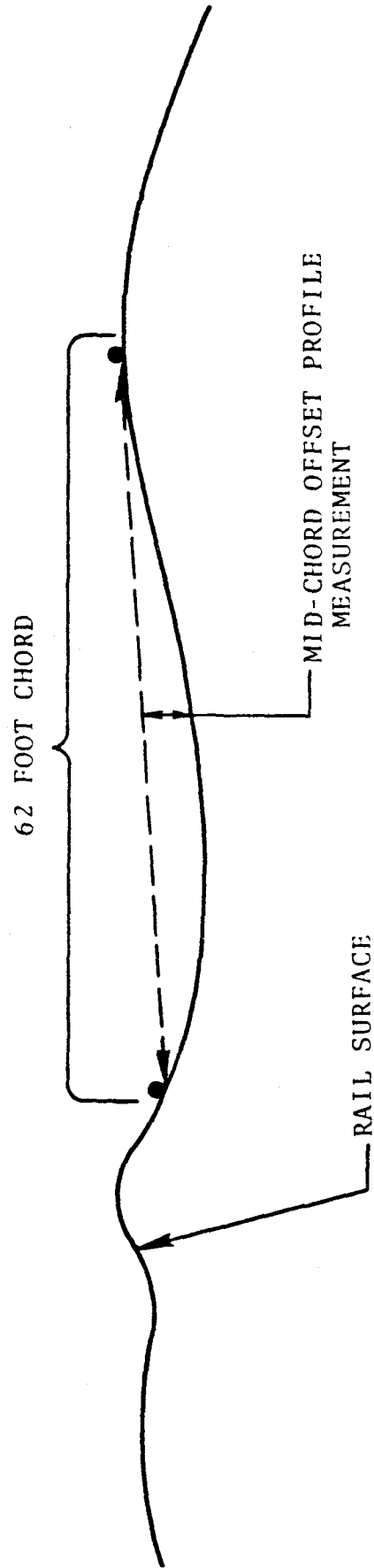


FIGURE B-3 PROFILE MEASUREMENT

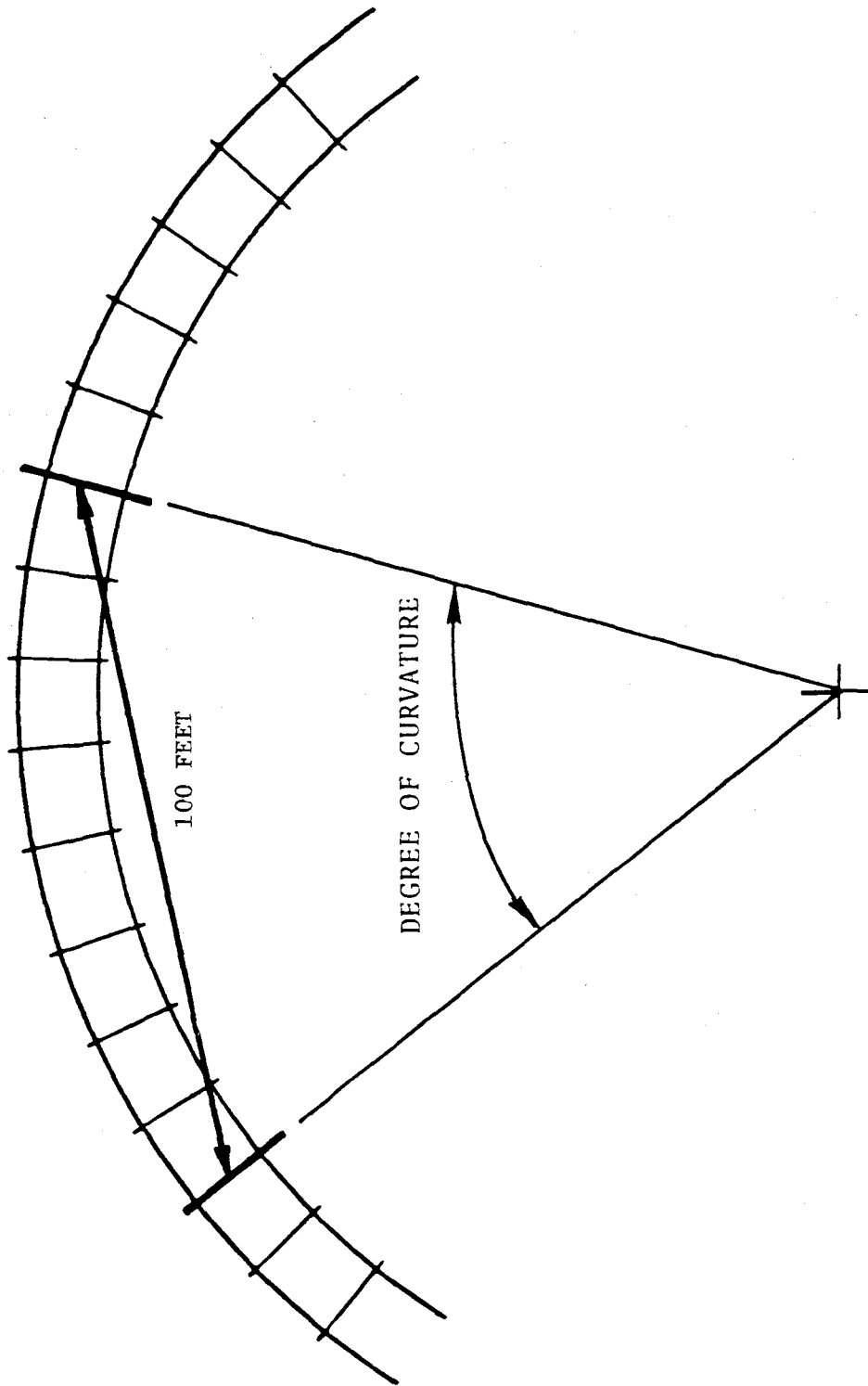


FIGURE B-4 CURVATURE MEASUREMENT

Although alignment is not measured directly by the track geometry survey cars T-1/T-3, some alignment information can be extracted from the gage and curvature measurements. For example, a variation in the measured gage is the result of a similar variation in the alignment of one or both rails. Similarly, the curvature measurement system sees the average alignment of the two rails as the truck traverses them. Each degree of curvature fluctuation above the mean can be interpreted as an alignment deviation of one inch (62-foot mid-chord offset).

From the data collected on the Chessie System it was observed that, within the selected test curves with bolted rail, the measured deviations in gage were predominantly due to high rail alignment variations at the joint (see Figure B-5). As a result, the gage measurement can be considered a good indicator of high rail alignment.

The curvature measurement is a measurement of the path of the trucks through the curve. Above balance speed, the trucks will tend to follow the high rail rather than the low rail. As a result, the curvature measurement is also a good indicator of the average high rail alignment. All but one of the selected test curves were measured above balance speed. Each of the geometry parameters was processed for the bodies of the selected curves to obtain the following statistical descriptors:

- Mean - the average value of a given parameter within a selected segment.

$$\bar{x} = \frac{1}{n} \sum_{i=1}^n x_i$$

- Standard Deviation - an indicator of the variation of the data for a given parameter within a selected segment.

$$\sqrt{\frac{\sum_{i=1}^n (x_i - \bar{x})^2}{n-1}}$$

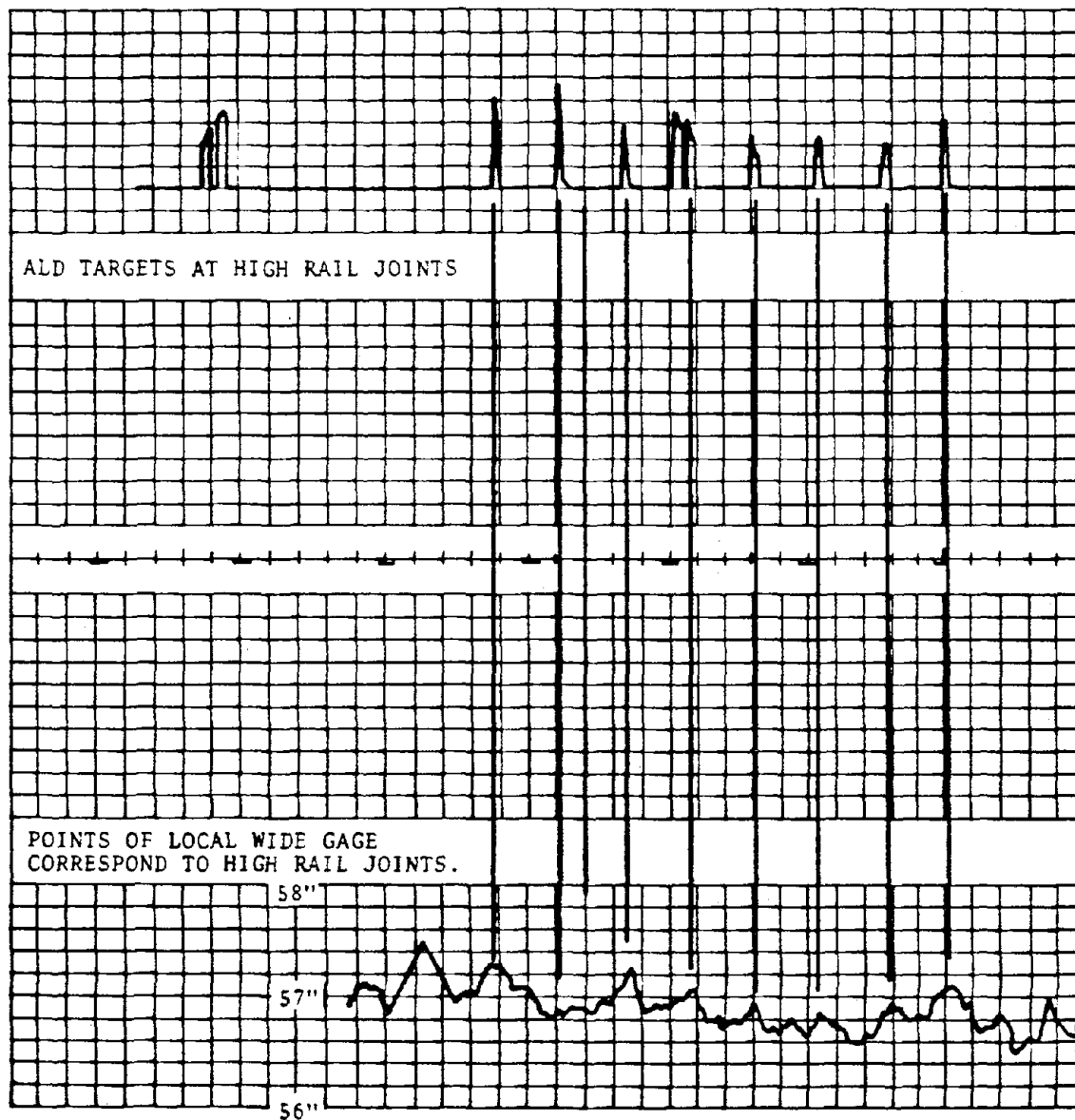


FIGURE B-5 ACTUAL STRIP CHART FROM CHESSIE TEST SITE AT MILEPOST 257.5

- Ninety-Five Percent Value - the level which 95 percent of the data within the segment falls below and five percent falls above.
- Peak Value - the maximum value for a given parameter within a selected segment.

When these four statistical descriptors are applied to the track geometry parameters, the standard deviation appeared to be the best indicator of the magnitude of the variations of a particular parameter. The mean, 95 percent and peak values are strongly affected by the average value of a parameter. This is particularly true for the gage and curvature measurements. Both of these measurements characteristically exhibit a small variation about a large mean on curved track.

Analysis indicated a strong relationship between the 95% values of lateral force in curves and the standard deviation of gage and curvature.

B.3 WAVELENGTH OF TRACK DISTURBANCE

Rail length-related high rail alignment deviations are of primary interest because of their observed relationship to lateral wheel/rail force. In calculating the standard deviation of a parameter over a given track segment, all wavelengths of deviations are considered equally. A series of short wavelength variations may have the same standard deviation as a single long wavelength defect (see Figure B-6).

However, the selected test segments on the Chessie were predominantly bolted rail. Within these track segments, rail length-related variations in alignment were the dominate contribution to the standard deviation of the gage measurements.

Being a single point measurement, the gage measurement is equally sensitive to all wavelengths of variations. The curvature measurement, however, is derived from the carbody yaw rate and speed. As a result, the wavelength response to alignment variations of the curvature system is dictated by the truck center distance on the track geometry vehicle. With a truck center distance of 60 feet, the track geometry cars are insensitive to alignment variations of wavelengths which are integer fractions of 60, i.e., 60, 30, 20, 15, 12... No oscillatory carbody yaw is induced by alignment variations of these wavelengths (see Figure B-7). However,

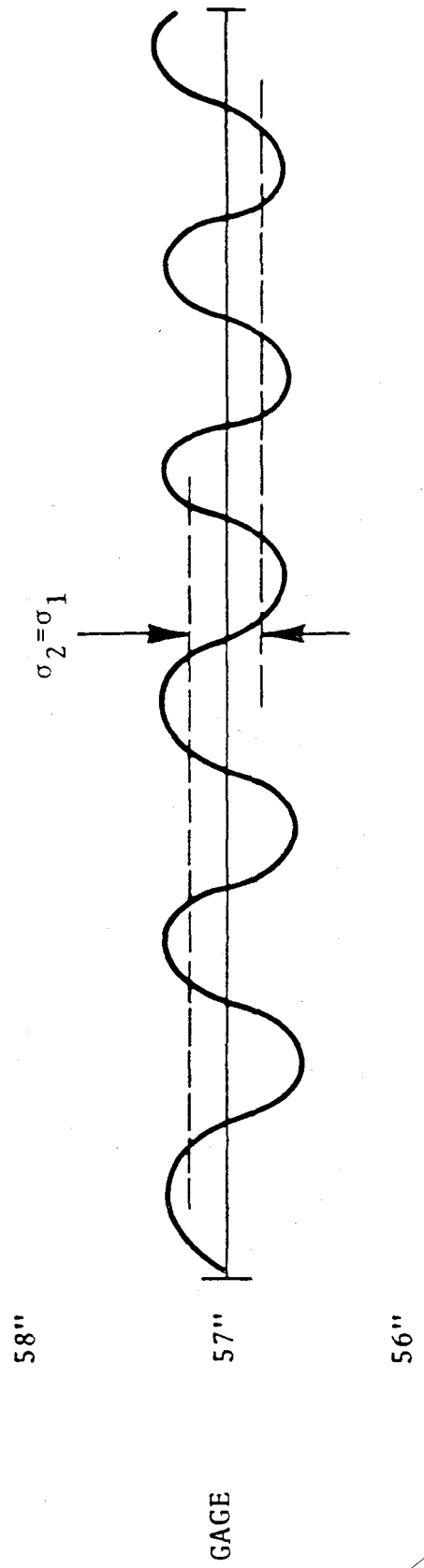
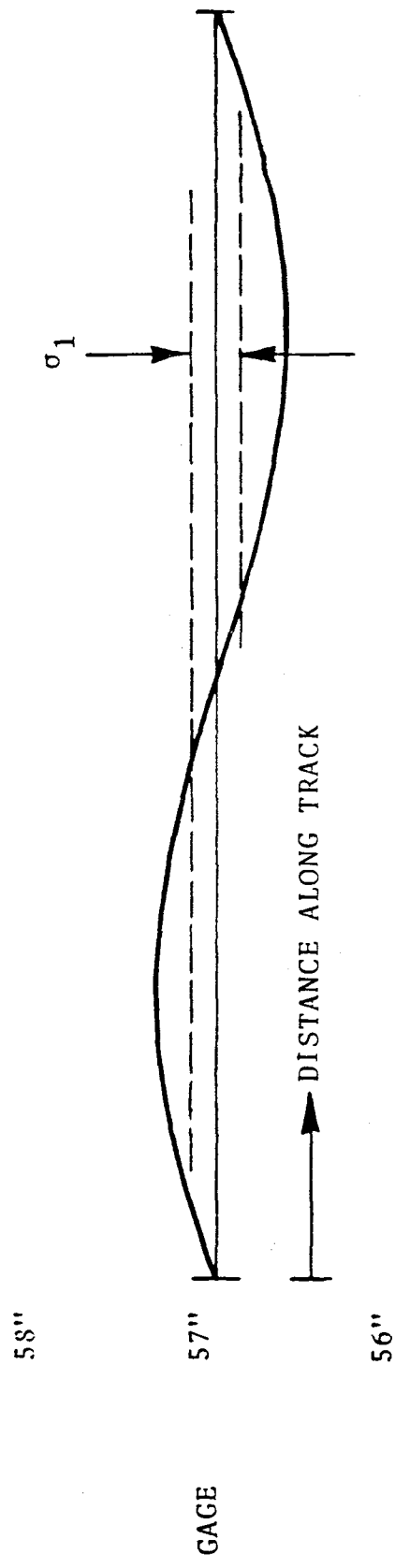


FIGURE B-6 COMPARISON OF STANDARD DEVIATION FOR WAVELENGTH DISTURBANCES DIFFERENT

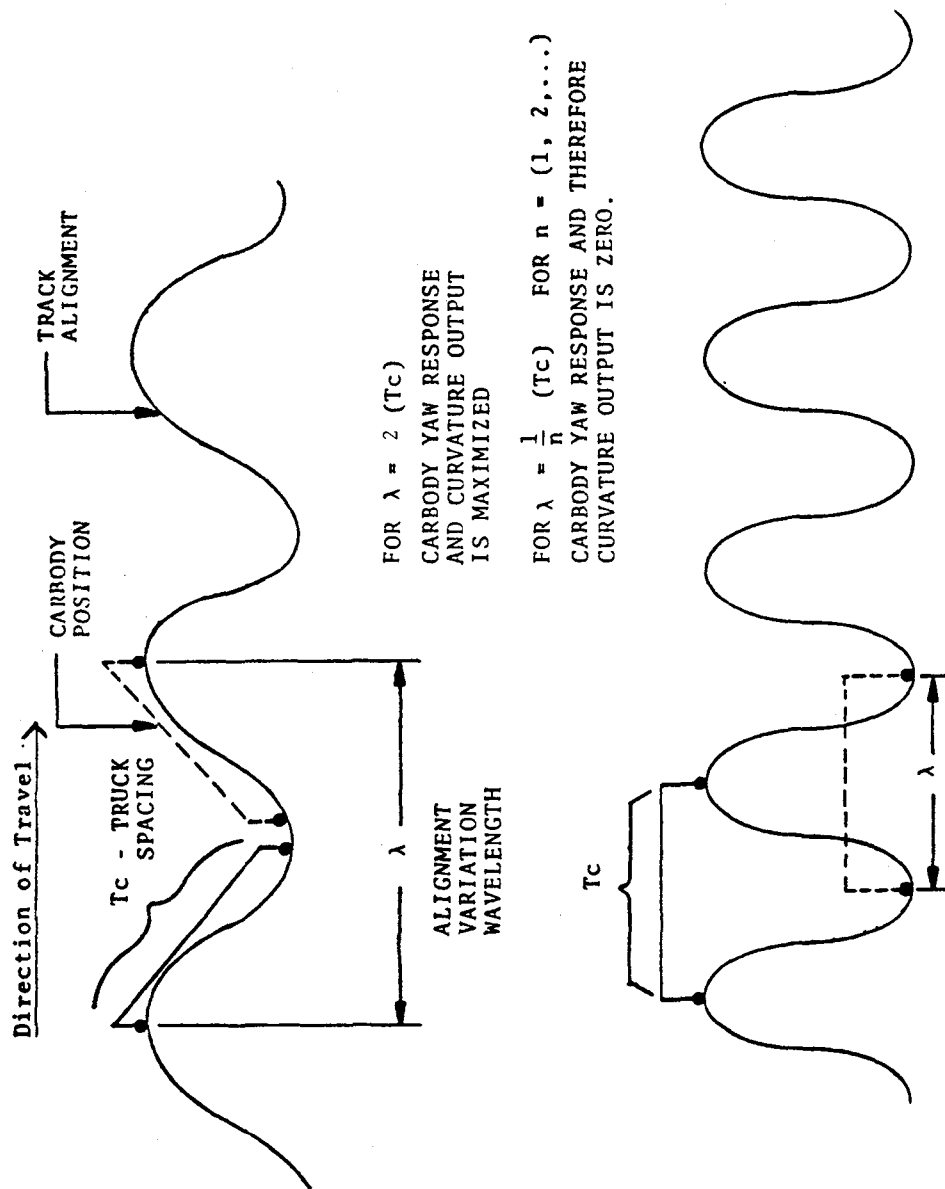


FIGURE B-7 CURVATURE SYSTEM RESPONSE

for wavelengths of twice the truck center spacing, oscillatory carbody yaw is accentuated.

As a result, the system is very sensitive to wavelengths of 120 feet, being twice the truck center distance. A plot of the sensitivity of the curvature system to track wavelengths is shown in Figure B-8.

Due to the characteristics of the gage and curvature systems described above, the curvature system is only sensitive to relatively long wavelengths (>80 feet) and the gage system is equally sensitive to long and short wavelengths. As a result, the rail length-related alignment deviations which existed in the bolted track were only seen by the gage system.

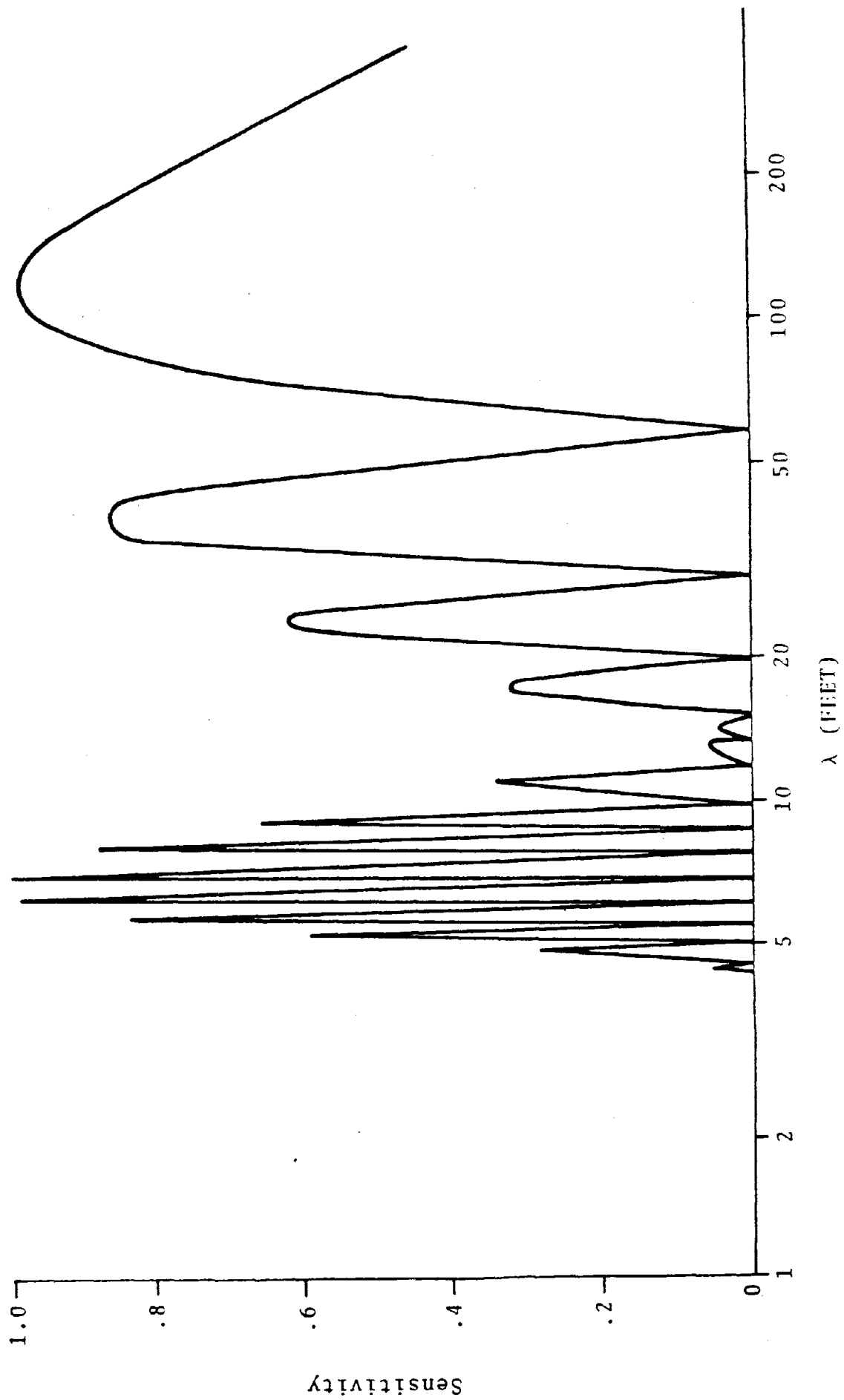


FIGURE B-8 CURVATURE SYSTEM SENSITIVITY

APPENDIX C

TRACK GEOMETRY DATA IN TEST ZONE

The test zone between MP 254 and 258 was divided into 18 segments. Each segment consists of a single (or a compound) curve or a tangent between two curves. Track geometry data for each of these 18 segments of track was analyzed manually according to FRA Track Safety Standards. Curvature and crosslevel analysis for each curve was extracted from the results of the computer-processed report.

The detailed analysis is given in Table C-1 for the eastbound pass. A westbound pass was also performed to demonstrate the repeatability of the data. The left-hand column in Table C-1 gives the start and the end points of the track segment, and the location of exceptions in milepost plus (or minus) number of feet measured from that milepost. The entries in the table are explained below:

1. **Average Curvature:** For a tangent track segment, a letter "T" is entered. For a curved segment, the average measured curvature is given in degrees/minutes. The average is computed by an FRA Safety Standard computer program based on points of spiral to curve and curve to spiral as estimated by a curve detection algorithm included in the computer program.
2. **Curvature Deviation from Average:** A letter "T" is entered for a tangent segment. For a curved segment, the maximum deviations above and below the average curvature are given in degrees.
3. **Average Crosslevel:** Average crosslevel in the segment as measured by the crosslevel system.
4. **Crosslevel Deviation from Average:** The maximum deviations above and below the average are given.
5. **Maximum Speed:** Maximum allowable speed in a curve computed by the formula

$$V_{\max} = \sqrt{\frac{E + 3}{0.0007d}}$$

TABLE C-1 TRACK GEOMETRY ANALYSIS (1 of 7)

EASTBOUND													
SEGMENT/LOC.	1 AVE CURV O	2 CURV DEV O	3 XLEVEL AVE "	4 XLEVEL DEV "	5 MAX SPD MPH	6 CURV O	7 XLEVEL "	8 LEFT PROF "	9 RT PROF "	10 GAGE (MAG) "	11 GAGE CHANGE "/39'	12 XLEVEL CHANGE "	13 WARP "
258-257.75	T	T	0	+ .75									
				-1.0									
258-580'								.625					
258-480'									1.0				
258-750'									1.0				
258-1140'									1.0				
258-810'										56.90			
258-0'											.8		
258-810'												1.0	
258-754'													1.57
CLASS								5	5	5		5	3
257.75-257.5	2.08	+ .45	2.27	+1.0									— TEST CURVE —
		- .40		-1.0									
258-1938'					52	2.83	2.41						
258-2200'								1.0					
258-2350'									.82				
258-2080'										57.62			
258-2050'											.80		
258-1780'												1.0	
258-1820													1.0
CLASS								5	5	3		5	5
257.5-257.4	T	T	0	+ .75									
				- .50									
253-3050'								.6					
253-2330'									1.0				
253-2950'										56.88			
258-2850'											.42		
258-3209'												1.0	
258-2750'													1.1
CLASS								5	5	5		5	4

Reproduced from
best available copy.



TABLE C-1 TRACK GEOMETRY ANALYSIS (2 of 7)

WORST MATCH

EASTBOUND

SEGMENT/LOC	AVE CURV	CURV DEV	XLEVEL AVE	XLEVEL DEV	MAX SPD	CURV	XLEVEL	LEFT PROF	RT PROF	GAGE (MAG)	GAGE CHANGE	XLEVEL CHANGE	WARP
57.4-257.05	2.58	+ .12	5.03	+ .6									
		- .10		- .75									
258-4964'					59	2.25	2.58						
58-4320'								1.0					
258-3790'									1.3				
258-3627'										57.79			
58-3627'											.90		
258-4570'												.75	
258-3730'													1.1
CLASS								5	4	3		5	4
257.05-256.9	T	T	-.4	+ .3									
				- .3									
57-210'								.75					
257-630'								.75					
58-5340'									.60				
58-5380'										56.76			
257-20'											.48		
58-5300'												.75	
58-5300'													1.0
CLASS								5	5	5		5	5
56.9-256.65	1.0	+ .08	1.68	+ .5									
		- .08		- .75									
					81								
57-1650'								1.0					
257-940'									.8				
57-1190'									.8				
257-740'										56.88			
257-740'											.56		
57-915'												.75	
257-915'													.75
CLASS								5	5	6		5	5

TABLE C-1 TRACK GEOMETRY ANALYSIS (3 of 7)

WORST MATCH

EASTBOUND

SEGMENT/LOC.	AVE CURV	CURV DEV	XLEVEL AVE	XLEVEL DEV	MAX SPD	CURV	XLEVEL	LEFT PROF	RT PROF	GAGE (MAG)	GAGE CHANGE	XLEVEL CHANGE	WARP
156.65-256.5	T	T	0	+.75									
				-.75									
						--	--	--					
257-1960'								.6					
257-2080'								.6					
257-1930'									.6				
257-2160'										56.80			
257-2700'											.44		
257-2240'												.75	
257-2240'													1.0
CLASS								5	5	5		5	5
256.5-256.35	1.0	+.05	1.75	+.5									
		-.05		-.75									
						82							
257-2940'								1.0					
257-3080'									.75				
257-3350'									.75				
257-3140'										56.76			
257-3200'										56.78			
257-3200'											.42		
257-2940'												.75	
257-2880'													1.25
CLASS								5	5	6		5	4
256.35-256.3	T	T	0	+1.25									
				-.5									
						--	--	--					
257-3750'								.8					
257-3860'									.75				
257-3740'										56.72			
257-3720'											.38		
257-3860'												1.25	
257-3840'													1.0
CLASS								5	5	5		4	5

TABLE C-1 TRACK GEOMETRY ANALYSIS (4 of 7)

EASTBOUND

WORST MATCH

SEGMENT/LOC	AVE CURV	CURV DEV	XLEVEL AVE	XLEVEL DEV	MAX SPD	CURV	XLEVEL	LEFT PROF	RT PROF	GAGE (MAG)	GAGE CHANGE	XLEVEL CHANGE	WARP
56.3-255.3	3.0	+.04	5.94	MAX.									
		-.08		-1.0									
256-94'					59	3.5	5.59						
57-4350'								.5					
256-600'								.5					
257-4100'									1.0				
57-4585									1.0				
257-4920'										57.48			
256-180'										57.42			
56-990'										57.45			
256-180'											.82		
56-540'												1.0	
56-600'												1.0	
256-750'												1.0	
56-480'													1.0
55								6	5	5		5	5
55.5-255.35	2.83	+.04	5.42	+.5									
		-.04		-.5									
					65								
56-3330'								.8					
56-2760'									.9				
256-3000'										57.17			
56-3000'											.72		
56-2940'												.5	
256-2940'													1.0
ASS								5	5	5		6	5

TABLE C-1 TRACK GEOMETRY ANALYSIS (5 of 7)

FASTBOUND

WORST MATCH

SEGMENT/LOC	AVE CURV	CURV DEV	XLEVEL AVE	XLEVEL DEV	MAX SPD	CURV	XLEVEL	LEFT PROF	RT PROF	GAGE (MAG)	GAGE CHANGE	XLEVEL CHANGE	WARP
55.35-255.3	T	T	0	+ .5									
				- .5	--	--	--						
56-3630'								.5					
56-3570'									.8				
256-3880'										56.68			
56-3540'											.47		
56-3900'												1.25	
256-3900'													1.0
ASS								6	5	6		4	5
255.3-255.1	3.25	+.04	5.88	+.5									
		-.04		-.75									
					60								
256-4260'								.85					
56-4050'									.5				
256-4180'										57.12			
56-4140'											.5		
56-4140'												.75	
256-4140'													1.25
CLASS								5	6	5		5	4
255.1-254.75	T	T	0	+.5									
				-1.0									
					--	--	--						
256-4975'								.8					
55-640'								.8					
56-4045'									.9				
255-635'										56.88			
55-440'											.42		
55-220'												1.00	
255-200'													1.25
CLASS								5	5	5		5	5

Reproduced from
best available copy.

TABLE C-1 TRACK GEOMETRY ANALYSIS (6 of 7)

WORST MATCH

FASTBOUND													
SEGMENT/LOC	AVE CURV	CURV DEV	XLEVEL AVE	XLEVEL DEV	MAX SPD	CURV	XLEVEL	LEFT PROF	RT PROF	GAGE (MAG)	GAGE CHANGE	XLEVEL CHANGE	WARP
54.75-254.55	2.33	+ .4	3.71	+ .75									
		- .1		- .5									
255-2100'					57	2.0	1.56						
55-1740'								.6					
55-1620'									.8				
255-1830'										57.18			
55-1470'											.64		
55-1830'												.75	
255-1600'													.75
55-1600'								5	5	5		5	5
54.55-254.5	T	T	0	+1.5									
				- .75									
55-2410'								1.0					
55-2230'									.8				
255-2600'										56.84			
55-2600'											.64		
55-2600'												1.5	
255-2600'													1.5
GLASS								5	5	6		3	3
254.5-254.1													
COMPOUND CURVE	2.42	+ .1	3.84	+ .5									
		- .08		- .75									
255-3250'					55	3.0	3.55						
	1.17	+ .6	1.69	+ .5									
		- .4		-1.25									
255-3598					59	1.75	1.39						
	2.83	+ .5	4.43	+ .6									
		- .5		- .75									
255-4287					55	3.17	3.86						

Reproduced from
best available copy.

TABLE C-1 TRACK GEOMETRY ANALYSIS (7 of 7)

WORST MATCH

SEGMENT/LOC.	AVE CURV	CURV DEV	XLEVEL AVE	XLEVEL DEV	MAX SPD	CURV	XLEVEL	LEFT PROF	RT PROF	GAGE (MAG)	GAGE CHANGE	XLEVEL CHANGE	WARP
4.5-254.1													
CONT.													
255+4580'									.7				
255+3840									1.1				
255+3000'										57.22			
255+2830'											.72		
255+3460'												1.25	
255+3520'													1.25
CLASS								5	5	5		4	4
254.1-253.95	2.33	+1	4.05	+1.5									
		-1		-1.75									
254-85'					59	2.58	3.33						
255-5220'									.6				
255-4850'									1.2				
255-5220'										57.20			
255-5220'											.8		
255-5250'												.5	
255-5250'													1.00
CLASS								5	5	5		6	5

based on the worst combination of measured crosslevel and curvature. The location of the worst combination is given at the left-hand end of the table.

6. Curvature: Value of measured curvature at location of worst combination of crosslevel and curvature.
7. Crosslevel: Value of measured crosslevel at location of worst combination of crosslevel and curvature.
8. Left Profile Evaluation: Worst measured profile on the left rail. Given in inches of mid-chord offset in a 62-ft. chord.
9. Right Profile Evaluation: Worst measured profile on the right rail.
10. Gage Evaluation: Widest measured gage in the segment, given in inches. The data is based on the magnetic gage system on the eastbound run and on the capacitive gage system for the westbound run.
11. Gage Change: Maximum observed change (variation of gage along distance) within a rail length. This parameter is a good indicator of alignment problem.
12. Crosslevel Change: Maximum observed change (variation of crosslevel along distance) within a rail length.
13. Warp: The worst measured warp in the segment. Warp is change in crosslevel between two points less than 62 feet apart.

Further details on some of these track geometry parameters are presented in Appendix B.

A track class analysis is given in Table C-1 at the end of each track segment; the track is rated by each parameter separately according to FRA Track Safety Standards. The purpose of the separate analysis is to give an idea of which of the track geometry parameters is the dominating factor in track classification. The actual class of the track segment should be taken as the lowest rating among all parameters.

Based on the eastbound data (where all measurement systems were functioning properly), the four-mile section between MP 254 and 258 satisfied at least FRA Class 3 according to the data (excluding alignment, which is not measured). Class 3 permits a maximum speed of 60 mph for passenger trains and 40 mph for freight trains. Based on the worst combination of crosslevel and curvature, the maximum allowable speed for the test curve at MP 257.5 ($2^{\circ}06'$) is 52 mph and is 59 mph for the adjacent curve at MP 257.2 ($2^{\circ}38'$). Therefore, the track section satisfies the standards required for the posted speed of 60 mph for passenger trains. However, this speed exceeded the maximum speed allowed by the rule of no more than 3" superelevation as defined in the FRA Track Safety Standards.

APPENDIX D

USE OF $L_{0.5}$ FOR ONBOARD DATA AS A VEHICLE RESPONSE DESCRIPTOR

There are various vehicle response descriptors that may be used for comparison of dynamic locomotive performance. For characterization of the lateral wheel/rail forces in curves, the maximum onboard value L_{max} may be used. However, lateral force data generally have sharp peaks associated with the maximum levels, which may lead to uncertainty in the data at these points. The fact that onboard L_{max} can have large variations for runs of nearly identical conditions, is shown in Figures D-1 to D-4, which depict this variation with speed at two joints ("C" and "D") in the curve at MP 257.2 for both the E-8 and SDP-40F. Upper and lower bound regions are depicted on the graphs along with regions of high density scatter. These onboard L_{max} curves show a great deal of scatter, most likely due to the sensitivity of L_{max} to the precise initial conditions of the wheelset entering a joint. These initial conditions are subject to "small" random variations, both for the track and operating conditions. It should be emphasized that this scatter is such that by taking different subsets of the total data points in a speed grouping it is possible to draw curves that show trends that are different from the previous data. For example, in Figure D-3, showing the SDP-40F L_{max} at joint "D", there are 7 data points in the region from 58-61 mph. Depending on which data points are omitted (for example, if only two points were available from two runs) it would be difficult to discern if the SDP-40F lateral forces were rising or flattening out in this speed range. Similarly, the data scatter for the E-8, at Joint "C", as shown in Figure D-2, at 60 mph could lead to a conclusion of rising L_{max} or falling L_{max} . It thus appears that it is difficult to use the value of onboard L_{max} at joint locations to establish accurate trend patterns.*

*It should be noted that the onboard L_{max} is not the same type of descriptor as the wayside lateral force descriptor L_{max} (the maximum single-wheel lateral force). By definition, the onboard L_{max} is that peak lateral force that occurs instantaneously with essentially no time duration. However, the wayside lateral forces are obtained as a spatial sampling (about 40" apart) of the lateral force trace, and accordingly, tend to filter out peaks of short

(Continued)

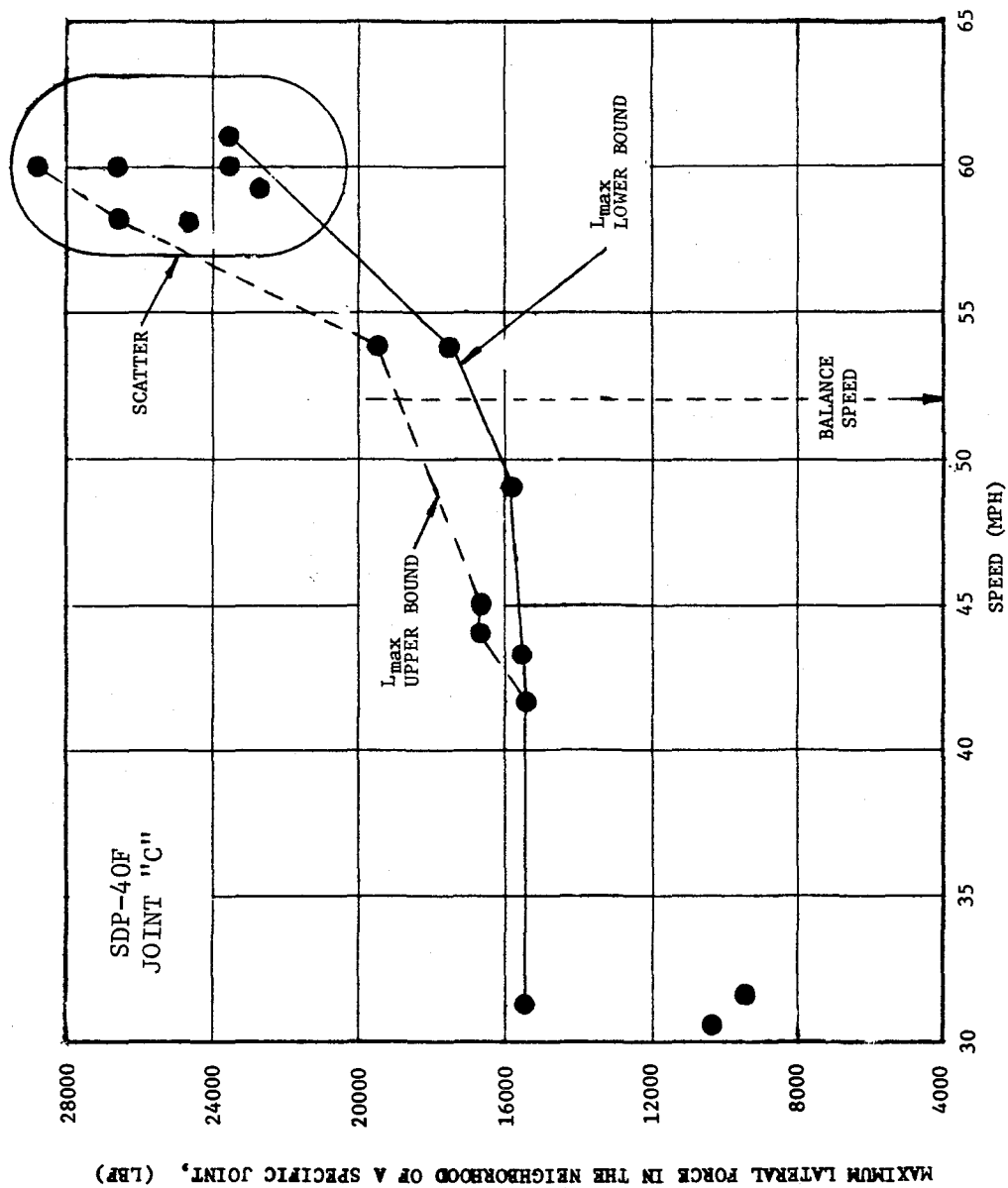


FIGURE D-1 VARIATION OF L_{max} FOR SDP-40F VERSUS SPEED AT JOINT "C" IN CURVE AT MP 257.2 (BASELINE RUNS, ONBOARD DATA)

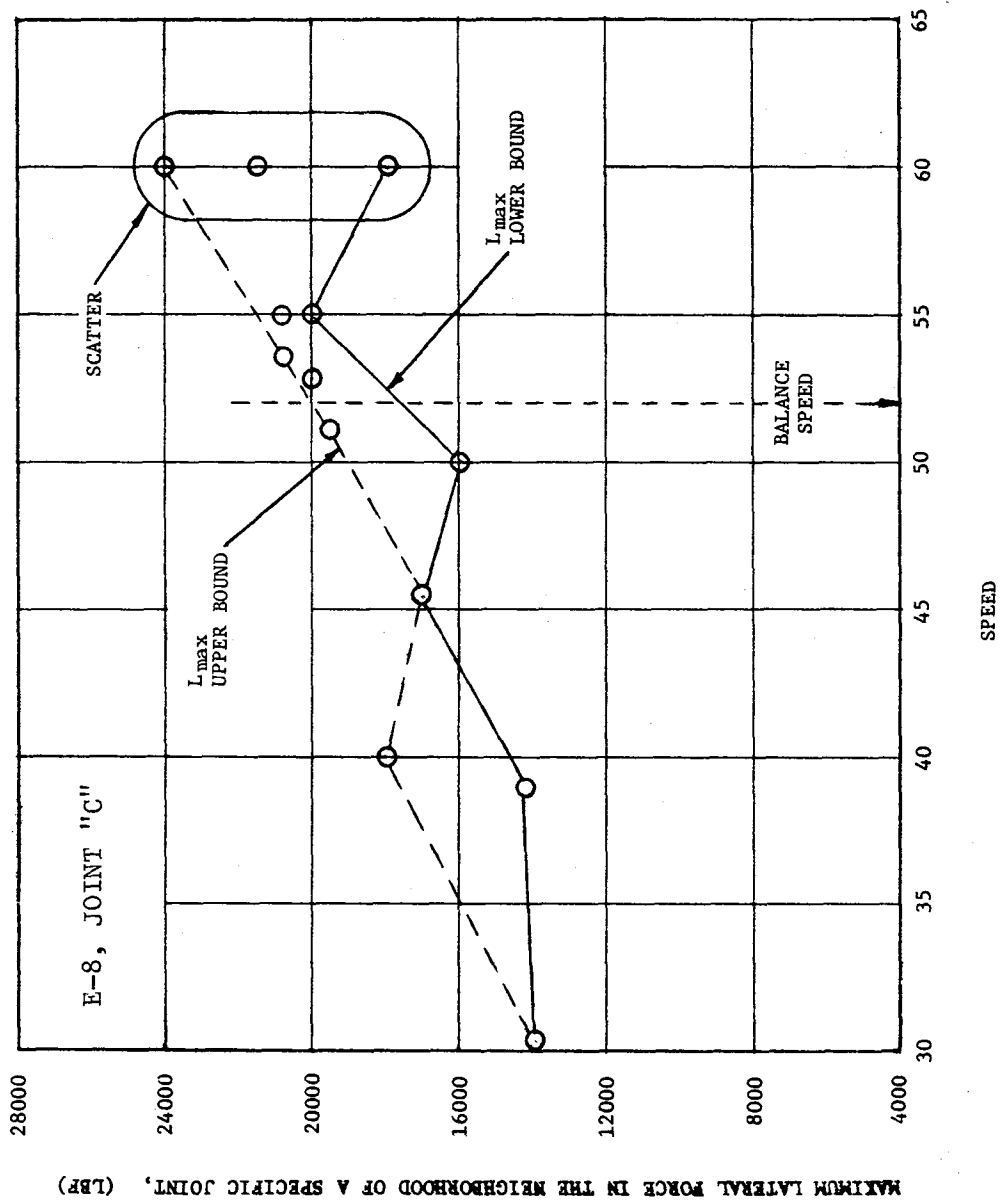


FIGURE D-2 VARIATION OF L_{max} FOR E-8 VERSUS SPEED AT JOINT "C" IN CURVE AT MP 257.2 (BASELINE RUNS, ONBOARD DATA)

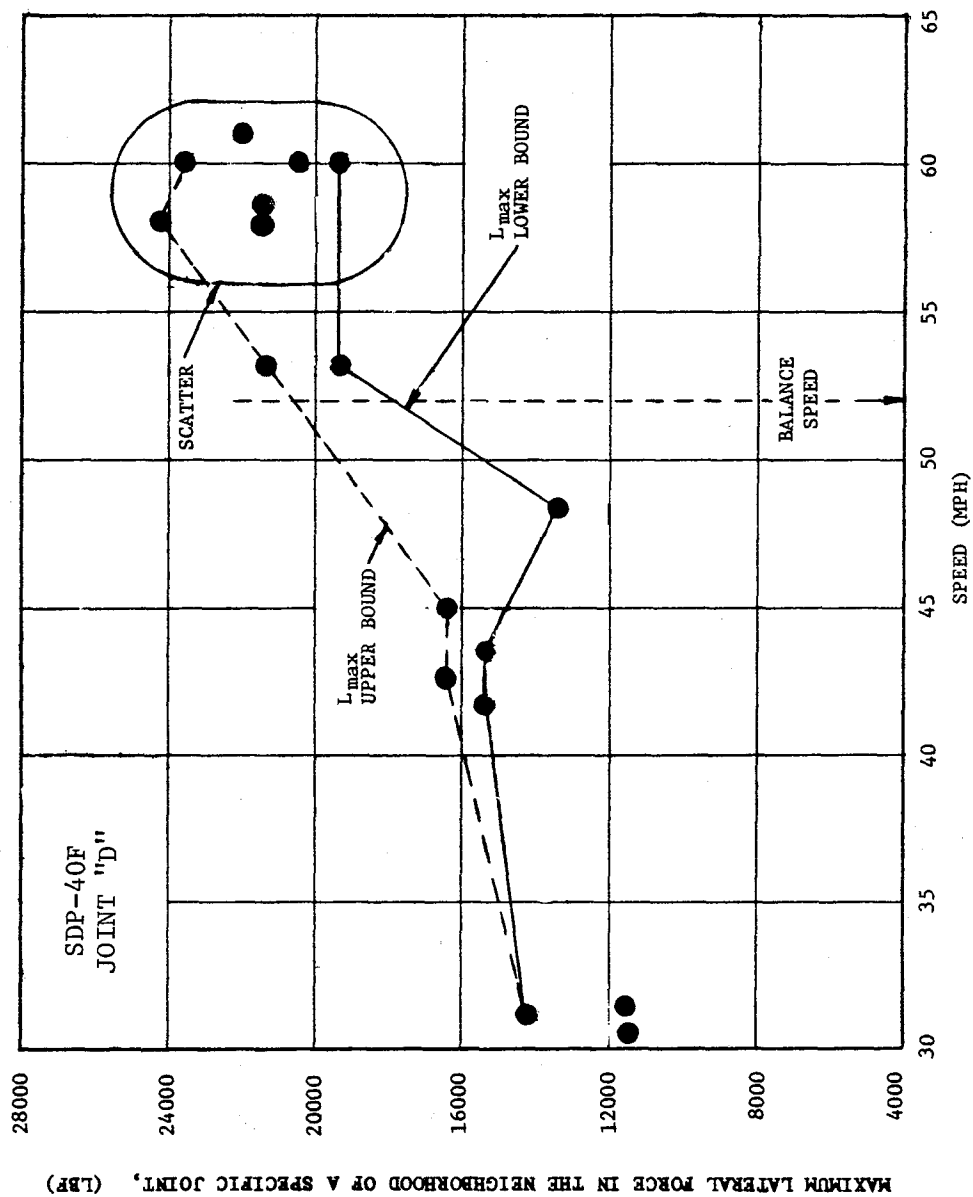


FIGURE D-3 VARIATION OF L_{max} FOR SDP-40F VERSUS SPEED AT JOINT "D" IN CURVE AT MP 257.2 (BASELINE RUNS, ONBOARD DATA)

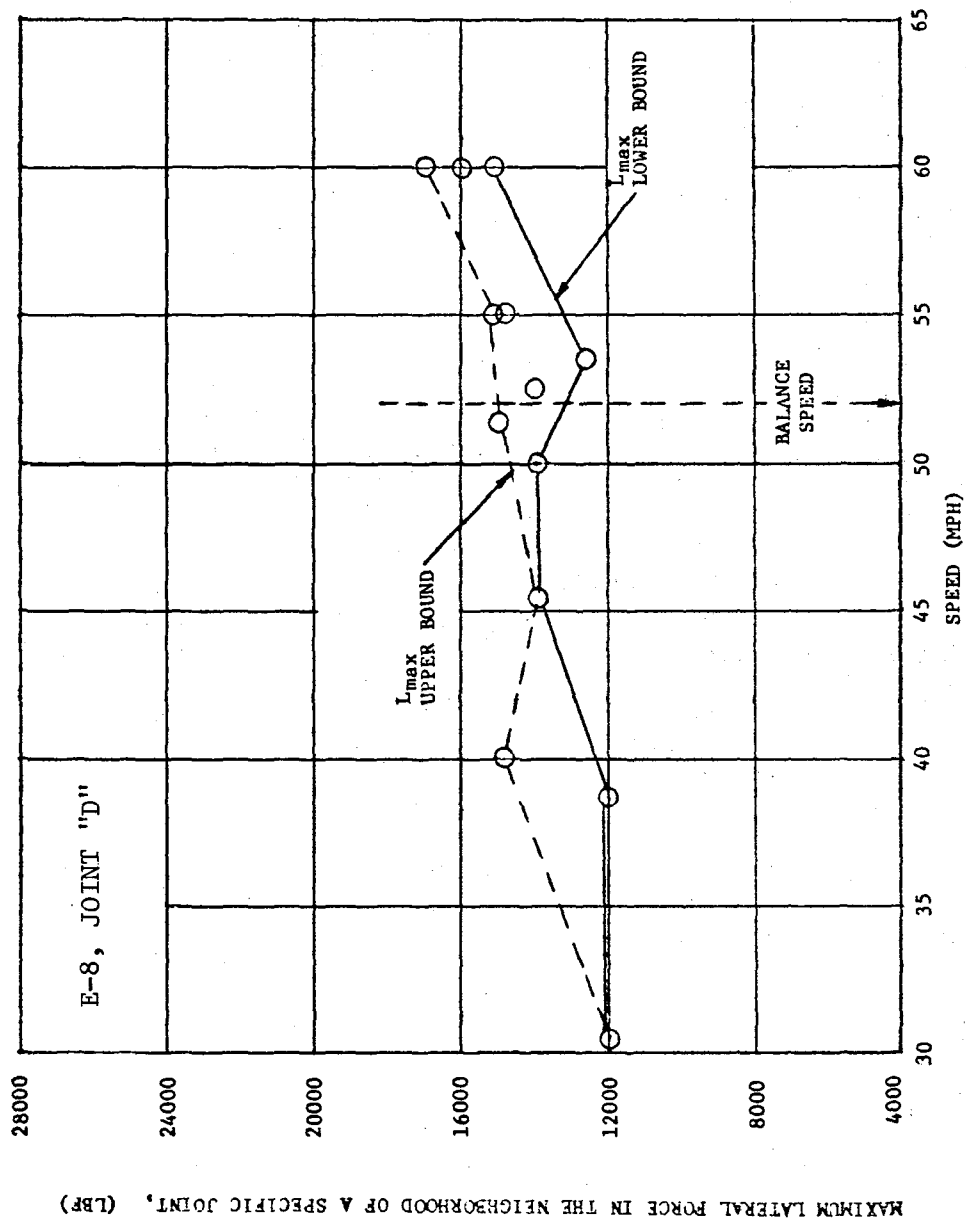


FIGURE D-4 VARIATION OF L_{max} FOR E-8 VERSUS SPEED AT JOINT "D" IN CURVE AT MP 257.2 (BASELINE RUNS, ONBOARD DATA)

An alternative for describing the vehicle response in curves is to develop a response descriptor that statistically characterizes the force distribution seen in the curve. Such a descriptor can be developed by examining the time distribution of the lateral forces, as shown in Figure D-5. The quantity L_x shown in the figure, is the Xth percentile value of lateral force; i.e., the value for which X% of the time the data falls below and 100 - X% of the time it exceeds this value. The calculation of L_x is depicted in Figure D-6, where T is a chosen convenient time interval, such as the time interval during curve traversal. By calculating the percent of time spent above various force thresholds (5, 10, 15 kips, etc.) and then plotting the cumulative probability distribution in a form similar to D-5, the value of L_x may be immediately found from the graph. For example, $L_{.5}$, represents a value that is exceeded only 5% of the time in the interval T. $L_{.5}$ was chosen as the specific descriptor for the analysis of the onboard data because it represented the highest force level consistent with significantly reduced scatter. The use of $L_{.5}$ as a vehicle response indicator provides a single measure that is characteristic of the vehicle response to repeated track geometry inputs. One of the important consequences of employing $L_{.5}$ is that it filters out forces of inconsequential time duration while being representative of the sustained high forces that could lead to derailment. In addition, $L_{.5}$ could also be used to characterize vehicle response to a transient input. For this case, T would then have to be a carefully chosen representative time interval.

An example of the difference between $L_{.5}$ and L_{max} on a time basis is shown in Figure D-7, which is a plot of the mean exceedance time duration (total time spent above a force threshold divided by the number of exceedances of that threshold) as a function of high wheel lateral force for the E-8 and SDP-40F for a specific run at 60 mph for each locomotive in the test curve at MP 257.5. For this speed and curve, the $L_{.5}$ points fall in the range of 20-25 milliseconds. Particularly for the SDP-40F, the $L_{.5}$ force was characteristic of a plateau in force around the 25 msec

(Continued)

time duration. Therefore, the wayside L_{max} , which is the maximum value obtained from these spatial samples of the force trace, is not equivalent to the onboard L_{max} , but is more closely related to a statistical measure of the force distribution such as $L_{.5}$.

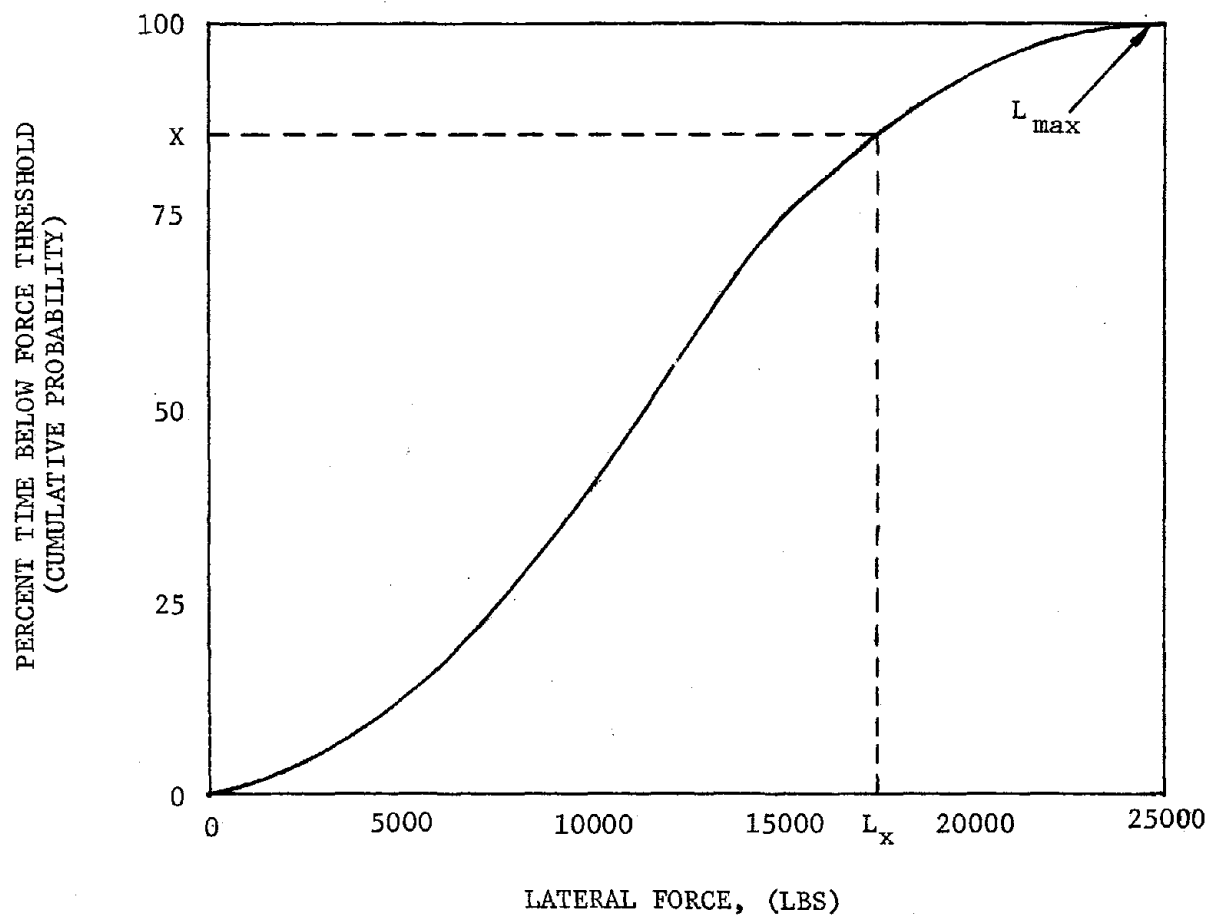


FIGURE D-5 PERCENT OF TIME LATERAL FORCE BELOW THRESHOLD
VS. LATERAL FORCE

$(\sum \text{---})/T$ = PERCENT OF TIME SPENT EXCEEDING 5 KIPS
 $(\sum \text{-----})/T$ = PERCENT OF TIME SPENT EXCEEDING 10 KIPS
 $(\sum \text{————})/T$ = PERCENT OF TIME SPENT EXCEEDING 15 KIPS

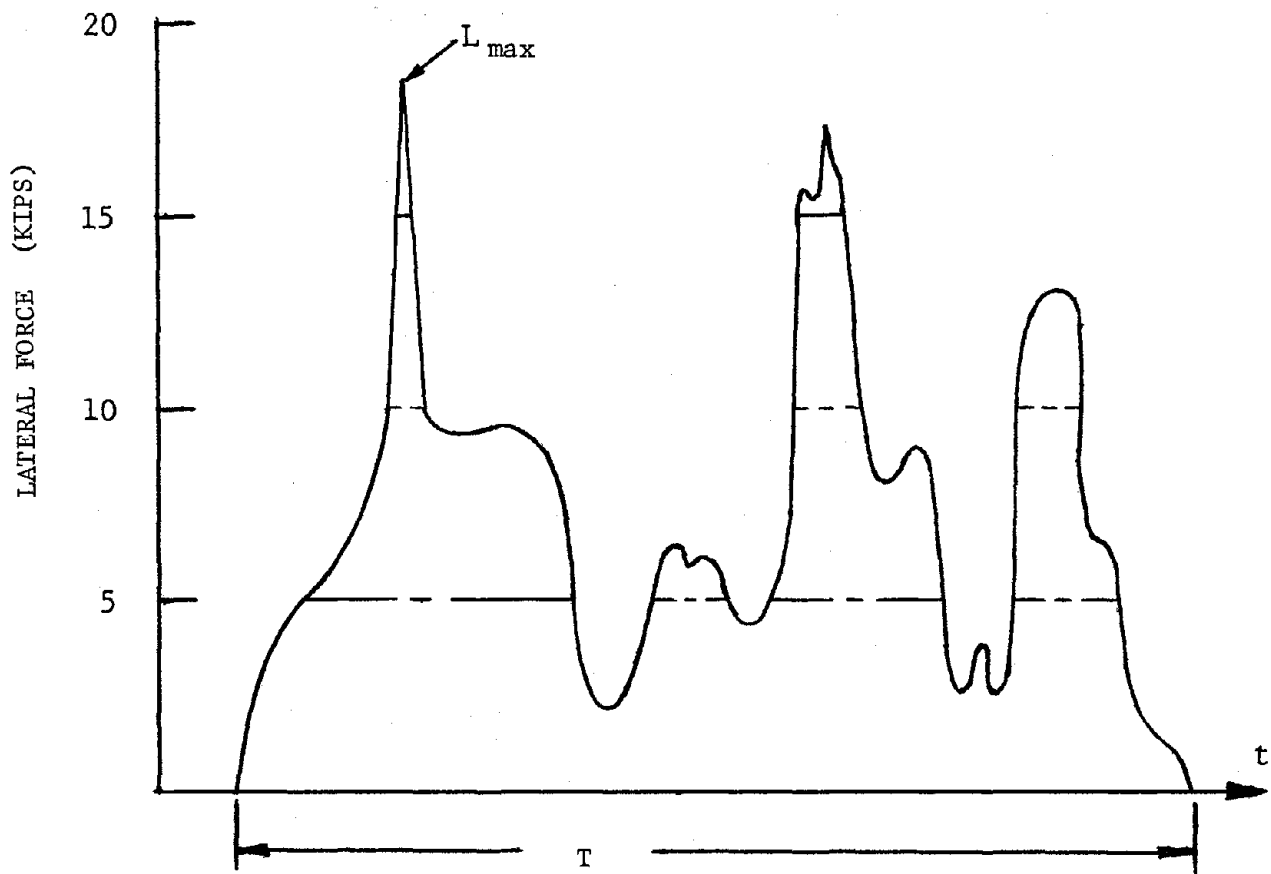


FIGURE D-6 CALCULATION OF TIME DISTRIBUTION OF LATERAL FORCE FROM TYPICAL DATA

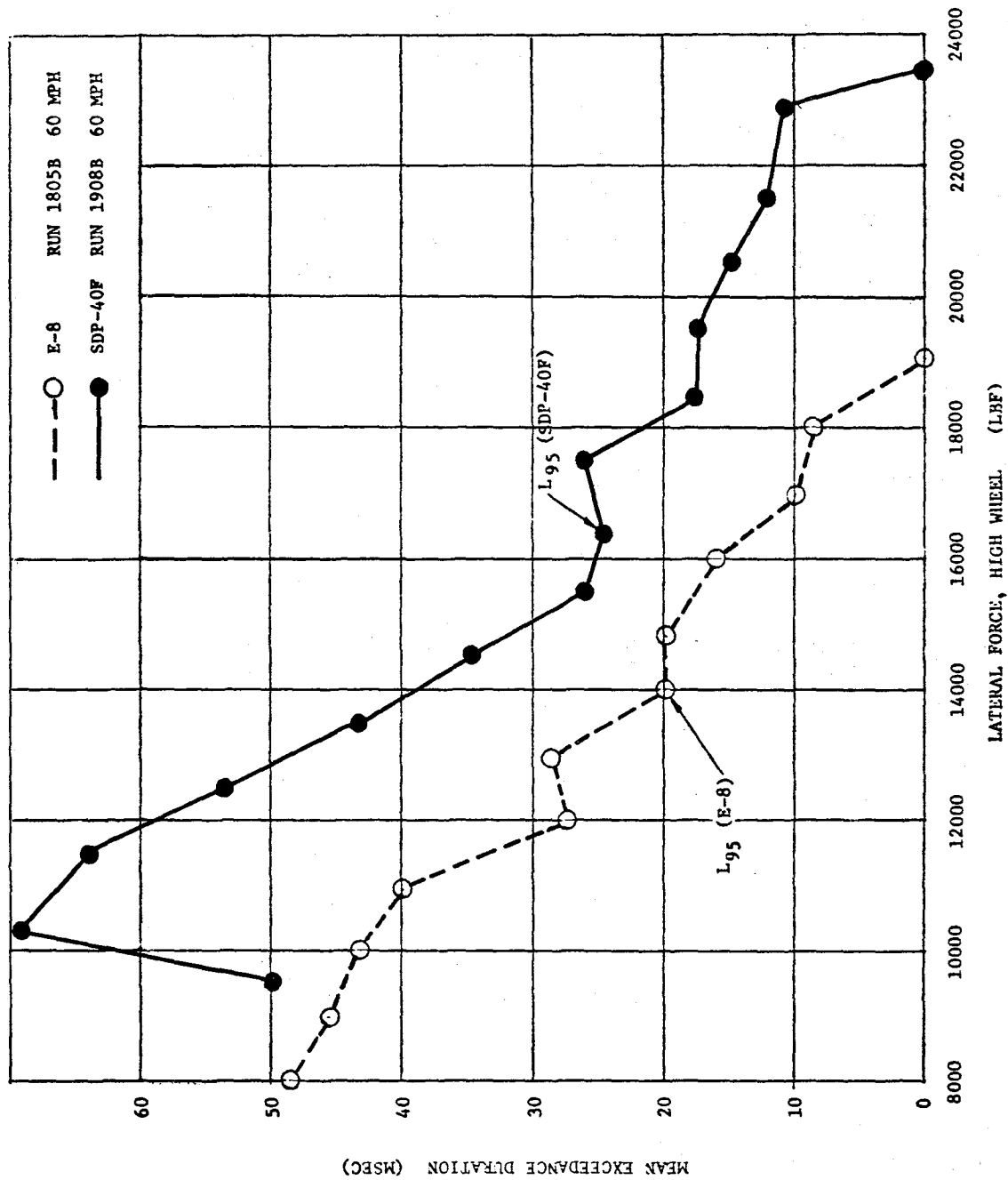


FIGURE D-7 MEAN EXCEEDANCE TIME VS. LATERAL FORCE THRESHOLD FOR AXLE 10
IN THE TEST CURVE (ONBOARD DATA, NOMINAL CONFIGURATION)

range. As we approach the L_{\max} region, there is a sharp drop-off in time duration. These results are quite typical and may be verified from analysis of a wide spectrum of observed Chessie System Test data. This analysis shows that the L_{95} time range is about 20-40 msec.

An analytical expression relating L_{\max} of a sinusoid and L_{95} can be developed for a periodic joint response, where the energy associated with the dynamic lateral curving force in the neighborhood of the joint is approximated by "fairing" in a sine wave under the spiked wave form, as shown in Figure D-8. The force distribution approximating the energy content of the dynamic curving forces can then be expressed in the form

$$\begin{aligned}
 L &= L_s & \lambda < X \leq X_0 - \lambda \\
 L &= L_s + (L_p - L_s) \sin \frac{\pi}{2\lambda} [X - (X_0 - \lambda)] & X_0 - \lambda < X < X_0 + \lambda
 \end{aligned}
 \tag{D-1}$$

where L_s is the steady state curving force and L_p is the faired peak force. To relate L_{95} to L_p , we note from Figure D-8 that

$$\begin{aligned}
 L &= L_{95} \quad \text{at } X = .95X_0 + \frac{1}{2} (.05) X_0 = .975X_0 \\
 \therefore L_{95} &= L_s + (L_p - L_s) \sin \frac{\pi}{2\lambda} (\lambda - .025X_0) & (D-2) \\
 &= L_s + (L_p - L_s) \sin \frac{\pi}{2} \left(1 - \frac{.025X_0}{\lambda}\right)
 \end{aligned}$$

For $\lambda = 3'$ (i.e., the dynamic portion of the lateral force changes from its minimum value to its peak value when the wheelset travels a distance of 3'),

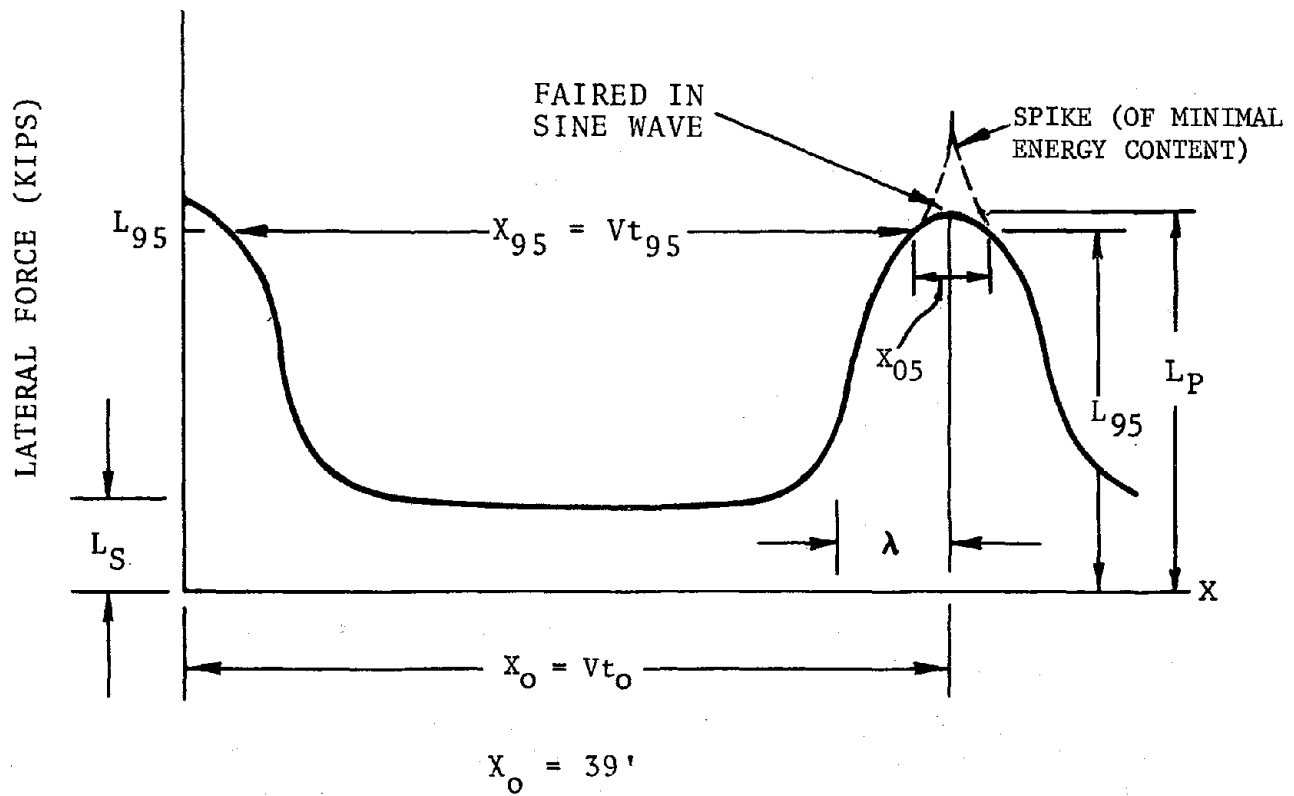


FIGURE D-8 RELATION BETWEEN L_{\max} AND L_{95}
FOR AN IDEALIZED SINUSOIDAL WAVEFORM

$$\begin{aligned}
 L_{95} &= L_s + (L_p - L_s) \sin\left(\frac{\pi}{2} \cdot \frac{2}{3}\right) \\
 &= L_s + (L_p - L_s) \frac{\sqrt{3}}{2}
 \end{aligned}
 \tag{D-3}$$

$$\therefore L_p = \frac{2}{\sqrt{3}} L_{95} - L_s \left(\frac{2 - \sqrt{3}}{\sqrt{3}} \right)$$

Now if $L_s = \alpha L_{95}$, then

$$L_p = \left(\frac{2}{\sqrt{3}} [1 - \alpha] + \alpha \right) L_{95}
 \tag{D-4}$$

then for $\alpha = 1/2$, it follows that

$$\begin{aligned}
 L_p &= \left(\frac{1}{\sqrt{3}} + \frac{1}{2} \right) L_{95} \\
 &= 1.08 L_{95}
 \end{aligned}
 \tag{D-5}$$

i.e., L_{95} is only 8% lower than the faired peak force. Similarly, if $\lambda = 6'$ then it may be shown that $L_p = 1.02 L_{95}$.

From the test data, it is seen that depending on the test speed, the dynamic curving force changed from a very small value to its peak in a distance of 3 to 6 feet. Then, as predicted from this analysis, L_{95} is about 2 to 8% lower than L_p . Thus, L_{95} can be used to estimate the energy content of the curving forces and therefore is a good vehicle response descriptor.

It should also be pointed out that the pulse duration at the L_{95} level can be estimated from

$$t = \frac{0.05X_0}{V} = 22 \text{ msec. at } V = 60 \text{ mph}$$

$$= 44 \text{ msec. at } V = 30 \text{ mph}$$

which is consistent with the actual measured values stated previously.

APPENDIX E

STATISTICAL REGRESSION ANALYSIS OF SURVEY RUN DATA

The regression analysis techniques used in analyzing the survey run data are part of a standard statistical package, the BMDP (BMDP-77, Biomedical Computer Programs, P-Series, University of California Press, Los Angeles, 1977). A brief review of the techniques is presented here, via a discussion of the L_{95} regression for the SDP-40F. Similar techniques were used in the regression analyses of V_5 and $(L/V)_{95}$.

1. Twenty-five curves were chosen. complete data were available in these curves for both the E-8 and the SDP-40F.
2. Each of these curves was represented by several independent variables representing track geometry and operational conditions. Examples of track geometry variables included the mean, maximum, minimum, standard deviation and 95th percentile values of the standard deviation curvature, gage, cross-level and high and low rail profiles. The values of these variables were extracted by computer analysis of the magnetic tape data. The value of L_{95} was obtained simultaneously.
3. A correction matrix was developed, showing correlations between the L_{95} values and the values of the independent variables for the 25 curves. This matrix also showed correlations among the independent variables. Independent variables showing a high correlation with L_{95} were chosen for the regression analysis.
4. In summary, the following variables were introduced into the regression analyses:

Dependent Variable: L_{95}

Independent Variables:

1. Mean curvature \bar{C}
2. Standard deviation of curvature σ_C
3. Variance of gage σ_G^2
4. Standard deviation of cross-elevation σ_{XE}

5. Standard deviation of high-rail profile σ_{PH}
6. Standard deviation of low-rail profile σ_{PL}
7. Underbalance ΔE

In addition, the following cross-product terms were defined as additional independent variables.

8. $\sigma_C \times \sigma_G$
9. $\sigma_C \times \Delta E$
10. $\sigma_C \times \delta_{XE}$
11. $\sigma_G \times \Delta E$
12. $\sigma_G \times \sigma_{XE}$
13. $\sigma_{XE} \times \Delta E$
14. $\bar{C} \times \sigma_G$

5. The use of fourteen independent variables meant that the regression for L_{95} could have had up to fourteen terms in it. However, the statistical analysis package contains criteria by which it decides whether the inclusion of any given term is justified by its contribution to the explanation of scatter in the L_{95} data. The specific statistic used is the F-statistic, which is the square of the t-statistic. The overall procedure is summarized below.
6. Determine the F-statistic for each independent variable. Enter into the regression equation the variable with the highest F, unless no variable meets a criterion requiring a minimum value of F.
7. Perform the regression analyses, and determine the regression, the multiple correlation coefficient and the residuals of all the L_{95} values.
8. Repeat step 4, now using the L_{95} residuals to determine the F values for the remaining independent variables.

9. Repeat step 5, now performing a regression with two independent variables.
10. Keep on entering new independent variables until none remains with sufficient explanatory power. The final regression equation is obtained.

APPENDIX F

HTC TRUCK LOW TEMPERATURE CHARACTERIZATION

(Prepared by Martin Marietta Corporation)

Introduction

A series of tests have been performed on two HTC locomotive trucks to determine their stiffness and damping characteristics and the variation of these characteristics with changes in ambient temperature. Specifically, the parameters of importance are the load-deflection and load velocity relations for primary and secondary suspension subassemblies. These parameters are required for use in analytical studies involving derailment and ride quality problems.

Two trucks were tested. The first one had hard secondary suspension elastomeric pads and was tested only at room ambient temperature. The second truck had soft secondary suspension elastomeric pads and was tested at two temperatures, room temperature (70°F) and a low temperature condition, approximately 0°F. From the low temperature test, it was found that the stiffness coefficients became higher from 20 to 70%, depending upon direction of the motion.

From these tests it was concluded that more emphasis is needed on determination of elastomer stiffness properties as a function of temperature. Variation of characteristics with frequency were also needed since the elastomeric pads may exhibit significant changes in both stiffness and damping with change in frequency. Because of these reasons it was decided that a comprehensive series of element tests be performed using only one elastomeric pad at a number of temperatures and excitation frequencies.

Test Setup

A rig was constructed to support one complete truck. Each wheel rested on a low friction pad which, in turn, was restrained by two mutually orthogonal actuators with load cells. Vertical load was applied through the bolster center plate; the lateral load, through the bolster. Several load conditions were tested. For example, static vertical load with an oscillatory component superimposed; lateral oscillatory load with static vertical load. In addition, several other conditions were superimposed, such as brake on

and off and thrust on and off. The oscillatory load was cycled at a relatively low frequency of 0.25 Hz. The oscillatory load was needed to display fully the hysteretic effects of the friction forces.

The reason for keeping the excitation frequencies low was twofold. First, the inherent limitations of the hydraulic supply system prevented reaching the frequencies in excess of 0.5 Hz. Second, the inertial forces are significant at higher frequencies. Hence, data interpretation becomes more difficult.

Test

Element tests were conducted to determine the load deflection/velocity characteristics in shear (lateral for the locomotive) of the secondary suspension system rubber pads. The tests were conducted at various frequencies of loading and various pad temperatures. Loading frequencies varied from .25 Hz to 3 Hz. Temperatures varied from -55°F to 70°F. During the test, the internal temperature of the pad was monitored with a thermocouple. No attempt was made to keep the internal temperature constant during the test. The data defined between -55°F and 0°F were obtained by cooling the specimen to -55°F, continuously loading the pad at .25 Hz and allowing the internal temperature to increase due to internal friction and 0°F ambient temperature. Hysteresis data (load/deflection) were then recorded in 5°F increments as the internal temperature increased. It took approximately one hour and 900 load reversals for the total 55°F change. This indicates an average change of 0.06°F per cycle.

Results

The suspension system load/deflection-velocity characteristics are the linear and nonlinear stiffness, linear damping and friction parameters associated with the suspension system elements and connections. Table F-1 gives a description of each element and the types and values of parameters measured for both of the trucks tested. This table illustrates that the only parameters affected by temperature were the secondary lateral and vertical stiffness. The vertical stiffness increased by approximately 70%, while the lateral increased by approximately 20%. The significance of these changes may be assessed as follows. The primary and secondary suspensions

TABLE F-1 HTC SUSPENSION CHARACTERISTICS

Suspension	Description of Suspension Element	Description of Characteristics	Parameter	Designation/Truck 1/70°F	Truck 2/70°F	Truck 2/0°F
Primary Vertical	Coil Springs	Linear Stiffness	K lbs/in.	44,000	50,000	50,000
	Journal box slides in pedestal liners	Coulomb friction (function of tractive effort or braking)	μ dimensionless	.16	.16	.16
Secondary Vertical	Rubber pads (compression)	Linear stiffness	K lbs/in.	475,000	257,000	440,000
	Bolster slides on tractive effort stops	Coulomb friction (function of tractive effort or braking)	μ dimensionless	.5	.5	.5
Primary Lateral	Rubber doughnut + clearance + small coulomb friction	Stiffness described by 9th order polynomial		← identical → could not measure		
Secondary Lateral	Rubber pads (shear)	Linear stiffness	K lbs/in.	23,000	14,300	17,500
	Bolster slides on tractive effort stops	Viscous damping	C lbs/in./sec	not measured adequately - see element test results		
		Coulomb friction	μ dimensionless	.4	.4	.4

are essentially in series; hence, the total suspension stiffness is given by the following expression:

$$K_T = \frac{K_S K_P}{K_S + K_P}$$

where

K_S - secondary stiffness,

K_P - primary stiffness, and

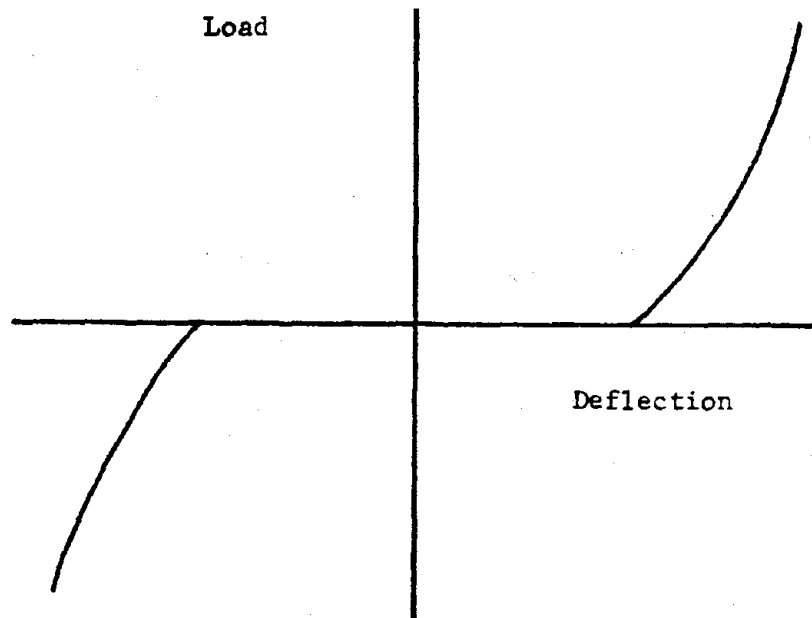
K_T - total stiffness.

In the vertical direction these values are:

	70°F	0°F
K_S	257,000	440,000
K_P	50,000	50,000
K_T	41,900	44,900

Hence, even though the secondary stiffness increased by 70% at low temperature, the net increase in vertical stiffness is only 7%.

The lateral case is not as simple as the vertical due to the fact that the primary lateral stiffness is nonlinear. This nonlinear characteristic has the following appearance:



When the locomotive is operating on rough track the excursions in this element make it appear very stiff. Similarly, when negotiating curves the biased load makes the element appear stiff. In this position or condition, the net suspension stiffness laterally is controlled by the secondary lateral stiffness; hence, changes in the secondary stiffness due to temperature are reflected in the total stiffness on a one-to-one basis. Therefore, in some circumstances the lateral suspension stiffness may change by as much as 20%, going from 70°F to 0°F.

Element test results exhibited the same trends for the lateral secondary stiffness versus temperature down to -55°F. Figure F-1 illustrates this trend for both the stiff and soft HTC pads.

Note a significant reduction in damping with increasing frequency. This type of behavior is typical for elastomeric materials. At the present time, work is in progress to try to fit the data to an analytical elastomeric model.

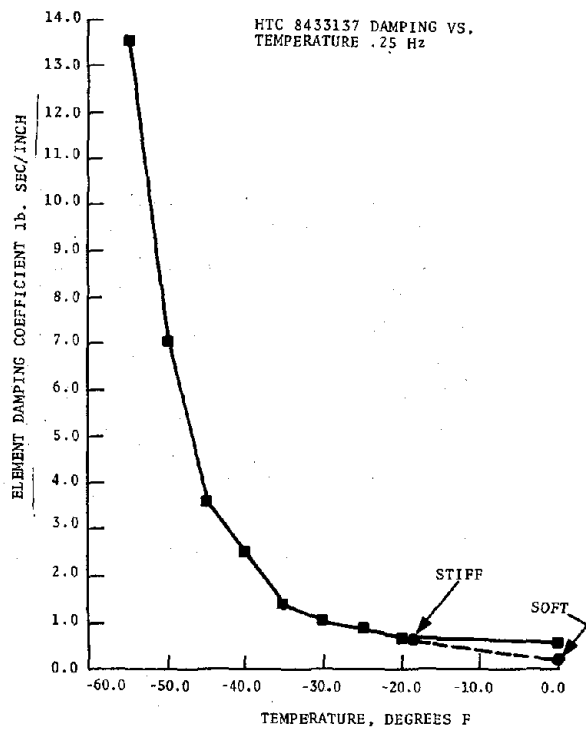
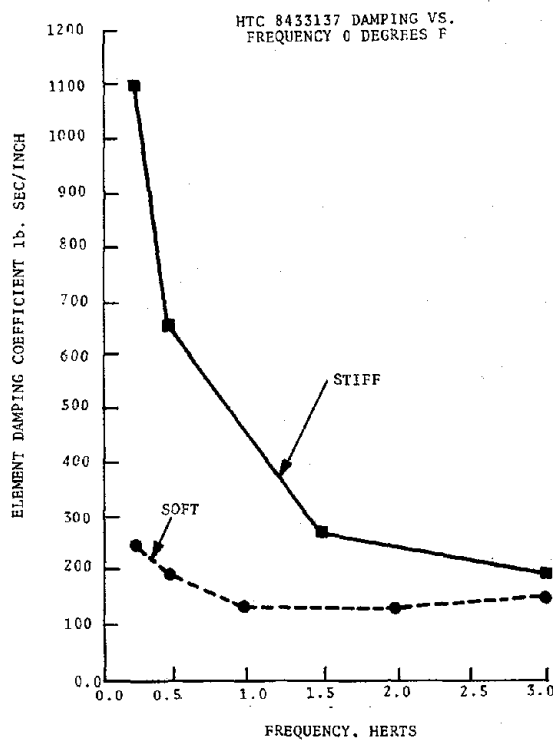
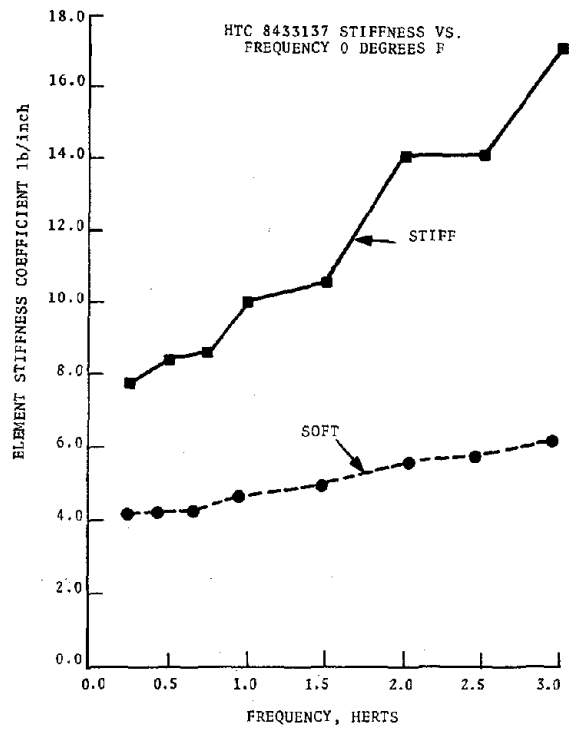
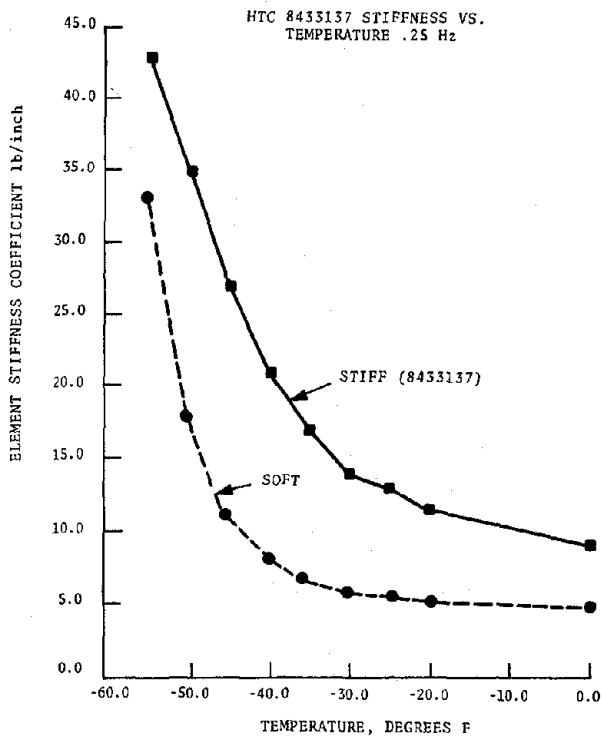


FIGURE F-1 HTC TRUCK STIFFNESS AND DAMPING PARAMETERS FOR STIFF AND SOFT ELASTOMERIC PADS

Conclusions

Until more comprehensive comparative analyses are performed, the effect on performance of the truck parameter variations due to temperature changes is not known. However, general deductions have been made based on our knowledge of the rail dynamic environment.

The key to ride quality for the HTC locomotive is the transmissibility of the suspension system. This transmissibility is controlled by three parameters: mass, stiffness and damping. Mass and stiffness control the frequency at which peak transmissibility occurs. Damping controls the magnitude of the peak. If the mass and stiffness are such that the transmissibility peaks occur where the damping is small, then a very rough ride can be expected.

The dynamic characteristics of the elastomeric pads seem to be the potential source of the rough ride problem experienced by the HTC locomotives equipped with stiff pads. No comprehensive analysis has been done to verify this; however, the changeover to soft pads has improved ride considerably based on EMD's ride quality tests* and subsequent railroad experience. This result seems consistent with our element test results for the two pads.

*See Table 1 and Figure 5 of the paper, "Tracking and Ride Performance of Electromotive 6-Axle Locomotives," by W.R. Klinke and C.A. Swenson in Railroad Engineering Conference, Pueblo, October, 1976, Proceedings: "Railroading Challenges in America's 3rd Century, Improved Reliability and Safety," FRA/ORD-77/13, pp. 106-108.

APPENDIX G

CORRELATION OF LATERAL FORCE DATA FROM WAYSIDE INSTRUMENTATION

A comparison of the vertical force measured from both the onboard data and the wayside data showed reasonable agreement. However, a similar comparison of the data for the lateral force showed a discrepancy in the wayside data. An example of the relationship between the high rail lateral force and corresponding wheel lateral force (axle 10) is shown in Figures G-1 and G-2 for the E-8 and SDP-40F, respectively. These figures trace the progression of the instrumented axle through the instrumented test site. It is seen that although there appears to be a discrepancy in the magnitudes of lateral force from the wayside instrumentation, the trends of the data are quite similar as axle 10 traverses the site. Due to the discrepancy, TSC personnel carried out a study of the strain gage circuit for measuring lateral loads. This circuit, originally used by the Swiss National Railways for the ORE, has been employed in a wide range of field investigations of wheel/rail loads in a series of TTD and AMTRAK programs by Battelle since its introduction to North American practice in 1975. Upon investigation, it was discovered that the measurement of the lateral force at the wayside could be substantially distorted due to a "crosstalk" arising from the response of the circuit to vertical load. The main error in the formulation of the circuit was in assuming that the cross-section of a rail, as shown in Figure G-3, behaved like a cantilever beam. Under this assumption, a vertical and lateral load would lead to a constant and linear bending moment along the web, respectively. For these ideal conditions, the ORE bridge circuit (shown in Figure G-3) would only measure the difference in the bending moments between the gage positions at points "a" and "b" on the web and would exclude any constant moments applied in this region. Thus, the output of the circuit would be independent of both vertical load and the location of lateral load on the rail head. However, a structural analysis study of an 8-inch high rail section of 39-foot length spiked on ties at discrete locations, shows that the response to a load is quite different from that predicted from beam theory for an 8-inch long cantilever beam. For example, when a load is applied at a point on the rail head, the force transmitted to the rail base through one rail section is affected by other adjacent rail sections as well as by the deflection of the rail head. Consequently, the distribution of the bending moment along a given section

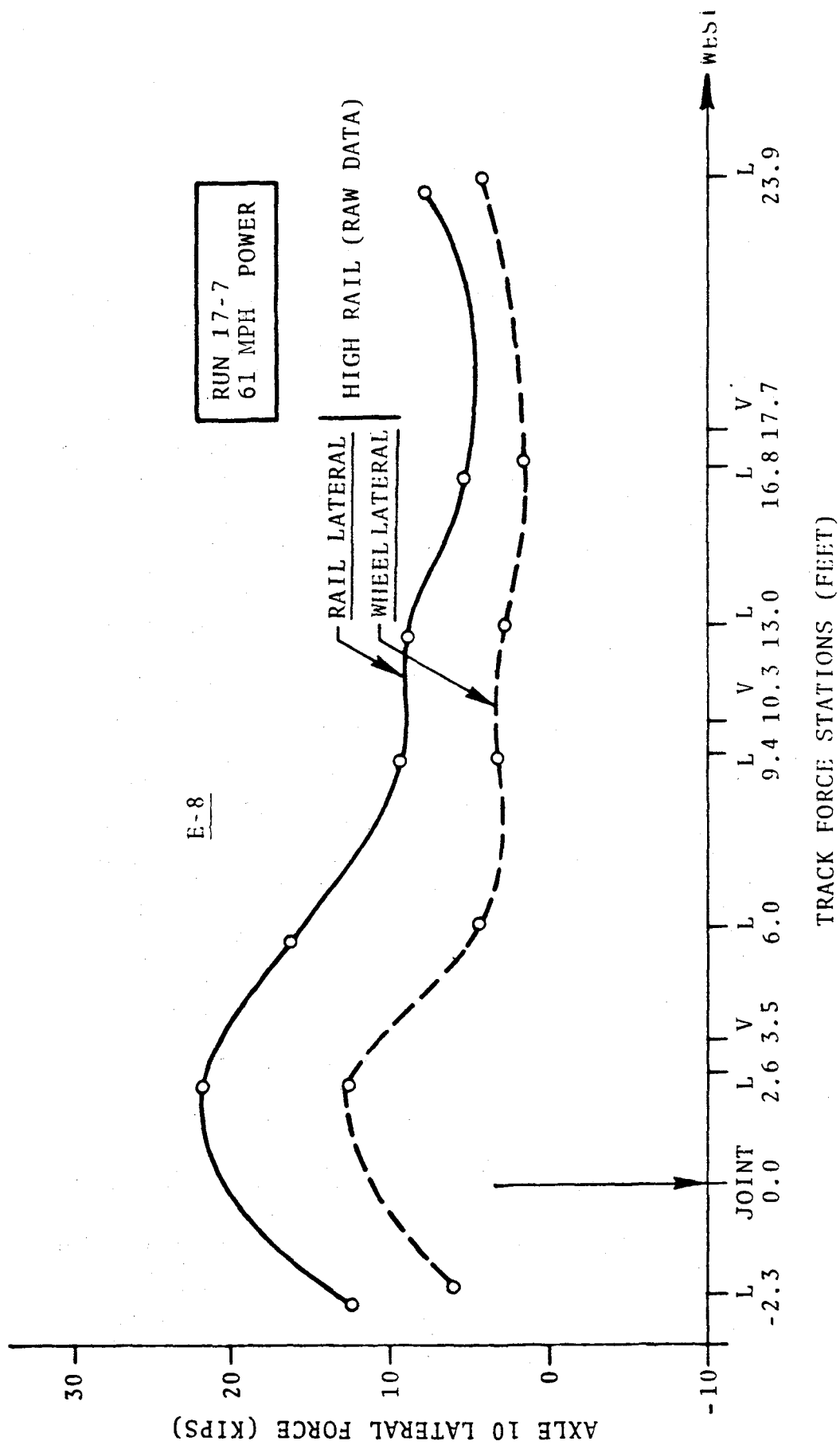


FIGURE G-1 COMPARISON OF TYPICAL ONBOARD AND WAYSIDE AXLE
 10 LATERAL FORCE TRACE FOR E-8 AT TEST SITE NEAR 60 MPH

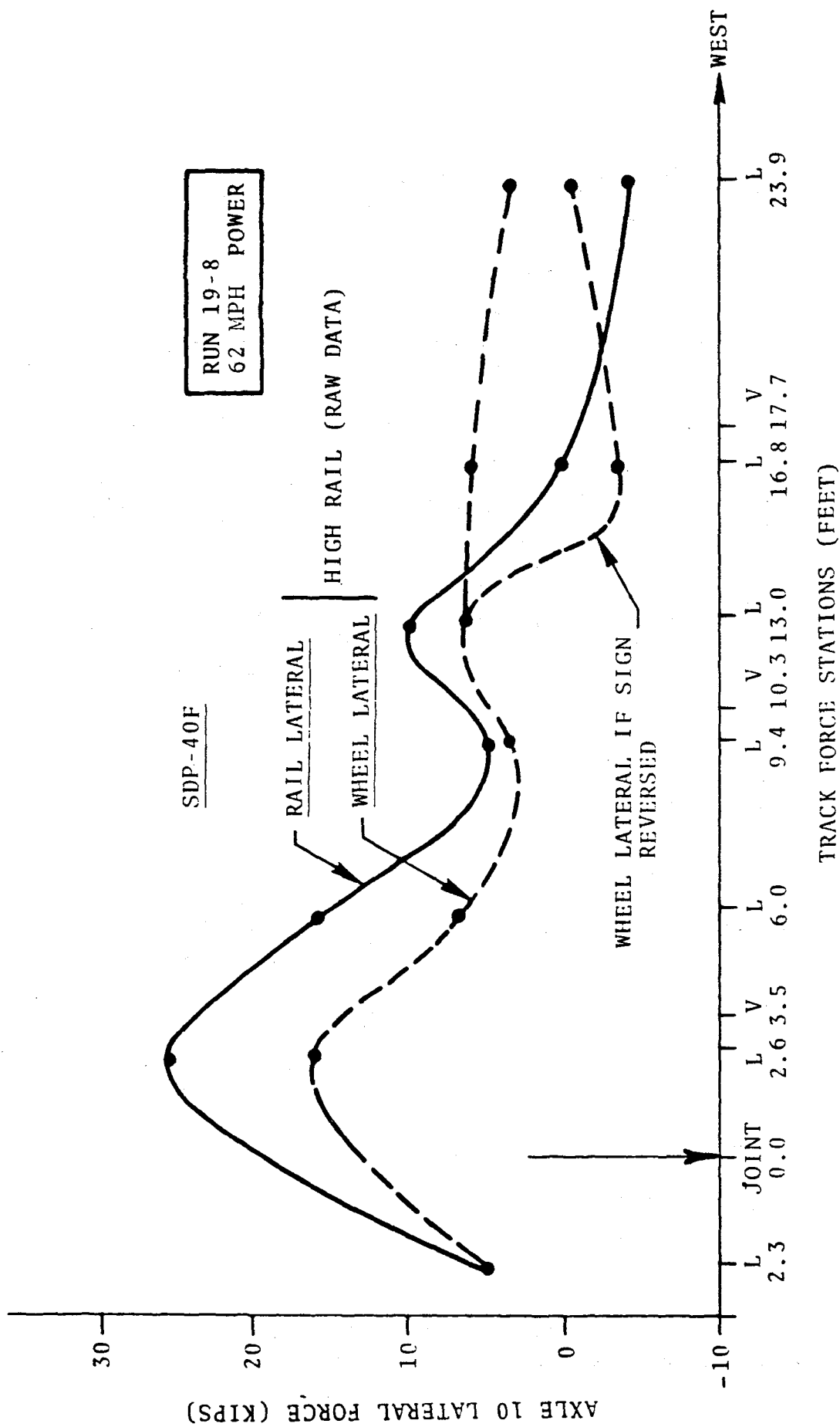
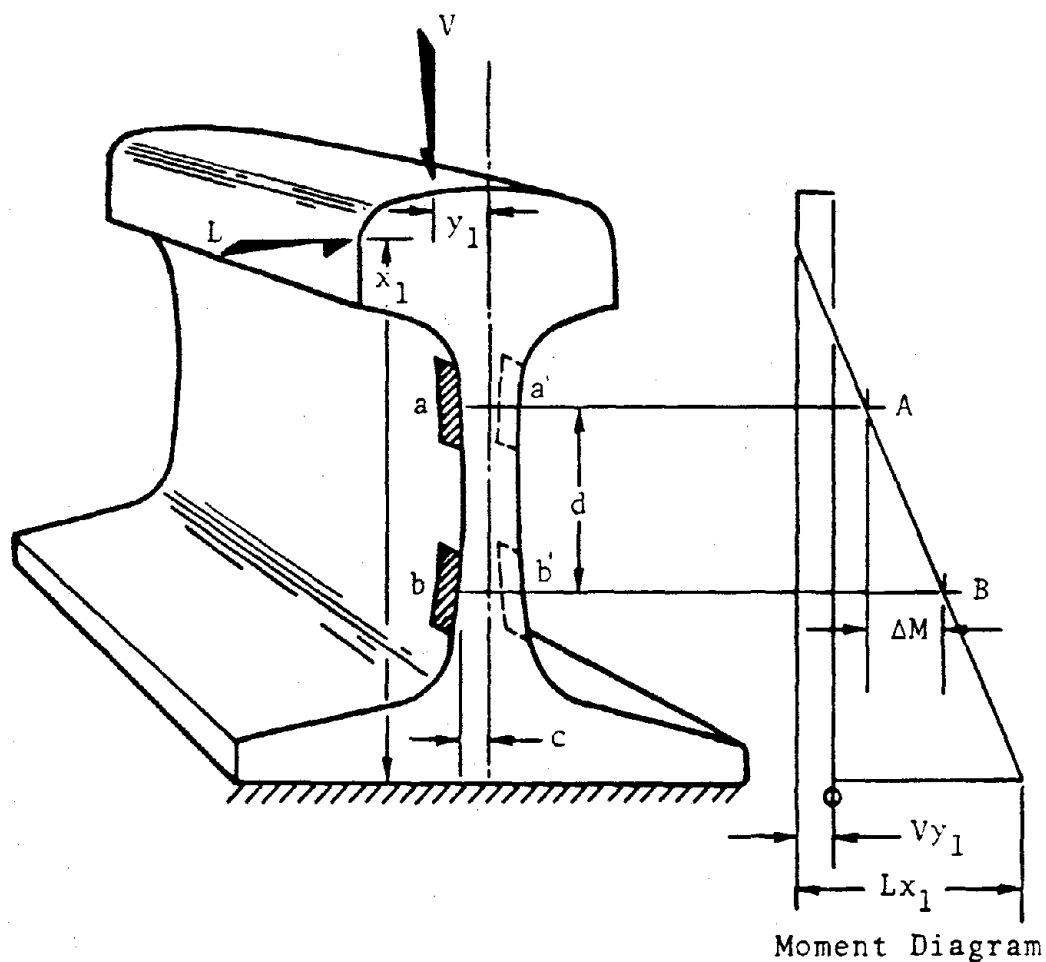


FIGURE G-2 COMPARISON OF TYPICAL ONBOARD AND WAYSIDE AXLE 10 LATERAL FORCE TRACK FOR SDP-40F AT TEST SITE NEAR 60 MPH



FORMULATION OF ORE CIRCUIT

$L \propto V$ (shear force)

$S = \frac{\partial M}{\partial X}$ (independent of V, x_1, y_1)

$$S = \frac{M_B - M_A}{d}$$

$$M_A = \left(\frac{EI}{c} \right) \epsilon_A$$

$$S = \frac{EI}{cd} (\epsilon_B - \epsilon_A)$$

$$L \propto (\epsilon_B - \epsilon_A) \text{ where } \begin{cases} \epsilon_A = \epsilon_a - \epsilon_{a'} \\ \epsilon_B = \epsilon_b - \epsilon_{b'} \end{cases}$$

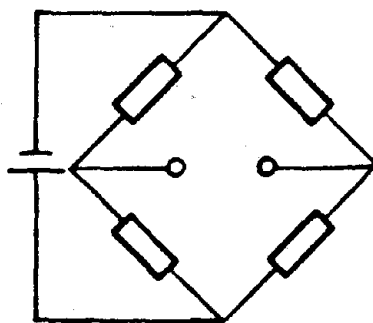


FIGURE G-3 ORE STRAIN GAGE CIRCUIT FOR MEASUREMENT OF LATERAL WHEEL/RAIL LOADS IN RAIL WEB

will depend upon the rail support condition, the location of load application, and also on the magnitude of both the vertical and lateral load.

As a result of this TSC study, Battelle was directed to carry out post-calibration tests to examine the crosstalk sensitivity at the test site and, in addition, to perform laboratory tests to further quantify the crosstalk, in general. The laboratory test fixture used for evaluating this rail circuit simulates one-half of a track structure 26 feet in length. As shown in Figure G-4, there are 14 crossties supported on two 10 x 12 wide flange I-beams. The crossties are aluminum I-beams, and they were simply supported so their bending stiffness simulated a nominal track modulus. This fixture allows testing of the circuit for an extreme range of support conditions ranging from unsupported (no center tie) to firmly supported. The rail was secured in the fixture with a combination of clips which could be changed to simulate either positive hold-down clips, simple lateral stops, or free lateral motion. Both the post-calibration and laboratory tests confirmed the sensitivity of the rail circuit to crosstalk. As an example, Figure G-5 shows the web strain for vertical loads applied at two different head locations, roughly 1/2 inch on either side of the centerline. These strain distributions do not correspond to a constant bending moment distribution along the web. Figure G-6 shows the ORE lateral circuit output is approximately proportional to the linear distance of vertical load from the rail head center. Figure G-7 shows the strain variation in the web for a lateral load applied at 0.44 inches below the rail running surface for different support conditions. The strain distribution does not correspond to a linear bending moment distribution along the web. Finally, Figure G-8 shows the sensitivity of the ORE lateral circuit output to various locations of the lateral load on the side of the rail head in the laboratory test.

Based on the results of the laboratory tests, it was obvious that the lateral circuit output from the Chessie System Test must be corrected both for the crosstalk from the vertical load and the change in sensitivity due to the position of the application of the lateral load. This latter correction is necessary since the lateral circuit was calibrated based on a lateral load application point at 0.81 inches below the rail head while the actual wheel/rail load due to flanging is more likely applied at the gage corner (which is much closer to the top of the rail). In order to obtain an exact correction, it would be necessary to ascertain the exact rail support condition, the location of the vertical and

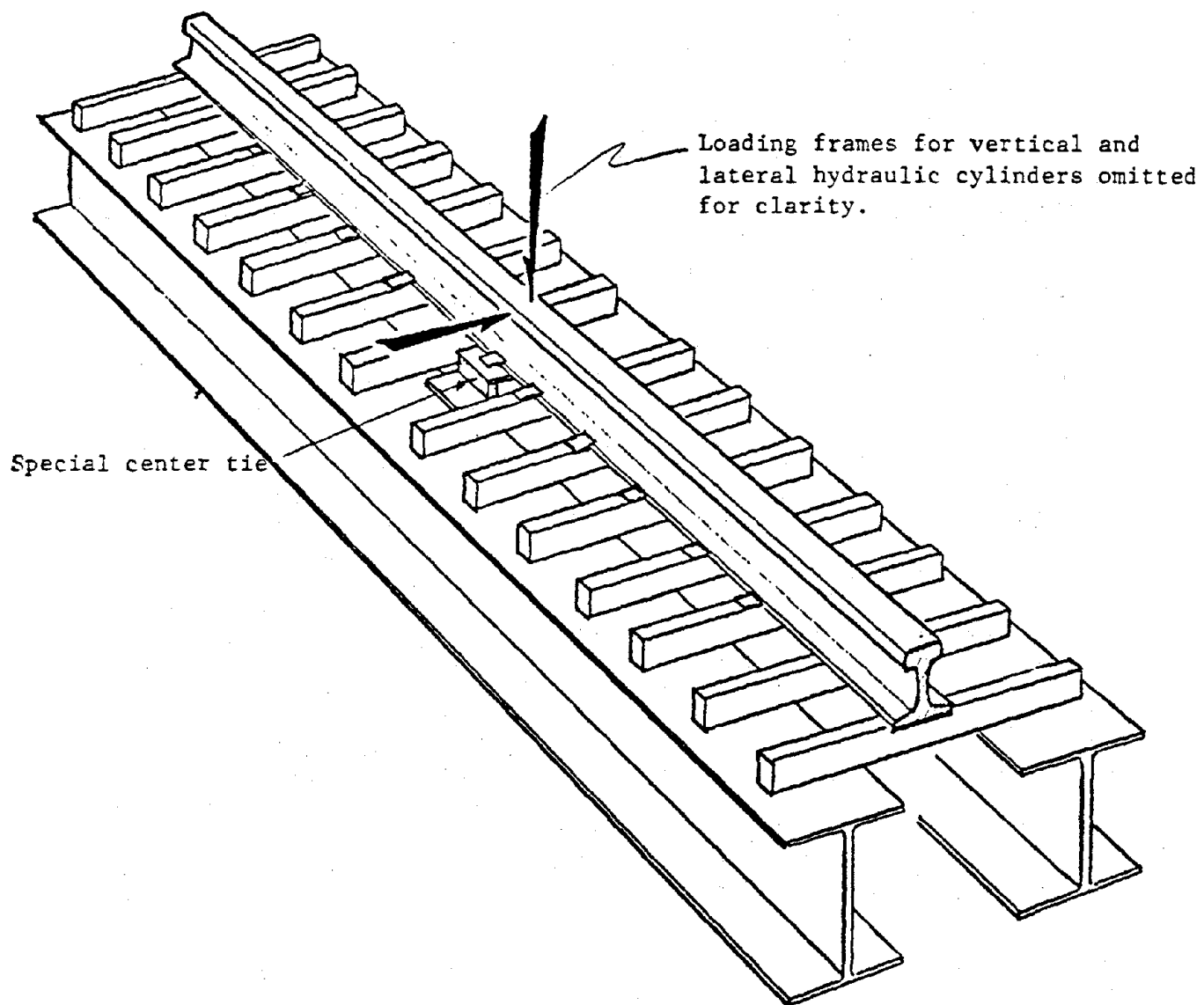


FIGURE G-4 LABORATORY RAIL TEST FIXTURE

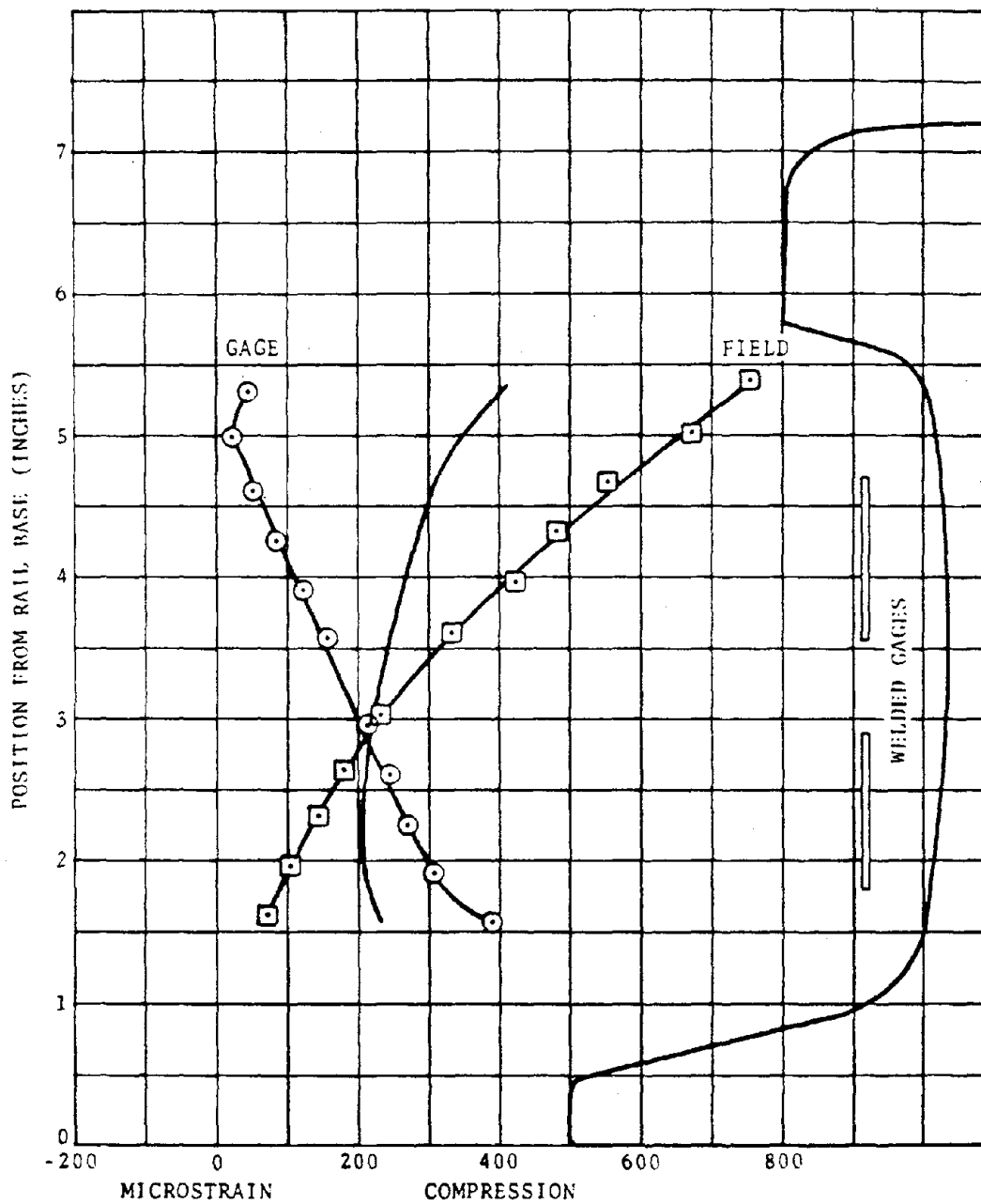


FIGURE G-5 WEB STRAIN PATTERN IN 131 LB/YD RAIL DUE TO 29-KIP VERTICAL LOAD APPLIED AT +0.53 INCH (TOWARD FIELD SIDE OF CENTERLINE), FIRMLY-SUPPORTED RAIL

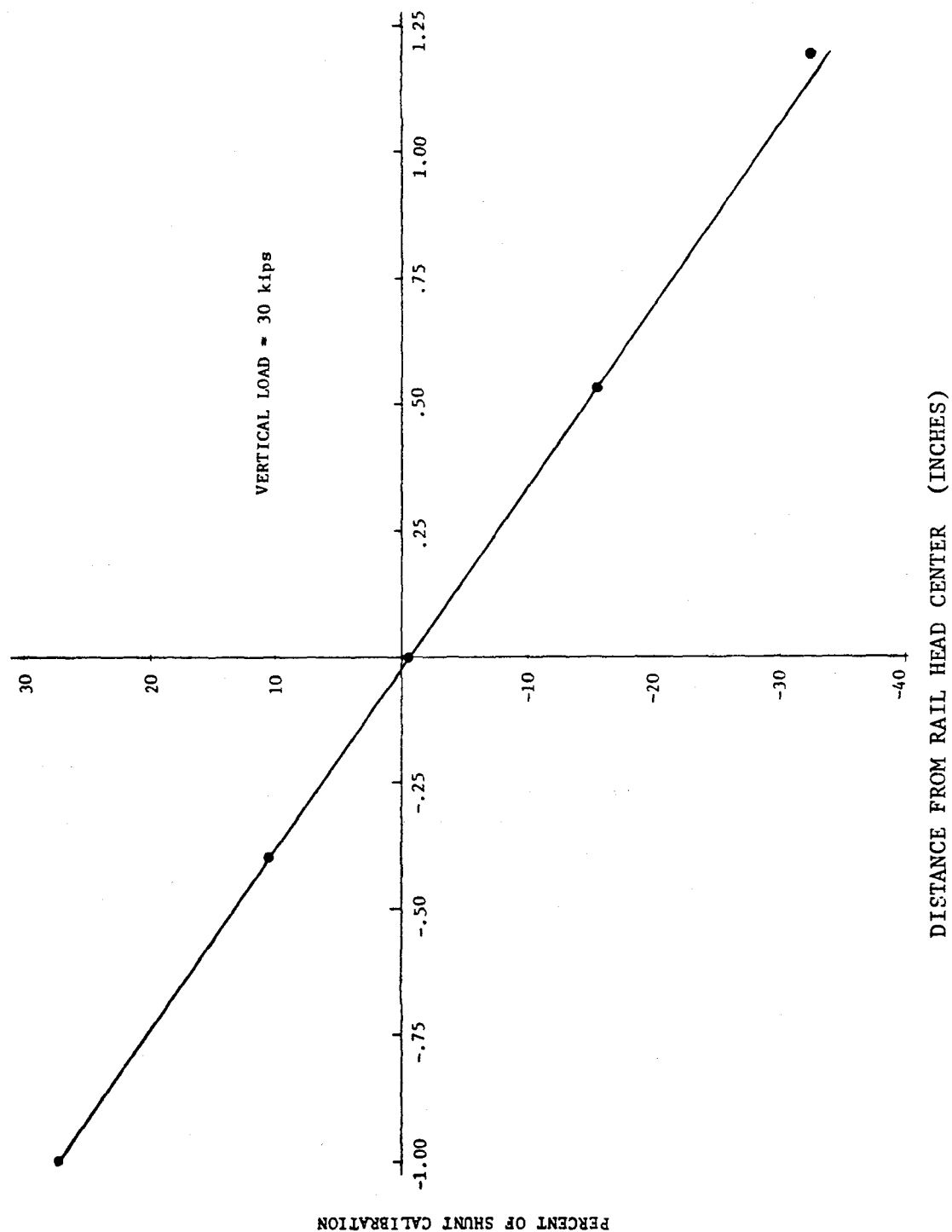


FIGURE G-6 LATERAL CIRCUIT CROSSTALK AS A FUNCTION OF LINEAR DISTANCE OF THE VERTICAL LOAD TO THE RAIL HEAD CENTER

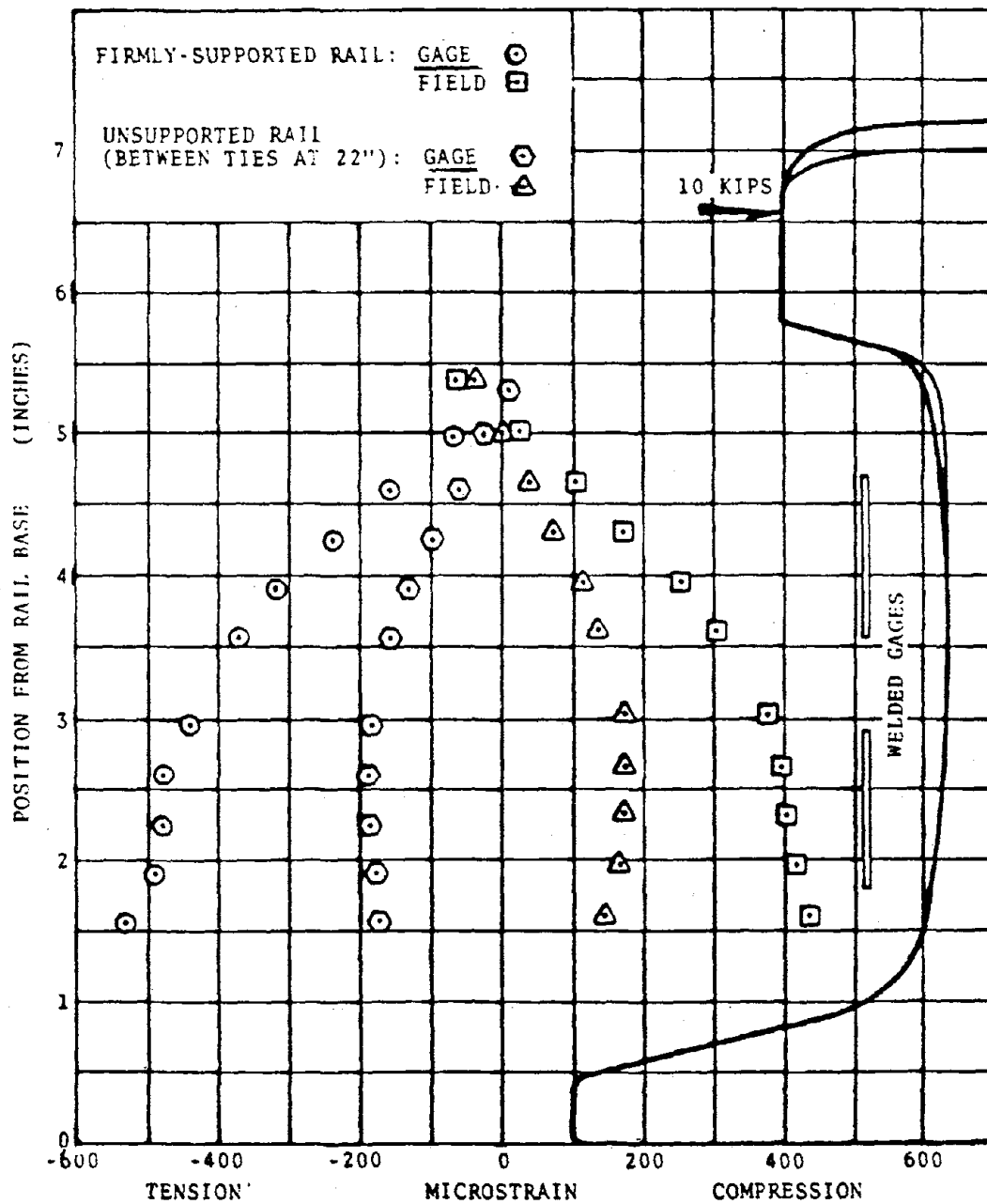


FIGURE G-7 WEB STRAIN PATTERN IN 131 LB/YD RAIL DUE TO 10-KIP LATERAL LOAD 0.44 INCH BELOW RUNNING SURFACE (6.56 INCHES ABOVE RAIL BASE)

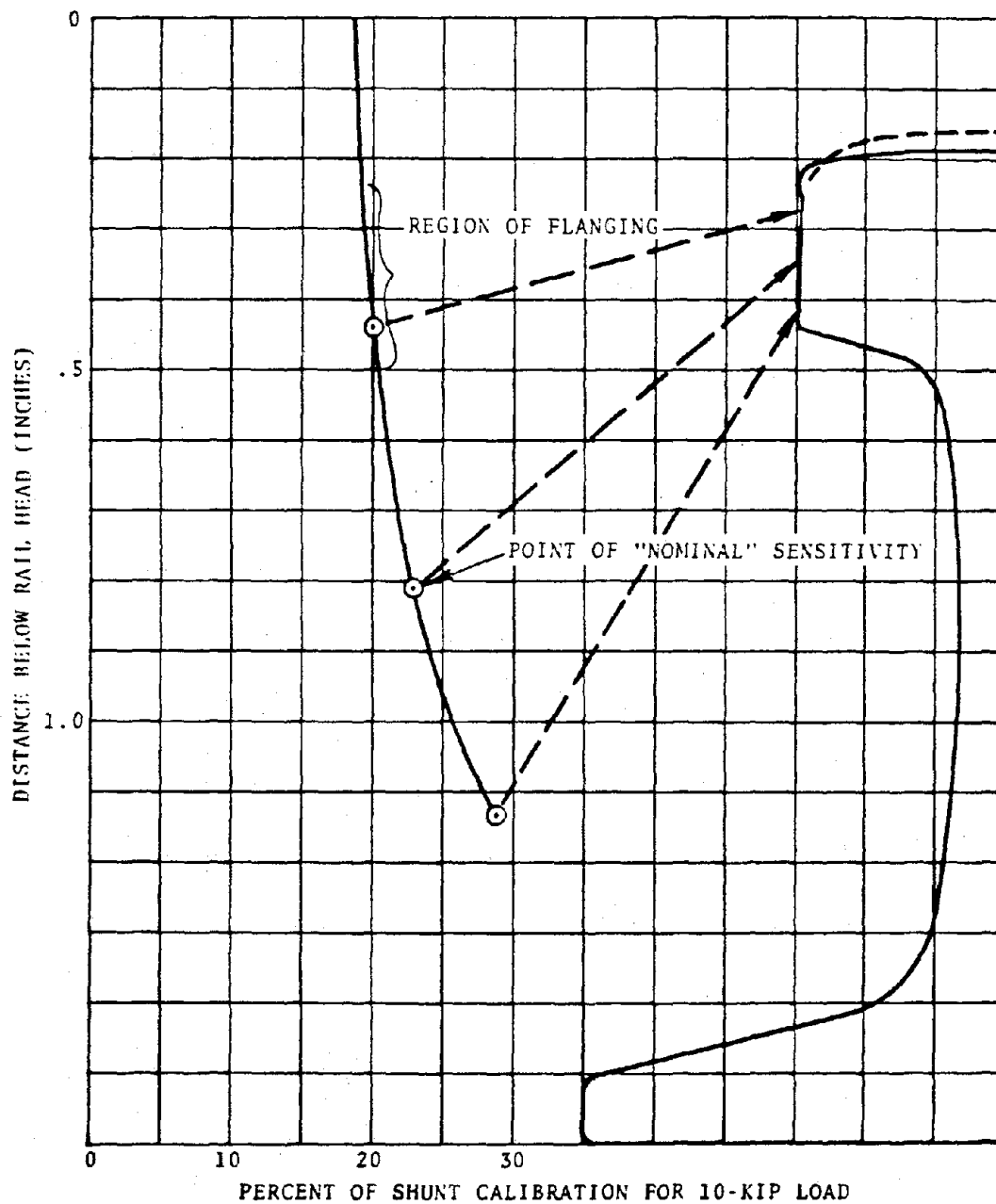


FIGURE G-8 VARIATION IN LATERAL CIRCUIT OUTPUT

lateral load and the magnitude of the applied loads. However, in a practical situation such as for the Chessie System wayside data, certain assumptions must necessarily be made in order to obtain the correction factor. First, since the field test sensitivity was similar to that of the laboratory test with a firm support condition, it was assumed that the change in sensitivity is proportional to that of the laboratory test associated with the different lateral load locations. Secondly, it was assumed that the wheel flanged on the curve so that the vertical wheel loads were applied on the rail at two different points as shown in Figure G-9. The portion of the vertical load at the gage corner, V_2 , is computed from Nadal's formula

$$\frac{L_2}{V_2} \leq \frac{\tan\delta - \mu}{1 + \mu\tan\delta} \quad (G-1)$$

where δ is the effective flange angle and μ is the coefficient of friction. For a worst case evaluation of the circuit, let the local L/V go to the limit and let $L_1 = 0$ (no creep force). Then

$$\frac{L}{V_2} = \frac{\tan\delta - \mu}{1 + \mu\tan\delta} \quad (G-2)$$

= C_3 (a worst case estimator)

The value of C_3 , as defined in equation (G-2), is given in Table G-1 for a variety of values of δ and μ . The lateral circuit output is now proportional to the combined effects of the applied lateral and vertical loads in the form

$$\begin{aligned} L \text{ output} &= C_1 L + C_2 V y \\ &= C_1 L + C_2 (V_1 y_1 + V_2 y_2) \end{aligned} \quad (G-3)$$

where V is the total vertical wheel load and y is the lateral offset of this vertical load from the center of the rail. In this relationship, C_2 is taken as the gage factor due to a vertical load positioned at 1" from the rail center, while C_1 is the ratio of the lateral sensitivity at

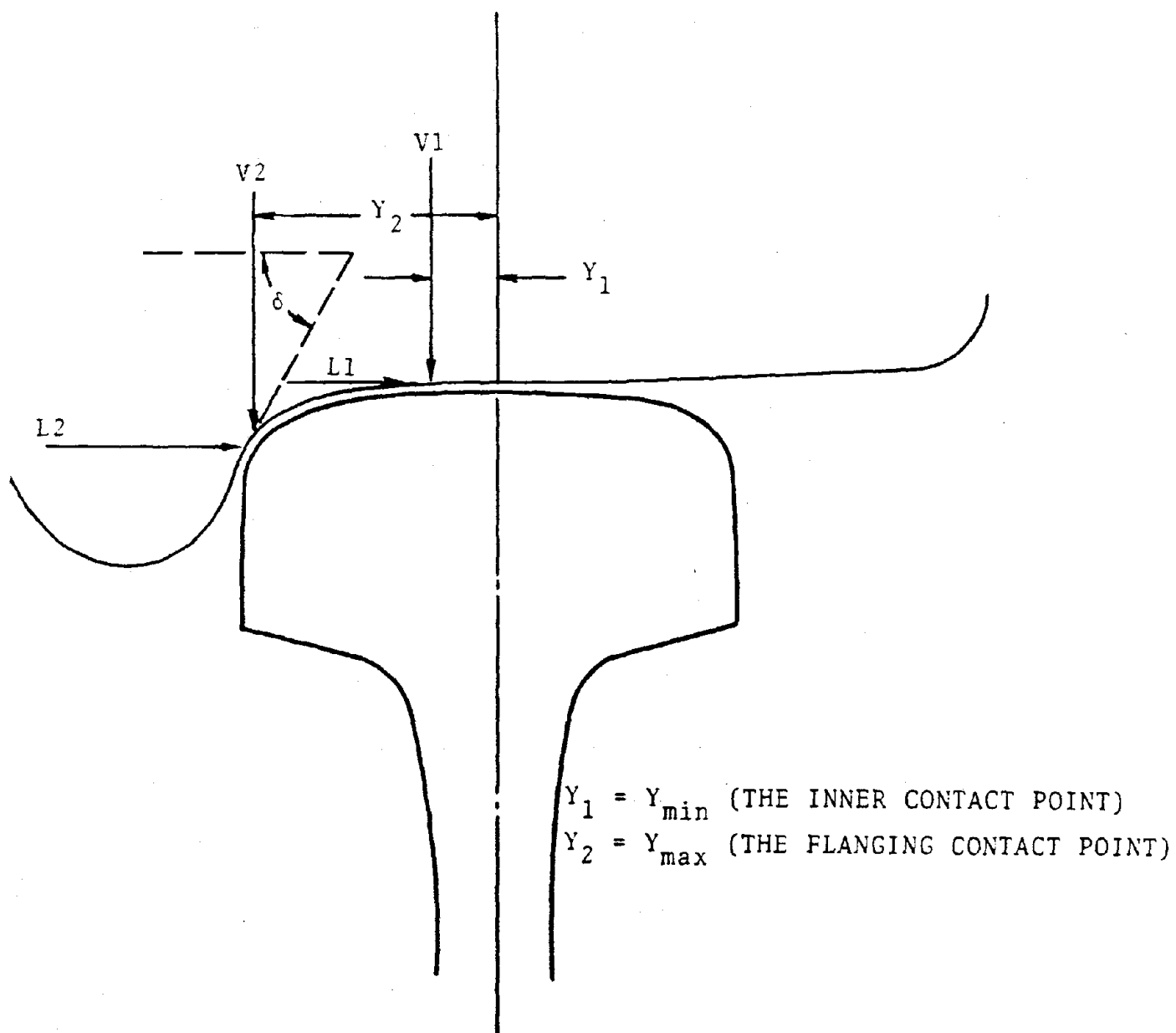


FIGURE G-9 NOMENCLATURE FOR TWO-POINT CONTACT

TABLE G-1 VALUES FOR C_3 , WORST CAST ESTIMATORS
OF NADAL'S LIMIT

		Coefficient of Friction - μ		
		.15	.20	.35
Flange Angle - δ	50°	0.88	0.80	0.59
	56°	1.09	0.99	0.74
	60°	1.26	1.14	0.86
	62°	1.35	1.22	0.92
	65°	1.51	1.36	1.03
	70°	1.84	1.64	1.22

the gage corner to that at 0.81 inches below the rail head. Using Nadal's formula to estimate V_2 , we have

$$L \text{ output} = [C_1 + \frac{C_2}{C_3} (Y_2 - Y_1)]L + C_2 VY_1 \quad (G-4)$$

Since Nadal's formula is only valid for $L \leq C_3 V_2$, the relationship of (G-3) must be altered for $L > C_3 V_2$. For this region, it follows that $V_1 = 0$ and the circuit output becomes

$$L \text{ output} = (C_1 + \frac{C_2}{C_3} Y_2) L \quad (G-5)$$

The results of equations (G-4) and (G-5) are plotted in Figure G-10 for $V = 30,000$ lbs. Using laboratory data, we can identify the following parameters:

$$\begin{array}{ll} Y_1 = 0.25" & Y_2 = 1.4" \\ C_1 = 0.85 & C_2 = 0.37 \end{array} \quad (G-6)$$

and C_3 is given in Table G-1. Results are shown in Figure G-10 for a flange angle of 50° and a friction coefficient of 0.15 and 0.35. From a study of these curves, it may be deduced that multiplying the circuit output by a factor of 0.6 will provide a simple correction factor that yields a good approximation for obtaining the actual lateral loads,

$$\begin{array}{l} L \\ \text{actual} \end{array} = 0.6L \begin{array}{l} \\ \text{output} \end{array} \quad (G-7)$$

particularly in the important range of circuit output from 10 kips to 30 kips. Therefore, this analysis suggests a scale factor 0.6 applied to the wayside data for comparison purposes with the onboard data.

Table G-2 examines the actual results for the maximum lateral force for various runs during the Chessie System Test. It includes a comparison of onboard data, raw wayside data and corrected wayside data for the SDP and E-8. It is seen that for the highest raw value of track force of 26 kips, the 0.6 correction factor produces a lateral force within 4% of the onboard wheel force. Further illustration

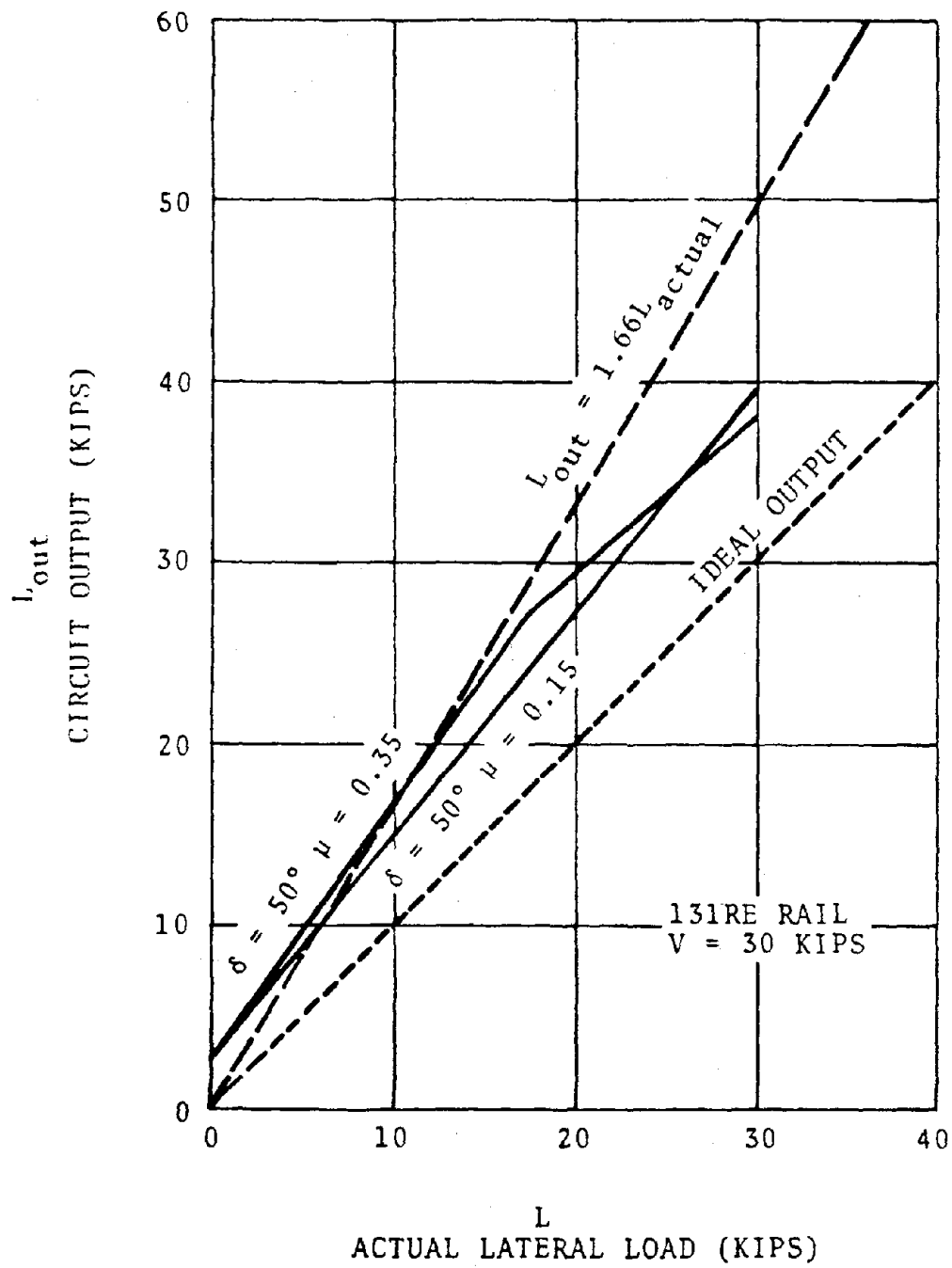


FIGURE G-10 CORRECTION CURVES FOR ORE LATERAL LOAD CIRCUIT

TABLE G-2. SDP-40F BASELINE RUNS
(1 of 2)

COMPARISON OF WHEEL AND TRACK FORCE MEASUREMENTS

MAXIMUM LATERAL FORCE AT INSTRUMENTED SITE

<u>Run Number</u>	<u>Speed</u>	<u>Wheel Force</u>	<u>Track Force</u>	<u>Corrected Track F</u>
19-1	30.6	6.0	11.0	6.6
19-2	41.2	7.0	10.0	6.0
19-3	41.7	8.0	11.0	6.6
*		*		
19-5	50.6	9.0	15.0	9.0
**		**		
19-7A	55.0	11.0	19.0	11.4
19-7B	55.7	10.0	23.0	13.8
19-8	62.0	16.0	26.0	15.6
19-9	29.2	6.0	10.0	6.0
20-1	60.1	15.0	24.0	14.4
20-2	33.1	5.0	11.0	6.6
20-3	42.5	6.0	12.0	7.2
20-4	61.8	10.0	19.0	11.4
20-5	29.8	6.0	13.0	7.8
20-6	45.6	7.0	13.0	7.8
20-7	58.9	12.0	21.0	12.6
20-8	50.6	11.0	20.0	12.0
20-9	60.7	15.0	25.0	15.0
*19-4	45.7	14.0		
**19-6	55.9	7.0		
Spurious Brush Chart Data				

TABLE G-2 E-8 BASELINE RUNS
(2 of 2)

COMPARISON OF WHEEL AND TRACK FORCE MEASUREMENTS

MAXIMUM LATERAL FORCE AT INSTRUMENTED SITE

<u>Run Number</u>	<u>Speed</u>	<u>Wheel Force</u>	<u>Track Force</u>	<u>Corrected Track Force</u>
17-1	28.7	7.0	15.0	9.0
17-2	34.8	11.0	18.5	11.1
17-3	38.2	10.0	21.0	12.6
17-4	46.3	12.5	23.0	13.8
17-5	52.1	11.0	21.0	12.6
17-6	54.5	12.0	20.0	12.0
17-7	60.7	14.0	22.0	13.2
18-1	55.4	15.0	26.0	15.6
18-2	55.7	13.0	20.5	12.3
18-3	38.8	10.0	15.0	9.0
18-4	50.2	12.0	20.0	12.0
18-5	60.1	11.5	18.0	10.8
18-6	48.3	11.5	22.5	13.5

of this correction factor is shown in Figure G-11. By using the 0.6 correction factor on the wayside data, we see that the comparison of onboard and wayside data is quite good at the higher speeds; furthermore, there is a good trend comparison throughout the entire test speed range.

Based on a review of laboratory strain distribution for the loaded rail, Chessie System Test data, and additional data generated under TSC's rail stress analysis projects, a number of alternative circuits for measuring lateral rail head loads were identified. Several of these circuits were investigated in the laboratory utilizing the rail loading fixtures originally developed for the rail stress program. Against the criteria of sensitivity to load, insensitivity to support conditions, linearity and crosstalk (Table G-3), the base chevron circuit of Figure G-12 was selected as the best overall transducer array. It is this circuit which TSC would recommend for use in future load characterization tests in combination with the existing rail web chevron circuit for vertical loads. This latter circuit shows excellent performance during the lab tests.

The newly developed based chevron circuit has a number of advantages over the old web circuit for measuring lateral loads, the most significant being the order of magnitude reductions in crosstalk which it permits. The additional advantages of this new circuit include:

- (a) The gages are mounted on the top surface of the rail base, which allows easy installation in the field.
- (b) Both lateral gage chevrons may be mounted over the same crib as the measurement circuit for vertical loads. This will enable the simultaneous measurement of the vertical and lateral loads with no phase shift.

As can be seen from the results of the laboratory tests, this new technique provides a substantial improvement over the existing system. These results were also proven out in a recent field test program.

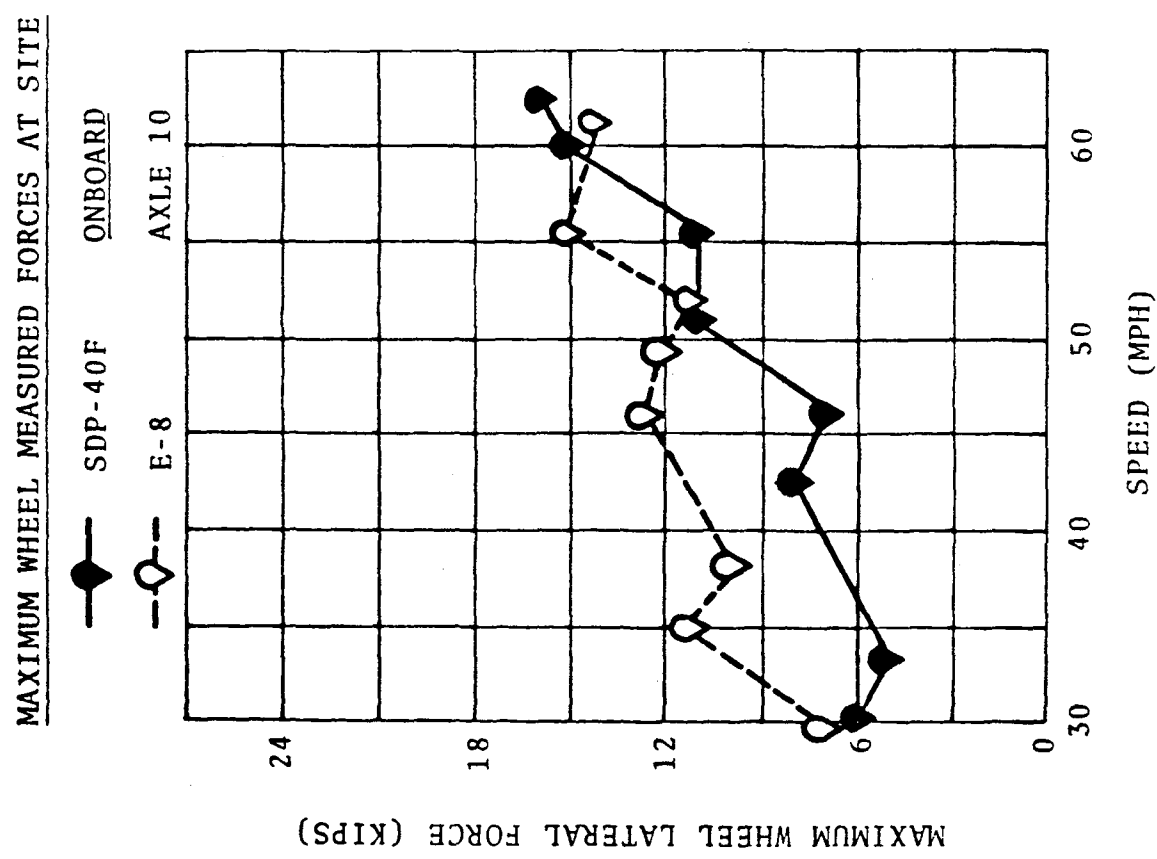
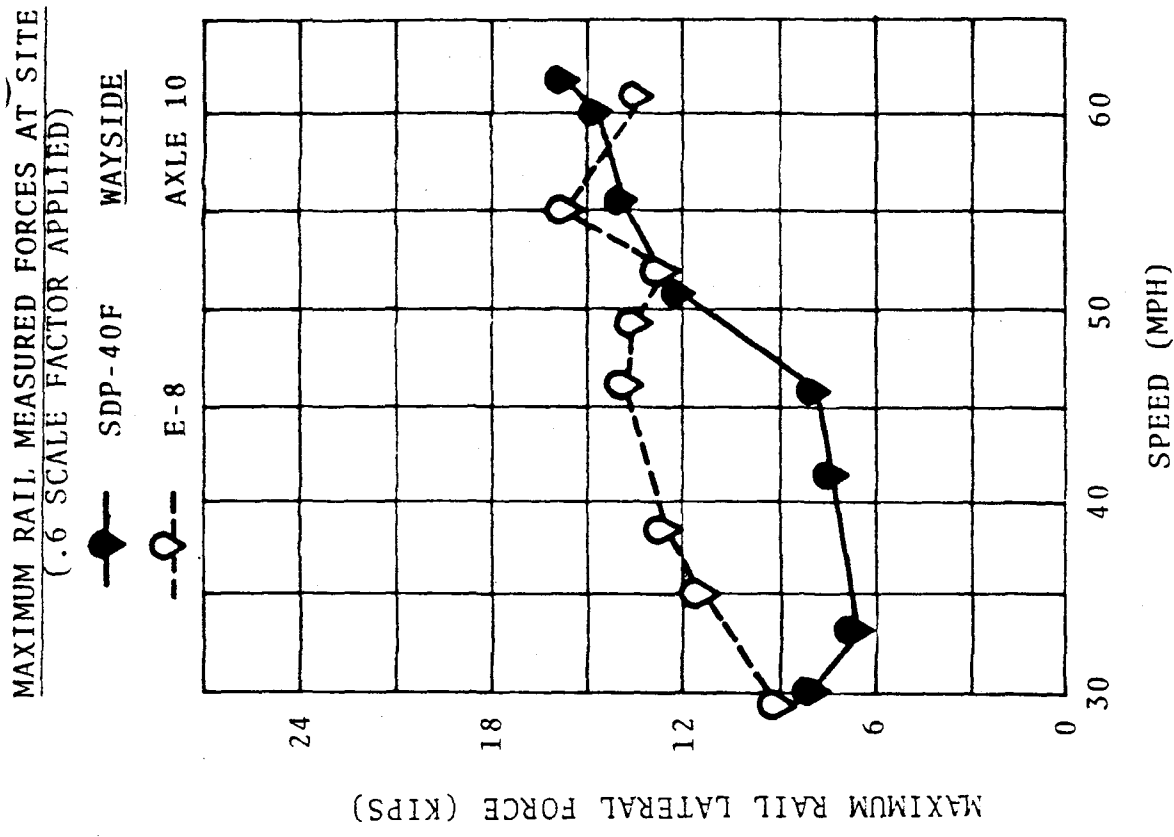
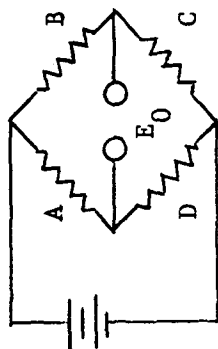
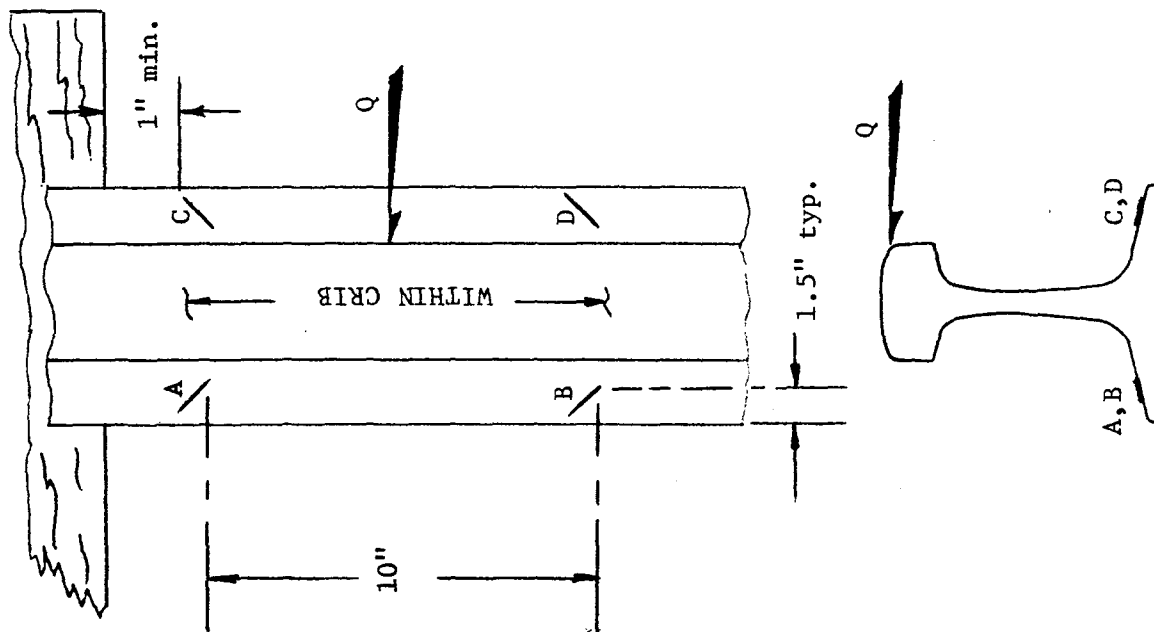


FIGURE G-11 COMPARISON OF AXLE 10 MAXIMUM LATERAL FORCE FROM
WAYSIDE AND ONBOARD, FOR E-8 AND SDP-40F AS A FUNCTION OF SPEED

TABLE G-3 COMPARATIVE EVALUATION OF LATERAL WHEEL/RAIL
LOAD-MEASURING STRAIN GAGE CIRCUITS

Criteria	Web Vertical Over Tie (Fully- Supported	Base Chevron
Sensitivity # 10K = % of calculated step or $\mu\epsilon$ *	Good 21%	Good 17.4%
Linearity (0 to 10K) at 5K, Error -	Fair +9%	Good -5%
Crosstalk * Lb per 1000 lb V at Flange Contact Pt.	Poor 580	Good -56/~132 ¹
Sensitivity to Support Clips off, field - Clips snugged -	Fair	Good -11% +10%
Sensitivity to Vertical Position of Lateral Load Z = -.44" to -.81"	Fair +18%	Good +8%
Change in Sensitivity under Vertical Load 30 K V, Y = 0	Good -4%	Good -3%

- # Clips loose on adjacent ties (normal condition)
 * Sensitivity for lateral load applied at Z = -.44"
 1 Near edge of chevron pattern



GAGE TYPE: Ailtech SG129, Type 6S weldable gage
(or equivalent)

RESISTANCE: 120 ohms

EFFECTIVE GAGE LENGTH: 1 inch

TEMPERATURE RANGE: 0° - 180° F

GAGE FACTOR: 2.0 (normal)

APPROXIMATE CIRCUIT SENSITIVITY: 1 m.v./volt/50 kips

CALIBRATION: Single 60 Kilo-ohm shunt resistor 25 kips

FIGURE G-12 TSC/ECL RAIL BASE CHEVRON CIRCUIT

APPENDIX H

SIMULATION OF LOCOMOTIVE VERTICAL RESPONSE

TSC's DYNALIST II computer program was used to simulate the vertical response of the SDP-40F locomotive with HTC trucks. A linear, tangent track model was used which contained thirteen degrees of freedom:

1. Leading wheel, leading truck, vertical response
2. Middle wheel, leading truck, vertical response
3. Trailing wheel, leading truck, vertical response
4. Leading wheel, trailing truck, vertical response
5. Middle wheel, trailing truck, vertical response
6. Trailing wheel, trailing truck, vertical response
7. Carbody center of mass
8. Carbody pitch angle
9. Hanging mass, vertical response
10. Leading truck, vertical response
11. Leading truck, pitch angle
12. Trailing truck, vertical response
13. Trailing truck, pitch angle

The program obtained the eigenvalues and eigenvectors corresponding to the model's equations of motion and printed the vertical response of the locomotive to a rectified sine wave track perturbation.

Based on comparing the analytical simulation with carbody acceleration test data obtained at the road crossing near MP 257.5 for the cases of no shocks, standard shocks (1200/400), and heavy-duty shocks (1800/1800), the following values were selected for the effective vertical primary damping (near resonance) of the truck assembly and of the external shock absorbers (two per truck on either side of the middle axle):

- Internal Truck Damping: 400 lbs - sec/inch (per truck)
- Standard Shock Absorber (1200/400): 25 lbs -sec/inch (per shock)
- Heavy-Duty Shock Absorber (1800/1800): 100 lbs - sec/inch (per shock)

The value of 400 lbs - sec/inch for the internal truck damping was selected by matching the trough-to-peak excursion of experimental and simulated acceleration data as the vehicle passed from its bounce to its pitch resonance. The data used in the matching procedure described the vertical acceleration of the locomotive carbody at the trailing truck attachment point; the value of the external shocks was zero. An independent calculation based on estimating the hysteresis damping in the springs and the friction damping between the axle journals and pedestal liner (under power in the resonant operating range) also produced a value of approximately 400 lbs - sec/inch for the internal truck damping.

The other constituent of this matching procedure was the track perturbation, which was approximated by a rectified sine wave. This rectified sine wave was represented by a ten-term Fourier series.* An amplitude of 0.6 inches was adopted to match the peak acceleration at the pitch resonance.

The upper curve in Figure H-1 shows simulated acceleration data obtained by following this matching procedure, as compared with the experimental data shown in Figure H-2. In the latter figure, the pitch resonance curve represents the

*Using a larger number of terms in the Fourier series did not change the results of the matching procedure, provided no more than 20 terms were used. Ten terms were used for reasons of economy. The use of more than 20 terms introduced unrealistically high forces attributable to the cusps in the track perturbation. The Fourier series representing these wheel/rail forces contained high frequency coefficients of alternate signs whose order approached the leading terms of the series. This increase in the order of the high frequency coefficients of the series representing the wheel/rail forces was avoided by limiting the number of terms to 20; i.e., limiting the number of terms effectively "smoothed-out" the cusps.

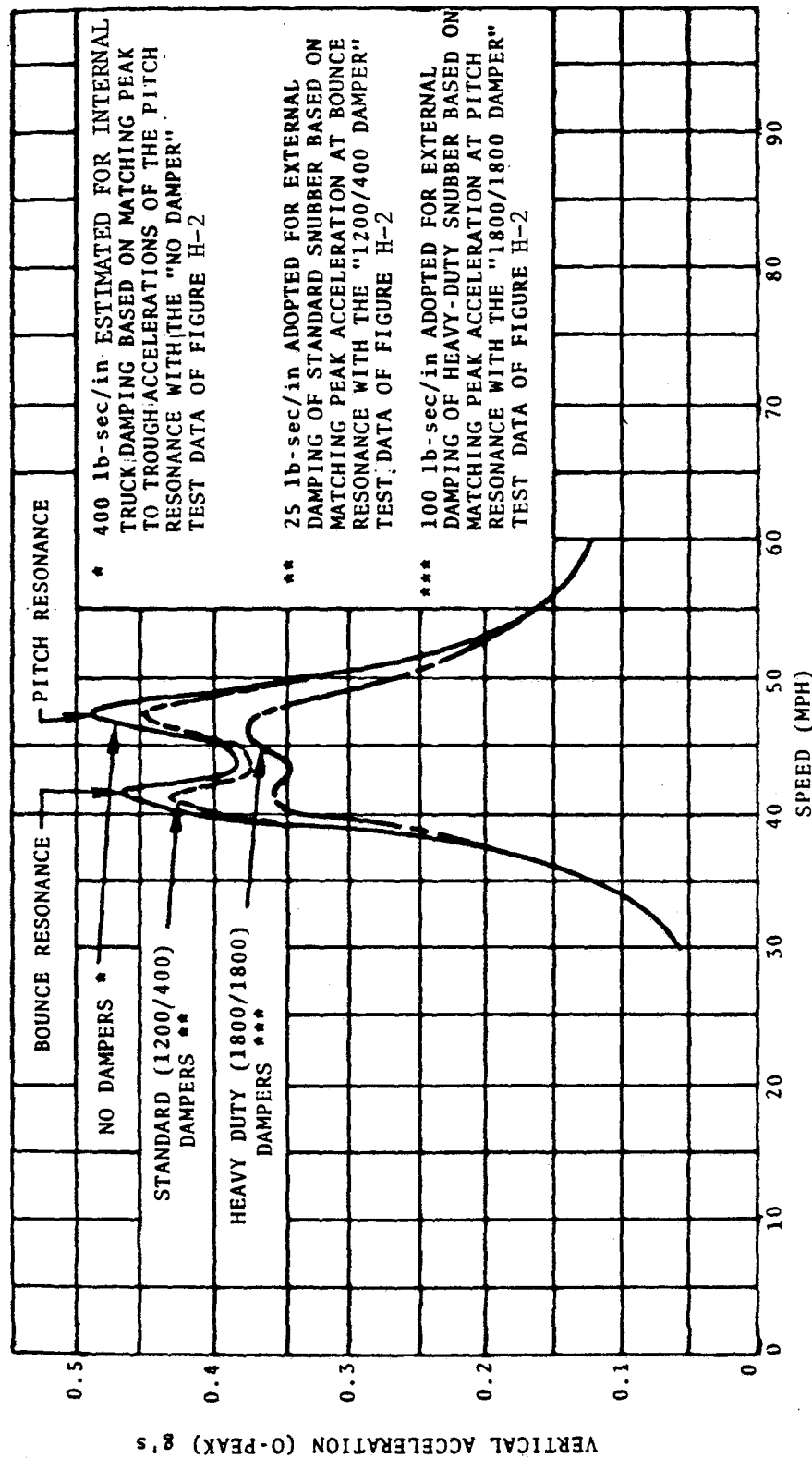


FIGURE H-1 ANALYTICAL SIMULATION OF EFFECT OF VARIATION IN THE VERTICAL PRIMARY DAMPING ON SDP-40F REAR END VERTICAL ACCELERATIONS. (TRACK REPRESENTED AS A .6" AMPLITUDE RECTIFIED SINE WAVE.)

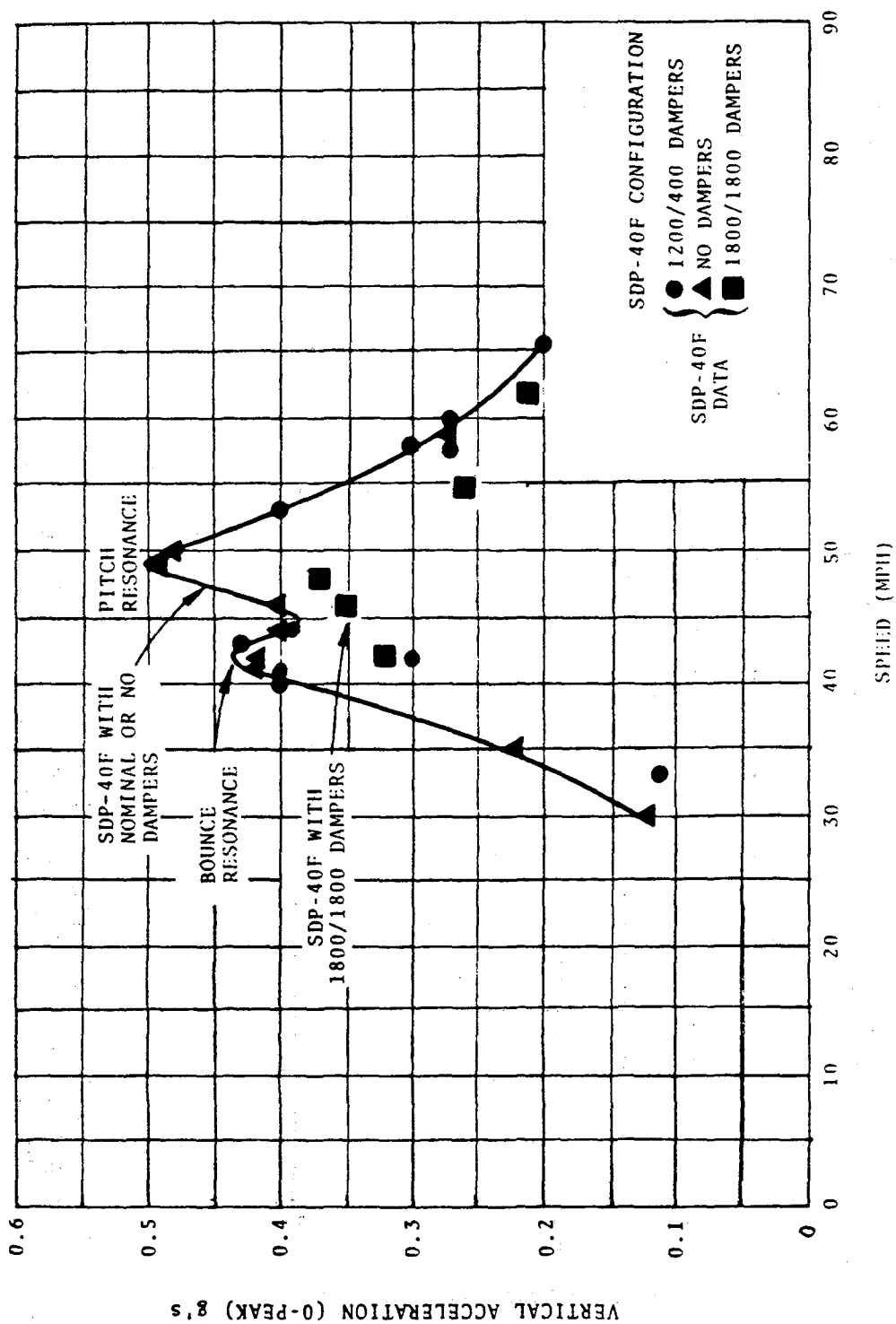


FIGURE H-2 TEST DATA SHOWING EFFECT OF VARIATION IN THE VERTICAL PRIMARY DAMPING ON SDP-40F REAR END VERTICAL ACCELERATION. (ALL RUNS FOR TRAILING LOCOMOTIVE AT ROAD CROSSING NEAR MP 257.5 IN POWER MODE.)

"no shock" test data, while the bounce resonance curve more closely corresponds to the standard shock data.

The two remaining curves in Figure H-1 were also obtained by matching simulated acceleration data with the experimental data of Figure H-2. In these cases, only the values of the external shocks were adjusted. The curve labeled "STANDARD (1200/400) DAMPERS" was obtained by matching simulated and experimental data in the vicinity of the bounce resonance near 41 mph. This matching procedure resulted in an effective value of 25 lb - sec/inch (per shock) for the standard shock in this operating region. The curve labelled "HEAVY-DUTY (1800/1800) DAMPERS" was obtained by matching data in the vicinity of the pitch resonance near 47 mph. This matching procedure resulted in an effective value of 100 lbs - sec/inch (per shock) for the heavy-duty shock.

It is of interest to compare the viscous damping coefficients obtained by using the matching procedures given in this appendix with values based on the result of an EMD study* of the shock absorber response characteristic. This EMD study had established that the standard shocks (1200/400) have an equivalent viscous damping coefficient of approximately 140 lb - sec/inch at a frequency of about 1.9 Hertz and a stroke of 2", as shown in Figure H-3. This frequency corresponds to the vertical resonance of the SDP-40F at about 50 mph. The 2" stroke is approximately equal to the amplitude of the simulated vertical response at resonance. It appears that the damping coefficient values based upon this EMD study are much greater than the values estimated by the TSC study (25 lb-sec/inch) to match the experimental values. Further work is being done to resolve this discrepancy. It is also of interest to note from Figure H-3 that the effective viscous damping coefficients for the standard external shock absorbers in this portion of the vehicle's operating range are greatly reduced from the maximum operating capability of these shocks.

*"Dynamic Performance of the HTC Suspension System under 6-Axle Locomotives," Southern Pacific Transportation Co., July 1977.

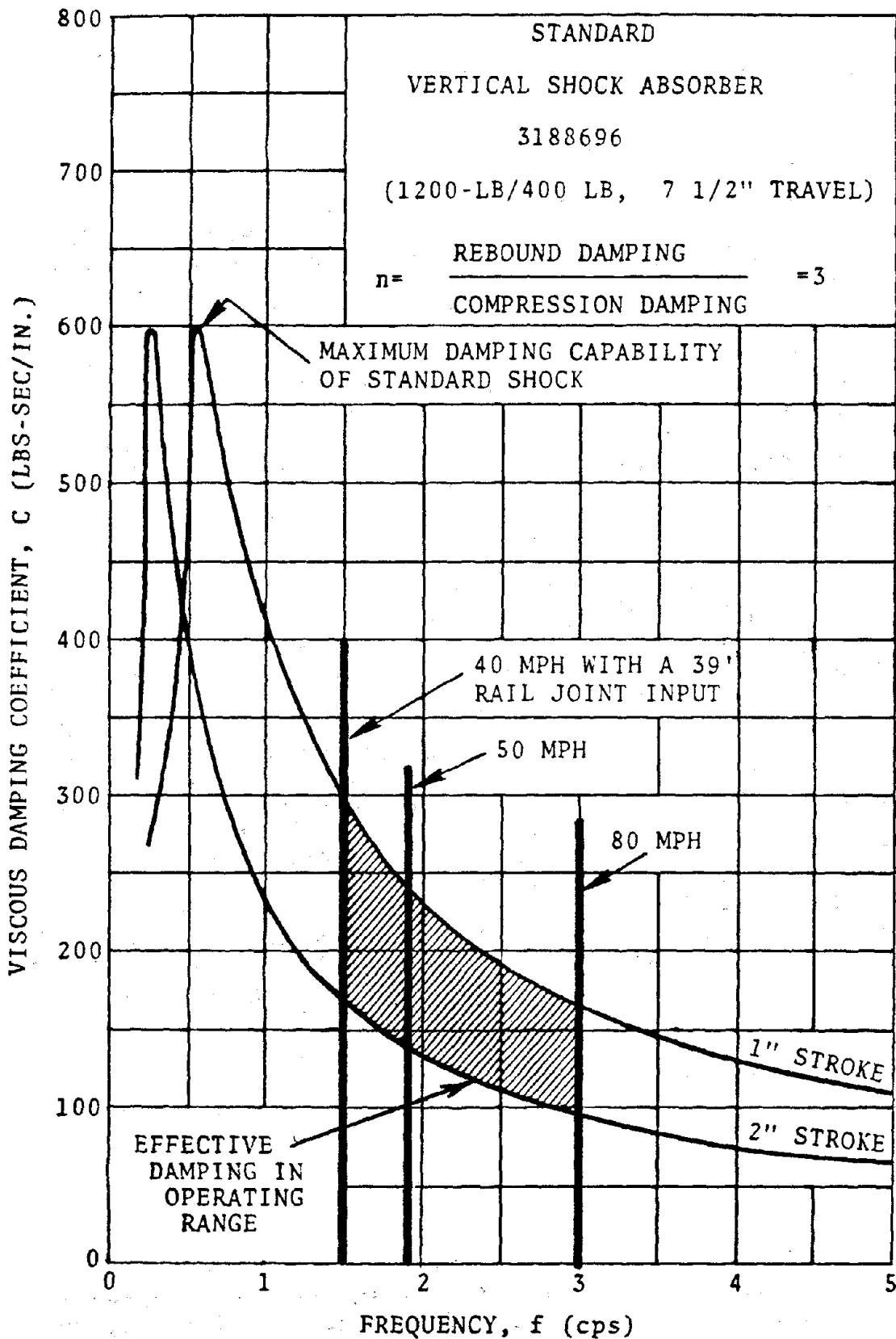


FIGURE H-3 VARIATION IN STANDARD SHOCK DAMPING CAPABILITY AS A FUNCTION OF FREQUENCY (BASED ON EMD STUDY)